COMPUTER SYSTEMS LABORATORY

STANFORD UNIVERSITY · STANFORD, CA 94305-2192

PERFORMANCE EVALUATION OF MULTIHOP PACKET RADIO NETWORKS BY SIMULATION

David Hilton Shur

Technical Report: CSL-TR-87-320

March 1987

This report is the author's Ph.D. dissertation which was completed under the advisorship of Professor Fouad A. Tobagi. This work was supported by the Defense Advanced Research Projects Agency under Contracts No. MDA 903-79-C-0201 and No. MDA 903-84-K-0249.

UNCLASSIFIED

SECURITY CLASSIFICATION OF THIS PAGE (When Data Entered)

REPORT DOCUMENTATION PAGE		READ INSTRUCTIONS BEFORE COMPLETING FORM
1. REPORT NUMBER 87-320	2. GOVT ACCESSION NO.	3. RECIPIENT'S CATALOG NUMBER
4. TITLE (and Subtitle) PERFORMANCE EVALUATION OF MULTIHOP PACKET RADIO NETWORKS BY SIMULATION		5. TYPE OF REPORT & PERIOD COVERED TECHNICAL REPORT 6. PERFORMING ORG. REPORT NUMBER 87-320
7. AUTHOR(s) David Hilton Shur		8. CONTRACT OR GRANT NUMBER(s) MDA 903-79-C-0201 MDA 903-84-K-0249
9. PERFORMING ORGANIZATION NAME AND ADDRESS Stanford Electronics Laboratory Stanford University Stanford, California 94305-2192		10. PROGRAM ELEMENT, PROJECT, TASK AREA & WORK UNIT NUMBERS
11. CONTROLLING OFFICE NAME AND ADDRESS Defense Advanced Research Projects Agency Information Processing Techniques Office 1400 Wilson Blvd., Arlington, VA 22209		12. REPORT DATE March 1987 13. NUMBER OF PAGES 217
14. MONITORING AGENCY NAME & ADDRESS(if different from Controlling Office) Resident Representative Office of Naval Research Durand 165 Stanford University, Stanford, CA 94305-2192		15. SECURITY CLASS. (of this report) UNCLASSIFIED 15a. DECLASSIFICATION/DOWNGRADING SCHEDULE

16. DISTRIBUTION STATEMENT (of this Report)

Approved for public release; distribution unlimited.

17. DISTRIBUTION STATEMENT (of the abstract entered in Block 20, if different from Report)

18. SUPPLEMENTARY NOTES

19. KEY WORDS (Continue on reverse side if necessary and identify by block number)

20. ABSTRACT (Continue on reverse side if necessary and identify by block number)

Packet switched networks provide an efficient and flexible method for interconnecting geographically distributed users for the purpose of digital data transmission. In packet radio networks, nodes transmit packets over multiple-access broadcast radio channels instead of wire, cable or fiber optics links. If the destination node of a packet is not within the power range of its source node, intermediate nodes are needed to deliver the packet in a store-and-forward fashion. Therefore, multihop packet radio networks have both the

DD FORM 1 JAN 73 1473 EDITION OF 1 NOV 65 IS OBSOLETE

S/N 0102-LF-014-6601

UNCLASSIFIED

SECURITY CLASSIFICATION OF THIS PAGE (When Data Entered)

multiple-access feature typical of broadcast networks and the store-and-forward feature of point-to-point networks. Since only under restrictive assumptions is performance analysis tractable, simulation techniques must be used.

The basic behavior of various existing channel access schemes, namely, ALOHA, CSMA, CDMA, and BTMA, and a new scheme referred to as Coded Activity Signalling Multiple Access (CASMA) is investigated. In networks with a regular structure and balanced traffic flow, the effects of transmission scheduling rate, the ratio of propagation delay to packet transmission time, store-and-forward buffer size, and to some extent network access flow control on throughput and delay performance are examined. We show that contrary to the case of single-hop, fully connected networks, the performance of CSMA is not only substantially degraded due to hidden nodes, but it is also affected to a much lesser extent by propagation delay. BTMA and CASMA on the other hand are observed to achieve a relatively high capacity, and to be more sensitive to propagation delay. The performance of a number of variants of a well known buffer management scheme, the Structured Buffer Pool (SBP) is also studied. The effect of the number of buffers per repeater differs according to the channel access scheme employed. The performance of ALOHA and CSMA is not very sensitive to the buffer size, while BTMA and CASMA exhibit up to a 50% degradation in capacity in certain examples. In more general networks, we show that the CSMA access scheme may exhibit a high degree of variance in the achievable capacity among different PRUs and links, as compared with the other access schemes. Simple sub-optimal transmission scheduling algorithms are introduced to treat the problem of large-scale realistic networks, and are shown to perform well in a 'real-world' example.

PERFORMANCE EVALUATION OF MULTIHOP PACKET RADIO NETWORKS BY SIMULATION

David Hilton Shur

Technical Report: CSL-TR-87-320

March 1987

Computer Systems Laboratory
Departments of Electrical Engineering and Computer Science
Stanford University
Stanford, California 94305-2191

Abstract

Packet switched networks provide an efficient and flexible method for interconnecting geographically distributed users for the purpose of digital data transmission. In packet radio networks, nodes transmit packets over multiple-access broadcast radio channels instead of wire, cable or fiber optics links. If the destination node of a packet is not within the power range of its source node, intermediate nodes are needed to deliver the packet in a store-and-forward fashion. Therefore, multihop packet radio networks have both the multiple-access feature typical of broadcast networks and the store-and-forward feature of point-to-point networks. Since only under restrictive assumptions is performance analysis tractable, simulation techniques must be used.

The basic behavior of various existing channel access schemes, namely, ALOHA, CSMA, CDMA, and BTMA, and a new scheme referred to as Coded Activity Signalling Multiple Access (CASMA) is investigated. In networks with a regular structure and balanced traffic flow, the effects of transmission scheduling rate, the ratio of propagation delay to packet transmission time, store-and-forward buffer size, and to some extent network access flow control on throughput and delay performance are examined. We show that contrary to the case of single-hop, fully connected networks, the performance of CSMA is not only substantially degraded due to hidden nodes, but it is also affected to a much lesser extent by propagation delay. BTMA and CASMA on the other hand are observed to achieve a relatively high capacity, and to be more sensitive to propagation delay. The performance of a number of variants of a well known buffer management scheme, the Structured Buffer Pool (SBP) is also studied. The effect of the number of buffers per repeater differs according to the channel access scheme employed. The performance of ALOHA and CSMA is not very sensitive to the buffer size, while BTMA and CASMA exhibit up to a 50% degradation in capacity in certain examples. In more general networks, we show that the CSMA access scheme may exhibit a high degree of variance in the achievable capacity among different PRUs and links, as compared with the other access schemes. Simple sub-optimal transmission scheduling algorithms are introduced to treat the problem of large-scale realistic networks, and are shown to perform well in a 'real-world' example.

Acknowledgments

I would like to acknowledge my dissertation advisor and first reader Prof. Fouad Tobagi for introducing me to the field of computer communications and for his constant interest in and critical attention to my work. The other readers of this dissertation, Profs. David Cheriton and Joseph Goodman kindly gave of their time and provided constructive comments, as did the fourth member of my Ph. D. Orals committee, Prof. Michael Flynn. My thanks also to Profs. Bernard Widrow and Ronald Bracewell for providing support and inspiration during my first years at Stanford.

My understanding of the field of computer communications was greatly enhanced by many interesting discussions with my knowledgable officemates, Michael Fine, Jose Brazio, Mehdi Nassehi, Yitzhak Birk, Tim Gonsalves and James Storey who also provided much appreciated support and turned into good friends. Other friends provided stimulation and friendship during the years at Stanford; special mention must be made of Alfred Bruckstein, Barry Medoff, Mati Wax, Howard Pein and Henk Goosen. Thanks to Jill Sigl for her guidance in dealing with administrative matters and to Willem Terluin for cheerfully drafting many of the figures in this dissertation.

To Janelle who shared much of this time with me, I offer my heartfelt thanks

for her steadfast support, advice and encouragement. To my family members in far-away lands, you were always in my thoughts. I dedicate this dissertation to the memory of my late mother Vivienne who sadly passed away during the course of my studies at Stanford, and to my father Abraham.

Contents

Figures

Tables

Chapter 1

Introduction

In this chapter, background information motivating the development of packet radio networks is briefly described. As the channel access policy is of particular importance, an overview of existing schemes is given. The problem that is the focus of this dissertation is outlined and the methodology discussed. Related research is surveyed and the contributions of the dissertation are stated. Finally, a brief description of some existing packet radio networks is given.

1.1 Background

As is well known, the technology of packet switching provides an efficient and flexible method for digital data communication [1]. Packet switching techniques have been applied to both point-to-point and broadcast communication networks, and transmission media such as twisted-pair wire, coaxial cable, fiber optics links and radio channels have been utilized. The radio medium is distinguished from the others in that not only is connectivity provided, but the users may be mobile and

rapid reconfiguration of the network is possible. The first example of an operational packet radio network was the ALOHA system at the University of Hawaii [2]. The ALOHA network was a two-channel, centralized configuration in which terminals transmitted packets to a central station on an inbound multiple access radio channel and received packets from the station on an outbound broadcast channel. While the ALOHA network did not utilize all the distinguishing features offered by the radio medium (for example, mobile users were not supported), the feasibility of the packet radio concept was very successfully demonstrated. Motivated in part by this fact, a research program was undertaken by the United States Defense Advanced Research Projects Agency (DARPA) on the design and implementation of a more general packet radio network (PRNET) [3]. The requirements for PRNET included support for mobile users in a distributed environment, wide geographical coverage, ease of deployment and resistance to interference (among others). Currently, the PRNET packet radio network is viewed as consisting of a collection of geographically distributed, possibly mobile, packet radio units (PRU's), communicating with each other over a single shared broadcast radio channel using omnidirectional antennas. Data originates at some PRU's (referred to as sources) and is destined for other PRU's (referred to as destinations). Since a radio transmitter may be unable to reach its destination, either due to power limitation or because the topology includes obstacles that are opaque to radio signals, PRU's also act as repeaters which relay packets in a store-and-forward manner between sources and destinations. In order to perform the functions required of a node in such a network, each PRU contains a radio section and a digital controller. The radio section consists of the antenna, a single transmitter and a single receiver and provides the connectivity among neighboring PRUs. Note that the operation of the transmitter and receiver is mutually exclusive since all communication in the network is assumed to take place in a single frequency band. The digital controller performs the various

packet switching functions such as the buffering of packets received from neighboring PRUs, the routing function which determines the path in the network followed by a packet, and the flow control function which controls the acceptance of packets by nodes of the network.

Packet radio networks combine the multiple access feature of broadcast networks with the store-and-forward feature of point-to-point, wire-based, store-and-forward communications networks. They are rather complex networks in that many interacting variables and functions need to be considered in their design. Among these are: the network topology, i. e., the number and connectivity of the PRUs, the data modulation and signalling schemes, the channel access policy which determines how the PRUs gain access to and share the channel, the routing and flow control protocols, the acknowledgment protocol whereby a source PRU learns of the success or failure of a previous transmission, and the nodal design, consisting of the selection, organization and management of buffer resources within a PRU. In this dissertation, we focus primarily on one variable that has a major impact on performance, namely, the channel access policy. We also study the nodal design, paying particular attention to interactions between the nodal design and the channel access policy. As a major portion of this thesis is concerned with the channel access policy, an overview of existing schemes is given below.

1.2 Overview of Existing Channel Access Schemes

Many channel access policies have been devised which allow a set of geographically distributed users to access a common channel. As discussed in [4], random access techniques can provide simple, efficient and distributed access to the channel and hence are most appropriate for the mobile radio environment. A random

access protocol is specified by both a random scheduling process which defines the points in time where a PRU may attempt a transmission, and a rule invoked at each point which determines whether or not the PRU actually transmits. The scheduling process is often parameterized by its rate, and we refer to methods for choosing scheduling rates or processes as scheduling algorithms. The simplest random access protocol is ALOHA [2,4], whose rule permits users to transmit whenever a packet is available. Under this protocol and in narrowband systems, the overlap in time and space of several transmissions which may occur on the shared channel may induce significant errors in some or all of these transmissions, thus resulting in low channel efficiency. Carrier sense multiple access (CSMA) attempts to alleviate this problem by requiring the transmitter to sense the state of the channel (busy or idle) prior to transmitting, and to inhibit transmission if the channel is sensed busy [5]. Studies of these access schemes have previously focused mainly on single hop environments, with the assumption that all nodes are within range and in line-of-sight of each other. In such environments, and when in addition the propagation delay is small compared to the transmission time of a packet, analysis has clearly demonstrated the high channel utilization of CSMA and its superiority over the pure and slotted ALOHA schemes [5]. Analysis, however, has also shown that CSMA suffers severe degradation when *hidden nodes* are present; i.e., when all nodes are not within range and in line-of-sight of each other [6]. This situation is clearly met in multihop packet radio networks, and hence, CSMA is not expected to perform as well in such networks as it does in fully connected networks. The busy tone multiple access scheme (BTMA) attempts to overcome the hidden node problem by having a node transmit a busy tone when it is busy receiving, thus preventing its neighbors from interfering with its reception [6,7]. Clearly, the reduction in interference is obtained at the expense of the increased bandwidth needed for the busy tone.

An alternative solution to the problem of collisions in multiaccess/broadcast

networks is based on spread spectrum and code division techniques. When these techniques are utilized, the number of collisions may be reduced by using orthogonal signalling codes in conjunction with matched filters at the intended receivers. Clearly, here too multiple orthogonal codes are obtained at the expense of increased bandwidth needed in order to spread the waveforms. When both code division signalling techniques and multiaccess protocols for accessing the channel are used, the resulting channel access schemes are known as code division multiple access (CDMA) schemes [3]. One CDMA scheme consists of assigning a unique code to each node; nodes then wishing to transmit to a particular node must utilize the code assigned to that node.

1.3 Statement of the problem

The fundamental behavior of channel access schemes in the single-hop fully-connected environment has been extensively studied and is well understood [1,4]; furthermore, the knowledge gained in the various studies has led to the development of scheduling algorithms for both radio and other broadcast networks [8-11]. The aim of this thesis is to characterize the basic behavior of channel access schemes in *multihop* packet radio networks and thus to lay the groundwork for the development of practical scheduling algorithms. The characterization of the behavior of channel access schemes is achieved by evaluating the effect of key parameters, namely, the scheduling rate, the propagation delay among nodes and the store-and-forward buffer storage size on the network performance measures of throughput and average packet delay.

1.4 Methodology

The difficulty of the analysis problem for multihop packet radio networks was discussed in [12] and [13], where it was pointed out that the network constitutes a system of interfering queues with the service time at a given queue depending on the state of neighboring queues. Additional complexity arises due to the non-zero propagation delay among nodes, and the exact analysis of delay turns out to be particularly intractable. Due to these difficulties the primary method used to obtain numerical results is simulation. In a small number of simple special cases, mathematical analysis based on renewal theory methods has been used (refer to Appendices 7.1.1 - 7.1.3). Simulation enables the consideration of general and realistic models without concern for analytic tractibility. Since arbitrary levels of detail of a packet radio network can be included in a simulation model, it is important to strike a balance between accuracy and complexity in the formulation of that model. Indeed, previous attempts to create simulation programs that encompass all operational aspects of a packet radio network have not been successful due to the size and complexity of the resulting programs [14]. In this work, we have thus included only the essential elements of packet radio networks in the simulation. Since the software is written in a modular form, we leave open the option of adding other aspects of network operation in the future. The simulation program structure, the validation of the program and the estimation of the performance measures are discussed in Appendix 7.2.

1.5 Related Work

A short survey of previous and related studies is given below. As single-hop, fully-connected networks have been extensively surveyed in several previous publications ([1, 14]), the emphasis will be on the more recent work on multihop networks.

A comprehensive descriptive survey of channel access protocols is given in [4]. The random access schemes covered include ALOHA, CSMA, BTMA and CDMA. The performance analysis of these and related protocols are surveyed in [14]. As discussed in [14], the difficulty in mathematical analysis has resulted in previous attempts at treating the general multihop problem taking one of two directions. Either detailed and accurate models have been formulated with the result that only small and rather simple networks are able to be analyzed, or less accurate models are considered in order to handle larger and more general networks. The first approach has been taken in [15-19]. Centralized two-hop configurations under the slotted ALOHA access scheme were analyzed in [15] and [16], and under CSMA in [17]. The work in [16] and [17] studied the throughput-delay performance and described the effect of two retransmission strategies, the delayed first transmission (DFT) and the immediate first transmission (IFT) schemes. In the DFT scheme, a PRU always delays a random amount of time before attempting to transmit a packet, while in the IFT scheme, if a packet arrives at a PRU whose buffers are entirely empty, the packet is transmitted immediately. It was shown that in the IFT scheme, the capacity was slightly diminished as compared to the DFT scheme, and that under low load the average packet delay tended to be lower than that of the DFT scheme. The effect of buffer size was also studied and it was concluded that the performance of the ALOHA and CSMA schemes were not limited by a lack of buffer storage, but were in fact channel bound. In [18], the capacity of the infinite tandem network under slotted ALOHA was derived under both so-called 'polite' and 'rude' scheduling policies. It was noted that as the number of nodes in the tandem network was increased, the capacity of the tandem remained essentially constant for the number of nodes more than four. It was also shown that the rude policy achieved a higher capacity than the polite policy. In [19], the throughput-delay performance of two multihop networks also operating under slotted ALOHA was obtained. Two

techniques for improving capacity were studied, namely, transmission suppression and transmission acceleration. In the former technique, a transmission is suppressed if no buffer storage space at the immediate intended destination is available. In the latter technique, given a source node i, if both the intended destination j and the neighbors of j other than i are all empty of packets, then i transmits with probability 1. It was also confirmed that little improvement in capacity was to be had by increasing the number of buffers per repeater to more than about 3.

The second approach has been taken in [20-39]. In [20,21], the capacity of slotted ALOHA networks with both a regular and random structure was obtained by simulation and analysis. It was shown that in one dimensional networks, the network capacity was basically independent of the nodal degree, while for two dimensional networks, the capacity grew in proportion to the square root of the number of nodes, provided the average degree was kept small. Also considered was the effect of variable transmitter power on network throughput. It was noted that there was a power range that maximized network capacity. The effect of variable transmitter power was considered in [22-24]. In [22], the effect of power capture was considered, and a tradeoff between the probability of successful transmission and the number of hops required to reach the destination was delineated. In [23], the optimal transmission range to maximize the expected one-hop progress in desired directions was obtained for the slotted ALOHA and CSMA access schemes. It was also noted that CSMA only slightly outperformed slotted ALOHA. In [24], three transmission strategies were considered, namely, most forward progress with fixed transmission radius (MFR) where a node chooses its destination so that most forward progress results, nearest neighbor with forward progress (NFP) where the transmission power is adjusted so as to just reach the nearest neighbor in the forward direction, and most forward progress with the transmission radius adjusted to be equal to the distance between the transmitter and the receiver (MVR). It was shown that higher

throughput and expected progress was achieved using the NFP strategy. In [25] spread spectrum slotted ALOHA networks were studied under the assumption of an inverse fourth power signal propagation law. It was concluded that if the spread spectrum system is able to effectively support K simultaneous transmissions, then the optimal transmission range is such that there are approximately $1.3\sqrt{K}$ nodes closer to the transmitter than the receiver.

In [26,27] new access schemes for multihop networks were proposed. In [26], a variant of CSMA called rude CSMA was introduced in which nodes transmit with a non-zero probability when the channel is sensed busy. Some improvement over conventional CSMA was noted in small regular lattice networks, but for other topologies such as rings, tandems and random networks conventional CSMA worked best. In [27] the spatial TDMA protocol was presented and analyzed. In spatial TDMA, it is assumed that sets of transmissions (referred to as cliques) that can take place concurrently and successfully are known. There is a periodic time cycle consisting of a number of time intervals with each time interval corresponding to a different clique. Transmissions within a clique are enabled during the corresponding time interval in the cycle. The average delay experienced by packets was calculated using an approximate queueing analysis.

Approximate analyses based on iteration procedures have been carried out in [28-30]. In [28], an approximate procedure for deriving throughput-delay performance was presented, which yielded results within a factor of 2 of simulation results for the (slotted ALOHA) examples considered. In [29] and [30] a more detailed model of the behavior of a node was developed, and the effect of interference by neighboring nodes was lumped into a single interference parameter, which allowed a solution for the throughput and delay of a node in a decoupled fashion. In [31-39] a Markovian model capable of throughput analysis of a large class of channel

access protocols, including ALOHA, CSMA and Conservative-BTMA (C-BTMA), was presented and analyzed under the assumption of zero propagation delay. In [31], the Markovian model was first presented for the CSMA protocol with perfect capture. Numerical results were derived for ring, chain and star topologies. In [32], the effect of imperfect acknowledgments was studied, and a new scheme for 'piggy-back' acknowledgments was proposed and analyzed. In [33], the analytical model was extended to ALOHA, C-BTMA and a version of the CDMA scheme. In [34], the model was extended to account for packet lengths distributions which possess rational Laplace transforms. In [35], an efficient algorithm for the numerical solution of the problem was described. In [36], a characterization of access protocols which result in product form solutions was presented, and general throughput expressions independent of capture assumptions were derived. In [37], the model was extended to spread spectrum networks. In [38], the CSMA, C-BTMA and CDMA protocols were compared in regular and random networks. In [39], the focus was on an approximate analysis of the CDMA access scheme in the presence of noise. In summary, the work of [31-39] constituted a major advance since it enabled the analysis of general topologies and traffic patterns for access schemes other than slotted ALOHA. Recall that the model considered was simplified in that the propagation delay was assumed to be zero; furthermore, the effect of the buffering of packets by store-and-forward repeaters was also not modelled, and hence information about packet delay could not be derived.

Simulation techniques offer the possibility of studying general models without restrictive assumptions, and can be used as a test for the validity of approximate analytic models. Simulation has been used more frequently for the latter purpose [5, 6, 13, 39] than for the former [40, 41, 42]. In [40], simulation was used to study a number of aspects of packet radio networks such as the effect of topological connectivity and two data signalling schemes. In the first data signalling scheme

the same data rate was used by all nodes, and in the second two signalling rates were available with the higher rate used to communicate with nodes with a heavy traffic load and the lower rate used to communicate with other nodes. It was concluded that the second scheme had a superior performance. In [41] simulations of slotted ALOHA networks with random topologies and various retransmission strategies was carried out as an integral part of that study. In [42] simulation was used to study buffering, transmission scheduling and acknowledgments in 4 and 5 node star and string topologies under a modified CSMA protocol. Finally we mention two examples outside the domain of packet radio where simulation has proved an effective tool. The performance of buffer management schemes in point-to-point communication networks has been evaluated in [55], and in [11] the effect of station locations and various access protocol parameters was examined for Ethernet networks.

1.6 Contributions

The above literature survey indicates that a number of key aspects of multihop packet radio networks have not been adequately studied. The contributions of this thesis consist of addressing certain of these, namely the effect of such parameters as the propagation delay among nodes and the store-and-forward buffer size, the exact determination of average packet delay, and the design and performance evaluation of scheduling algorithms.

In chapters 3 and 4, multihop networks that have a regular structure and balanced traffic flow are considered. In such networks, matters are simplified as the number of parameters is greatly reduced, since all nodes perform in a statistically identical manner. In chapter 3, the effect of transmission scheduling rate, the ratio

of propagation delay to packet transmission time, and to some extent network access flow control on throughput and delay performance is examined. The performance of various existing channel access schemes, namely, ALOHA, CSMA, CDMA, and BTMA is compared. A new scheme referred to as Coded Activity Signalling Multiple Access (CASMA) is introduced and studied for the purpose of determining a bound on performance. We show that contrary to the case of single-hop, fully connected networks, CSMA is little affected by propagation delay (its performance being primarily limited due to hidden nodes). Propagation delay also has little effect on ALOHA and CDMA, but when the propagation delay is greater than about 20% of the packet transmission time the performance of BTMA and CASMA is substantially degraded. As well as providing useful numerical data, these results also indicate that analytic models that use the zero propagation delay assumption are more applicable for ALOHA, CSMA and CDMA than for BTMA and CASMA.

In chapter 4, multihop packet radio networks with finite buffers are studied. The use of the deadlock-free SBP scheme enables the study of multihop packet radio networks with finite buffers by means of simulation without fear of deadlocks. Several variants of the SBP scheme are proposed and their performance evaluated. The effect of the prioritization (based on pathlength) introduced by the SBP scheme is examined and the effect of finite repeater buffer size on the performance of the various channel access schemes is also obtained. We confirm the results of previous studies that have indicated that for ALOHA and CSMA, the performance bottleneck lies not in the finite repeater buffer storage, but in the utilization of the channel [16,17,19]; thus relatively few buffers per repeater suffice. For BTMA and CASMA on the other hand, we show that the performance of these schemes is indeed limited by finite buffer storage (by up to 50% in certain examples). In the latter examples, the largest value of buffer storage size required in order to make performance degradation negligible was approximately 40.

In chapter 5 we consider networks with more general topologies than were considered in chapters 3 and 4. Both simple small-scale networks and more complex and realistic large-scale networks are studied. We show that the CSMA access scheme may exhibit a high degree of variance in the achievable capacity among different PRUs and links. A number of simple sub-optimal transmission scheduling algorithms are introduced and numerical results given for an example consisting of a 51 node network obtained from measurement over real terrain. We show that the strategy of selecting a single scheduling rate for all PRUs, followed by a local perturbation of scheduling rates in the vicinity of saturated PRUs leads to a capacity of within 20% of the theoretical maximum capacity in the case of ALOHA. We conclude that this is a promising approach to packet scheduling in large multihop networks.

1.7 Existing Packet Radio Networks

There are currently three existing experimental PRNET networks operating in the high VHF to UHF bands at data rates of 100 to 400 Kbits/sec. One is deployed in the San Francisco Bay Area, and the other two are located in Ft. Bragg, North Carolina and Omaha, Nebraska and are aimed at determining the applicability of the technology to battlefield conditions [43]. The US navy has also worked on the development of packet radio networks. The High Frequency Intra-Task Force network is a general purpose network providing extended line-of-sight communications (50 to 1000 km) for mobile naval task force units [44]. Communication takes place in the HF band (2 to 30 MHz). Network connectivity and initialization are achieved via a distributed linked cluster algorithm and the time division multiple access protocol is used for the propagation of control messages.

The Stanford Packet Radio Network [45] is designed to provide line-of-sight access (within about 50km) to the local area network (LAN) based Stanford University Network (SUNET). The Stanford Packet Radio Network is configured as a two channel star, and operates in the low UHF band (at about 440MHz) at data rates of 9.6 to 56 Kbits/sec. The network is scheduled to begin operation in 1986. Packet radio networks have also been developed in the United Kingdom. The Royal Signals and Radar Establishment has carried out development of a medium size packet radio network with signalling rates of 16Kbits/sec in the low VHF band [46]. The use of the lower frequency band greatly reduces line-of-sight problems, which together with the smaller size of the network under consideration permits a non-hierarchical organization. Channel access is controlled via the CSMA protocol. Finally, the amateur ham-radio community has been actively developing hierarchical packet ham-radio networks in the VHF band at 300 and 1200 bit/sec data rates [47]. Amateur networks exist not only in the USA based on the AX.25 protocol, but also in Europe and Japan.

Chapter 2

Channel Access Protocols, Network Model and Performance Measures

2.1 Introduction

In this chapter, we describe the channel access protocols, the multihop packet radio network model and the measures of network performance. A precise description of the various protocols considered and the assumptions made in this study is given. The channel access protocols are described in section 2.1, operational protocols such as flow control, routing, acknowledgments and buffer management in section 2.2, the traffic model is discussed in section 2.3, the scheduling of packet transmissions in section 2.4, and the measures of performance presented in section 2.5.

2.2 Channel Access Protocols

We consider a network consisting of N nodes distributed over some geographical area. The connectivity of the network is specified by an $N \times N$ hearing matrix H, in which the (i,j)'th element h_{ij} is 1 if node j hears node i, and zero otherwise. (We let $h_{ii} = 1, \forall i$). Each nonzero element $h_{ij}, (i \neq j)$ of the hearing matrix corresponds to a directed radio link in the network from node i to node j, and vice versa. Alternatively, a network can be represented graphically by a directed graph in which vertices represent nodes in the network, and directed edges represent one-way connectivity. For simplicity, we assume in this work that H is symmetric, and thus all edges in the graph are bidirectional. For any node i, let $\mathcal{N}(i)$ denote the set of all nodes connected to it including itself. Let $\mathcal{N}^*(i) \triangleq \mathcal{N}(i) - i$. The elements of $\mathcal{N}^*(i)$ are called neighbors of i. For a collection of nodes A, we define $\mathcal{N}(A)$ to be

$$\mathcal{N}(A) \triangleq \bigcup_{i \in A} \mathcal{N}(i).$$

We let $\mathcal{N}^2(A) \triangleq \mathcal{N}(\mathcal{N}(A))$, and $< i,j >$ denote a transmission from node i to node j (assuming $h_{ij} = 1$). Given transmission $< i,j >$, a node k is said to be hidden with respect to the transmitting node i if $k \in \mathcal{N}(j) - \mathcal{N}(i)$.

Capture refers to the ability of a receiver to successfully receive a packet destined to it, in spite of the presence of other overlapping signals on the same channel. By *perfect capture*, we mean that once a receiver has begun to receive a packet, capture is achieved independent of the number of overlapping signals on the channel and their times of arrival. *Zero capture* refers to that situation in which any overlap of transmissions results in mutual destructive interference. We consider that all schemes, with the exception of CDMA, operate in a narrow band channel with zero capture. In the CDMA scheme, we assume that the channel is operating in

the spread spectrum mode, (together with bit-by-bit code changing and receiver directed codes), in which case the probability of capture is high, and thus perfect capture is assumed.

For all the protocols described below, it is considered that nodes attempt transmission of their packets at discrete random points in time defined by some point process. In the event that a packet scheduled for transmission is inhibited by the operation of the protocol, or in the event that a transmitted packet is not captured, then that packet is again considered for transmission at some future point in time determined by the scheduling point process.

2.2.1 ALOHA

In this mode, it is assumed that a node is allowed to transmit only if it is not already transmitting, regardless of the activity in the rest of the network. In the **pure ALOHA** version of this mode, packets are scheduled for transmission asynchronously (and independently). Clearly, this implies that the reception of a packet by a node is aborted if a packet transmission is scheduled at that node during the time of reception.

In the **Slotted ALOHA** version of this mode, the time axis is considered to be universal for all nodes and divided into equally sized slots. A node with a packet scheduled for transmission in a particular slot transmits that packet, synchronizing the start of transmission to coincide with the beginning of the slot. Note that since the slot size is fixed in advance, arbitrary distributions of packet length cannot be accommodated by this protocol. Note also that, due to the non-zero propagation delay among nodes, in order to have a universal slotted time axis, the slot size must be large enough to accommodate the packet transmission time plus a 'guard band'

equal to the maximum of the propagation delays between pairs of neighboring nodes in the network.

2.2.2 CSMA

In this mode, it is required that a node be able to sense the presence of transmissions by its neighbors. A packet will be transmitted by a node only if that node is not already transmitting and no ongoing transmissions are sensed. In spite of carrier sensing, two factors remain which contribute to collisions. The first is the non-zero propagation delay between neighbors: given that a transmission $< i, j >$ has been initiated, all nodes in the set $\mathcal{N}^*(i)$ are not blocked from transmitting until the transmission from node i has been sensed by them all; thus the propagation time from node i to its neighboring nodes constitutes a *vulnerable period* for the transmission $< i, j >$ as far as transmissions from $\mathcal{N}^*(i) \cap \mathcal{N}(j)$ are concerned. The second factor is *hidden nodes*: given that a transmission $< i, j >$ has been undertaken, all nodes in $\mathcal{N}(j) - \mathcal{N}(i)$ cannot sense the presence of $< i, j >$, and are thus never blocked; in this case the entire packet transmission time constitutes a vulnerable period for $< i, j >$ as far as transmissions from hidden nodes are concerned.

2.2.3 BTMA

The problem of collisions caused by hidden nodes can be alleviated by the use of a busy tone on a separate channel, which is emitted by a node to indicate that it is currently receiving a packet. The busy tone is then used to inhibit the receiving node's neighbors from transmitting and thereby interfering with it. Several variants of BTMA exist depending on which set of nodes transmit a busy tone in any given situation, as outlined below.

a. Conservative BTMA (C-BTMA): Whenever a node senses a transmission, it emits a busy tone regardless of whether it is the immediate destination or not. Then any node that wishes to transmit is allowed to do so only if it is not already transmitting and no busy tone is sensed. Given that a transmission $< i, j >$ has been undertaken, then after a one-hop propagation delay, all nodes in the set $\mathcal{N}^*(i)$ sense the presence of $< i, j >$, and emit a busy tone. After another propagation delay, busy tone is detected by all nodes in $\mathcal{N}^2(i) - \mathcal{N}(i)$. Thus, for the transmission $< i, j >$, a one-hop propagation delay constitutes a vulnerable period as far as transmissions from nodes in $\mathcal{N}^*(i) \cap \mathcal{N}(j)$ are concerned, while a two-hop propagation delay constitutes a vulnerable period as far as transmissions from nodes in $\mathcal{N}(j) - \mathcal{N}(i)$ are concerned. Note that, if the propagation delay between nodes is zero, then C-BTMA is collision free.

b. Receiving Destination BTMA (RD-BTMA): This scheme is similar to C-BTMA except that whenever a node senses a transmission, it emits a busy tone only if it is the immediate destination. As without prior knowledge, a node may not know if a particular transmission is destined to it or not, the RD-BTMA scheme is considered here for comparison purposes. Given that transmission $< i, j >$ has been undertaken, then after a vulnerable period equal to a two-hop propagation delay, all nodes in the set $\mathcal{N}^*(j)$ are blocked from transmitting. Alternatively, one may additionally make use of carrier sensing. This way, all nodes in $\mathcal{N}^*(i)$ (which includes $\mathcal{N}^*(i) \cap \mathcal{N}(j)$) are blocked after a vulnerable period of only a one-hop propagation time, while nodes in the set $\mathcal{N}(j) - \mathcal{N}(i)$ are blocked after a vulnerable period equal to a two-hop propagation time. In this work, only the latter scheme is studied.

We now examine in more detail some of the ramifications of these two BTMA schemes. Assume for the purpose of this discussion, that the propagation delay

is zero. Consider the following situation depicted in figure 2.1. Let node i be transmitting to node j and let all other nodes be silent. Assume that a packet from node $k \in \mathcal{N}^2(i) - [\mathcal{N}(i) \cup \mathcal{N}(j)]$ destined to node $m \in \mathcal{N}^2(i) - \mathcal{N}(i)$ is scheduled for transmission during the transmission $< i, j >$. In C-BTMA the transmission $< k, m >$ is blocked, while in RD-BTMA it results in a successful transmission.

On the other hand, in RD-BTMA (and CSMA for that matter) it is possible to allow a transmission to take place that will be unsuccessful, and whose presence may block a number of other potentially successful transmissions, while in C-BTMA, the former transmission would be inhibited by the protocol, allowing the later potentially successful transmissions to then take place. For example, referring to figure 2.1, consider now that a packet from node k destined to node $l \in \mathcal{N}(i)$ is scheduled for transmission during the transmission time of $< i, j >$. Furthermore, let $n \notin \mathcal{N}^2(i)$ and $r \in \mathcal{N}^2(i) - \mathcal{N}(i)$, and consider a transmission $< n, r >$ to be scheduled at some point in time during the transmission time of $< k, l >$. In RD-BTMA, the transmission $< k, l >$ is not blocked, but is unsuccessful; the transmission $< n, r >$ is blocked if $n \in \mathcal{N}(k)$; the transmission $< n, r >$ is unblocked but unsuccessful if $n \notin \mathcal{N}(k)$ and $r \in \mathcal{N}(k)$. In the latter case n's unsuccessful transmission will have blocking and interfering effects on its neighbors similar to those of node k's transmission. However, in C-BTMA, the transmission $< k, l >$ is blocked and the transmission $< n, r >$ is successful. It is not clear which of the effects outlined above would predominate in a given situation, and hence we resort to simulation to compare the different schemes.

c. Hybrid Destination BTMA (HD-BTMA): In RD-BTMA, we assume hypothetically that as soon as a node receives a packet it knows immediately whether or not that packet is destined to it. In practice this information is obtained from the packet header. Assuming that the packet header is processed as soon as it is

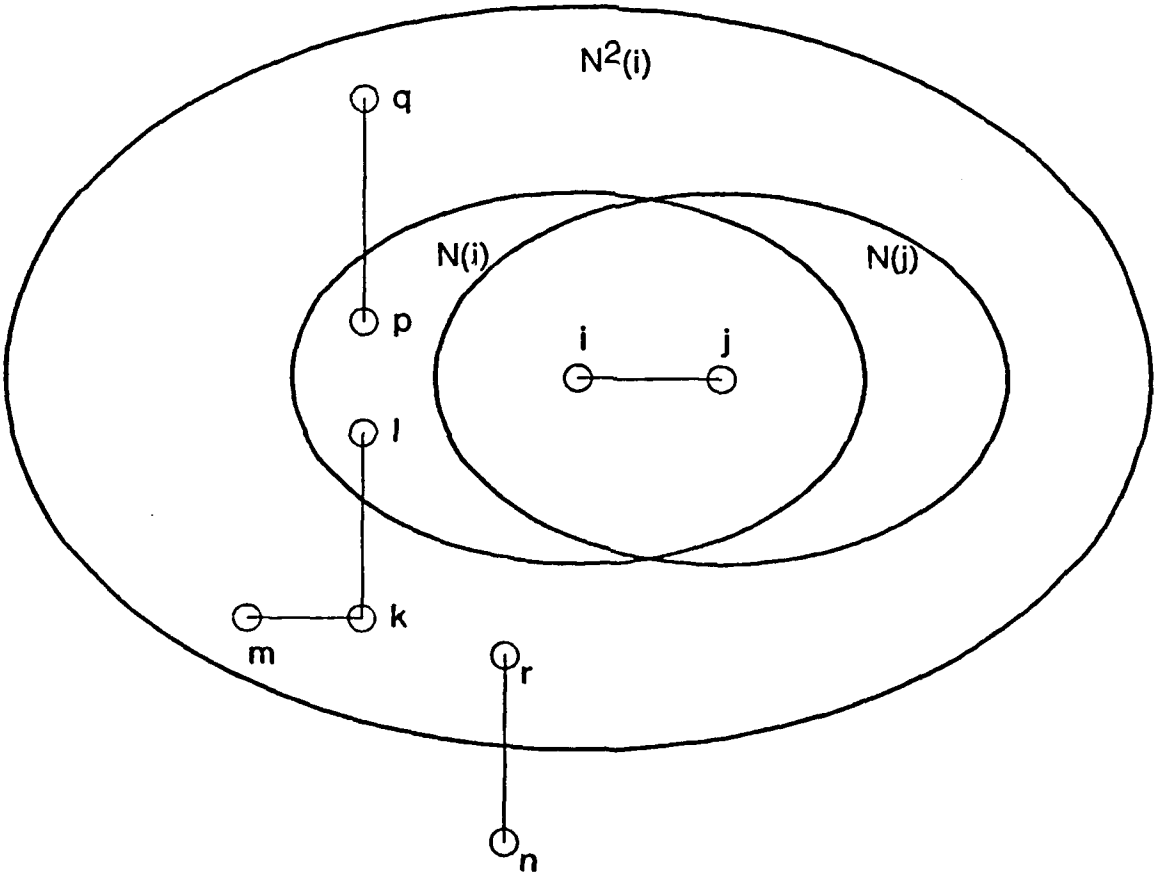

Fig. 2.1 Example of a set of transmissions in a multihop packet radio network.

received and before the entire packet is received, the time at which a node can first determine whether or not it is the intended immediate destination for a particular packet reception is at the end of the processing of the packet header. In HD-BTMA, a node operates as in C-BTMA until the header is processed, upon which time it operates as in RD-BTMA. (Alternatively one may conceive of a scheme in which the node operates as in CSMA until the header is processed prior to switching to RD-BTMA. We consider only the former scheme in this study.)

2.2.4 CASMA

As discussed above, depending on the particular situation, both C-BTMA and RD-BTMA have their shortcomings. In order to see how good a performance is achievable using random multiaccess protocols in narrowband multihop packet radio networks, we consider the following hypothetical *CASMA protocol*: *a node is* allowed to transmit only if it is not already transmitting, it is not already receiving a packet destined to it, no neighbor is receiving a packet destined to that neighbor, and its immediate destination is currently neither transmitting nor sensing carrier.

Clearly, as with RD-BTMA, without prior knowledge a node may not know if a particular transmission is destined to it or not. Hence, in practice, a hybrid form of this protocol would be used. In such a hybrid scheme, before the header is processed the protocol operates in one mode (such as C-BTMA), and after the header is processed it operates in the CASMA mode. In this study, in order to obtain a bound on performance, we consider only the idealized case where prior knowledge of the immediate destination is assumed. We assume that the activity signalling functions required by this protocol are implemented by means of a busy tone emitted by a node when it is receiving a packet destined to it, and the use of a carrier sense tone emitted by a node when it is transmitting or detecting carrier

due to a packet transmission not destined to it. In addition, it is required that the carrier sense tone be coded so that it allows unique identification of the node emitting it.

The essence of CASMA is that, given the state of the network in terms of ongoing transmissions, a scheduled transmission in the network is allowed to take place only if it has a high probability of not interfering with an ongoing transmission; furthermore, once allowed, the transmission has a high probability of success since all other nodes operate under the same protocol. (If the propagation delay is zero, then both probabilities would be unity.) Given that transmission $< i, j >$ has been undertaken, then after a vulnerable period equal to a two-hop propagation delay, all nodes in the set $\mathcal{N}^*(j)$ are blocked and all transmissions destined to nodes in $\mathcal{N}(i)$ are inhibited.

To illustrate the benefits gained by this scheme, we reexamine the various situations considered above and depicted in figure 2.1. Let nodes i, j, k, l, n and r, and the scheduled transmissions among them be as defined above. Transmission $< k, l >$ is inhibited due to l's carrier sense tone, and thus transmission $< n, r >$ can take place successfully (as in C-BTMA). Consider, on the other hand, transmission $< k, m >$; $< k, m >$ can take place successfully in CASMA, while it is blocked in C-BTMA; as for transmission $< n, r >$, in CASMA it is inhibited if $r \in \mathcal{N}(k)$, but is successful if $r \notin \mathcal{N}(k)$. Moreover, given an on-going transmission from node i to node j and all other nodes silent, any node $p \in \mathcal{N}(i) - \mathcal{N}(j)$ with a packet scheduled for transmission to a node $q \in \mathcal{N}^2(i) - \mathcal{N}(i)$ during the transmission $< i, j >$ will transmit successfully in CASMA; (note that node p is blocked in CSMA, C-BTMA, as well as RD-BTMA). Thus the action taken in CASMA in each situation is expected to lead to a performance that is superior to both that of RD-BTMA and C-BTMA. (We thus consider CASMA to provide an upper bound on the performance of the

other schemes.)

2.2.5 CDMA

In this case we assume that spread spectrum operation is in effect. Each node is assigned a unique code for reception. Nodes wishing to transmit to a particular node must use the code assigned to that node. A receiver that is idle 'locks onto' a packet with the appropriate code by correctly receiving a preamble appended in front of the transmitted packet. When reception of a packet is completed, the receiver becomes free again until another packet with the correct preamble is received. A node is allowed to transmit only if it is neither transmitting nor 'locked on'.

This is not the only way to make use of spread spectrum modulation. A number of access schemes that operate in the CDMA mode have recently been proposed and analyzed, such as Destination Code Sensing Multiple Access [37], and Channel Load Sensing [48]. In the former access scheme, the source node monitors the channel for activity using the code assigned to the destination of the packet being considered for transmission, prior to attempting to transmit. Transmission is inhibited if such activity is detected. In the latter scheme, the source node is assumed to be able to sense the number of transmissions on the channel. Transmission is inhibited if the node is either transmitting, 'locked on', or if the number of transmissions sensed exceeds a predetermined threshold. In this study, for the sake of simplicity, we consider that the presence of any number of overlapping transmissions on the channel does not affect the captured packet's reception. (Thus perfect capture is assumed). We also assume that preambles are of zero length. Note that in the numerical results obtained, when the scheduling rates were correctly set the number of overlapping transmissions was typically small, implying also that the probability of preamble overlap for non-zero length preambles would also be small. Thus the assumptions made here for CDMA turned out not to be overly restrictive.

2.3 Operational Protocols

It should be kept in mind that a primary aim of this dissertation is to investigate the performance of various channel access policies and buffer management schemes. Hence, in order to limit the scope, and to keep the simulation task manageable we have made certain simplifying assumptions below as a first step in achieving our goal. These assumptions are thought to have little impact on the comparative evaluation of the access schemes.

We assume that the acceptance rate of destinations is unlimited, and thus we do not consider end-to-end flow control schemes. We do consider, however, network access flow control, and make use of a particular scheme referred to as the input buffer limit (IBL) scheme [49]. Such a scheme restricts network access for new packets attempting to join a given queue by causing rejection of such new packets whenever the total number of packets (new and in transit) in that queue exceeds a certain number m. An alternative scheme, also considered here, consists of rejecting new packets when the total number of such packets exceeds a certain number m'.

The routing algorithm used throughout this work is a static shortest path scheme, with the path length based on number of hops. Where several shortest paths between a source-destination pair exist, all such paths are selected with equal likelihood.

We assume that acknowledgments are instantaneous and for free; that is, the sender learns of the success or failure of its transmission as soon as the packet has been completely received at the intended immediate destination, and the acquisition of this knowledge is assumed not to require any communication bandwidth. This assumption clearly will result in the absolute performance of the various channel access schemes being over estimated, as acknowledgments constitute some non-zero fraction of the overall channel traffic. The relative performance of the access schemes

should not, however, be affected. Refer to section 6.2 for a brief discussion of issues relating to hop-by-hop acknowledgments.

Contrary to the case of point-to-point networks where each outgoing link has its own transmitter, in a packet radio network, a radio unit possesses a single transmitter which is shared among all such links. Accordingly, we consider two intra-node queueing structures, namely,

(i) all packets at a node form a single queue,

(ii) packets are enqueued in separate queues, with each queue corresponding to a unique neighboring node.

In the latter case, the PRU's radio transmitter is shared by all queues of the PRU.

2.4 Traffic Model

We define the network input traffic requirement by the matrix $[\gamma_{ij}]$, where γ_{ij}, $i \neq j$, is the average number of packets per unit time offered at node i and ultimately destined for j. (We let $\gamma_{ii} = 0, \ \forall i$). The total traffic offered to the network is denoted by γ and is given by $\sum_{i=1}^{N} \sum_{j=1}^{N} \gamma_{ij}$. In this study, we consider two types of input traffic matrices, namely, the *uniform* traffic matrix in which γ_{ij} is constant for all pairs of nodes, and equal to $\gamma/N(N-1)$, and the *neighbors-only* traffic matrix in which $\gamma_{ij} = \gamma/dN$ if $h_{ij} = 1, \ i \neq j$, and $\gamma_{ij} = 0$ otherwise.

The generation of packets at a source node forms a random process considered here to be Poisson. We assume that packets are of constant length. Thus the transmission time of a packet is also a constant. We define a to be the ratio of the propagation delay to packet transmission time.

2.5 Packet Transmission Scheduling Algorithm

Associated with each node of the network, there is a random point process which defines the points in time when transmissions may be attempted. These points are referred to as *scheduling points*. At each scheduling point, the node executes the following algorithm:

(i) If the transmitter is already engaged in a transmission, or if all the queues of a node are empty, then the scheduling point is ignored.

(ii) Otherwise (the transmitter is free and one or more queues are not empty), the packet at the head of some non-empty queue is considered for transmission. The selection of the non-empty queue, whose head is to be considered for transmission, is random according to a uniform distribution. Clearly, actual transmission of the packet may or may not take place depending on the state of the network and the blocking property of the particular channel access protocol in use:

a) If the attempted transmission is inhibited, then the scheduling point is lost.

b) Otherwise the transmission is undertaken.

Once the packet has been transmitted successfully, then it is deleted from the head of its queue. In this study, the scheduling point process for node i is assumed to be Poisson (with rate G_i scheduling points per packet transmission time) for the ALOHA, CSMA, BTMA, CASMA and CDMA protocols, and Bernouilli (with probability G_i of transmitting in a slot) for the slotted ALOHA protocol. Note that it has been shown in [50] for single-hop slotted ALOHA networks, that the network performance is sensitive to the scheduling rate but not to the actual scheduling distribution. It is thought that the same insensitivity holds for other random access schemes in multihop networks.

2.6 Measures of System Performance

There are two primary measures of performance which we consider in this study, namely network throughput and packet delay. We define the throughput matrix $[S_{ij}]$ so that its (i,j)' th element S_{ij}, $1 \leq i,j \leq N$, is the average number of successful receptions at destination node j of packets that originated at source node i, per packet transmission time. The total end-to-end network throughput is

$$S = \sum_{i=1}^{N} \sum_{j=1}^{N} S_{ij}.$$

Another measure of throughput performance of interest in this study is the nodal throughput denoted by s_i, $1 \leq i \leq N$, where s_i is the average number of successful transmissions by node i to all its neighbors, per packet transmission time.

We define the delay matrix $[\delta_{ij}]$ so that its (i,j)'th element δ_{ij} specifies the average time a packet from source node i destined to ultimate destination node j spends in the system from the time it is accepted at node i until it is finally successfully received at node j, normalized to the packet transmission time. If, due to the input buffer limit control scheme, a newly generated packet is not accepted at a source node, then it is considered lost and does not contribute to the measured delay. The average packet delay over the entire network is given by

$$D = \sum_{i=1}^{N} \sum_{j=1}^{N} \frac{S_{ij}}{S} \delta_{ij}.$$

We also consider the distribution of buffer occupancy per queue. For a given queue i, let L_i denote the number of new and transit packets in the queue in steady state. Let $q \in [0,1]$. We define a buffer occupancy qth quantile to be an integer n_q such that $\Pr[L_i > n_q] \leq 1 - q$.

Chapter 3

Regular Networks with Infinite Buffering

3.1 Introduction

In this and the following chapter, we have considered networks in which the structure, traffic requirement and operational algorithms are such that all nodes perform in a statistically identical manner and all links carry the same traffic load. Furthermore, in this chapter, it is assumed that at every PRU buffer resources are unlimited and that there exists a separate queue corresponding to each neighboring PRU with a First Come First Served (FCFS) service discipline at each queue. The performance of various existing channel access schemes, namely, ALOHA, CSMA, CDMA, and BTMA, and the new scheme (CASMA) is studied. Network throughput and packet delay are evaluated, as well as the effects on performance of the nodal transmission scheduling rate, the ratio of propagation delay to packet transmission time, and to some extent network access flow control.

The remainder of this chapter consists of a description of the structure of the

regular networks under consideration in section 3.2, numerical results in section 3.3, and a chapter summary in section 3.4.

3.2 Network Structure

Several classes of regular topologies are considered: closed planar topologies, regular (Platonic) solids and ring topologies. (See figures 3.1 and 3.2). The two closed planar topologies considered are the square lattice with number of nodes N equal to 25 and the triangular lattice with N equal to 36. The regular solids are symmetric three-dimensional structures with N varying from 4 to 20, and nodal degree, denoted by d, varying from 3 to 5. These structures are chosen so as to represent planar networks of different nodal degree that are totally symmetric and that do not present special boundary conditions. For example, note that the dodecahedron is equivalent to a closed hexagonal tiling with $N = 20$. Ring topologies with $d = 2$ (referred to as simple rings) approximate a linear string of repeaters in a packet radio network. In this chapter, we also consider 'multiconnected' rings with nodal degree $d > 2$, as shown in figure 3.1. Multiconnected rings represent a string of repeaters where the transmission radius extends beyond the nearest neighbors. They are simple topologies in which the number of nodes N and the nodal degree d can to a large extent be arbitrarily chosen, thus enabling us to experiment with the effects of N and d on the performance of the channel access schemes. In all regular solid topologies, the same propagation delay exists between all pairs of adjacent nodes. This is also assumed to be the case in the simulation model for closed planar and ring topologies (simple and multiconnected).

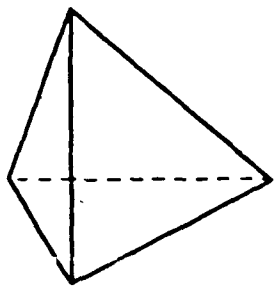

TETRAHEDRON
$N = 4 \quad d = 3$

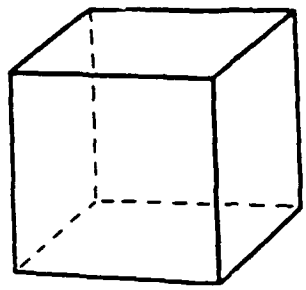

CUBE
$N = 8 \quad d = 3$

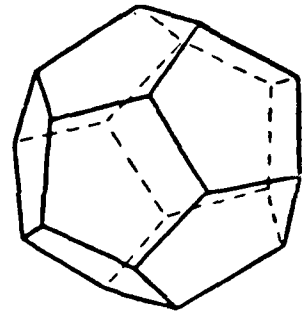

DODECAHEDRON
$N = 20 \quad d = 3$

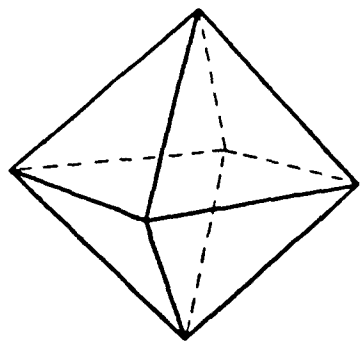

OCTAHEDRON
$N = 6 \quad d = 4$

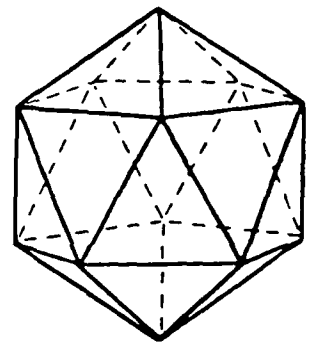

ICOSAHEDRON
$N = 12 \quad d = 5$

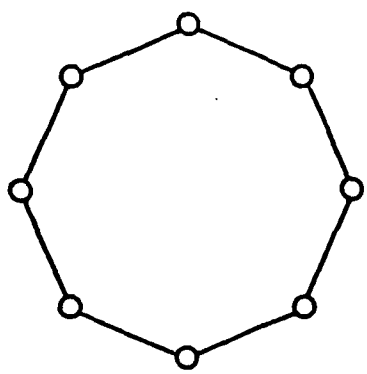

RING
$d = 2$

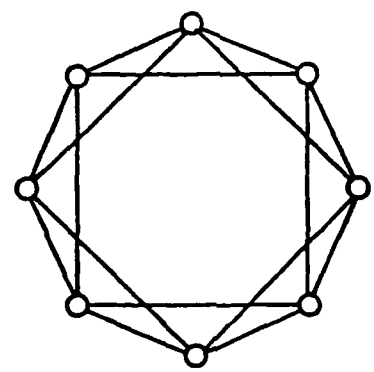

MULTICONNECTED RING
$d = 4$

Fig. 3.1 Regular solid and ring topologies.

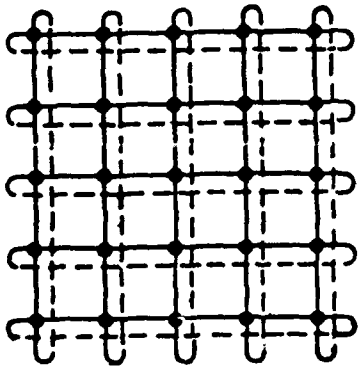

CLOSED SQUARE LATTICE ($N = 25,\ d = 4$)

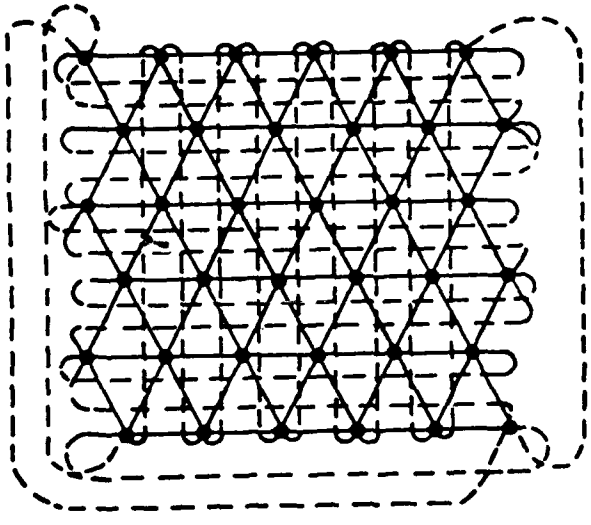

CLOSED TRIANGULAR LATTICE ($N = 36,\ d = 6$)

Fig. 3.2 Closed planar topologies.

3.3 Numerical Results

Consider a packet radio network according to the model described in chapter 2 and section 3.1. The topology may be any of the regular structures introduced with the exception of multiconnected rings. The latter will be examined in more detail in subsection 3.2.3. Due to the assumptions of uniformity in the offered input traffic matrix, and the balanced shortest path routing, all nodes behave in a statistically identical manner*. Hence we may consider all nodal scheduling rates to have the same value denoted by G. Moreover, all nodes have equal nodal throughput s, all source-destination pairs have equal end-to-end throughput, (which is $S/N(N-1)$ in the case of the uniform traffic matrix, and $S/Nd = s/d$ in the case of the neighbors-only traffic matrix), and all paths of equal length have identical end-to-end average packet delay. Note that $S = Ns/\overline{n}$, where $\overline{n}$ denotes the mean number of hops between a source and a destination.

Let $S(\gamma, m, G)$ denote the total end-to-end throughput for γ, m, and G. Assume $m = \infty$ (i.e., no external packet is ever rejected), and heavy-traffic conditions (i.e., $\gamma = \infty$). Under these conditions, given the (regular) network structures under consideration and the random nature of the access schemes, it is guaranteed that all queues in the network will always be non-empty. Since the number of nodes in the network is finite and no incoming transit packet at a node is ever rejected (due to the infinite buffer assumption), it is intuitively clear that the mean service time X for a packet at the head of a queue, (defined as the expected time from when a packet moves to the head of the queue until it is successfully transmitted to its immediate destination) is finite and constant over time, and entirely determined by the network topology, the access scheme, and the scheduling rate G. This also means that the link throughput (i.e., the fraction of time that a link is engaged

*For the closed triangular lattice, the neighbors-only traffic matrix is assumed.

in successful transmissions) is nonzero and equal to $1/X$ packets per second. Let $C(G) \triangleq \lim_{\gamma \to \infty} S(\gamma, \infty, G)$. $C(G)$ is the total end-to-end network throughput under heavy-traffic for the scheduling rate G, and is called the *capacity* of the network at scheduling rate G. We define nodal capacity in a similar fashion. Let $s(\gamma, m, G)$ denote the nodal throughput for γ, m and G, and define the nodal capacity as $c(G) \triangleq \lim_{\gamma \to \infty} s(\gamma, \infty, G)$. As with the network and nodal throughput, $C(G)$ and $c(G)$ are related according to $C(G) = Nc(G)/\overline{n}$. With $m = \infty$, it is clear that for $\gamma \leq C(G)$ we must have $S(\gamma, \infty, G) = \gamma$, and for $\gamma > C(G)$, $S(\gamma, \infty, G) = C(G)$. Such expectations are entirely confirmed by simulation, as will be shown in the following subsection. Note that $c(G)$ is the same for both traffic matrices considered in this study, while $C(G)$ differs due to the differences in $\overline{n}$.

As a first step in the discussion of the numerical results, a representative example network consisting of the simple six node ring topology together with the C-BTMA access scheme is selected for an in-depth study with the purpose of identifying explicitly the effect of the scheduling rate and the input flow control on throughput and delay performance. As all other network topology and access scheme combinations (again with the exception of multiconnected rings) exhibit similar behaviour, we limit the remainder of the section to a comparison of the performance of the various access schemes in the different networks, on the basis of their capacity and throughput-delay characteristics.

3.3.1 A Representative Example

The example considered here is a simple six node ring with $a = 0.01$ operating under C-BTMA with a uniform offered traffic matrix and balanced shortest path routing. In figure 3.3 we plot the network throughput $S(\gamma, m, G)$ versus γ with m set to 50 (a somewhat arbitrary but large value). The difference between the

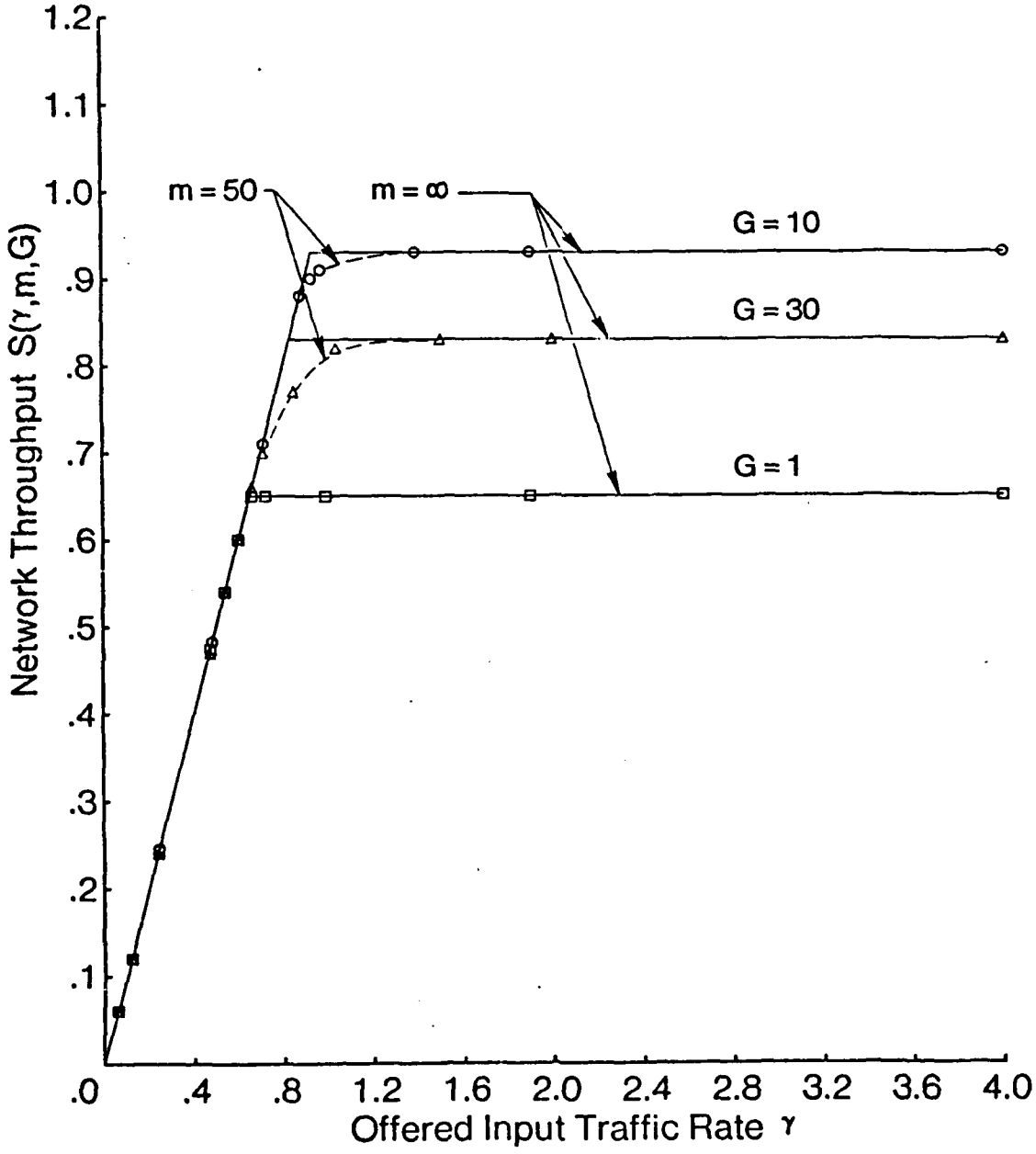

Fig. 3.3 Network throughput versus offered input traffic rate in a simple six node ring network, under the C-BTMA protocol, with a uniform traffic matrix and $a = 0.01$.

simulation points and the expected curves in the vicinity of $\gamma = C(G)$ is due to the finite value used for m, which causes some new packets to be rejected. Indeed, the probability $P_b(\gamma, m, G)$ of an input packet being rejected is nonzero for $m < \infty$, and increases for decreasing values of m. The larger m is, the closer the simulation points are to the expected curve ($m = \infty$) as can be seen in figure 3.4. We note, however, that regardless of the value of m, we have

$$\lim_{\gamma \to \infty} S(\gamma, m, G) = C(G).$$

The results shown in figures 3.3 and 3.4 correspond to the IBL scheme where a new packet is rejected if the total number of packets in the queue (new and transit) exceeds m. The alternative scheme (as described in section 2.2) considers that a new packet offered to a queue is rejected if the number of new packets in that queue reaches m'. (Transit packets are again not affected, since we have assumed infinite buffers at each queue). In figure 3.5 we show S versus γ for various values of m'. For equal values of m and m', this IBL control scheme clearly achieves a higher throughput than the former scheme, since the blocking probability is smaller; in all other respects the behaviour is the same. We also have

$$\lim_{\gamma \to \infty} S(\gamma, m', G) = C(G)$$

where $C(G)$ is the same in both IBL schemes. In the remainder of this chapter, we shall consider only the first IBL control scheme.

The scheduling rate G has an important effect on the network capacity $C(G)$. The latter is maximized for a particular value of G, denoted by G^*. $C(G^*)$ is referred to as the *optimum network capacity*. The effect of G is illustrated in figure 3.6 where we plot $C(G)$ versus G. To the left of G^*, $C(G)$ is limited by the small value of G (and hence the large intervals between scheduling points); to the right of G^*,

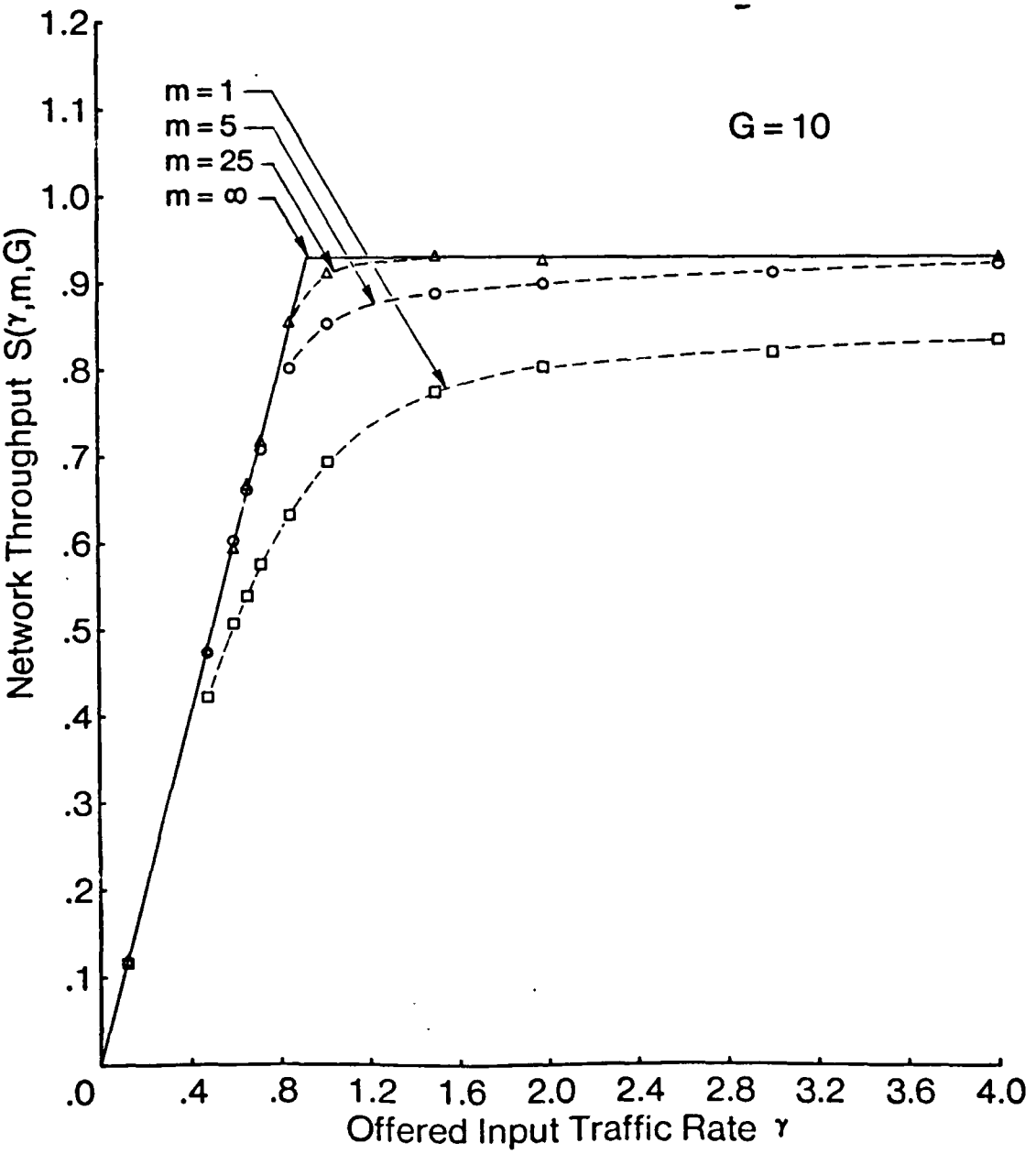

Fig. 3.4 Network throughput versus offered input traffic rate, for various input buffer limits m, (with rejection of new packets when new and transit packets exceed m), in a simple six node ring network under the C-BTMA protocol, with a uniform traffic matrix, $a = 0.01$ and $G = 10$.

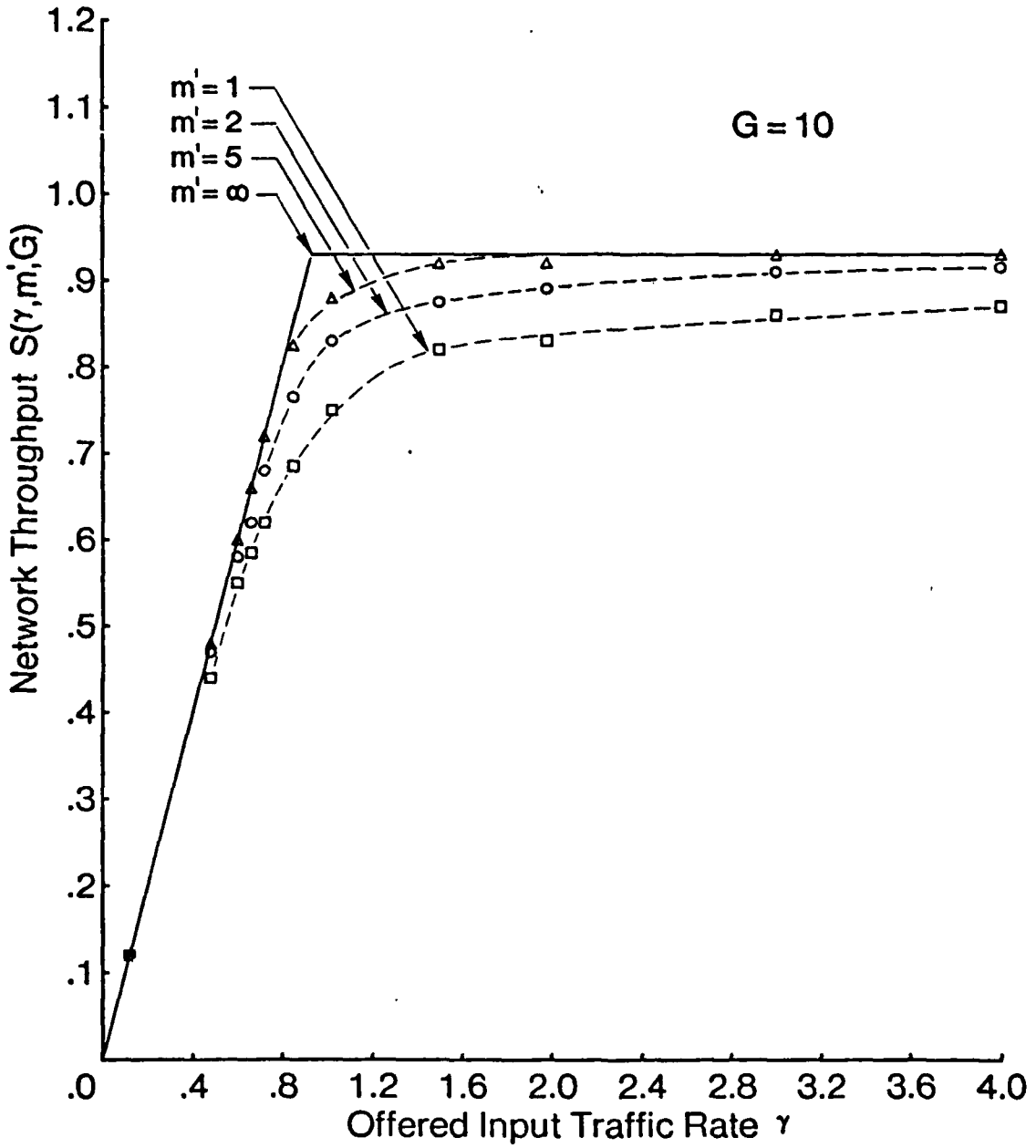

Fig. 3.5 Network throughput versus offered input traffic rate, for various input buffer limits m', (with rejection of new packets when m' new packets are already present), in a simple six node ring network under the C-BTMA protocol, with a uniform traffic matrix, $a = 0.01$ and $G = 10$.

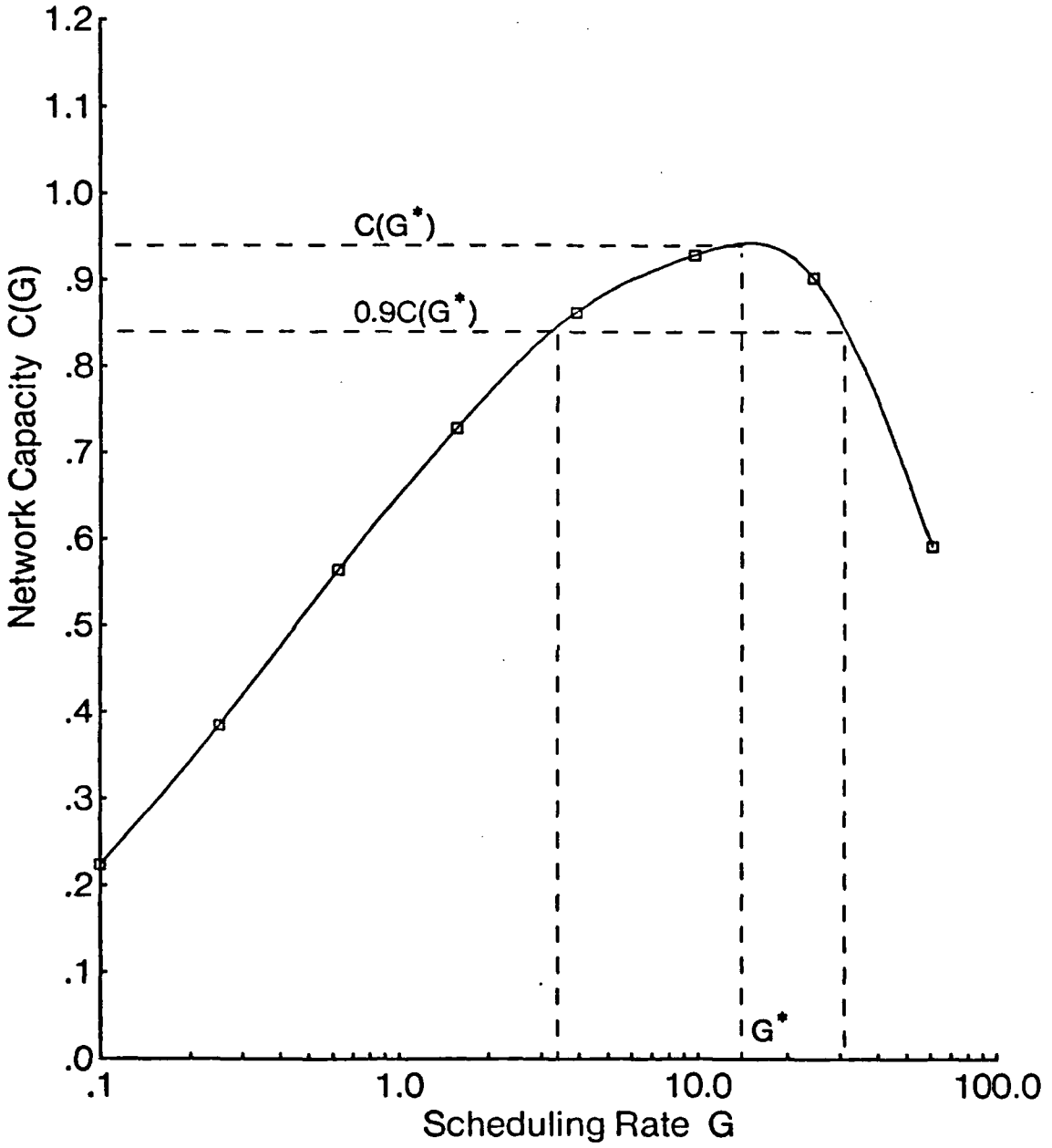

Fig. 3.6 Network capacity versus scheduling rate in a simple six node ring network, under the C-BTMA protocol, with a uniform traffic matrix and $a = 0.01$.

$C(G)$ is limited by an increase in the rate of collisions. (We note here that the determination of $C(G)$ by simulation is obtained by guaranteeing that all queues are always non-empty, which is simply achieved by considering the first IBL scheme with $m = 1$ and $\gamma = \infty$). Note that the variation of $C(G)$ with respect to G is small in the vicinity of G^* implying a degree of insensitivity to G. For instance, we see in figure 3.6 that $C(G) \geq 0.9C(G^*)$ for $0.2G^* \leq G \leq 2G^*$.

We now examine the network packet delay D. As defined in section 3.4, D is the average delay of a packet from when it is admitted to the network, until it is delivered to its ultimate destination. It is a function of γ, m and G, which we denote by $D(\gamma, m, G)$. In figure 3.7 we plot $D(\gamma, m, G)$ versus γ for various values of m and $G = 10$. Recall that when m is finite, all rejected (external) packets do not contribute to the calculation of $D(\gamma, m, G)$. Accordingly, it is not surprising to see the network delay increase with γ, but level off at a limit which is a function of m. In practice, data packets that are blocked at the network input are stored by the host attached to the local PRU, (thus undergoing a delay), and are resubmitted at a later time. Thus a more reasonable measure of the total packet delay is obtained for a value of $m = \infty$, where new packets are accepted without limitation. As expected, for $m = \infty$, the delay becomes unbounded as $\gamma \rightarrow C(G)$.

The case $\gamma = \infty$, $m = 1$ is an interesting one to examine more closely. By setting $m = 1$, given the IBL scheme under consideration, no new packet is admitted to a queue until that queue empties. Furthermore as soon as the queue empties, a new external arrival is created ($\gamma = \infty$). This represents the situation where traffic is heavy, (hosts have infinite queues of packets to be offered to the network,) but priority service is given to transit packets in a first-come-first-served (FCFS) order. $D(\infty, 1, G)$ represents the network delay of packets that are admitted to the network. In figure 3.8, we plot the network delay for 1-, 2- and 3-hop traffic,

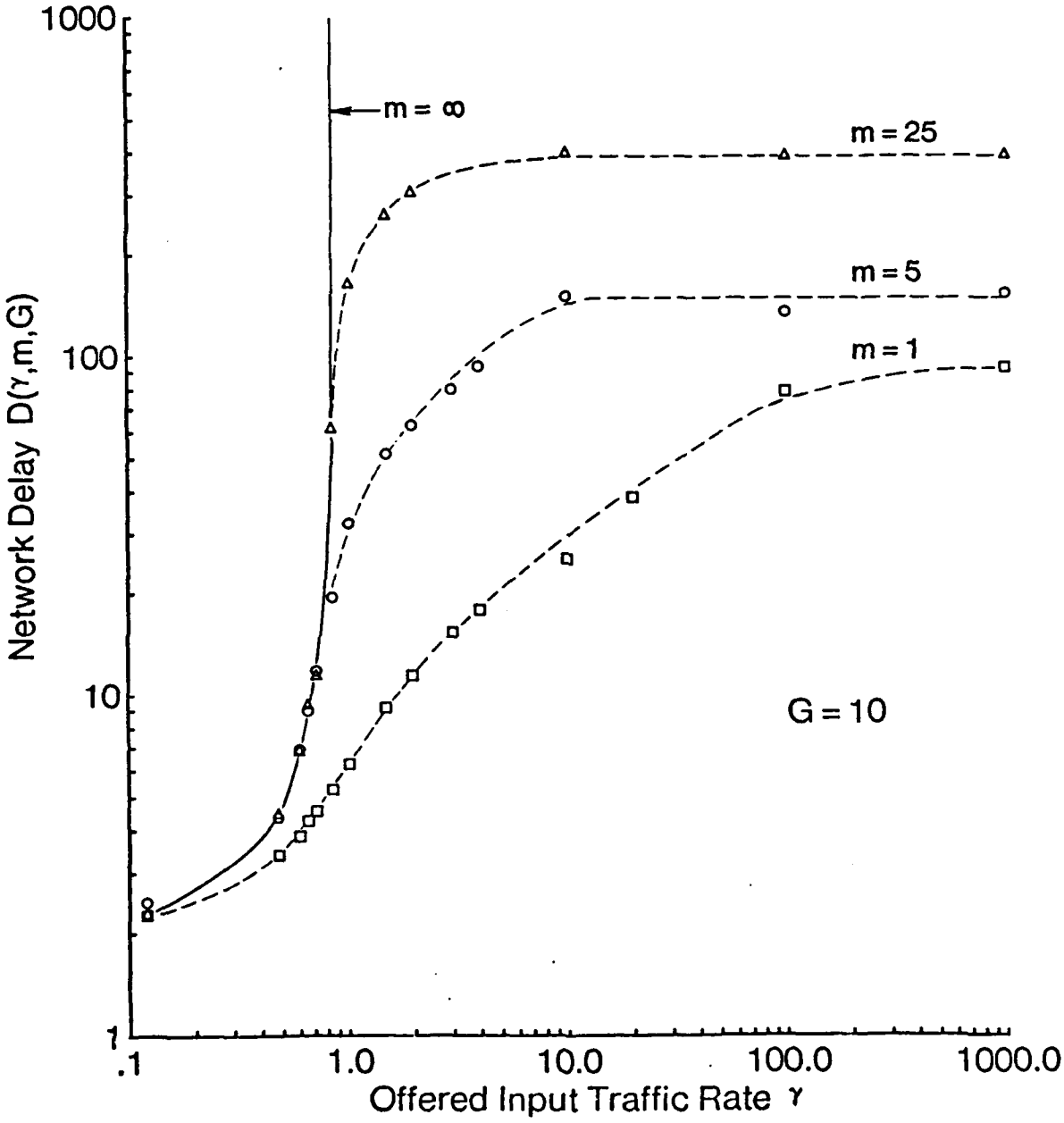

Fig. 3.7 Network delay versus offered input traffic rate, for various input buffer limits, in a simple six node ring network under the C-BTMA protocol, with a uniform traffic matrix, $a = 0.01$ and $G = 10$.

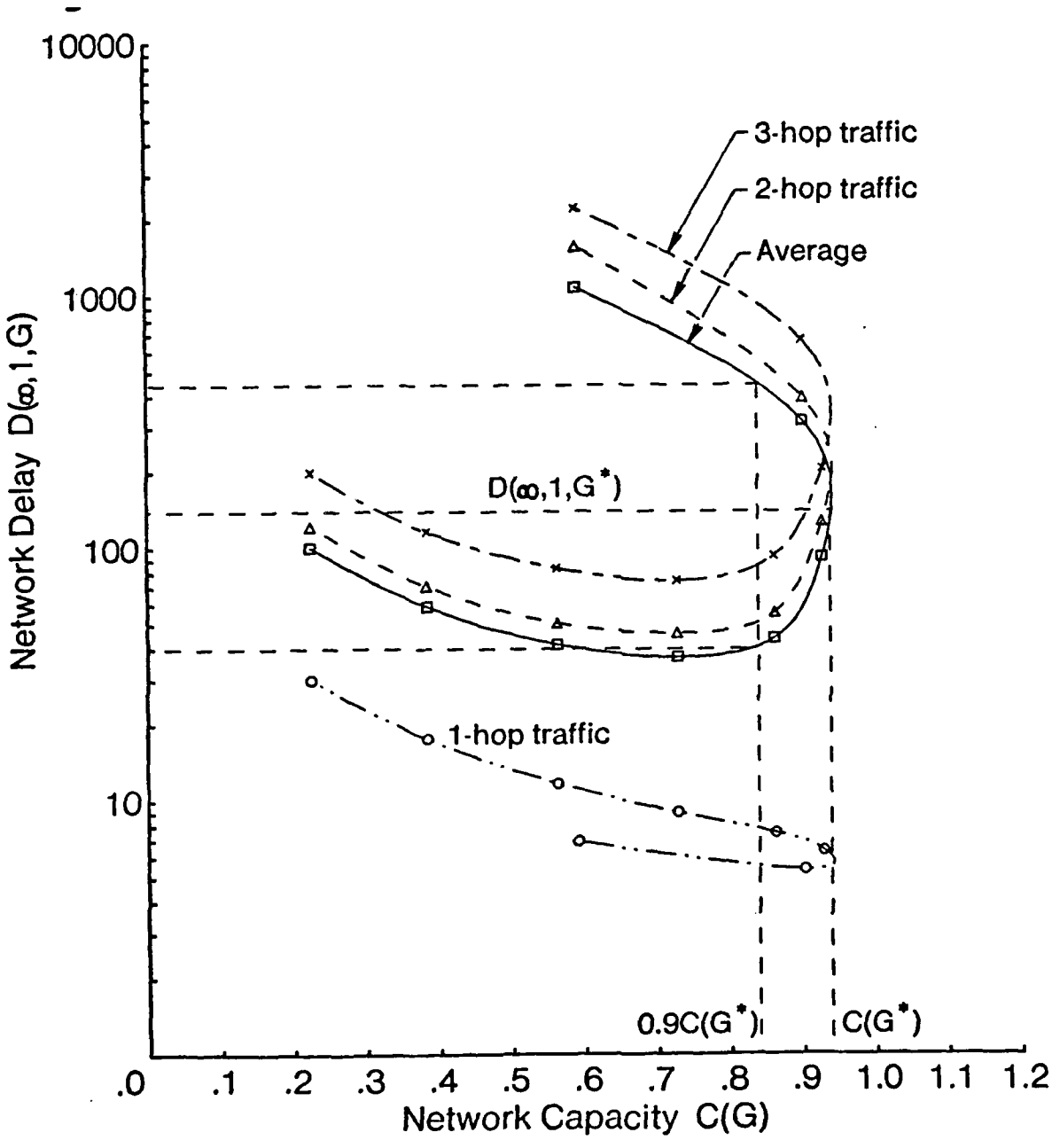

Fig. 3.8 Network delay versus network capacity in a simple six node ring network, under the C-BTMA protocol, with a uniform traffic matrix, $a = 0.01$, $\gamma = \infty$ and $m = 1$.

as well as the average delay over all traffic ($D(\infty, 1, \gamma)$) versus $C(G)$. Observe that 1-hop traffic does not pass through intermediate nodes, while 2-hop traffic is forwarded through 1 intermediate queue, and 3-hop traffic through 2 intermediate queues. As before, let the service time of a packet be the time from when the packet first reaches the head of its queue, until the time it is successfully received by its intended immediate destination. Then, the 1-hop delay consists of 1 service time, the 2-hop delay consists of 2 service times and 1 queueing delay, and the 3-hop delay consists of 3 service times and 2 queueing delays. $D(\infty, 1, G)$ is observed to first decrease with $C(G)$, and then increase as $C(G)$ increases. The explanation for this is that low values of $C(G)$ correspond to low values of G, and for low values of G packets remain at the server for long periods of time due to large scheduling delays. However, as G and $C(G)$ increase, the scheduling delay decreases, which tends to decrease the network delay. As G increases further however, the system begins to operate close to capacity, and hence queueing delays begin to increase significantly, and in addition, the probability of collision and hence retransmission also increases, causing a sharp increase in network delay, and ultimately a reduction in $C(G)$. We observe that in the vicinity of network capacity $C(G^*)$, network delay is more sensitive to the scheduling rate than is the case for throughput; (an effect similar to that observed for fully connected networks [50]): we see that approximately $0.4D(\infty, 1, G^*) \leq D(\infty, 1, G) \leq 4D(\infty, 1, G^*)$ for $C(G) \geq 0.9G^*$ which corresponds to $0.2G^* \leq G \leq 2G^*$.

The buffer occupancy statistics for the case of $\gamma = \infty$ and $m = 1$ represent the buffer requirement for *transit* packets, (and potentially a single external packet,) under heavy traffic conditions. In figure 3.9 we plot the qth quantiles of buffer occupancy n_q versus capacity $C(G)$ for different probabilities q of exceeding n_q buffers. As $C(G)$ approaches $C(G^*)$, the qth quantiles of buffer occupancy n_q increase with $C(G)$, indicating that more and more buffers are being occupied by

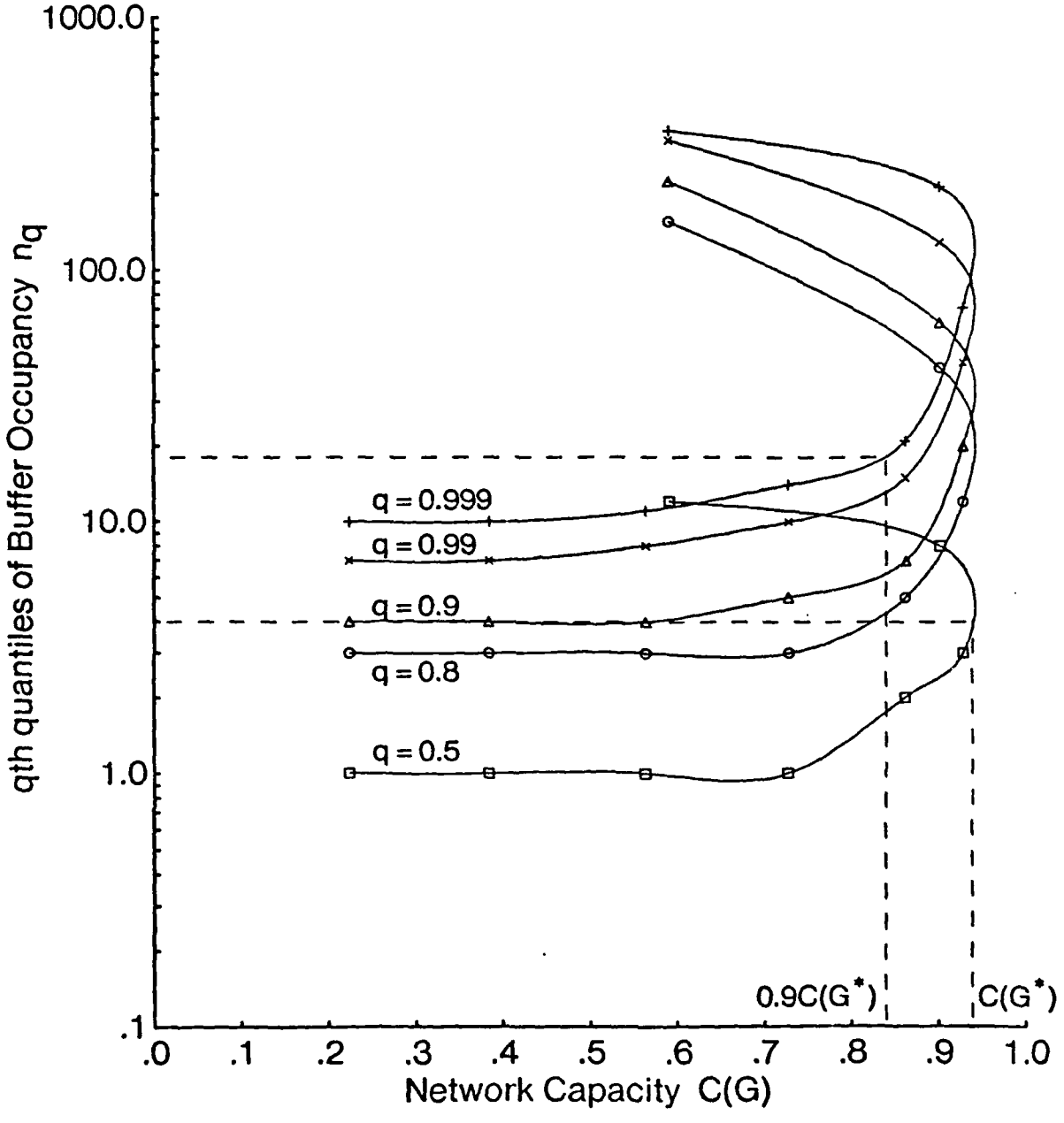

Fig. 3.9 qth quantiles of buffer occupancy versus network capacity in a simple six node ring network, under the C-BTMA protocol, with a uniform traffic matrix, $a = 0.01$ and $m = 1$.

packets in transit. The curves of figure 3.9 can be used as a guide for the selection of a finite transit buffer size. For example, at a throughput $S = 0.9C(G^*)$, the probability q that the buffer occupancy exceeds 20 is less than 0.001, implying that a buffer size of 20 would be a safe choice as far as achieving $0.9C(G^*)$ goes.

The previous discussion has focused on a particular access scheme (C-BTMA) and a particular topology (a simple six node ring). For other network and access scheme combinations similar behaviour is observed in general, except for certain quantitative differences. For example, in the simple six node ring, the degree of sensitivity of the network capacity $C(G)$ to the scheduling rate G in the vicinity of G^* differs according to the access scheme. ALOHA and CSMA exhibit the highest sensitivity, while CDMA, CASMA, and the BTMA schemes exhibit the lowest sensitivity. The reason for the greater robustness of BTMA and CASMA is that, given that a node has begun to receive a packet, the reception of this packet may be interfered with only by other transmissions that were initiated during the vulnerable period. The robustness of CDMA is due to the fact that once a reception is initiated, given the assumption of perfect capture it cannot be subsequently interfered with. The ALOHA and CSMA schemes are less robust due to the fact that a packet being received is vulnerable to interference over its entire period of reception. Note that, in ALOHA and CSMA a certain degree of insensitivity to G is still evident since, in the simple six node ring network for example, a factor of 2 or 3 variation in G leads to a variation in $C(G)$ of $\leq 10\%$. Note further that the robustness of BTMA and CASMA is expected to diminish as a increases.

In the remainder of this chapter, the performance of the various access schemes is studied and compared in the regular networks under consideration, in terms of their capacity and throughput-delay characteristics.

3.3.2 Nodal Capacity

The optimum network capacity $C(G^*)$ is the most important single parameter that characterizes the performance of a network under a given set of operational protocols. Not only does it give the maximum throughput that a network can support, but in addition it is the most determining factor in the throughput-delay characteristic of a network; indeed, the delay in a network increases from $\bar{n}$ at a throughput approaching zero, to infinity at an asymptote determined by the network capacity. However, since $C(G^*)$ depends on the type of traffic matrix assumed (either uniform or neighbors-only), in comparing the performance of the various channel access schemes, we focus on the optimum nodal capacity $c(G^*)$. The latter is the same for all traffic matrices that induce balanced link traffic; it is the maximum rate at which a node may transmit successfully over the channel, and hence is a more intrinsic measure of the performance of the access schemes.

For certain networks and access schemes, analyses leading to $c(G^*)$ or $C(G^*)$ have been performed and used to derive numerical results and validate the simulation. These cases consist of (i) the ALOHA schemes in arbitrary multihop topologies, (ii) CSMA, C-BTMA and CASMA in fully connected topologies, and (iii) C-BTMA and CASMA in simple ring topologies for $a = 0$.

(i) **ALOHA schemes in arbitrary multihop topologies.** For the pure ALOHA scheme, we have adapted the approach of [33], where the analysis assumed exponential packet lengths, to the case of fixed packet lengths, while for slotted ALOHA the approach of [20] is used (refer to appendix 1). For the regular topologies considered here with a uniform or neighbors-only traffic matrix, the optimum nodal capacities are expressed as

$$c_{pure\ ALOHA}(G^*) = \left(\sqrt{\frac{d}{d+1}}\right)^{d+1} \frac{\sqrt{d+1}-\sqrt{d}}{\sqrt{d}} e^{-(\sqrt{d^2+d}-d)}, \qquad (3.1)$$

$$c_{slotted\ ALOHA}(G^*) = \frac{1}{(1+a)(d+1)}\left(\frac{d}{d+1}\right)^d. \tag{3.2}$$

Note that the nodal capacity for the ALOHA schemes is only dependent on d and is independent of N. Note also that, for the pure ALOHA scheme, the nodal capacity is not a function of the parameter a; (in fact, of the access schemes under study, it is the only one to exhibit such an independence). Table 3.1 exhibits the optimum nodal capacity $c(G^*)$ for various network topologies considered and $a = 0$, as well as and the optimum network capacity $C(G^*)$ for uniform traffic.

				Pure ALOHA		Slotted ALOHA	
N	d	*Topology*	$\bar{n}$	$c(G^*)$	$C(G^*)$	$c(G^*)$	$C(G^*)$
6	2	Ring	1.80	.078	.260	.148	.494
12	2	Ring	3.27	.078	.286	.148	.543
4	3	Tetrahedron	1.00	.055	.220	.106	.422
8	3	Cube	1.71	.055	.257	.106	.495
20	3	Dodecahedron	2.63	.055	.418	.106	.806
6	4	Octahedron	1.20	.042	.210	.082	.410
25	4	Closed Lattice	2.50	.042	.336	.082	.656
12	5	Icosahedron	1.64	.034	.249	.067	.491

Table 3.1. Network and nodal capacities in regular topologies for uniform traffic requirement for pure and slotted ALOHA protocols, with $a = 0$.

(ii) **CSMA, C-BTMA and CASMA in fully connected topologies.** A simple adaptation of the analysis in [5] to a fully connected network with N identical nodes gives the following approximate expressions for the nodal capacities (refer to appendix 2):

$$c_{CSMA}(G) = \frac{(N-1)Ge^{-a(N-1)G}}{(1+2a)N(N-1)G + Ne^{-a(N-1)G} - 1}, \tag{3.3}$$

$$c_{C-BTMA}(G) = \frac{(N-1)Ge^{-a(N-1)G}}{(1+3a)N(N-1)G + Ne^{-a(N-1)G} - 1}, \tag{3.4}$$

$$c_{CASMA}(G) = \frac{(N-1)(N-2)Ge^{-aG(2N-3)}}{(N-1)[N(N-2)(1+4a)G - 2] + Ne^{-aG(N-2)} + N(N-2)e^{-aG(2N-3)}}. \tag{3.5}$$

The difference between the results for CSMA and C-BTMA is due to the fact that, in the latter case, the period of time during which nodes are blocked is extended by an additional time period a, due to the presence of busy-tone. The difference between the results for CASMA and C-BTMA is due to the fact that, in CASMA, once a transmission is initiated, the intended receiver is blocked from transmitting after a time units, while the remaining $N-2$ nodes are blocked after $2a$ time units (when the busy and carrier sense tones are detected). This implies that the period during which a transmission is vulnerable to collisions is increased by a time units over that of CSMA and C-BTMA; furthermore, the period during which nodes are blocked is extended by a time units over that of C-BTMA. Both effects lead to a decrease in the achievable capacity. Note that the difference in performance between all three schemes is rather slight for a small, but becomes more noticeable for a large.

(iii) **Simple N-node ring networks with $a = 0$.** When $a = 0$, C-BTMA and CASMA are conflict-free; hence $G^* = \infty$. The capacity is then simply determined by the maximum number of transmissions that can concurrently exist in the network.

C-BTMA: The maximum number of concurrent transmissions in the network is achieved when one in every three nodes is transmitting and the intermediate ones are blocked, and is simply expressed as $\lfloor N/3 \rfloor$. The nodal capacity is obtained by normalizing to the number of nodes and is expressed as*

$$c(\infty) = \frac{1}{N}\left\lfloor \frac{N}{3} \right\rfloor. \tag{3.6}$$

CASMA: The maximum number of concurrent transmissions in the network is achieved by minimizing the number of *unused* nodes (i.e., neither transmitting nor receiving). Given the CASMA protocol, it is clear that this condition corresponds to the situation whereby a transmitting node is adjacent to its destination and another transmitting node; likewise, a receiving node is adjacent to its sender and another receiving node. Furthermore, the number of unused nodes will vary between 0 and 2 depending on the value of N. The maximum number of concurrent transmissions is expressed as

$$\begin{cases} 1, & N = 2,\ 3 \\ 2k & N = 4k + l,\ \ l = 0, 1, 2;\ \ k \geq 1, \\ 2k + 1 & N = 4k + 3\ \ k \geq 1. \end{cases}$$

The nodal capacity is obtained by normalizing to the number of nodes and is expressed as

$$c(\infty) = \frac{1}{N} \begin{cases} 1, & N = 2, 3 \\ 2k & N = 4k + l,\ \ l = 0, 1, 2;\ \ k \geq 1, \\ 2k + 1 & N = 4k + 3\ \ k \geq 1. \end{cases} \tag{3.7}$$

Using simulation and analysis whenever possible, we plot in figures 3.10 to 3.18 the optimum nodal capacity $c(G^*)$ versus a for the various schemes in the regular topologies under consideration. We note that for all schemes but pure ALOHA (which is independent of a), the nodal capacity decreases as a increases, due to the fact that the information obtained by channel sensing is increasingly out of

*We note here that, when N is a multiple of 3 and $G^* = \infty$, the maximum number of concurrent transmissions, $N/3$, is achieved by a subset of $N/3$ nodes equally spaced. The nodes in this subset remain the same over time, each achieving a nodal capacity equal to 1, while all others achieve a nodal capacity of 0. We shall nevertheless consider that in this case $c(\infty)$ exists and is equal to 1/3. For G finite but large, a nodal capacity close to 1/3 is truly attained by all nodes. However in this case, there may be long periods of time during which the same subset of $N/3$ nodes transmit before another subset of nodes gains access to the channel. Note that in CASMA, a similar effect occurs (for N a multiple of 4), but with respect to subsets of transmissions.

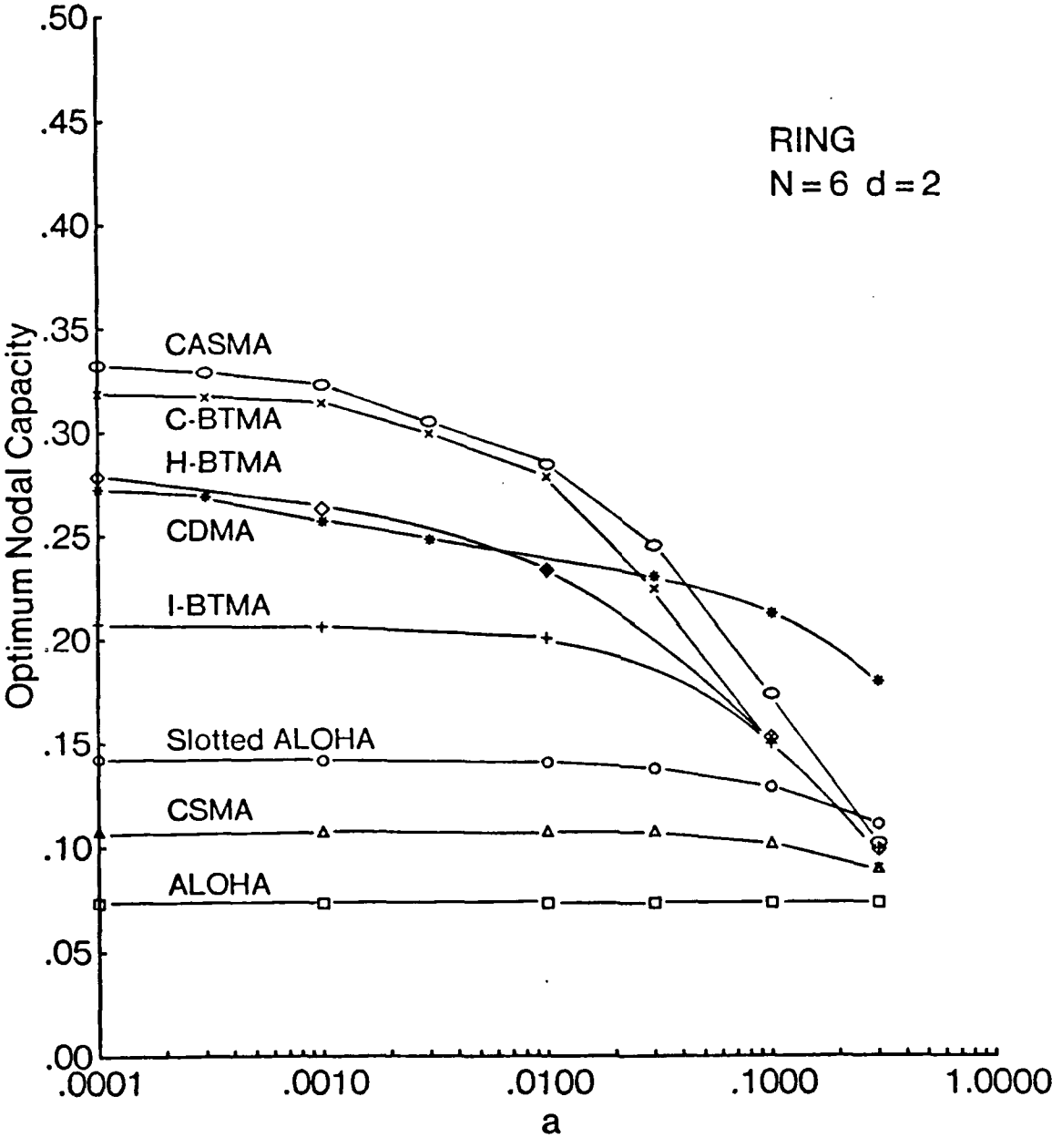

Fig. 3.10 Optimum nodal capacity versus a for the simple six node ring topology.

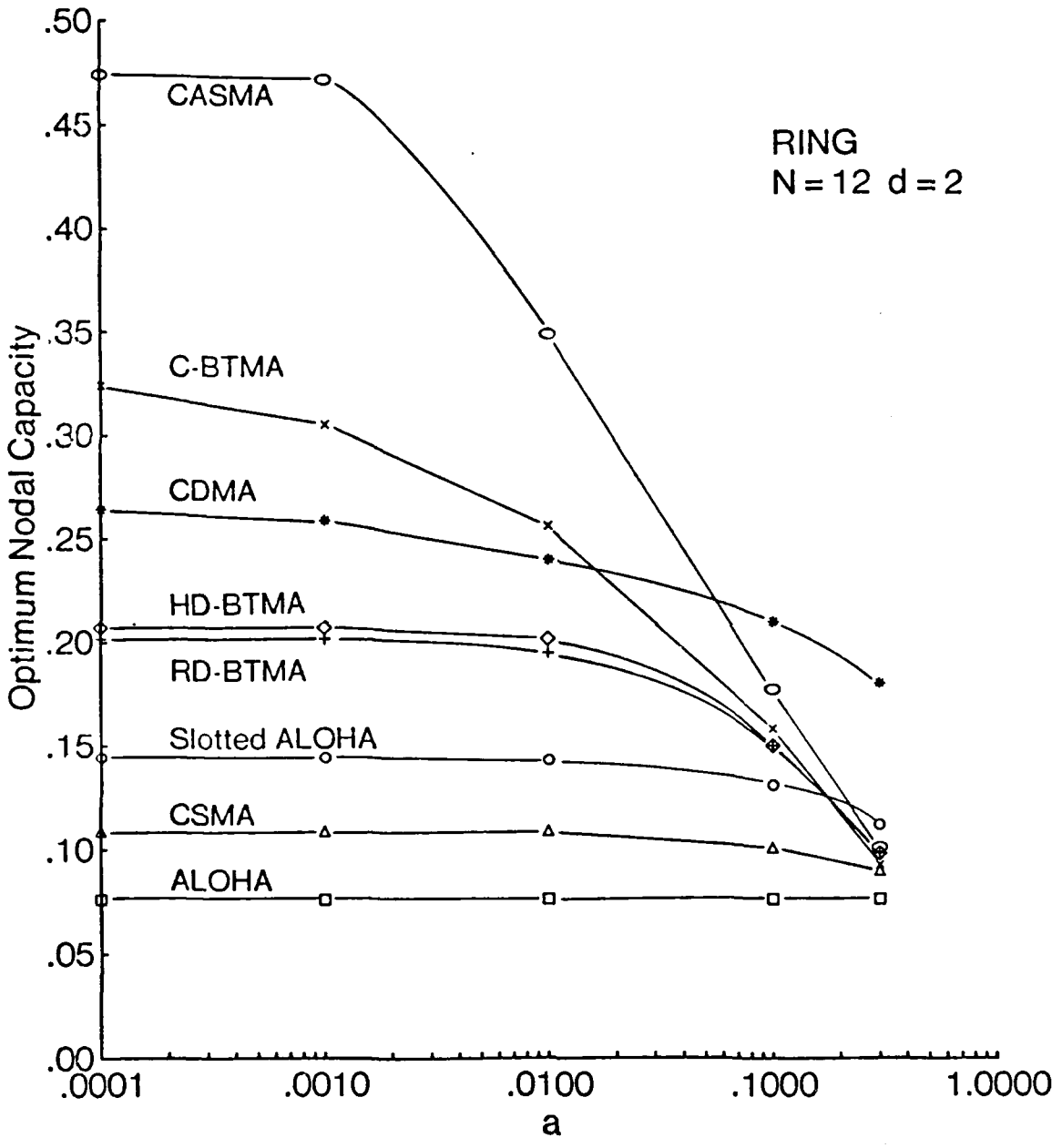

Fig. 3.11 Optimum nodal capacity versus a for the simple twelve node ring topology.

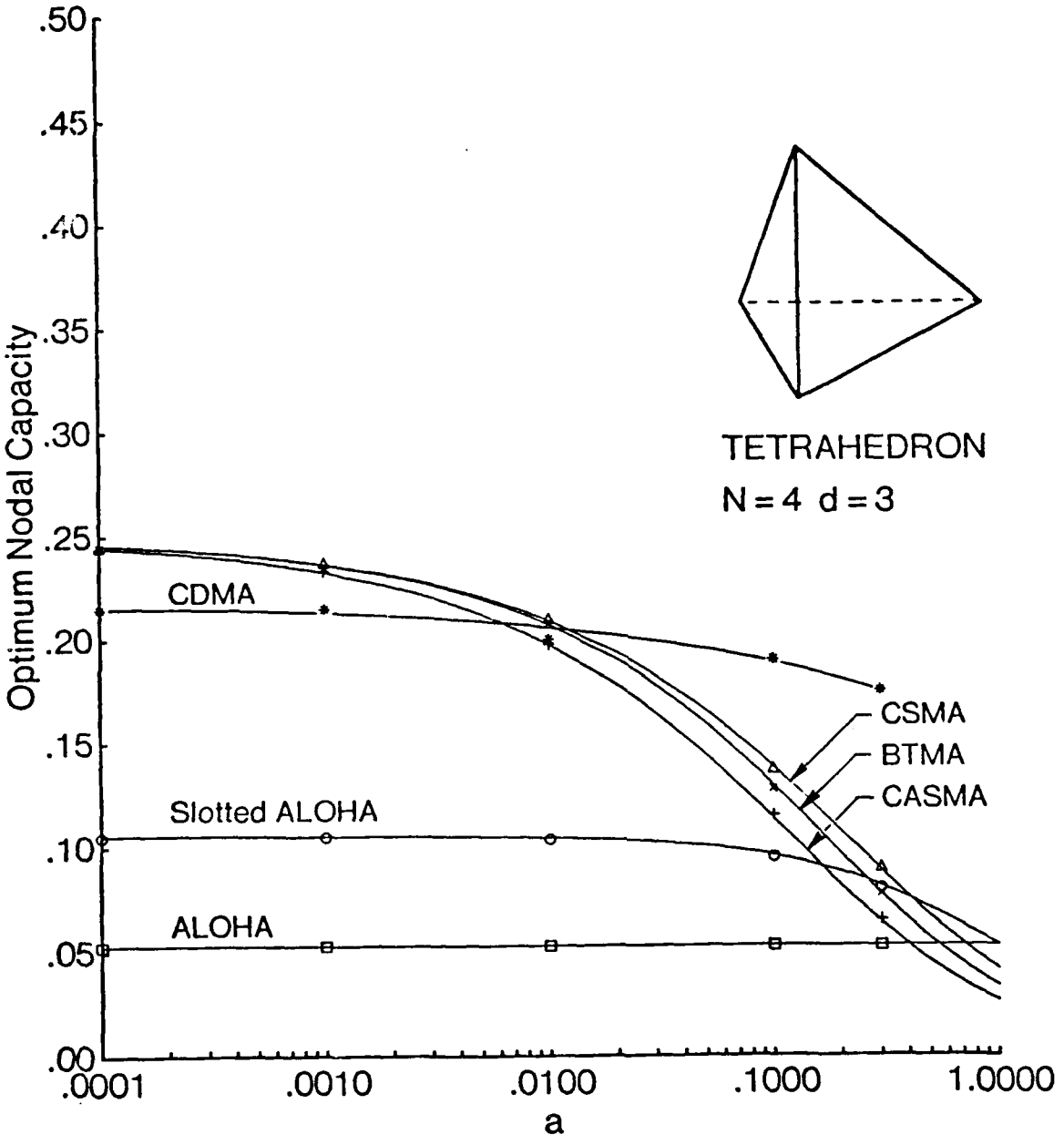

Fig. 3.12 Optimum nodal capacity versus a for the tetrahedron topology. (All symbols represent simulation results. For CSMA, C-BTMA, CASMA and ALOHA, the curves drawn are obtained from analysis.)

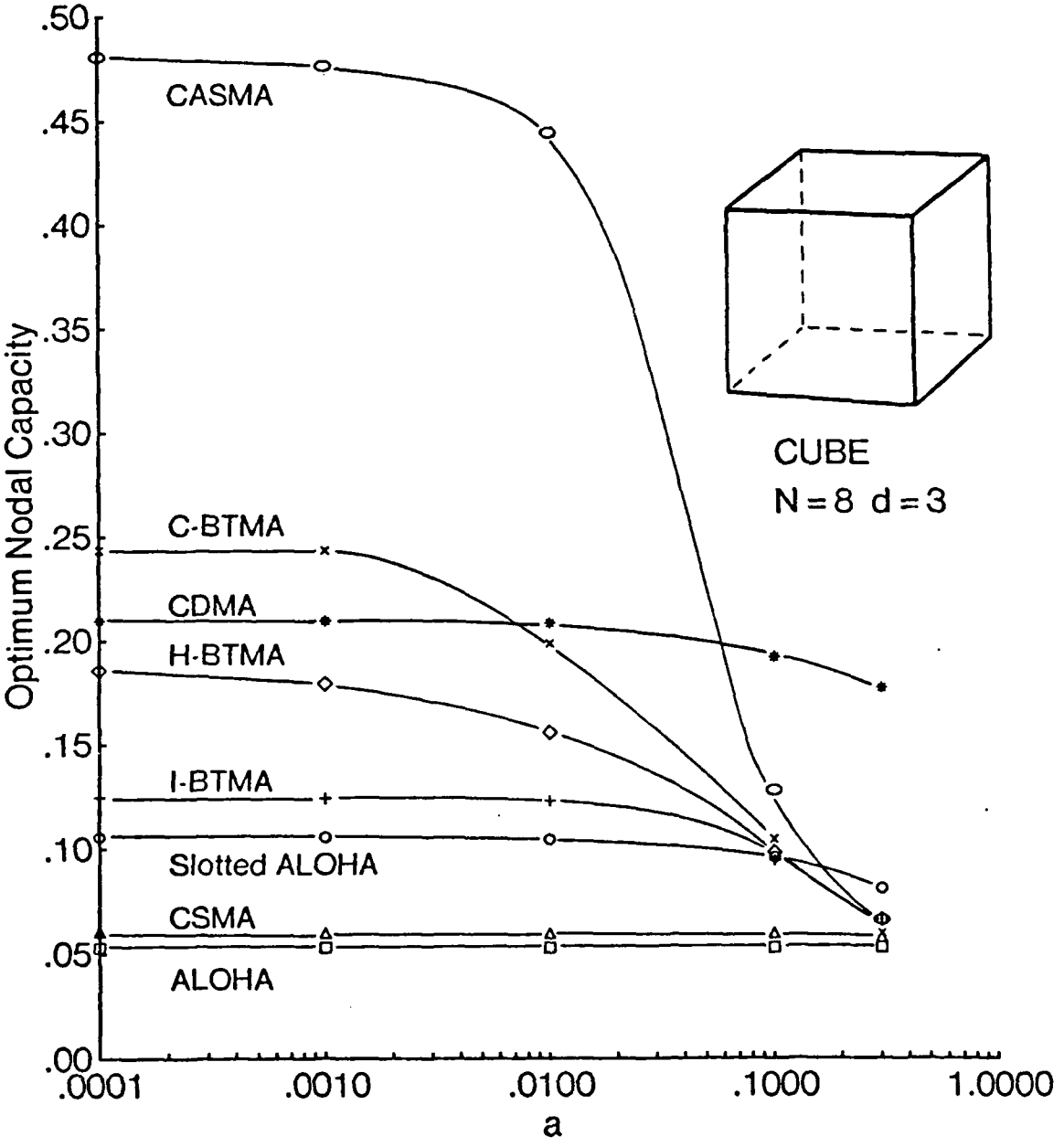

Fig. 3.13 Optimum nodal capacity versus a for cube topology.

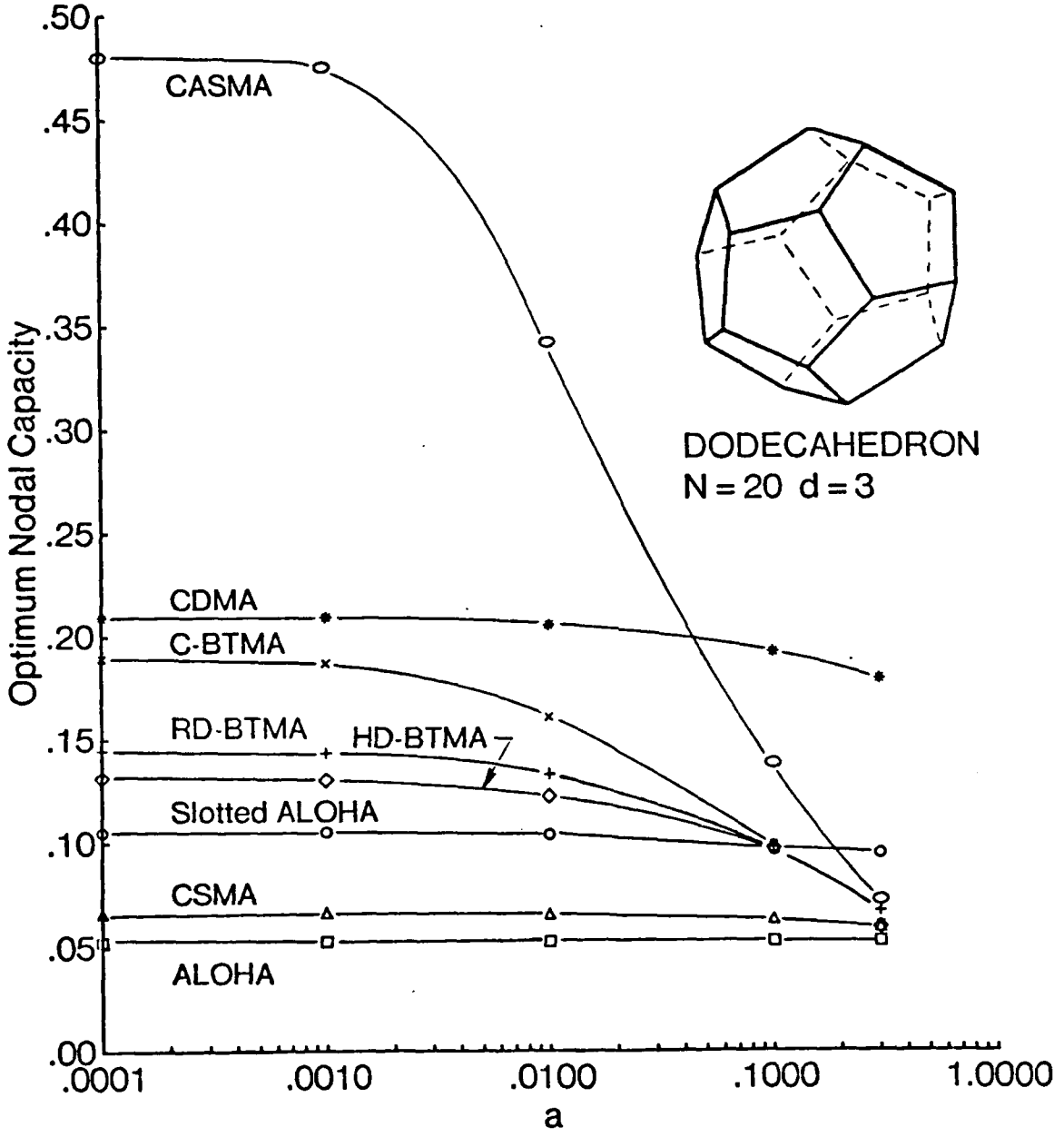

Fig. 3.14 Optimum nodal capacity versus a for dodecahedron topology.

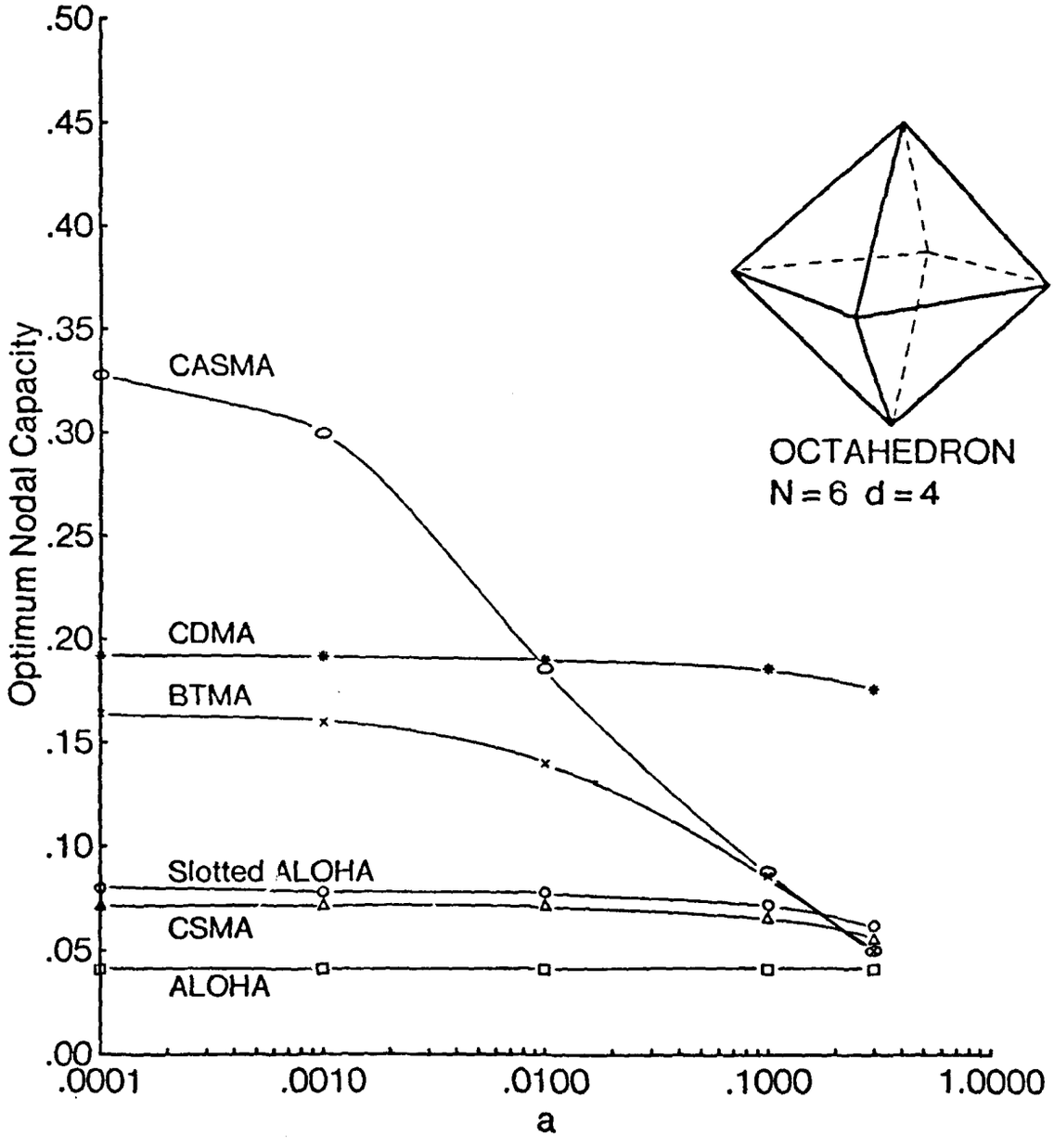

Fig. 3.15 Optimum nodal capacity versus a for the octahedron topology.

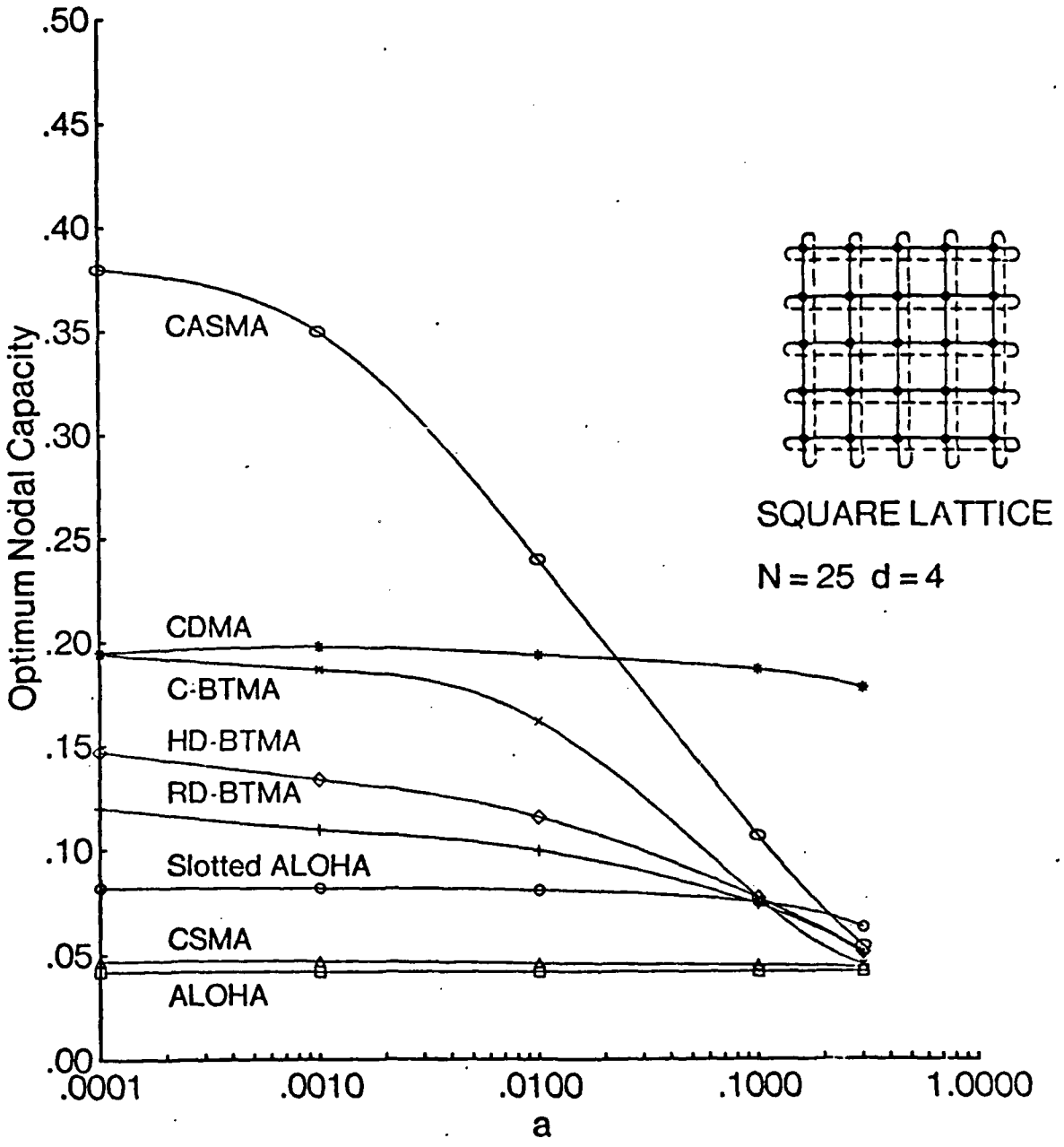

Fig. 3.16 Optimum nodal capacity versus a for the closed square lattice topology.

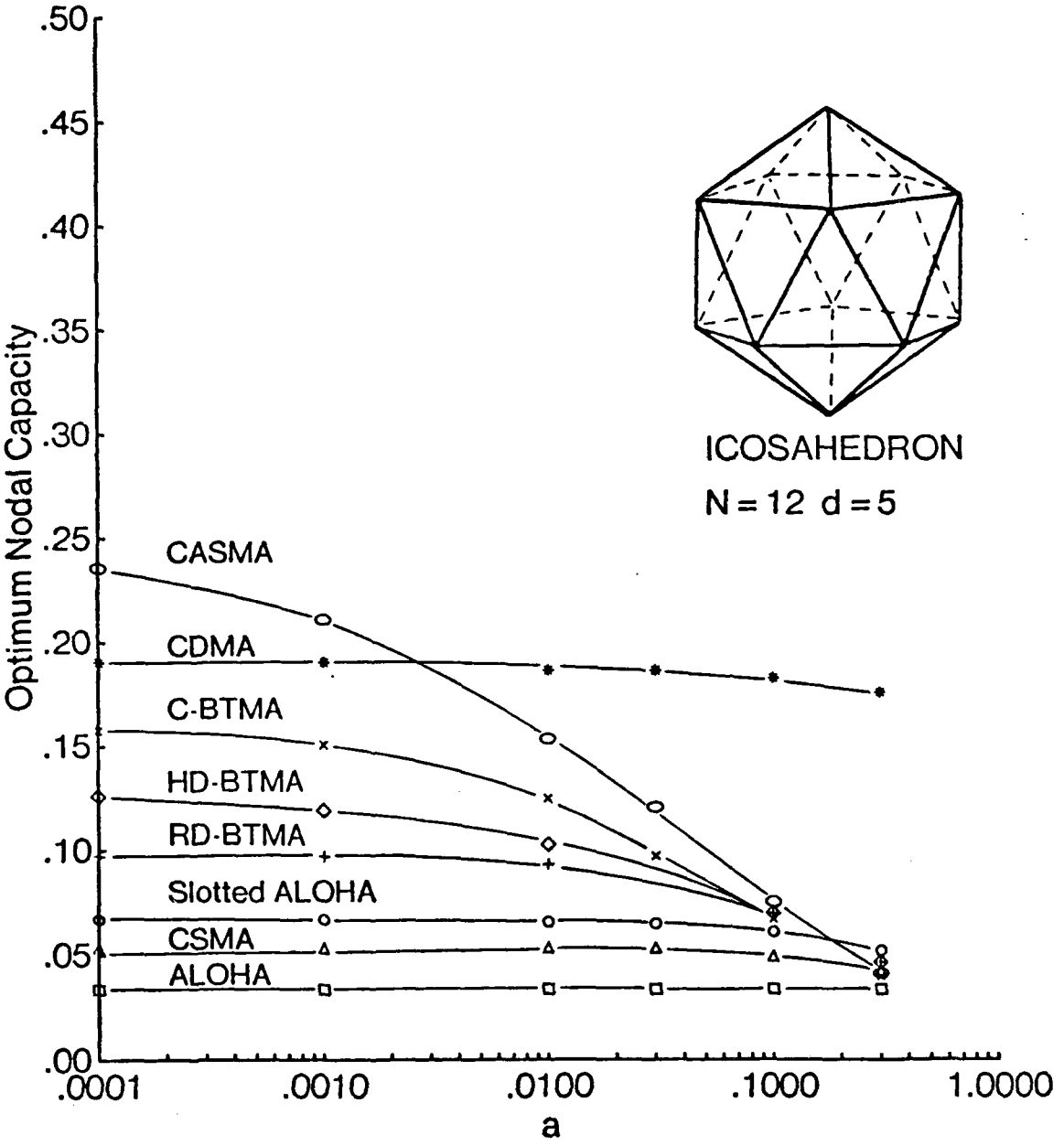

Fig. 3.17 Optimum nodal capacity versus a for icosahedron topology.

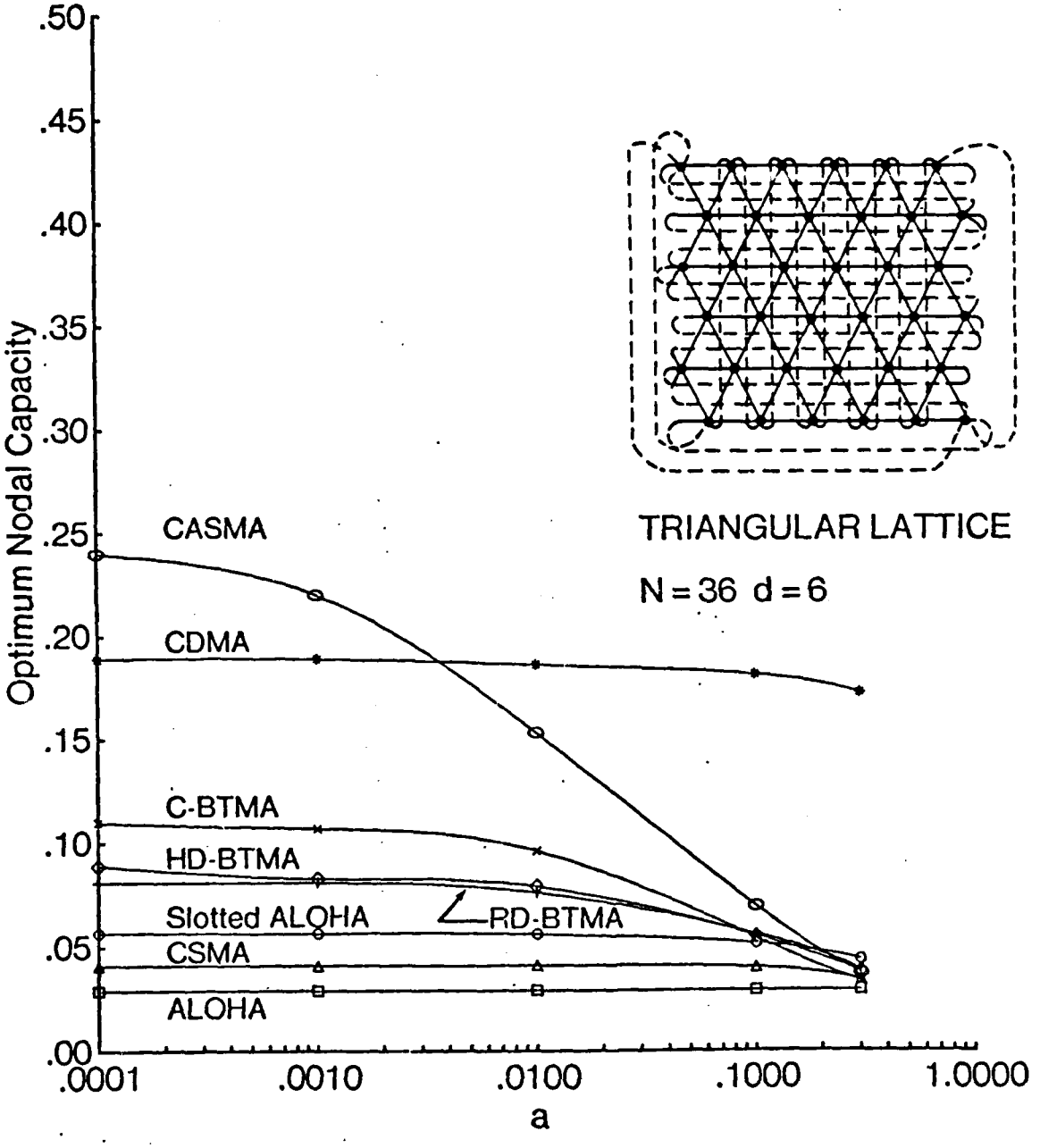

Fig. 3.18 Optimum nodal capacity versus a for closed triangular lattice topology.

date; however, for BTMA and CASMA, a greater decrease with a is seen than for the other schemes. In the remaining access schemes, the nodal capacities are less sensitive to a for the following reasons: for slotted ALOHA, equation (3.2) shows that the capacity varies as $1/(1+a)$, a quantity which is rather small for $0 \leq a \leq 0.3$ (the range of values depicted in figures 3.10 to 3.18). While CSMA is also affected to some extent by a, its performance is primarily limited by collisions due to hidden nodes where these exist, (an effect independent of a). For cases where there are hidden nodes, the nodal capacity of CSMA is low over the entire range of a and thus the effect of a is slight. Only in the case of the fully connected tetrahedron topology (where there are no hidden nodes and the capacity of CSMA is high), is a severe degradation exhibited as the value of a increases (as is also the case for BTMA and CASMA). In CDMA, channel sensed information is not utilized and hence we expect the nodal capacity to be basically insensitive to a; the decrease in the capacity of CDMA with a is due to the fact that, for a large, the probability that a node will begin to transmit while a transmission to it is already on the way, but before the latter transmission is detected, becomes significant. This results in the probability of wasted transmissions increasing with a.

Excluding the CDMA scheme (where the required channel bandwidth may be orders of magnitude greater than for the narrow band schemes), for a small (< 0.1), the protocols may be 'approximately' ranked in order of increasing performance as follows*: pure ALOHA, CSMA, slotted ALOHA, RD-BTMA, HD-BTMA, C-BTMA and CASMA. One exception to this ordering is CSMA in the (fully connected) tetrahedron topology, where it achieves the highest performance (as expected). The other exception to this ordering occurs in the dodecahedron topology, where the performance of HD-BTMA is inferior to both C-BTMA and ID-BTMA.

*The cost of the busy tone channel for BTMA, and the activity signalling channel for CASMA is ignored here.

Note that for HD-BTMA, the capacity achieved depends on the value of header processing time assumed, (here the value is 50% of the packet transmission time in all cases). The effect of the header processing time is clearly seen in figure 3.19 for the dodecahedron, cube and six node ring topologies. We note that for a header processing time of zero, performance is identical to ID-BTMA, while for a header processing time equal to a packet transmission time, performance is identical to C-BTMA. We note further that in the case of the dodecahedron, the capacity of HD-BTMA is less than that of both ID-BTMA and C-BTMA, over a wide range of header processing times, including the 50% point; for the cube and the ring, the capacity of HD-BTMA lies between that of ID-BTMA and C-BTMA for all values of header processing time. This rather surprising result in the case of the dodecahedron is somewhat corroborated by the following scenario in HD-BTMA: suppose that at a given scheduling point, node i attempts a transmission to node j, where j is currently receiving a packet not destined to it (transmitted by a node p), has already processed the header of that packet, and hence is not emitting a busy tone. Assume that all other nodes in $N(i)$ are neither transmitting nor receiving. If $< i, j >$ is undertaken it will be unsuccessful; furthermore, for a period of time equal to the header processing time h, the nodes in $\mathcal{B} = \mathcal{N}^*(i) - \mathcal{N}(p)$ emit busy tone thereby blocking all nodes in $\mathcal{N}(\mathcal{B})$. After h, the nodes in $\mathcal{B}$ turn off their busy tone, and for the remainder of the transmission $< i, j >$, only the nodes in $\mathcal{N}^*(i)$ are blocked (due to carrier sensing). Since $< i, j >$ is unsuccessful, the blocking of nodes by $< i, j >$ is clearly wasteful, and the more nodes blocked, the greater the waste. Note that in ID-BTMA, only the set $\mathcal{N}^*(i)$ is blocked for the entire transmission time of $< i, j >$, and hence the inefficiency is decreased over the case described above. In C-BTMA, $< i, j >$ would have been blocked in the first place, thus entirely avoiding this particular inefficiency. Note further that this effect depends on the sizes of the sets $\mathcal{N}^*(i)$, $\mathcal{B}$ and $\mathcal{N}(\mathcal{B})$, and also on the probability

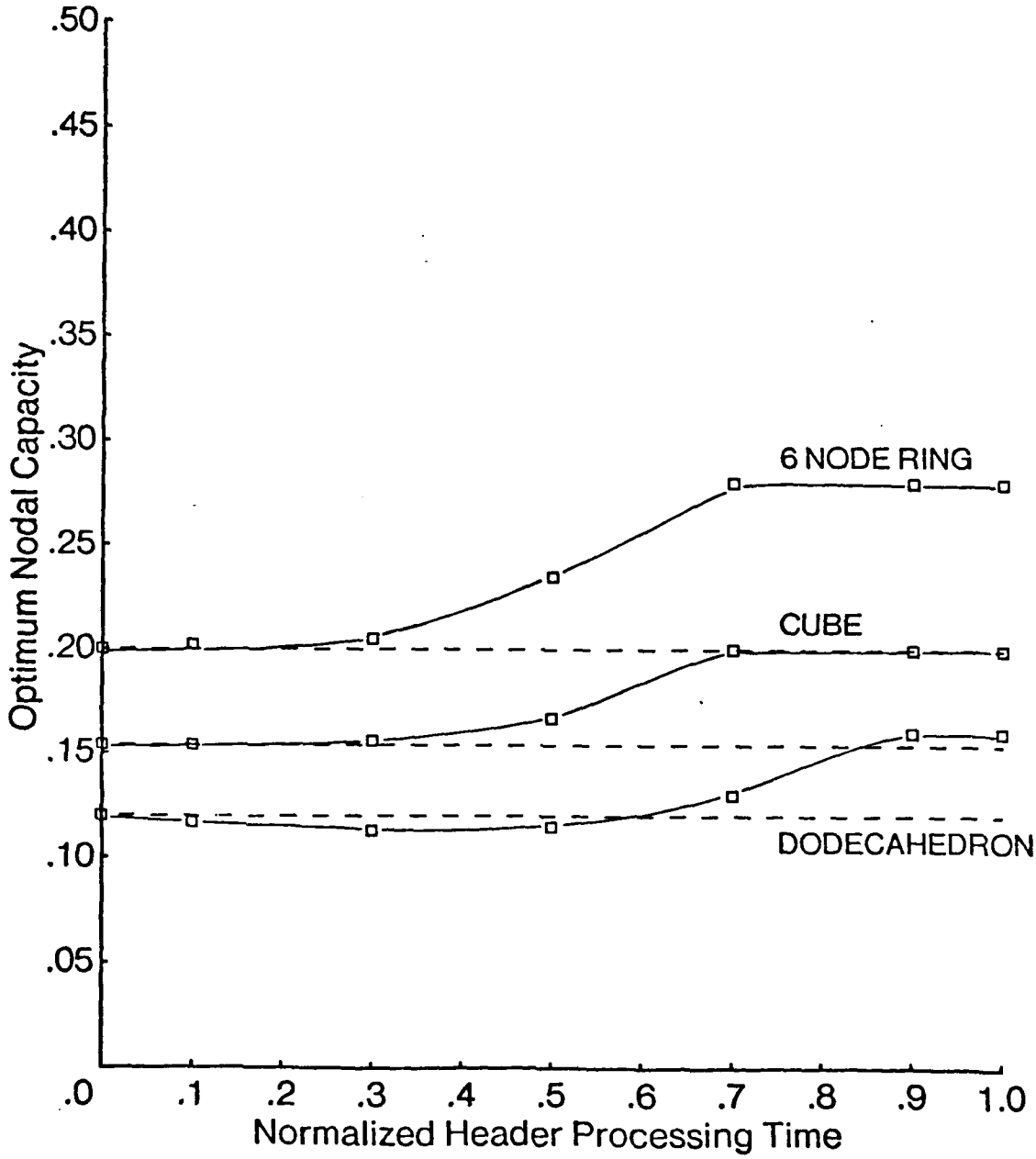

Fig. 3.19 Optimum nodal capacity versus header processing time for H-BTMA protocol in dodecahedron, cube and six node ring topologies, with $a = 0.01$.

that $< i, j >$ will be unsuccessful as described above. To summarize, a phenomena of spurious blocking in the neighborhood of an ongoing unsuccessful transmission $< i, j >$ during the header processing period exists. As the relative amount of such blocking turns out to be greater in the dodecahedron as compared with the other topologies, it is certainly conceivable that in the dodecahedron topology, the performance of HD-BTMA is indeed inferior to both C-BTMA and ID-BTMA. Regarding the relative performance of C-BTMA and ID-BTMA, the C-BTMA scheme achieves higher throughput than the ID-BTMA scheme in all networks under study, indicating that the potential collisions permitted by the ID-BTMA scheme are more harmful to performance than the blocking of potentially successful transmissions caused by C-BTMA. Note that for $a > 0.1$, the capacity of BTMA and CASMA continues to decrease, becoming less than that of slotted ALOHA, and approaching that of CSMA and pure ALOHA. We now examine in more detail the performance of certain access schemes in simple ring networks with different values of N. We limit the discussion to the case $a = 0$ for which we make use of equations (3.6) and (3.7). In figure 3.20, we plot the nodal capacity $c(G^*)$ versus N for the ALOHA, Slotted ALOHA, C-BTMA and CASMA schemes. Figure 3.20 suggests that, in the 6-node ring for a small, CASMA and C-BTMA achieve similar performance, while in the 12-node ring CASMA achieves a higher performance than C-BTMA, which explains why this is indeed observed in figures 3.10 and 3.11. Note that as $N \rightarrow \infty$, the nodal capacity for each access scheme becomes insensitive to N and approaches a limit. For the case of the uniform traffic matrix, from [20],

$$\bar{n} = \lfloor (N+1)/2 \rfloor (1 - \frac{\lfloor (N-1)/2 \rfloor}{N-1}). \tag{3.8}$$

The graph of $\bar{n}/N$ versus N is shown in figure 3.21. Note that $\lim_{N \rightarrow \infty} \bar{n} = N/4$. In figure 3.22, we plot the network capacity $C(G^*)$ versus N for the uniform traffic matrix. Since in the case of the ring, $\bar{n}$ is proportional to N, it is not surprising to

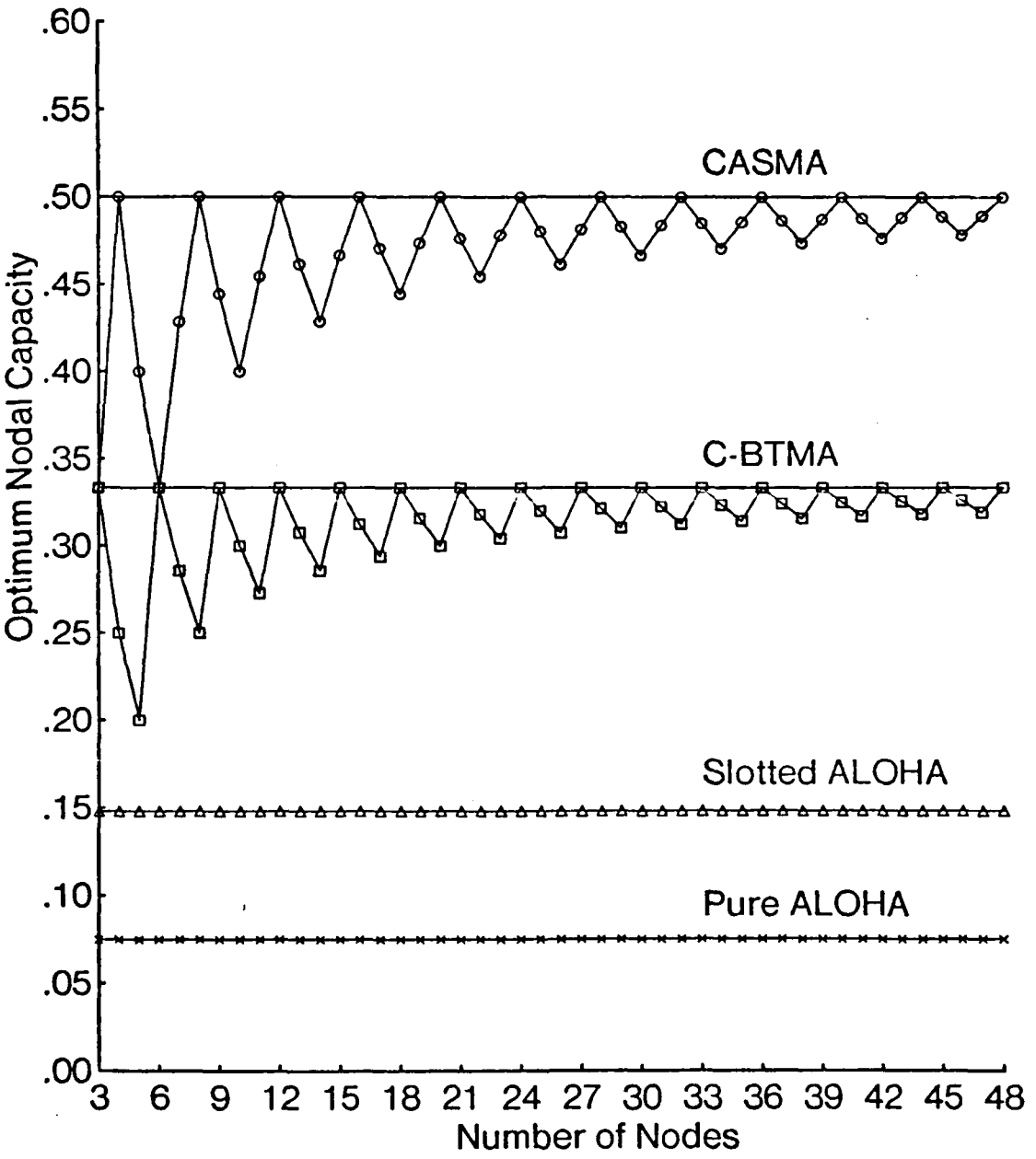

Fig. 3.20 Optimum nodal capacity versus number of nodes for the simple ring topology.

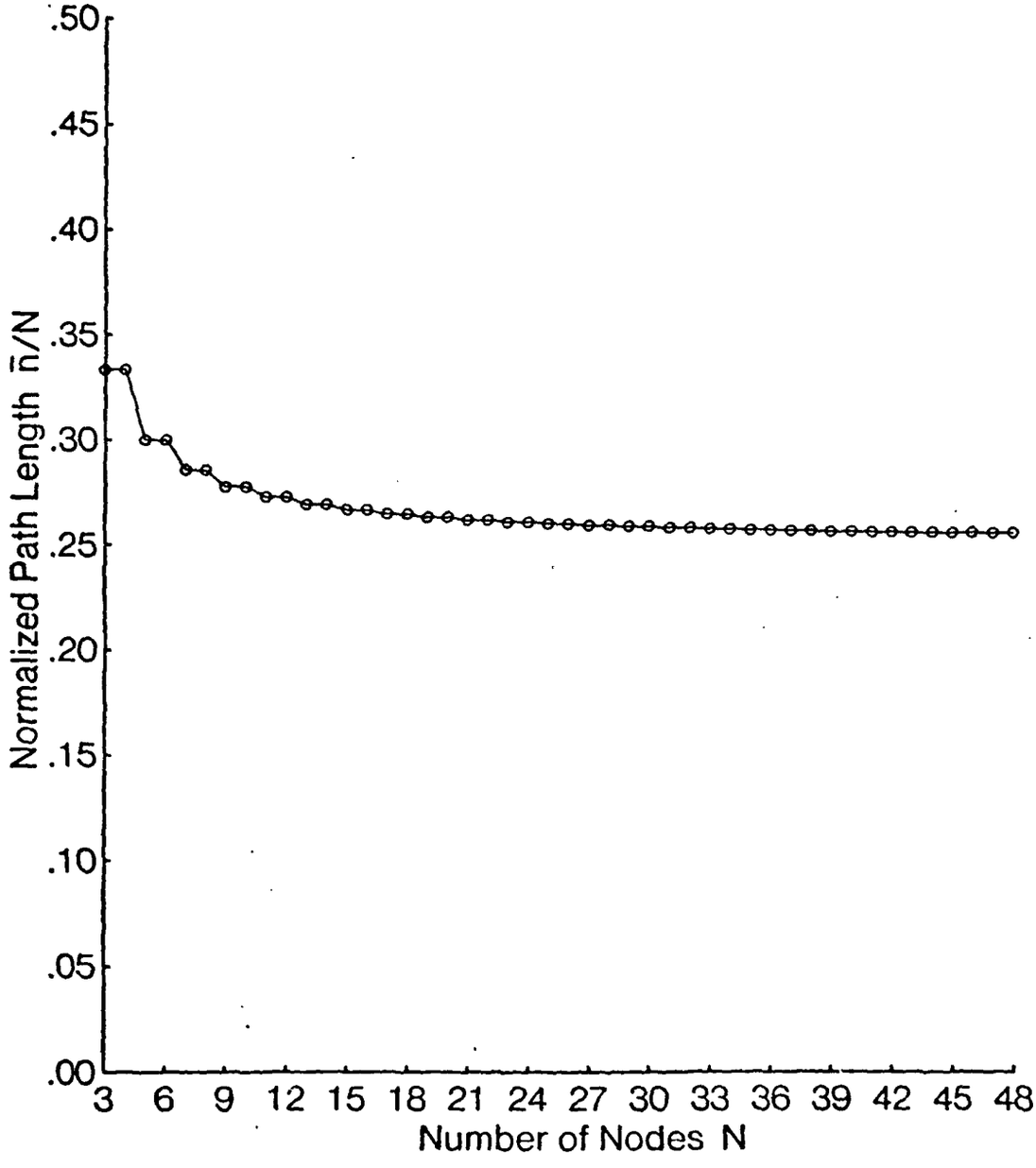

Fig. 3.21 Normalized path length versus number of nodes for the simple ring topology.

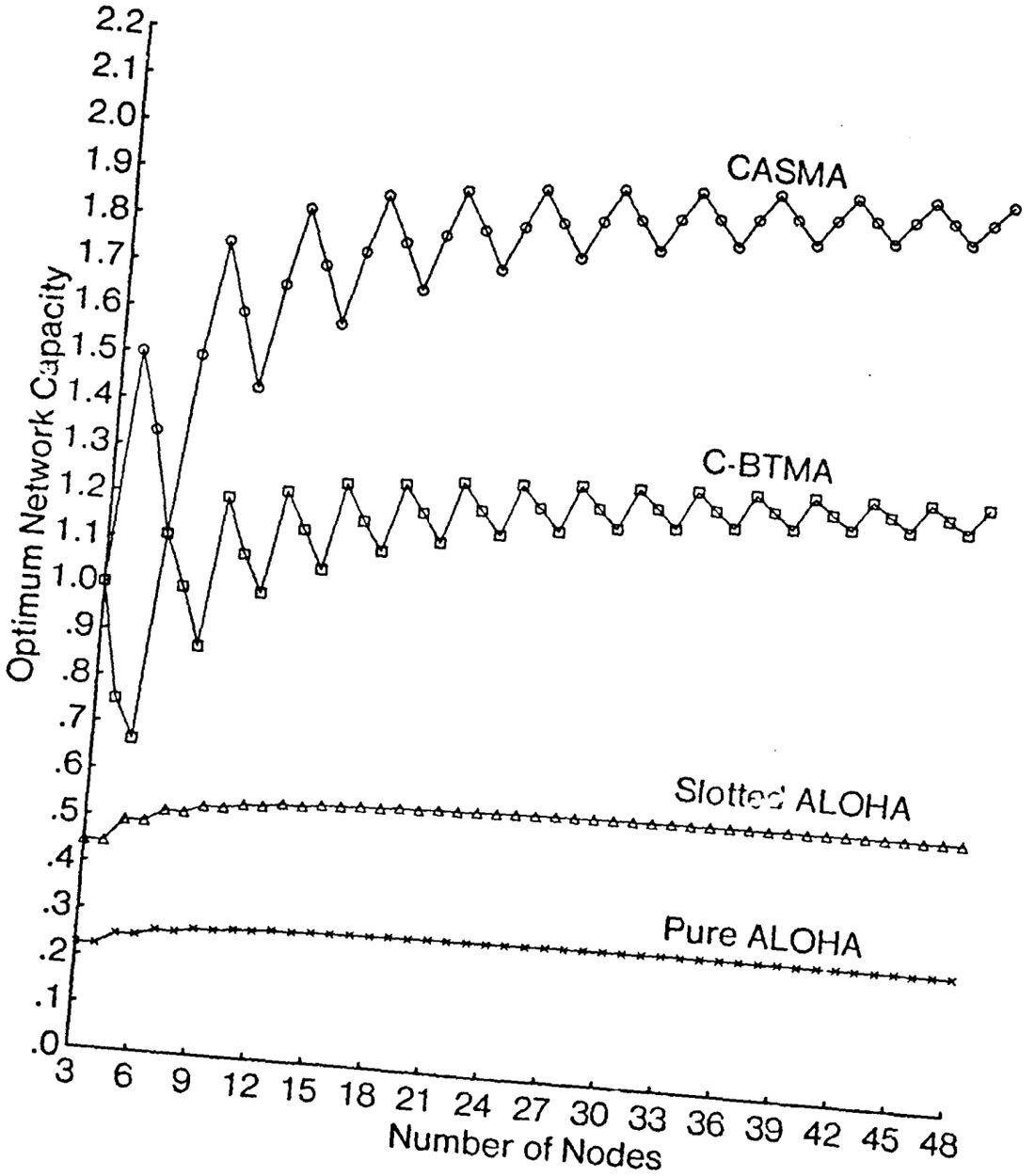

Fig. 3.22 Optimum network capacity versus number of nodes for the simple ring topology.

see that $C(G^*)$ approaches a limit as $N \rightarrow \infty$ as well. The results of figures 3.20 and 3.22 can be compared with those in [33] where the nodal capacity of C-BTMA and ALOHA (among others) was analyzed for the case of exponential packet lengths. We find that there is a minor difference (6%) for the case of ALOHA, while the results are identical for C-BTMA. We attribute the former difference to the different assumptions concerning packet length distribution, since, in pure ALOHA, once a transmission is undertaken, the probability of success is dependent on the packet length; in C-BTMA for $a = 0$, once a transmission is undertaken, the probability of success is unity, and is thus independent of the packet length.

3.3.3 Effect of d on the Nodal Capacity

In figures 3.23 and 3.24, we plot for $a = 0.01$ and 0.1 respectively the nodal capacity versus d for various access schemes in the closed planar networks, regular solids and simple rings. The results clearly indicate that the nodal capacity $c(G^*)$ decreases as the nodal degree d increases. Note that there is a variation in $c(G^*)$ with N for d and a fixed, due to the finite values of N in the topologies considered. However, this variation is less pronounced when a is large. Furthermore, as remarked earlier for simple rings, the variation is also less pronounced for large N. Thus we conclude that d is the topological parameter which affects performance the most. Note however that the CDMA scheme is seen to be less affected by d than are the narrow band schemes, with the difference in performance between CDMA and the other schemes increasing with d. This is due to the directional capture assumption of CDMA as described in section 3, which enables it to achieve a potentially higher number of successful, concurrent transmissions than the narrow band protocols.

In order to further study the effect of the degree d on nodal capacity without constraints on N and d, we consider multiconnected ring networks with a neighbors-

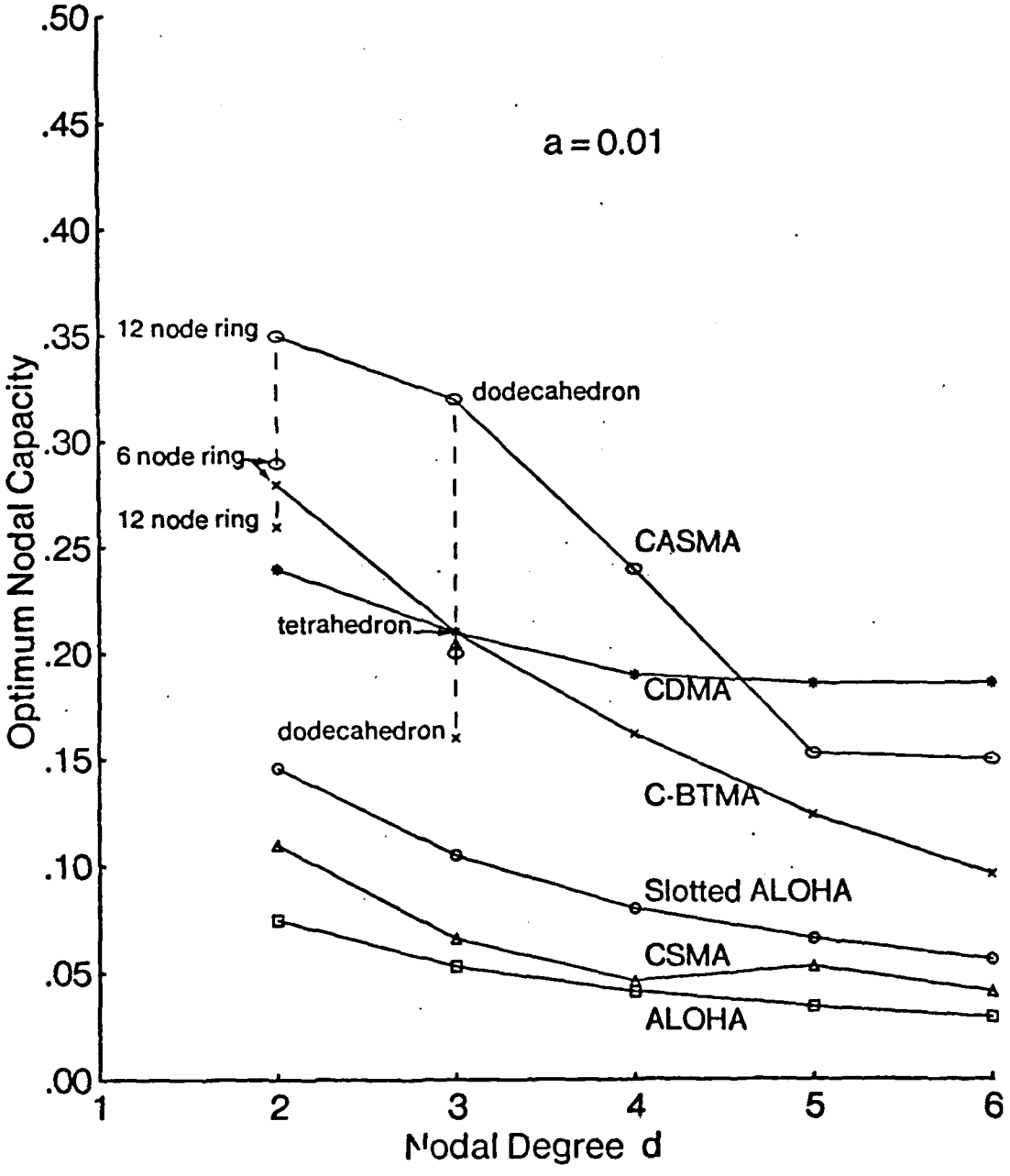

Fig. 3.23 Optimum nodal capacity versus degree for closed planar, regular solid and simple ring networks, with $a = 0.01$.

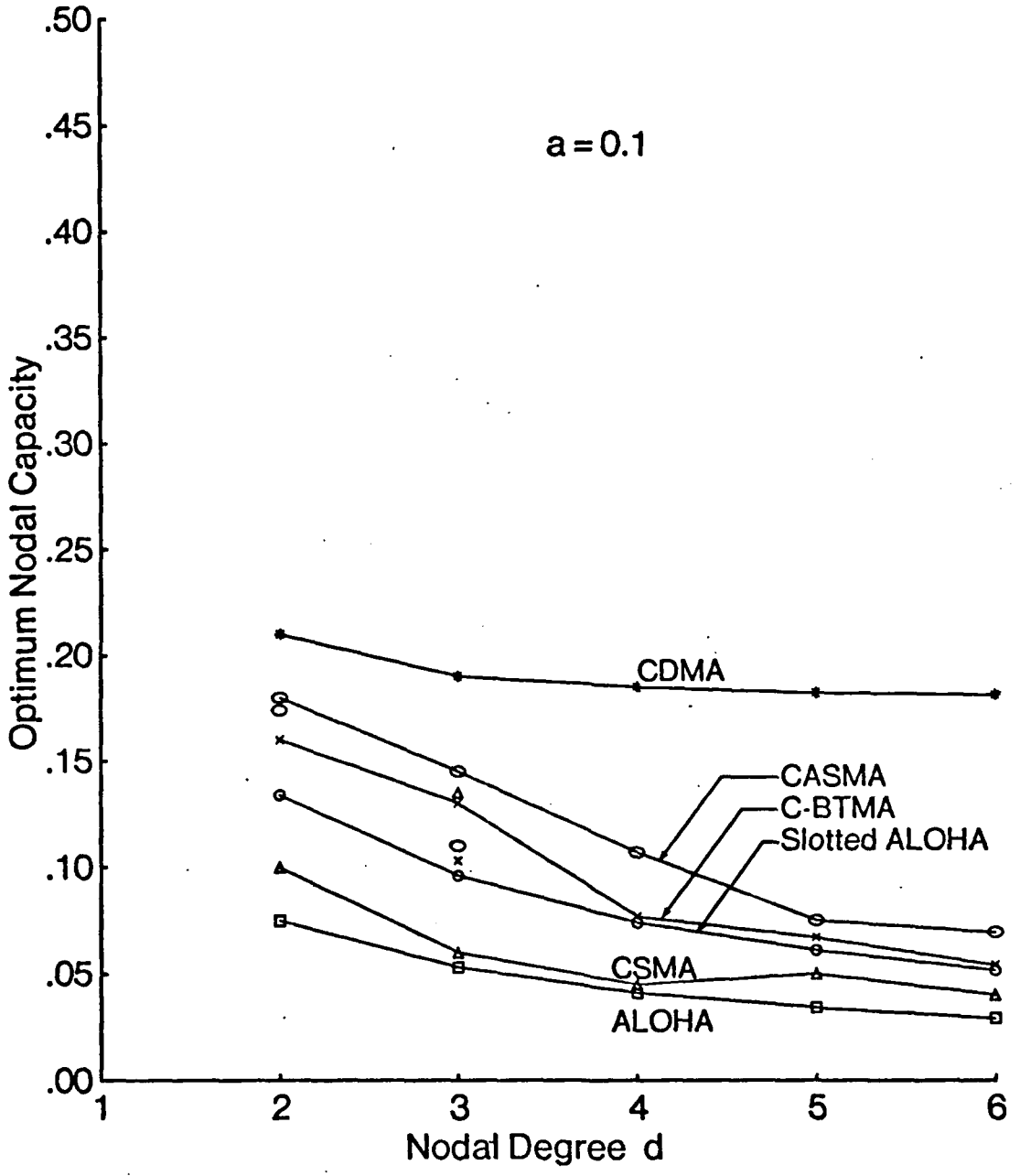

Fig. 3.24 Optimum nodal capacity versus degree for closed planar, regular solid and simple ring networks, with $a = 0.1$.

only traffic matrix. Note that, in this case, contrary to the simple ring ($d = 2$) and the regular solid networks considered previously, the link traffic processes under the CSMA, BTMA and CASMA access schemes are no longer statistically identical. This is due to the fact that for the aforementioned access schemes, the probability of successful reception p_s is different on each link; (p_s is not link dependent for ALOHA and CDMA, hence all link traffic processes are statistically identical for these schemes). For example, consider a multiconnected ring with N nodes of degree 4, operating under CSMA with $a = 0$. Consider the nodes to be numbered sequentially and consider transmissions from node 1 to its neighbors (i.e, nodes 2, 3, $N-1$, and N). The transmission $< 1,2 >$ is vulnerable to transmissions from node 4 only, (the other neighbors of 2 being blocked by carrier sensing), while $< 1,3 >$ is vulnerable to transmissions from both nodes 4 and 5. Let $S'(\gamma, m, G) \triangleq 2NS_{12}(\gamma, m, G)$ and $S''(\gamma, m, G) \triangleq 2NS_{13}(\gamma, m, G)$; these represent the sum of link throughputs summed over all links which are statistically identical to $S_{12}(\gamma, m, G)$ and $S_{13}(\gamma, m, G)$ respectively. We expect that $S_{12}(\gamma, m, G) \geq S_{13}(\gamma, m, G)$ and hence $S'(\gamma, m, G) \geq S''(\gamma, m, G)$ for all γ. This expectation is confirmed in figure 3.25 where $S'(\gamma, m, G)$, $S''(\gamma, m, G)$ and their sum $S(\gamma, m, G)$ (the network throughput) are plotted versus the offered input traffic rate γ, for the case of $N = 12$, $d = 4$, $a = 0.01$, $m = 50$ and $G = 0.5$. Furthermore, we note that $S'(\gamma, m, G) = S''(\gamma, m, G)$ for $\gamma < \gamma_1$, $S'(\gamma, m, G) > S''(\gamma, m, G)$ for all $\gamma > \gamma_1$, and $S'(\gamma, m, G)$ and $S''(\gamma, m, G)$ approach limits $C'(G)$ and $C''(G)$ respectively for γ large, as indicated in figure 3.25. (Note that the ratio $C'(G)/C''(G)$ can be altered by varying the queue scheduling distribution; however, in this chapter, we consider only a uniform queue scheduling distribution). The additional complexity in the behaviour of such a network indicates the reason why we have chosen to initially focus only on entirely regular topologies. In chapter 5, we study further the multiconnected ring and consider several other networks that are not entirely

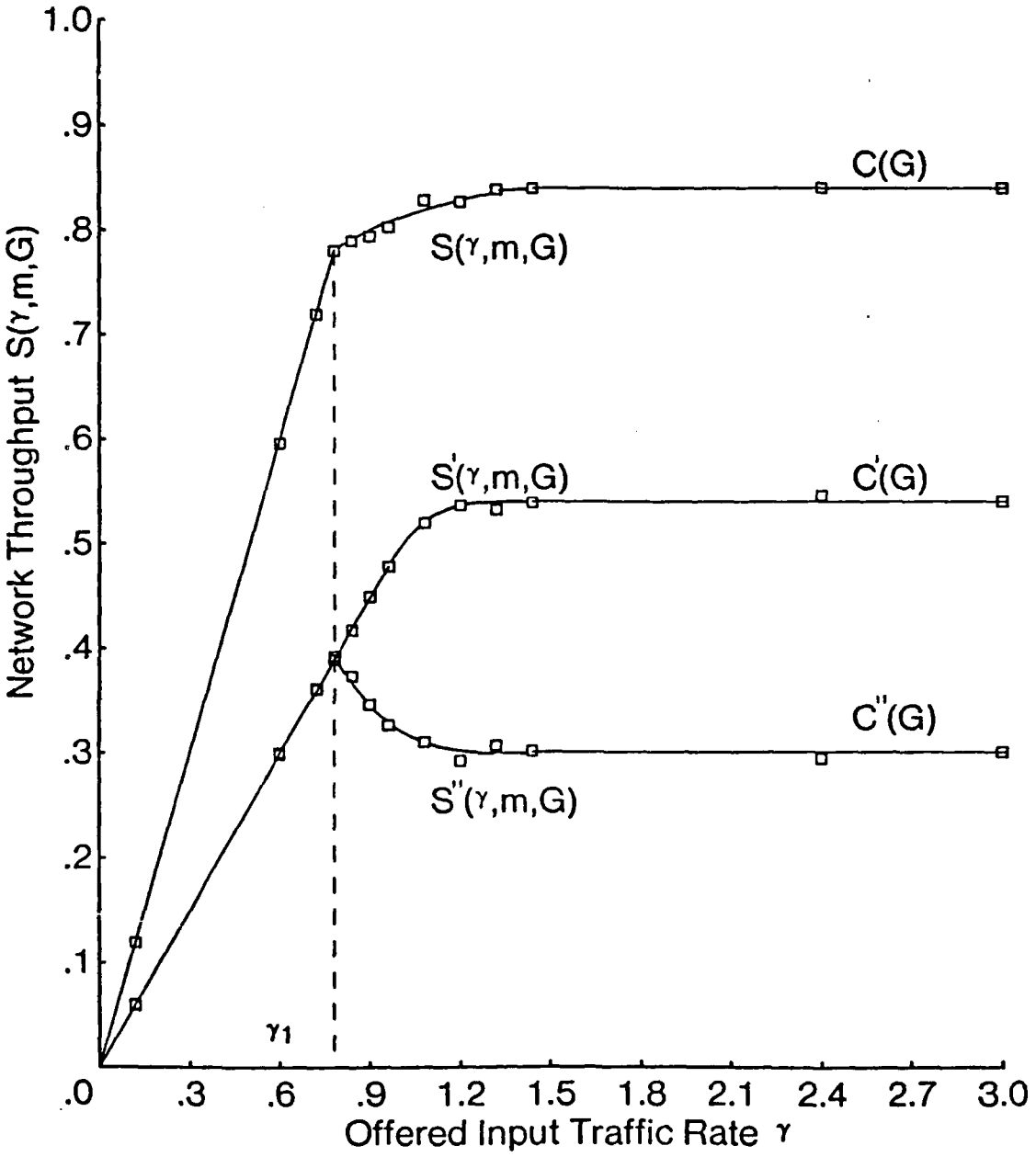

Fig. 3.25 Network throughput $S(\gamma, m, G)$ versus offered input traffic rate γ, in a 12-node multiconnected ring of degree 4, under the CSMA protocol with a neighbors-only traffic matrix, $a = 0.01$, $m = 50$ and $G = 0.5$.

regular.

In figures 3.26 and 3.27, for $a = 0.01$ and $a = 0.1$, the optimum nodal capacity for various access schemes considered are plotted versus the nodal degree d for $N = 12$. The results generally confirm those of figures 3.23 and 3.24, and allow us to observe the effect of d for $d > 5$; in particular, we note that for large d, the capacity of CDMA is significantly higher than of the narrow band schemes. We also observe that, in multiconnected rings, the performance of CSMA first decreases with d and then increases as the connectivity of the network increases; at $d = N - 1$, as expected, the performance of CSMA is the best among the narrow band schemes.

3.3.4 Throughput - Delay Performance

For the case of uniform traffic and finite values of input traffic rate γ, we examine the throughput-delay tradeoff for the various access schemes in two representative topologies, namely, the simple six node ring and the icosahedron. Unlimited acceptance of both new and transit packets (i.e., $m = \infty$) and a value of $a = 0.01$ are assumed. For $\gamma \leq C(G^*)$, we find that the network delay $D(\gamma, \infty, G)$ is minimized by a particular value of G denoted by $G_{opt}(\gamma)$, for each γ. This is depicted in figure 3.28 for the case of CSMA in the simple six node ring topology. Note that as $\gamma \rightarrow 0$, $G_{opt}(\gamma) \rightarrow \infty$, and as $\gamma \rightarrow C(G^*)$, $G_{opt}(\gamma) \rightarrow G^*$; refer to figure 3.8 and the discussion pertaining thereto. Furthermore, we observe that the sensitivity of $D(\gamma, \infty, G)$ to G increases with γ; such behaviour had been encountered previously in the context of single-hop, fully connected networks [5], [50]. In figures 3.29 and 3.30, we plot the minimum network delay $D(\gamma, \infty, G_{opt}(\gamma))$ versus the network throughput $S(\gamma, \infty, G_{opt}(\gamma))$ in the simple six node ring and the icosahedron topologies for all access schemes under consideration. Note that all curves share certain properties, namely, $\lim_{\gamma \rightarrow 0} D(\gamma, \infty, G_{opt}(\gamma)) = \bar{n}$, (the average path length),

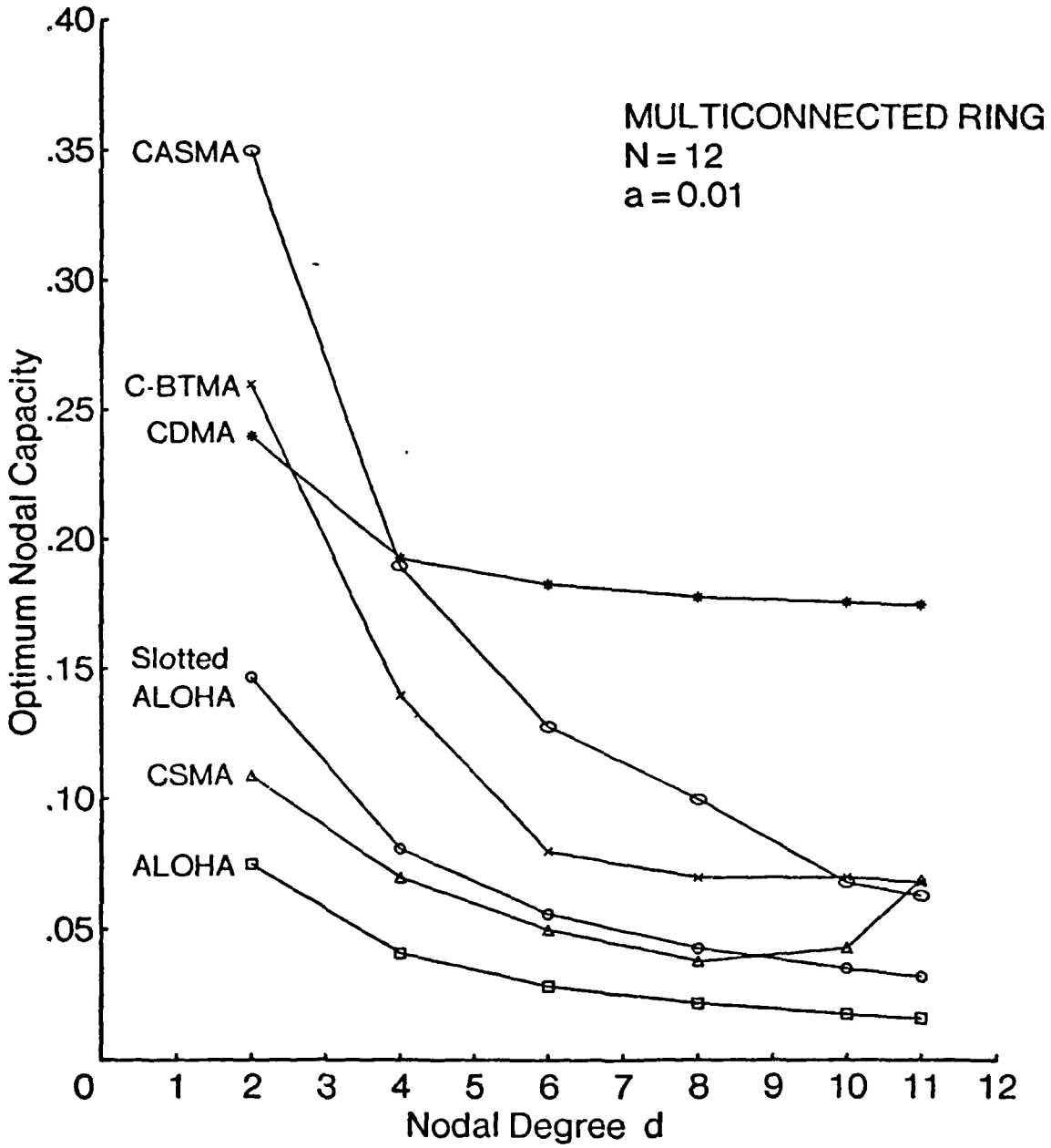

Fig. 3.26 Optimum nodal capacity versus degree for 12-node multiconnected ring, with $a = 0.01$.

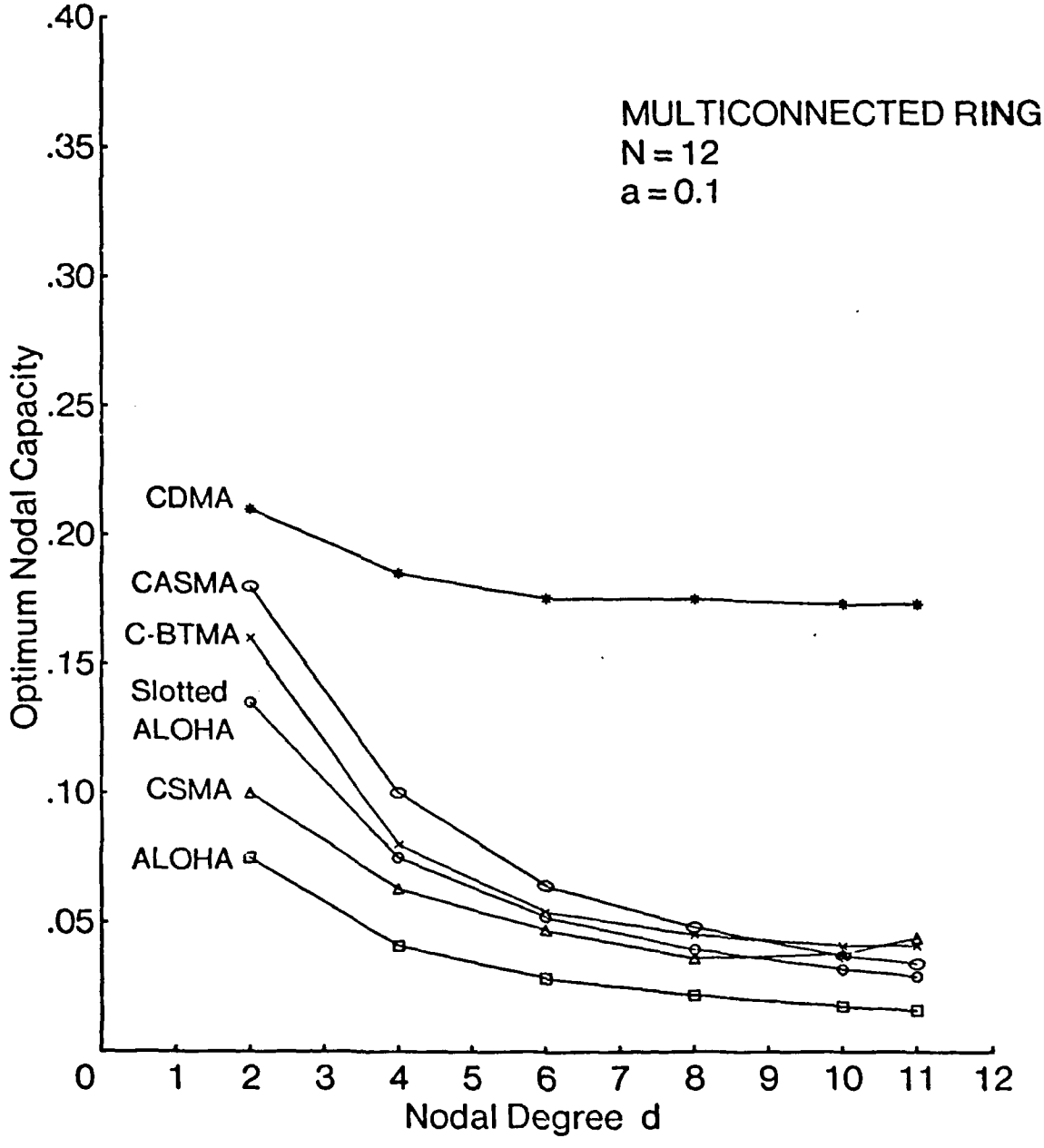

Fig. 3.27 Optimum nodal capacity versus degree for 12-node multiconnected ring, with $a = 0.1$.

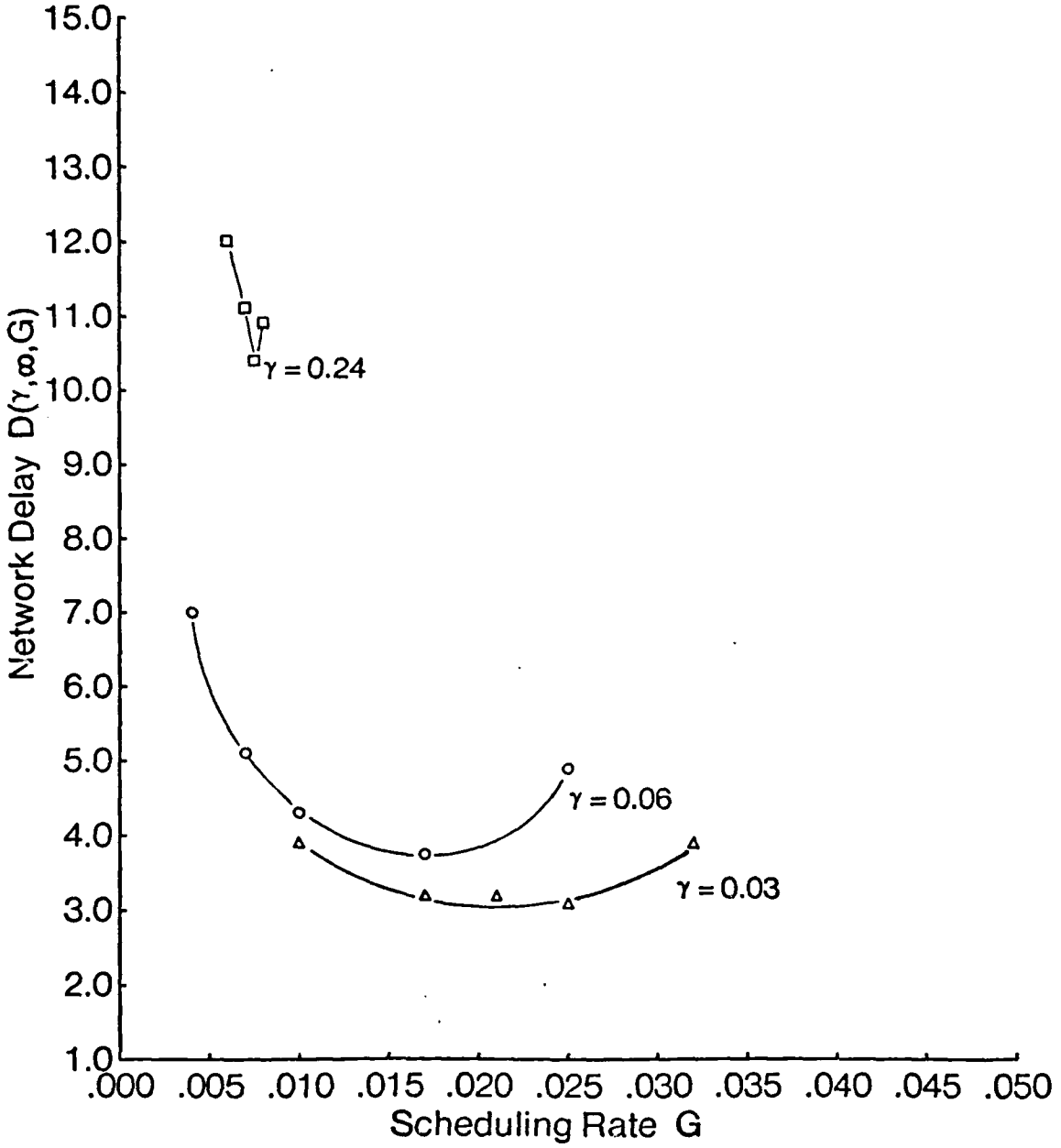

Fig. 3.28 Network delay versus scheduling rate for CSMA protocol in the simple six node ring topology, with uniform traffic and $a = 0.01$.

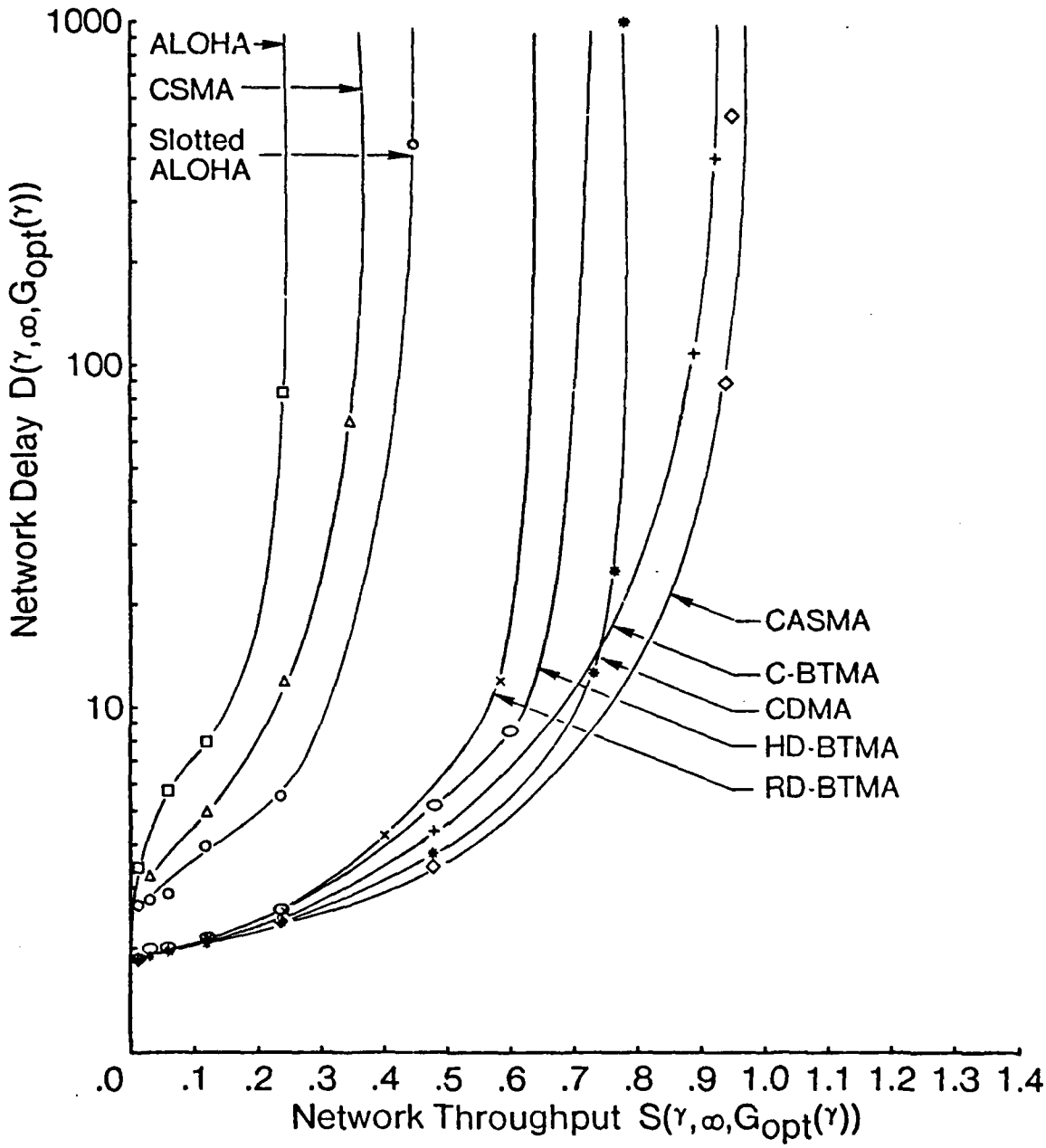

Fig. 3.29 Network delay versus network throughput for the simple six node ring topology, with uniform traffic and $a = 0.01$.

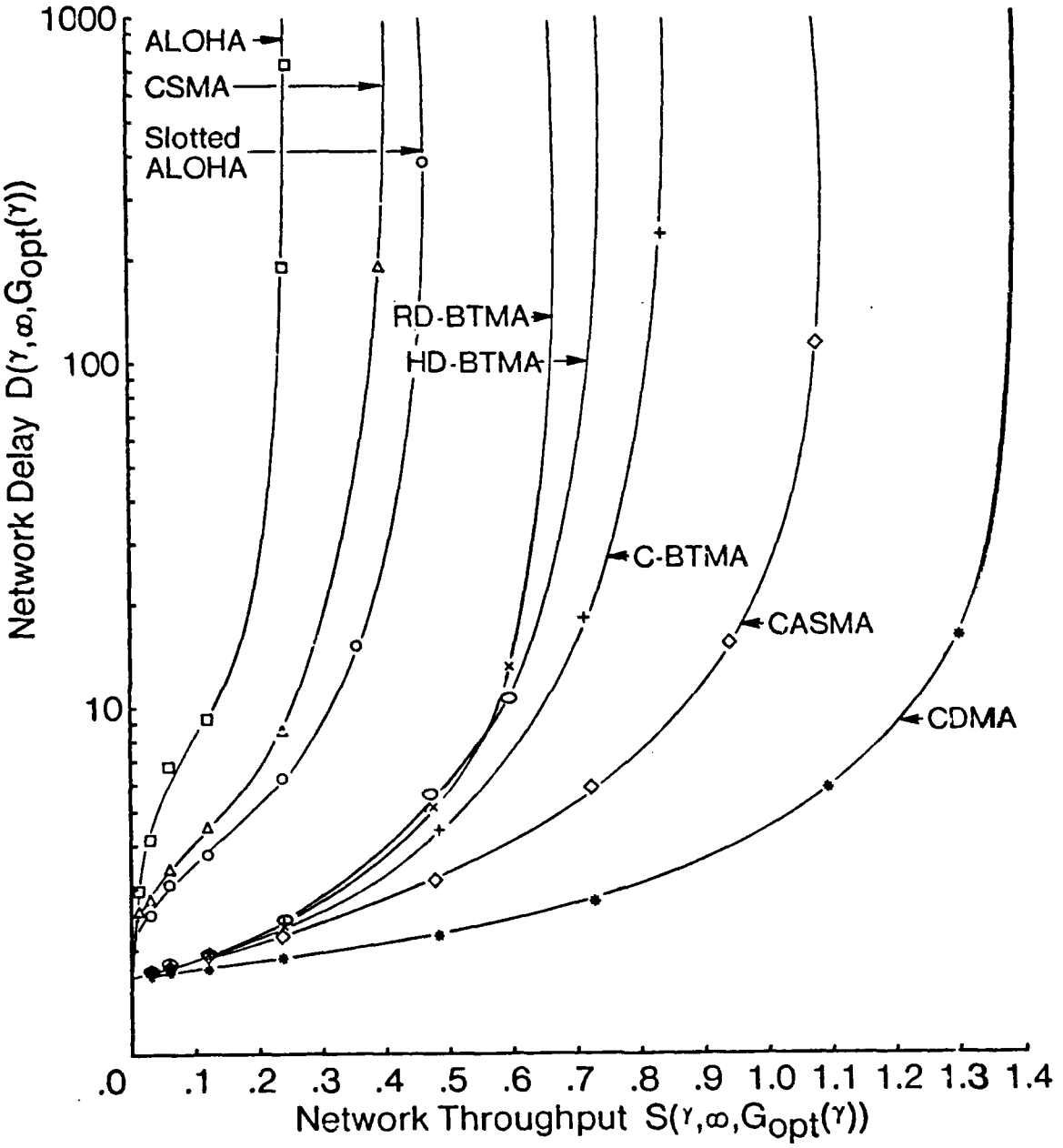

Fig. 3.30 Network delay versus network throughput for the icosahedron topology, with uniform traffic and $a = 0.01$.

$\lim_{\gamma \to C(G^*)} S(\gamma, \infty, G_{opt}(\gamma)) = C(G^*)$, and $\lim_{\gamma \to C(G^*)} D(\gamma, \infty, G_{opt}(\gamma)) = \infty$. Note further that the ordering of the access schemes in terms of the maximum network throughput is as predicted in figure 3.17 for the icosahedron and in figure 3.10 for the simple six node ring for $a = 0.01$.

3.4 Summary

In this chapter, we have studied the performance of multihop packet radio networks with regular structure. The effect of the nodal scheduling rate, and the input flow control on performance was detailed, and the sensitivity of the performance measures to these variables was explored. It was found that network delay was much more sensitive to the nodal scheduling rate than was network throughput. Regarding flow control, it was seen that when the flow control scheme caused blocking at the network input, a reduction in throughput resulted. The performance of the various access schemes was compared in terms of their nodal capacity, and throughput-delay characteristics. The performance of CSMA was shown to degrade severely in multihop networks. Regarding the effect of a, the performance of the BTMA and CASMA schemes were seen to be rather sensitive to this parameter, but for a small, relatively high capacities were achieved by these schemes as compared with CSMA and ALOHA (by factors of typically ≥ 3). The CDMA scheme also achieved relatively high throughput and was also only slightly sensitive to a. Regarding the effect of nodal degree, it was seen that nodal capacity decreased with d; however, a smaller decrease was observed for CDMA than for the narrow band schemes. It was also noted that for certain networks of the same nodal degree but with a different number of nodes, different nodal capacities resulted. The latter effect is due to the finite size of the networks considered. Finally, it should be kept

in mind in comparing the performance of these schemes that a penalty has not been assessed neither for the busy tone in BTMA, nor for the activity signalling in CASMA, nor for the additional bandwidth required for spread spectrum operation in CDMA. However, with reference to BTMA, in environments where the channel bandwidth is the limiting resource, the improvement in channel utilization achieved may well more than compensate for the cost of the busy tone.

Chapter 4

Regular Networks with Finite Buffering

4.1 Introduction

In the previous chapter, the performance of various channel access schemes was studied under the idealized assumption of infinite buffer resources. In this chapter, we address the same problem but considering that buffers are finite. Given the lower cost of memory at the present time, buffer storage minimization is a less critical issue now than it was 10 years ago. Nevertheless, it is important to know how many packet buffers are sufficient to prevent performance degradation. Furthermore, in the case of packet radio more so than for other types of computer networks, there may exist constraints on the size, weight and cost of individual nodes that limit the memory that may be installed.

Previous experience with store-and-forward networks such as ARPANET [51] has indicated that the management of the buffer resources has a significant impact on efficiency and reliability. In particular, if the (finite) buffer resources of a

store-and-forward network are improperly managed, then deadlocks may occur, in which some or all data packets never get through to their destinations. Deadlocks have been considered in several previous studies ([52] - [55]). In [52], deadlocks in computer systems are studied by means of a model for process interactions based on so-called resource graphs. Resources are defined as objects shared by processes, and deadlock is defined as the situation in which processes are permanently blocked because their resource requirements are never satisfied. Using an approach similar to that of [52], packet-switched store-and-forward networks are considered in [53-55]. Among the major results of these studies are (i) that the necessary and sufficient condition for a buffer management scheme to be deadlock-free is that the resource graph associated with every possible network state be "knot-free", and (ii) a simple deadlock-free buffer management scheme called the Structured Buffer Pool (SBP). The latter scheme is based on the resource-ordering principle; deadlock-free operation is ensured even if packets are never 'dropped' from the network but are repeatedly retransmitted until they are successfully received. The SBP scheme enables us to study multihop packet radio networks with finite buffers by means of simulation without the risk of deadlocks. We note here that it is also possible to achieve deadlock-free operation if packets are dropped from the network following a certain number of unsuccessful retries; such schemes are not considered here. In this chapter, the performance of several variants of the SBP scheme is evaluated. The effect of the prioritization (based on pathlength) introduced by the SBP scheme is examined and the effect of finite repeater buffer size on the performance of the various channel access schemes is obtained.

The remainder of this chapter consists of a description of the buffer structure and management schemes in section 4.2, the measures of performance pertaining to networks with finite buffering in section 4.3, numerical examples and results in section 4.4, and a chapter summary in section 4.5.

4.2 The Buffer Structure and Management schemes

A key function of a buffer management scheme is the prevention of deadlocks. In figure 4.1, a well-known example of deadlock is depicted [49]. The network consists of nodes configured in a ring, and each queue is filled with packets all of which are destined to a node two or more hops away. Under these conditions no traffic can move in the network. The deadlock occuring in the unidirectional ring network of figure 4.1 may be prevented by employing a network access flow control which prohibits the acceptance of an externally generated packet into the last empty buffer of a queue; thus it is always possible to transfer packets within the network [56]. In topologies other than the ring however, the above flow control scheme may not prevent deadlocks. This is illustrated in figure 4.2. The queues of nodes 1, 2 and 3 may be filled with packets originating at nodes 4, 5 and 6 respectively, all of which are destined to a node 2 hops away, and a deadlock results. In general topologies, deadlocks may be prevented by means of the SBP scheme, which is proved to be deadlock-free in [53]. The SBP scheme is based on:

(i) the classification of packets according to some criteria (e.g., the number of hops travelled so far, or the number of hops remaining to the destination),

(ii) assigning at each node a well defined set of buffers that can be occupied by packets of each class,

(iii) the acceptance of packets according to their class and the class of the available buffers,

(iv) always servicing packets in a queue in an order which is a function of their respective classes.

There are a number of variants of the SBP scheme. For example, in this work we consider packet and buffer classification based solely on the counting of hops. In

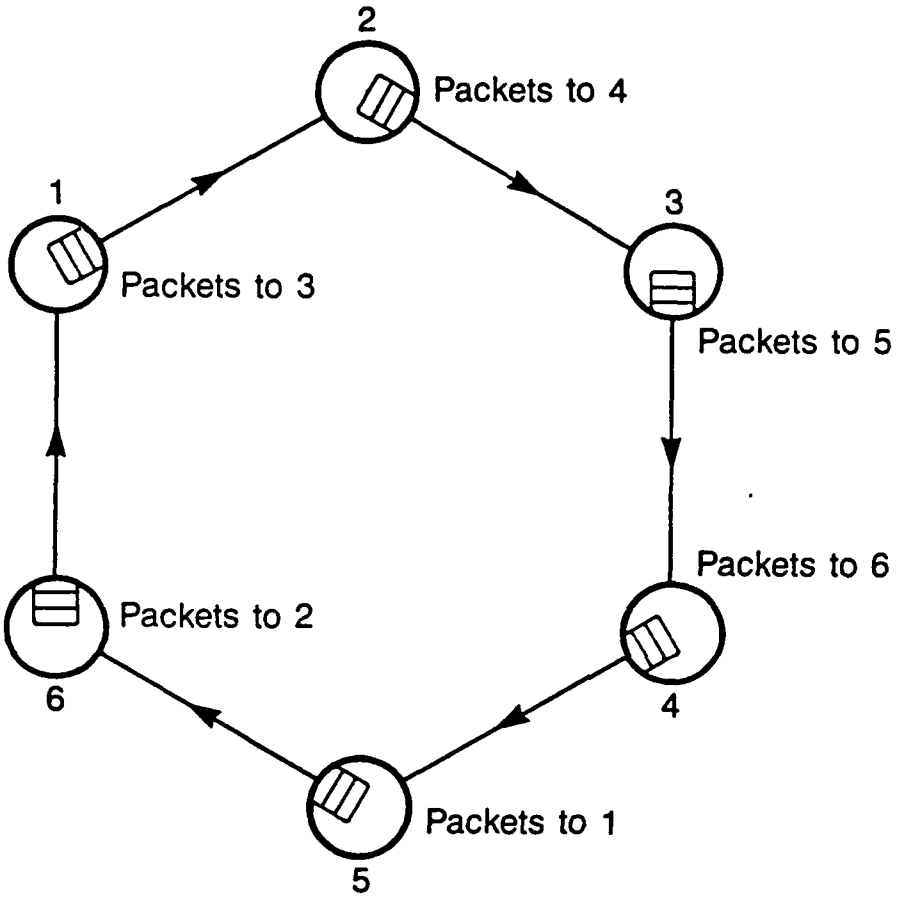

Fig. 4.1 Example of a store-and-forward deadlock.

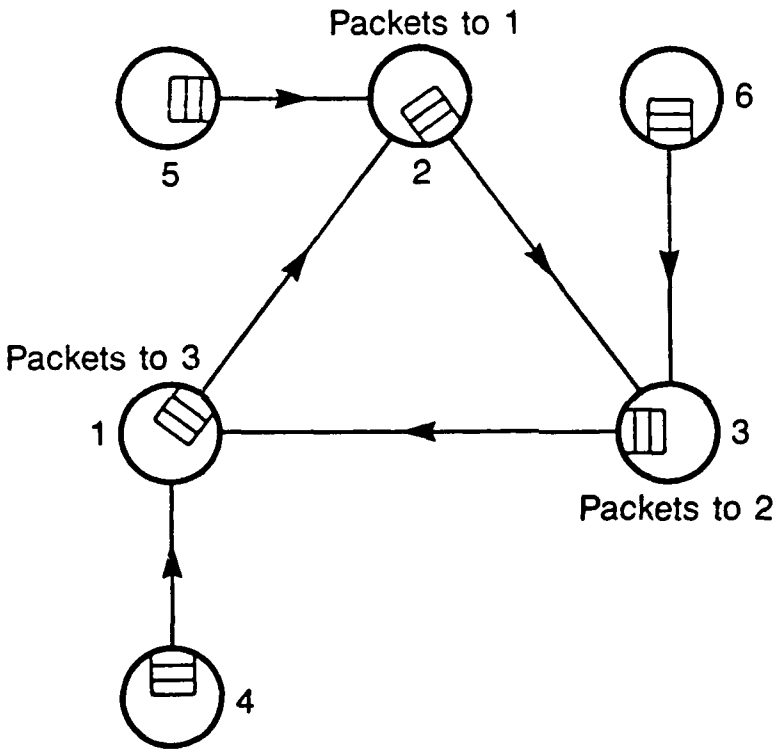

Fig. 4.2 Store-and-forward deadlock with flow control.

the hops-so-far (HSF) scheme, the packet class is defined to be the number of hops travelled so far. We let h_{max} denote the maximum path length in the network. In the hops-to-go (HTG) scheme, the packet class is defined as the difference between h_{max} and the number of hops remaining to the destination. In both these cases, the packet class increases with the length of the path travelled. Other methods of classification such as 'counting reversal of direction' are described in [53] and 'negative hop count' in [57].

In this chapter, we study both intra-node queueing structures introduced previously, namely, (i) all packets at a node form a single queue, and (ii) packets are enqueued in separate queues, with each queue corresponding to a unique neighboring node. Note that in the case of multiple queues, the buffers may be shared among the queues in several ways (refer to [58]). Here we consider the case of fixed partitioning, i.e., the buffers are partitioned into separate queues.

We consider that each queue is as depicted in figure 4.3. A total of $B_T + B_0 = B$ buffers per queue is assumed. B_T buffers are reserved for packets that are in-transit and en-route to their destination. We assume that a packet which arrives at its final destination does not need to be buffered among the B buffers of that destination. Therefore, the constraints of the SBP scheme require that $B_T \geq h_{max} - 1$. B_0 buffers may be occupied by packets that are newly generated by an external user (referred to as *new* packets). Out of these B_0 buffers, m buffers are always reserved for new packets, and the remaining $B_0 - m$ buffers may be shared by both in-transit and new packets. The m buffers may be viewed as representing the buffering capability of the external user or users attached to the local PRU. If so, all other buffers (i.e., $B - m$) would represent the buffering capability of the PRU itself.

We now describe the organization and management of the $B - m$ (PRU) buffers. These buffers are partitioned into h_{max} disjoint nonempty subsets labelled $0, 1, 2, \cdots,$

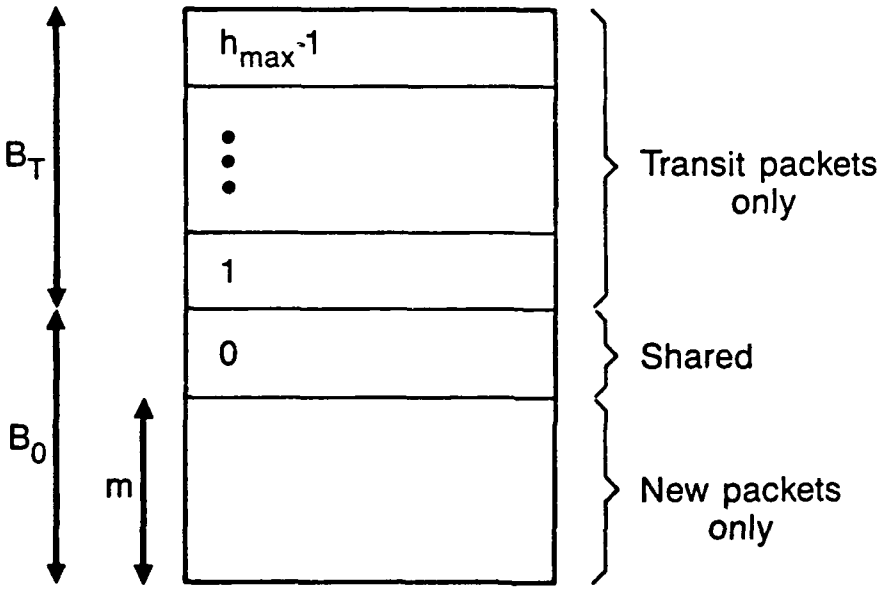

Fig. 4.3 The structure of a queue.

$h_{max} - 1$. There are several ways according to which the $B - m$ buffers may be occupied by arriving packets. First of all, we let buffer subset 0 consist of the $B_0 - m$ buffers. It is possible to consider that buffer subset i is reserved for packets of class i so that no sharing of resources takes place. Alternatively, one may assume that a packet of class $i + 1$ may access all buffers available to packets of class i plus those in subset $i + 1$, thus enabling a high degree of sharing of buffers among packet classes. In the sequel, we consider the case where the sharing of transit buffers is maximized, i.e., all buffer subsets numbered 2 and above consist of a single buffer, and all remaining transit buffers are allocated to class 1. (The remaining transit buffers are not allocated to class 0 in order to prevent new packets from using them). Given that the latter scheme is employed, a further decision regarding packet placement needs to be made. For example, incoming transit packets which are accepted may be placed in the buffer of the highest class or, alternatively, the lowest class available. Furthermore, the PRU's queue may be updated after a buffer is released (due to the dequeueing of a packet) so that packets in the queue move to occupy the highest or lowest class buffer currently available and allowable. The former packet placement policy is referred to as the 'push-up' (PU) policy and the latter is referred to as the 'push-down' (PD) policy. These strategies trade off storage for lower class packets versus that for higher class packets. In the PD variant, the presence of higher class packets may block acceptance of lower class packets in instances where space is indeed available for such lower class packets. This rather conservative policy reflects the idea that highest class packets are to be given utmost priority. In the PU variant, a packet of a given class is not accepted only if there is truly no space available given the necessity to structure the buffer pool for deadlock prevention; thus it is less discriminatory than the PD policy.

The m (user) buffers are organized as a FIFO queue and are not classified. When a new packet is generated by a user, the following algorithm is executed:

if the buffers in B_0 are entirely occupied, then the packet is lost; otherwise, the packet is enqueued in B_0. If there is space available among the $B_0 - m$ buffers of the PRU, then the packet is enqueued there; otherwise, it is stored in one of the m (user) buffers. Note that, due to the successful transmission and reception of packets, a buffer in the set $B_0 - m$ may become free and available for a new packet at a future point in time. At that time, and if the m (user) buffers are not entirely empty, then the head-of-queue of the user buffer is transferred to the free PRU buffer. Thus, packets from the user buffer are always 'pushed up' to the PRU buffer if there is space available. For the case of $B_0 - m = 0$, when the B_T (PRU) buffers are all empty, the head-of-queue of the packets stored in m may be considered for transmission.

The order of service of packets among the packets in the $B - m$ buffers is according to highest class first. It is clear that among packets of the highest class any order may be imposed; here we use a FCFS discipline. Note that servicing packets according to their class may result in a distribution of packet delay different from that of a global FCFS discipline over all packets irrespective of class. The performance of the global FCFS discipline may be desirable (since in this case, there is no discrimination on the basis of class), but the discipline is deadlock-prone in general. In an attempt to reach the performance of the global FCFS scheme but remain deadlock-free, we propose here a deadlock-free scheme which performs similarly to FCFS with a sufficiently large number of buffers. This scheme is referred to as SBP with threshold service (TSBP). In TSBP, buffers subsets 1 through $h_{max} - 1$ consist of a single buffer. The classification of packets and the packet acceptance conditions are the same as that of the SBP scheme but the service discipline is altered as follows: service is FCFS over all packets irrespective of class as long as the total number of packets does not exceed a threshold T. If the threshold T is exceeded, then service is according to highest class first. For a

total of $B - m$ buffers in a given PRU queue, deadlock-free operation is ensured by limiting T to at most $B - m - h_{max} + 1$. In the sequel, we consider only the case $T = B - m - h_{max} + 1$. It is clear that as B and T increase, the order of service approximates FCFS more closely, and that for B and T infinite, the order of service is exactly FCFS.

4.3 Network Structure and Measures of Performance

The same regular networks and uniform traffic requirements described in chapter 3 are considered here. As before, the performance of the network is measured by means of the network throughput and the average packet delay. For given γ, G, B_0, m, and B_T, the total end-to-end network throughput is denoted $S(\gamma, G, B_0, m, B_T)$, and the average packet delay is denoted $D(\gamma, G, B_0, m, B_T)$. $\bar{n}$ denotes the average number of hops. In addition to throughput and delay, we define the following measures (the same for all PRUs) which are useful in interpreting the numerical results:

$P_c(\gamma, G, B_0, m, B_T)$, the probability that a packet transmitted by a node is not accepted at the intended receiver due to a collision (i.e., interference over the channel);

$P_b(\gamma, G, B_0, m, B_T)$, the probability that a packet transmitted by a node is received free from interference at its intended receiver, but is rejected due to a lack of buffer storage space at that intended receiver;

$P_l(\gamma, G, B_0, m, B_T)$, the probability that an external packet is lost due to the network access flow control mechanism (i.e., all B_0 buffers occupied); and finally,

$r(\gamma, G, B_0, m, B_T)$, the average number of packet transmissions (successful or not) undertaken by a PRU per packet transmission time.

In the sequel, we will suppress the arguments γ, G, B_0, m, B_T, where no ambiguity results.

The following relations hold:

$$S = \frac{N}{\bar{n}} r(1 - P_b - P_c) \tag{4.1}$$

$$S = \gamma(1 - P_l), \quad B_0 < \infty. \tag{4.2}$$

4.4 Numerical Results

4.4.1 General Network Behaviour

We consider the general network behaviour for two cases of structuring the buffers in the set B_0, namely,

(a) no sharing of buffer storage between new and transit packets ($B_0 = m$),

(b) new and transit packets share all buffers in the set B_0 ($m = 0$).

4.4.1.1 No sharing ($B_0 = m$)

Consider first the case of $B_0 = m = \infty$. In this case, the general behaviour of the network is similar to the behaviour seen in the previous chapter except for the additional effect of B_T. Due to the uniform traffic requirement, the balanced routing, and the fact that for $B_0 = m$, all new packets contend equally for service by the PRU, all source-destination pairs have equal end-to-end throughput and the end-to-end packet delay for paths of equal length is the same. Let $S(\gamma, G, m, B_T)$

denote the network throughput for γ, G, m, and B_T. Let $\gamma = \infty$ (i.e, heavy traffic conditions exist). In this case, it is guaranteed that all queues in the network are non-empty, and hence there is always a packet to be transmitted at every scheduling point. Therefore the mean service time X_k for a packet of class k (the expected time from when the packet is first considered for transmission until it is successfully received by its immediate destination) is finite and constant over time. Let X be the mean service time averaged over all packet classes. X is determined by the network topology, the access scheme and the scheduling rate G (as in the previous chapter), as well as the buffer management scheme and the transit buffer size B_T (since B_0 is always entirely occupied by new packets). The $\lim_{\gamma \to \infty} S(\gamma, G, m, B_T)$ is thus the same irrespective of the value of m and is denoted by $C(G, B_T)$. Note that in the case of separate queues per link, $C(G, \infty)$ for all variants of the SBP and TSBP schemes is the same as the capacity $C(G)$ derived in the previous chapter for networks with infinite buffers. This is because for $B_T = \infty$, $P_b = \mathbf{0}$ and thus neither the packet acceptance policy nor the order of service affects the successful acceptance of packets over the channel. The order of service does however affect packet delay; refer to subsection 4.4.4.

It is evident that for $\gamma \leq C(G, B_T)$, we must have $S = \gamma$, and, since heavy traffic conditions exist whenever the input traffic rate γ exceeds the network throughput S, for $\gamma > C(G, B_T)$, $S = C(G, B_T)$. When $\gamma < C(G, B_T)$ we say that the network is underloaded, since the average number of buffered new and transit packets is finite and the average delay is bounded. When $\gamma \geq C(G, B_T)$ we say that the network is overloaded, since the average number of buffered new packets increases linearly with time and average delay grows without bound. For the case where $m < \infty$, new packets may be lost when all m buffers are occupied, leading to a situation where S is always below γ. Hence a delineation between underload and overload states like the one above does not hold. However, it is expected that for a sufficient number

of B_0 buffers, the network behaviour is very similar to that of the infinite B_0 case.

In the remainder of this chapter unless stated otherwise, a representative example network consisting of a six PRU ring topology, with the C-BTMA protocol, the HSF buffer scheme, the PD placement policy and a single queue per PRU is assumed. In addition, since the effect of propagation delay has been extensively studied in the previous chapter, throughout the remainder of this chapter it is assumed that the ratio of propagation delay to packet transmission time (a) = 0.01. The network behaviour for the case of $m = \infty$ is seen in figure 4.4 where network throughput versus offered input traffic rate is plotted. As in the previous chapter, the scheduling rate G has an important effect on the throughput asymptote $C(G, B_T)$. For every value of B_T, $C(G, B_T)$ is maximized by a particular value of G denoted $G^*(B_T)$ (or G^* where no ambiguity results). The effect of G is illustrated in figure 4.5 where we plot $C(G, B_T)$ versus G for various values of B_T. Recall that in order to obtain deadlock-free operation, the minimum value of B_T required is $h_{max} - 1$, which is equal to 2 for the example network under consideration. We observe that $C(G^*, B_T)$ for the case of $B_T = 2$ is reduced by a factor of 2 over that for the case of $B_T = \infty$. This indicates that the transit buffer size B_T has a significant impact on achievable performance. Figure 4.5 also indicates that for B_T larger than some threshold, little improvement in performance is to be had. In this particular case, as B_T increases from 40 to ∞, a performance increase of $< 5\%$ is obtained. Note that $G^*(B_T)$ increases with B_T and reaches a finite value $G^*(\infty)$ as $B_T \rightarrow \infty$. In general, the effect of B_T on performance will depend on the particular topology and channel access protocol.

As stated earlier, for $m < \infty$ new packets may be lost due to a lack of input buffers; this results in a throughput S which is lower than the offered traffic rate γ for all values of γ. This effect is shown in figure 4.6 where S is plotted versus

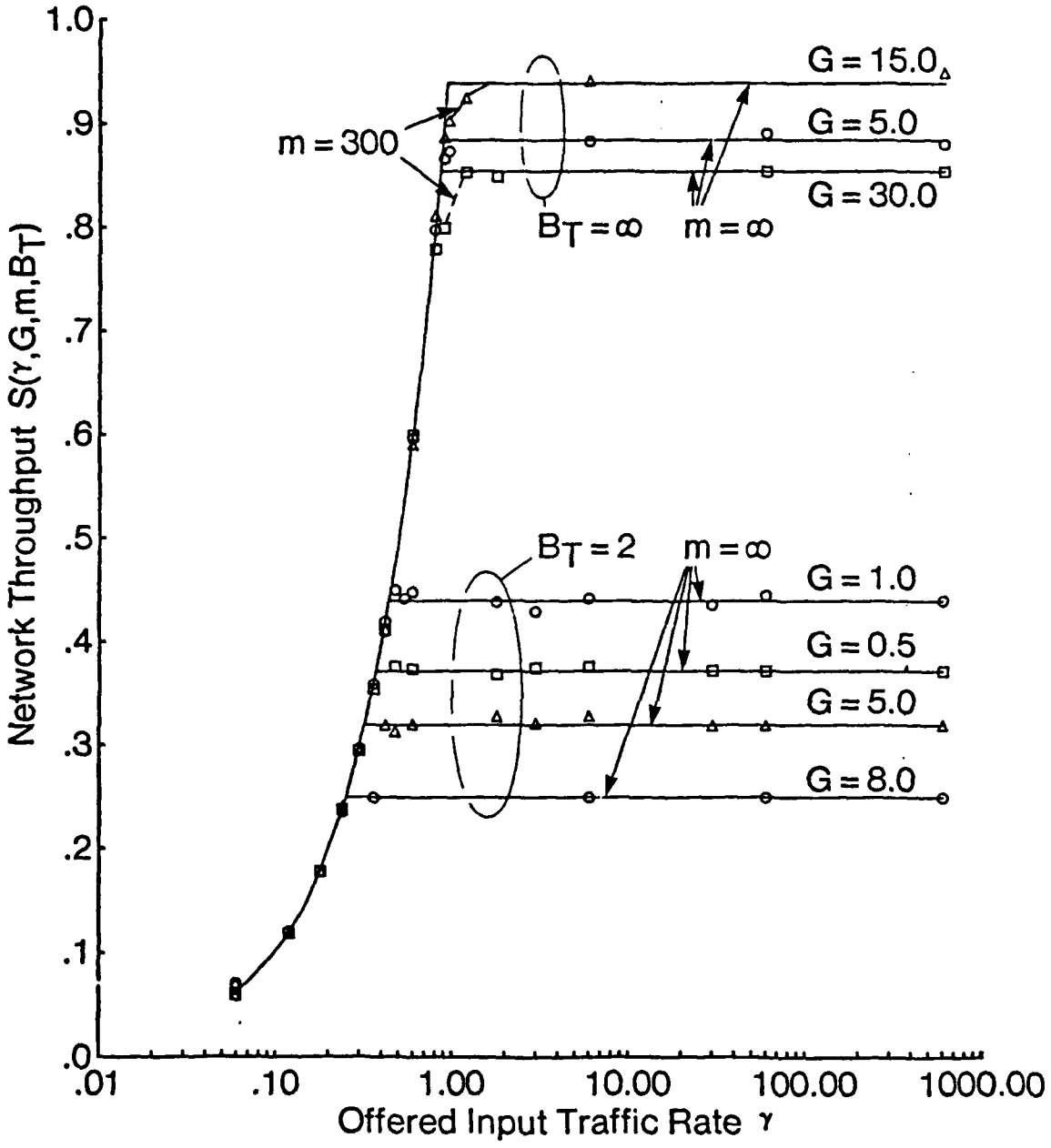

Fig. 4.4 Network throughput versus offered input traffic rate in a six PRU ring network, with the C-BTMA protocol, the HSF buffer scheme, a single queue per PRU, and various values of scheduling rate G and transit buffer size B_T.

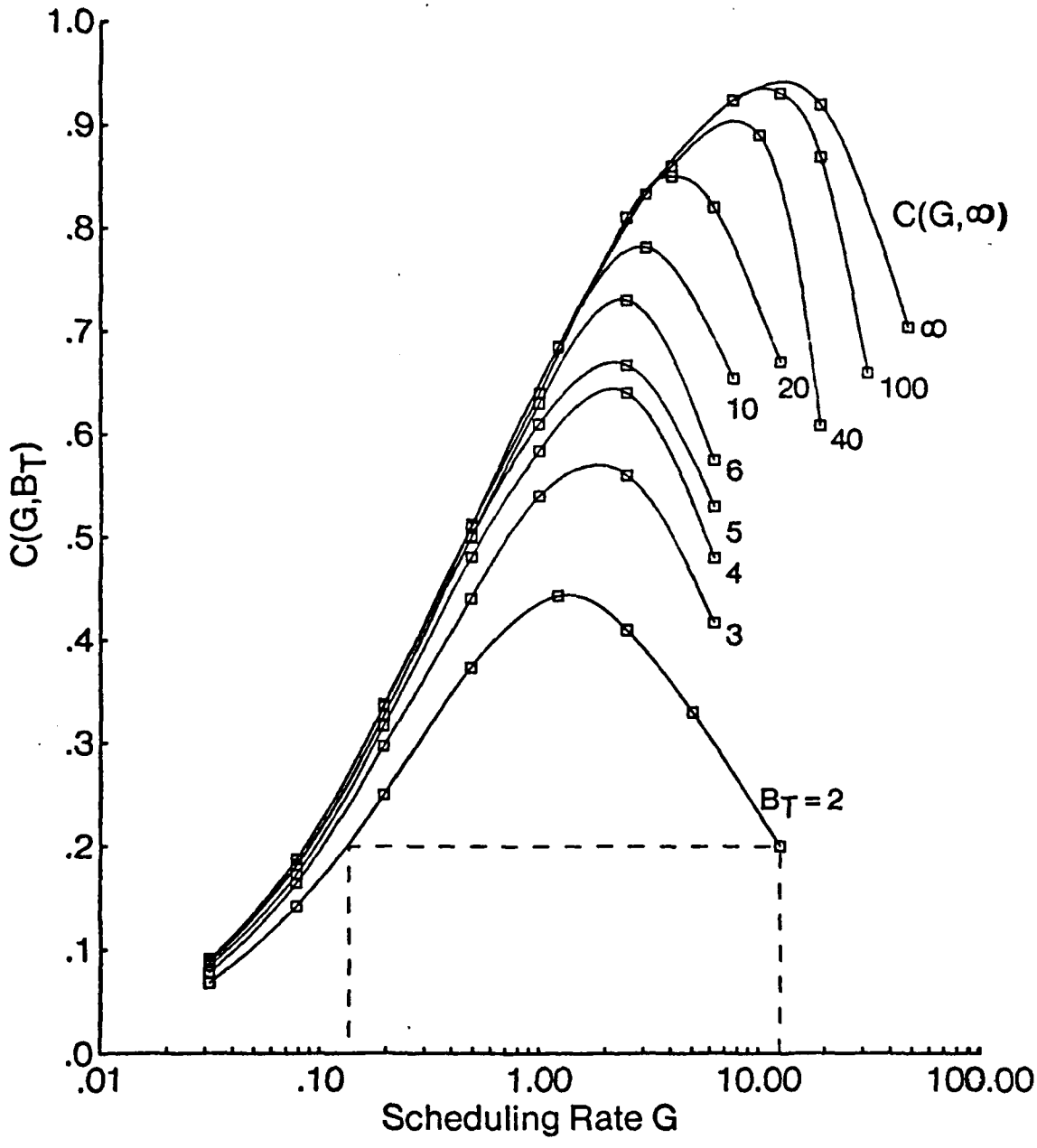

Fig. 4.5 $C(G, B_T)$ versus nodal scheduling rate G in a six PRU ring network, with the C-BTMA protocol, the HSF buffer scheme, a single queue per PRU, and various values of B_T.

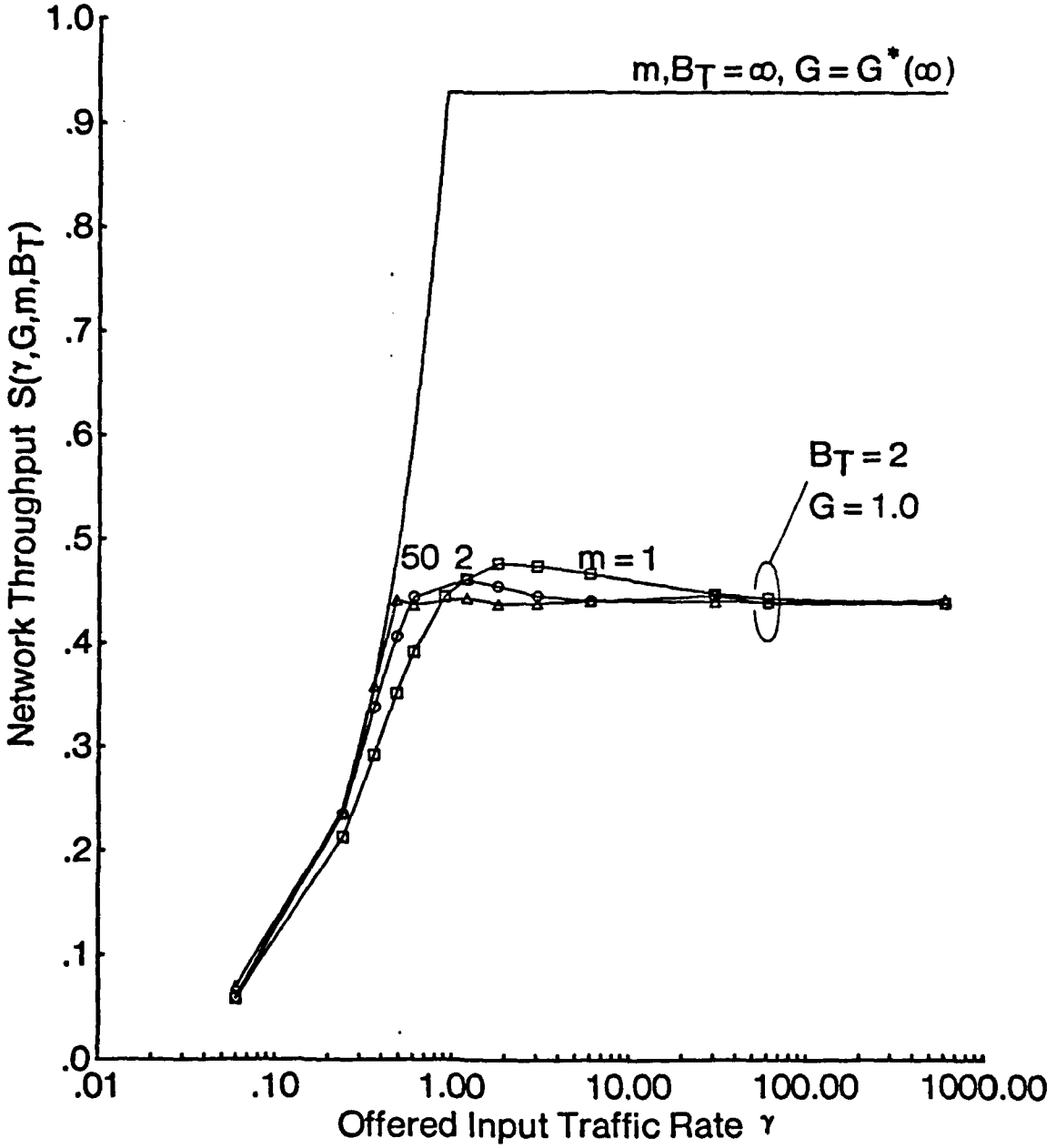

Fig. 4.6 Network throughput versus offered input traffic rate in a six PRU ring network, with the C-BTMA protocol, the HSF buffer scheme, a single queue per PRU, $B_T = 2$, $G = 1$, and various values of m.

γ for various values of m. It is interesting to observe that for given values of B_T and G, with m finite, S may exceed $C(G, B_T)$ for certain values of γ (while never exceeding $C(G^*, \infty)$). This effect (most pronounced for $m = 1$) is due to the fact that certain PRU's, having lost new packets, will be less likely to attempt transmission at scheduling points and therefore

(i) are less likely to interfere with other ongoing transmissions, and

(ii) are less likely to transmit packets which may require buffering at a neighboring node; this causes more buffer storage space to be available for the buffering of transit packets already in the network.

The above effects result in reductions in r, P_c and P_b. Clearly, for specific combinations of γ, G, and B_T, the decrease in $P_b + P_c$ outweighs the decrease in r leading to the behaviour of figure 4.6 (see equation 4.1). Which of P_b and P_c has the greatest impact on performance depends on the particular network under consideration. In the example considered here, the improvement in throughput is caused primarily by the reduction in P_b, as can be seen from figure 4.7 in which we plot P_b, P_c and r as a function of γ. For the same network but using the CSMA access scheme instead of C-BTMA, the opposite is true. This can be seen in figure 4.8 in which we plot S, P_b, P_c and r versus γ for CSMA with $G = 0.01$ and $m = 1$. We observe that for γ large the value of P_b is small (thus little improvement is to be had by decreasing P_b), while P_c on the other hand is large. In general, for examples where the value of P_b is significant, the network is said to be *storage bound.* For examples where the value of P_b is small (and P_c is large) performance is said to be *channel bound.* (This issue is addressed further in section 4.4.3). The case of $m = 1$ is further examined in figure 4.9 in which we plot throughput versus traffic rate for various values of G. Consider two values of G, (namely, $G_1 = 0.15$ and $G_2 = 12.5$) such that $G_1 < G^*(2) < G_2$ (where $G^*(2) = 1.0$) and $C(G_1, 2) = C(G_2, 2)$. Note that

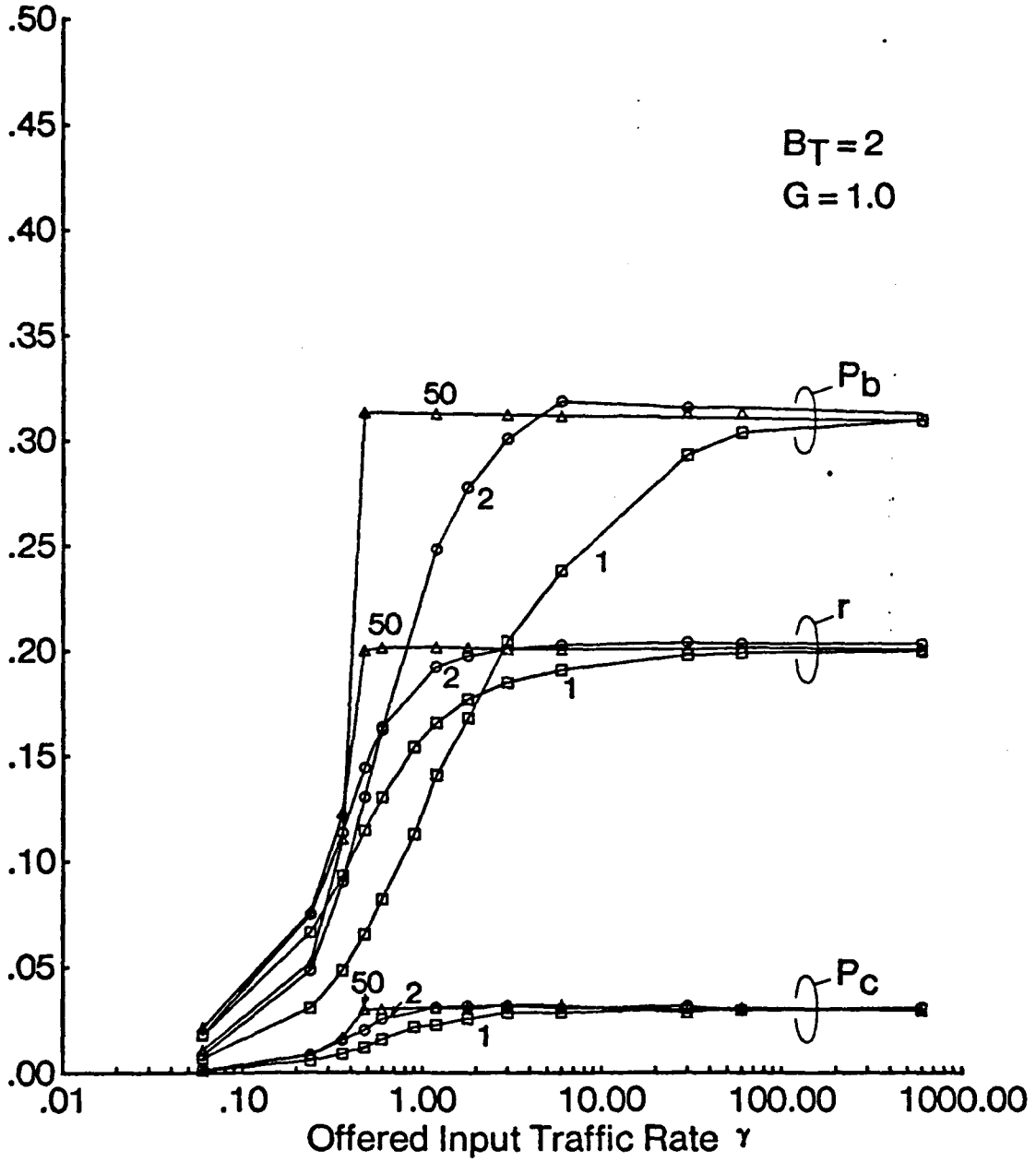

Fig. 4.7 P_c, P_b and r versus offered input traffic rate in a six PRU ring network, with the C-BTMA protocol, the HSF buffer scheme, a single queue per PRU, $B_T = 2$, $G = 1$, and various values of m.

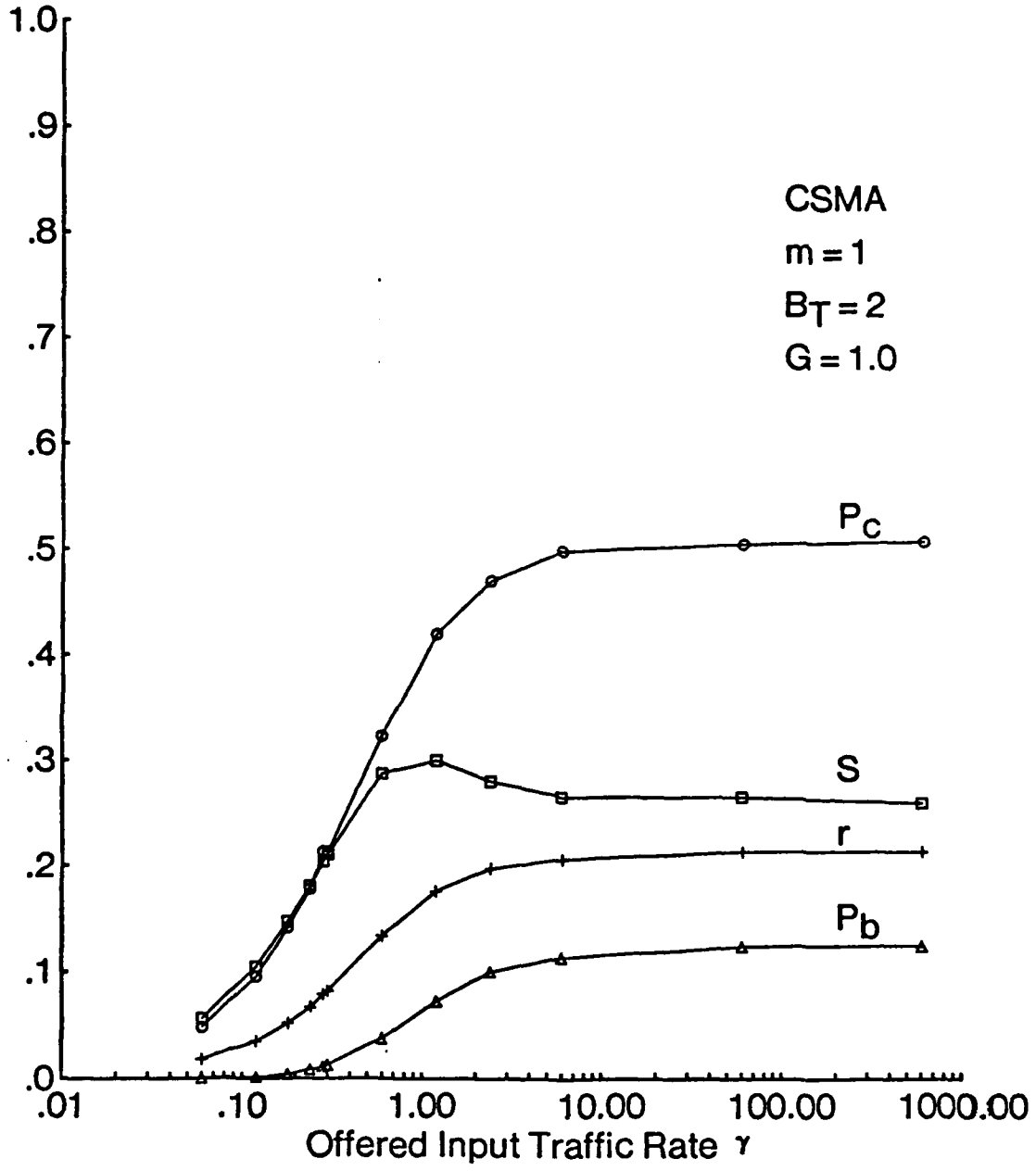

Fig. 4.8 S, P_c, P_b and r versus input traffic rate γ in a six PRU ring network, with the CSMA protocol, the HSF buffer scheme, a single queue per PRU, $B_T = 2$, $m = 1$, and $G = 0.01$.

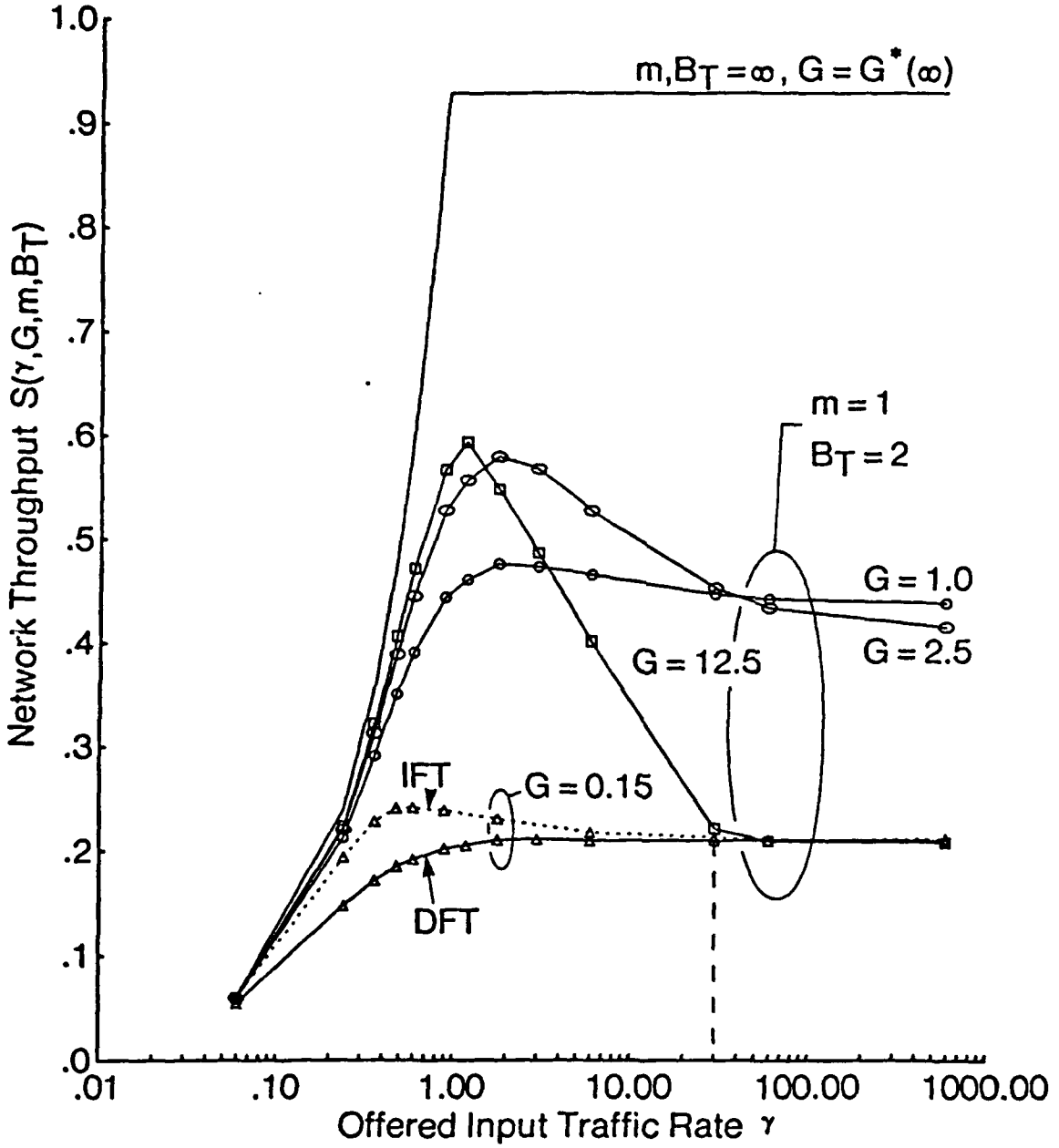

Fig. 4.9 Network throughput versus offered input traffic rate in a six PRU ring network, with the C-BTMA protocol, the HSF buffer scheme, a single queue per PRU, $B_T = 2$, $m = 1$, and various values of G.

for $\gamma > 30.0$, the throughputs corresponding to G_1 and G_2 are approximately the same, but the behaviour for each differs considerably over the range of $\gamma < 30.0$. Clearly, too small a value of G (namely G_1) tends to cause long scheduling delays before a transmission may be attempted. A new packet may therefore remain in the user buffer for long periods of time (with the channel idle), and block acceptance of other new packets; this leads to an excessive value of P_l and a reduction in throughput (refer to equation 4.2). The behaviour seen for $G = G_1$ occurs in part because the scheduling algorithm (described in chapter 2) corresponds to a delayed first transmission (DFT) protocol. For $G = G_1$, P_l may be reduced somewhat by means of an immediate first transmission (IFT) protocol, whereby a packet is transmitted immediately if it arrives at an empty PRU. A graph of S versus γ for the IFT case and $G = G_1$ is depicted in figure 4.9. For the IFT case and $G = G_2$, there is little difference as compared with the DFT case; for γ large (> 30 in this case), the throughput of the DFT scheme is slightly greater than that of the IFT scheme. For a detailed discussion of the DFT and IFT protocols refer to [16] and [17]. Consider now a fixed value of γ. As G increases from a value $< G^*(2)$, S increases and achieves a maximum at some value of $G \geq G^*(2)$. In this case, the network achieves its maximum throughput, maximized over both G and γ, for the value of $G = G_2$. To show that the long sojourn times of new packets in the user buffer is indeed the cause of the excessive value of P_l, we plot in figure 4.10 S versus average buffer occupancy over all B buffers for the same case. We also show the constant γ contours. This graph indicates that, for γ constant and < 1.2, a reduction in average buffer occupancy occurs as G increases. This is because as G increases, the average scheduling delay is reduced, resulting in a shorter sojourn time for new packets in the user buffer. The latter causes a reduction in P_l and hence an increase in throughput S.

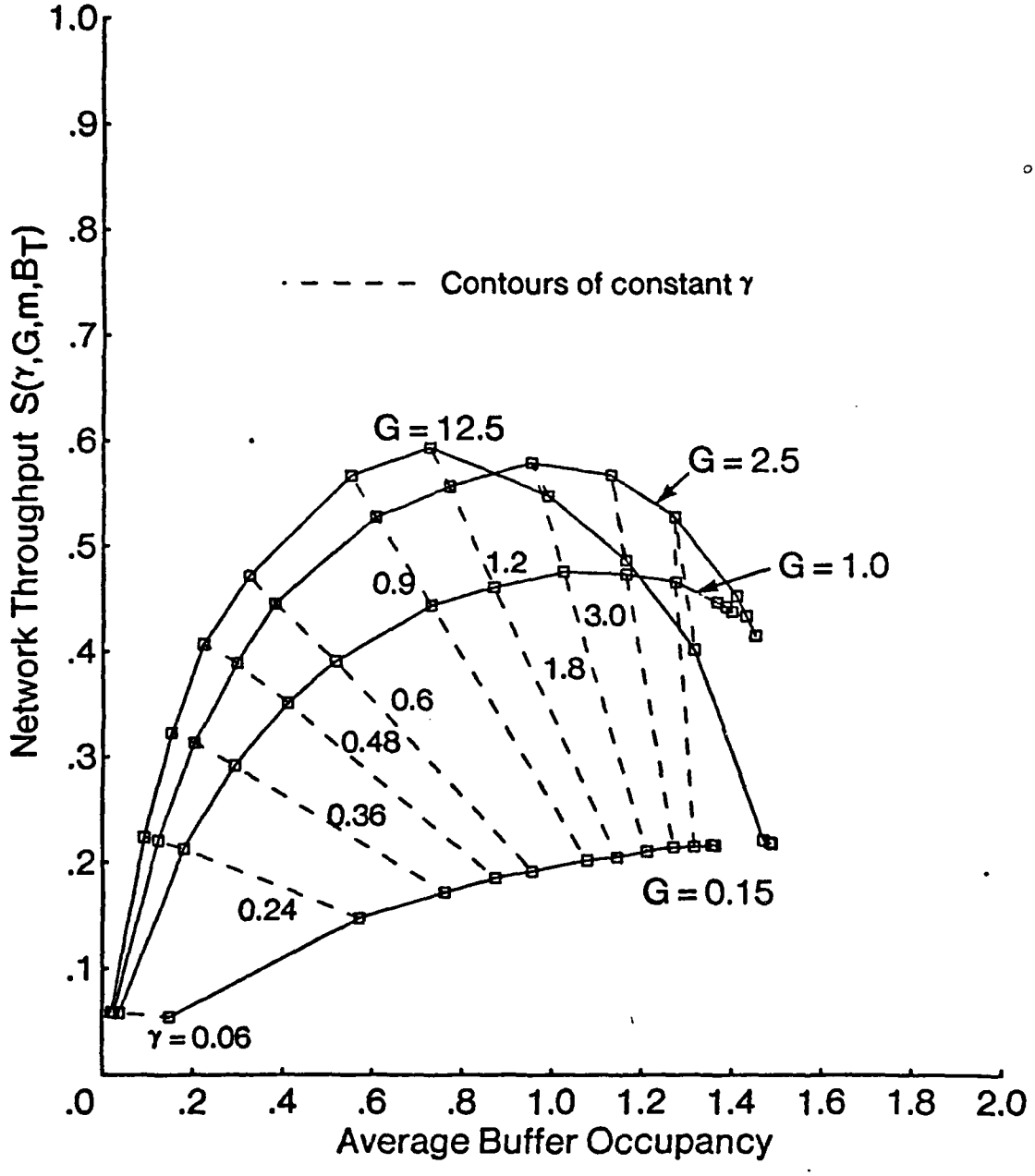

Fig. 4.10 Network throughput versus average buffer occupancy in a six PRU ring network, with the C-BTMA protocol, the HSF buffer scheme, a single queue per PRU, $B_T = 2$, $m = 1$, and various values of G.

4.4.1.2 New and transit packets share B_0 ($m = 0$)

For $B_0 - m > 0$, as will be seen from the discussion below, the overall network behaviour for the HSF and HTG schemes differs. Consider first the case of the HSF scheme. In this case, all new packets are classified as class 0, and hence for a given source PRU new packets corresponding to each destination have equal access to both the PRU buffers and the transmitter irrespective of the value of B_0 and m. Therefore, given the uniform traffic requirement and the balanced routing scheme, the end-to-end throughput for all source-destination pairs is the same. Consider the case of $m = 0$. Assume now that $B_0 = \infty$ and B_T is finite. For any value of $\gamma < C(G, \infty)$, a throughput of $S = \gamma$ is achieved since transit packets are able to utilize buffers in the set B_0 and hence are accepted without limitation; thus the network is underloaded. For $\gamma > C(G, \infty)$, the network is overloaded and the set B_0 tends to be occupied primarily by new packets. For a given γ ($> C(G, \infty)$ but finite), there is a non-zero probability that transit packets may occupy a subset of B_0 thus increasing the 'effective' B_T; however, as γ increases further, a larger number of new packets is accepted which compete with transit packets, reducing the effective B_T. At $\gamma = \infty$, all B_0 buffers are occupied by new packets and the effective B_T is exactly B_T. In summary, for $\gamma \leq C(G, \infty), S = \gamma$; and for $\gamma > C(G, \infty), S < C(G, \infty)$ but is $> C(G, B_T)$ and approaches the limit $C(G, B_T)$ as $\gamma \rightarrow \infty$. This behaviour is depicted in figure 4.11 for $B_T = 2$ and various values of G. (Clearly similar behaviour will be seen for the case of $B_0 - m = \infty$ for any value of m.) If B_0 is finite, then the maximum throughput attained lies between $C(G, 2)$ and $C(G, \infty)$ depending on the exact value of B_0. This is shown in figure 4.12. The special case of $B_0 = 1$ ($m = 0$) is expected to be rather similar to the case $B_0 = m = 1$ which was previously shown in figure 4.9. The results for $B_0 = 1$ and various values of G are plotted in figure 4.13. Comparing figures 4.13 and 4.9 we see that the shapes of the curves are generally similar. For the same G, a slightly

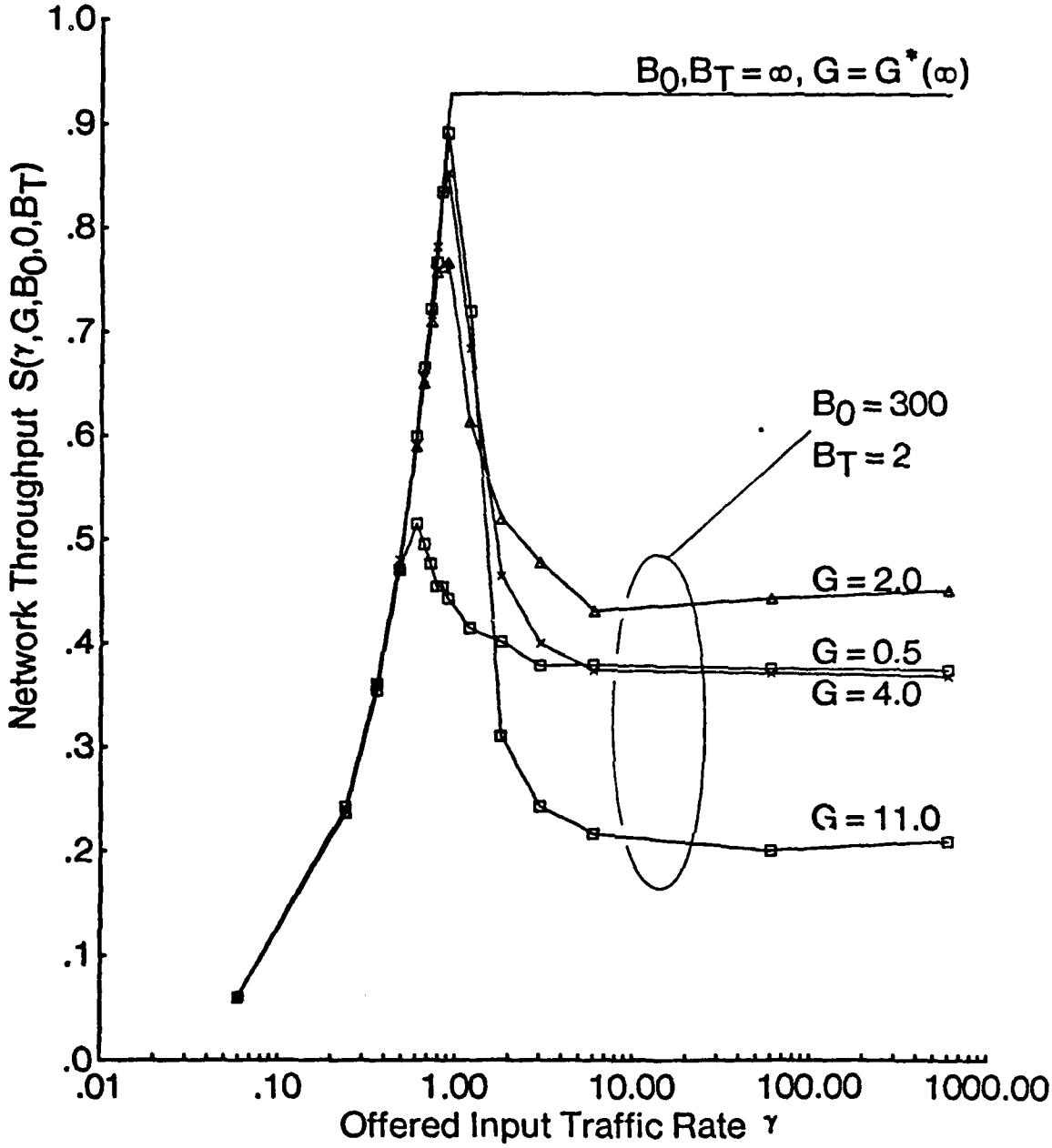

Fig. 4.11 Network throughput versus offered input traffic rate in a six PRU ring network, with the C-BTMA protocol, the HSF buffer scheme, a single queue per PRU, $B_0 = 300$, $B_T = 2$, and various values of G.

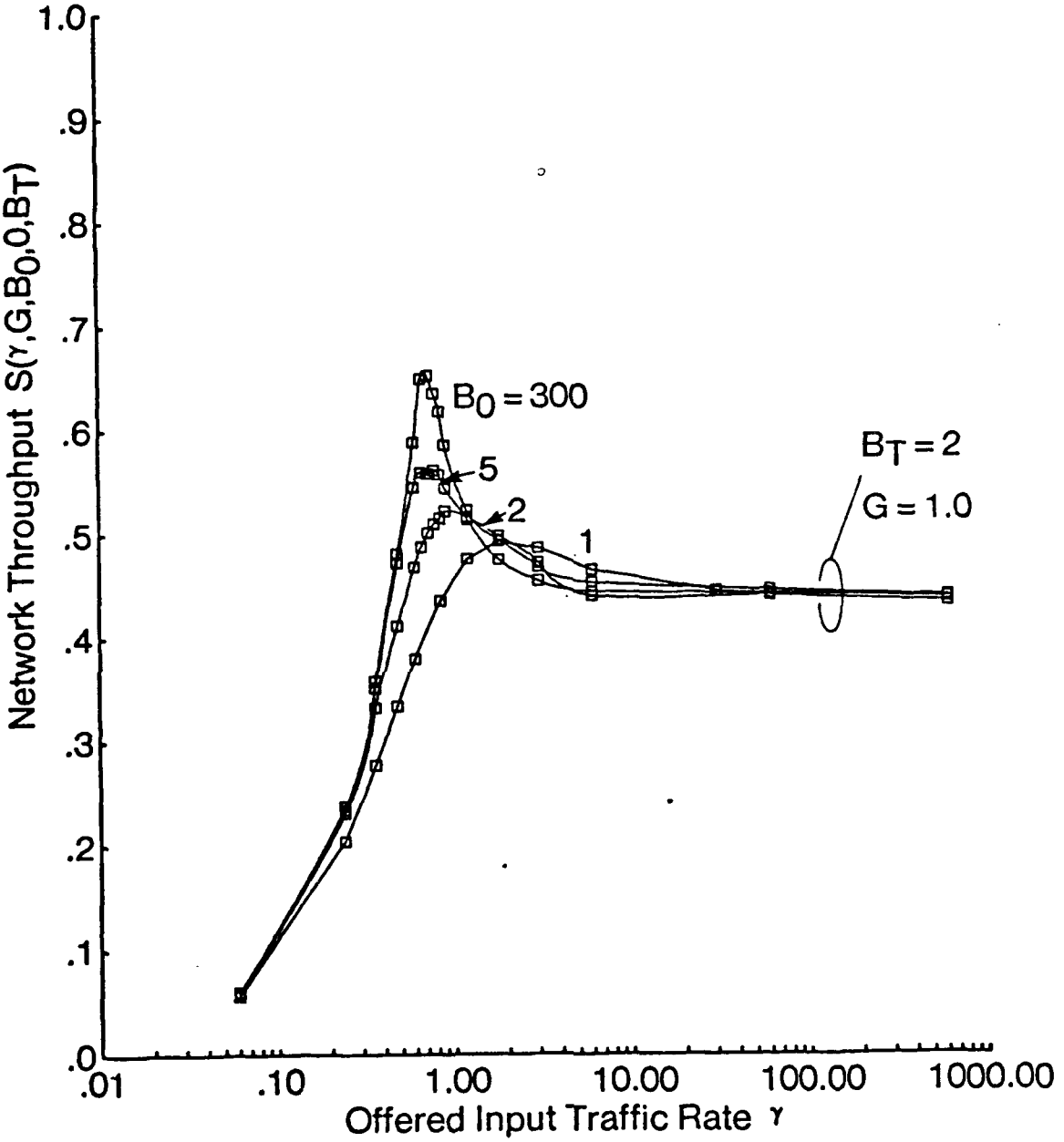

Fig. 4.12 Network throughput versus offered input traffic rate in a six PRU ring network, with the C-BTMA protocol, the HSF buffer scheme, a single queue per PRU, $B_T = 2, G = 1.0$, and various values of B_0.

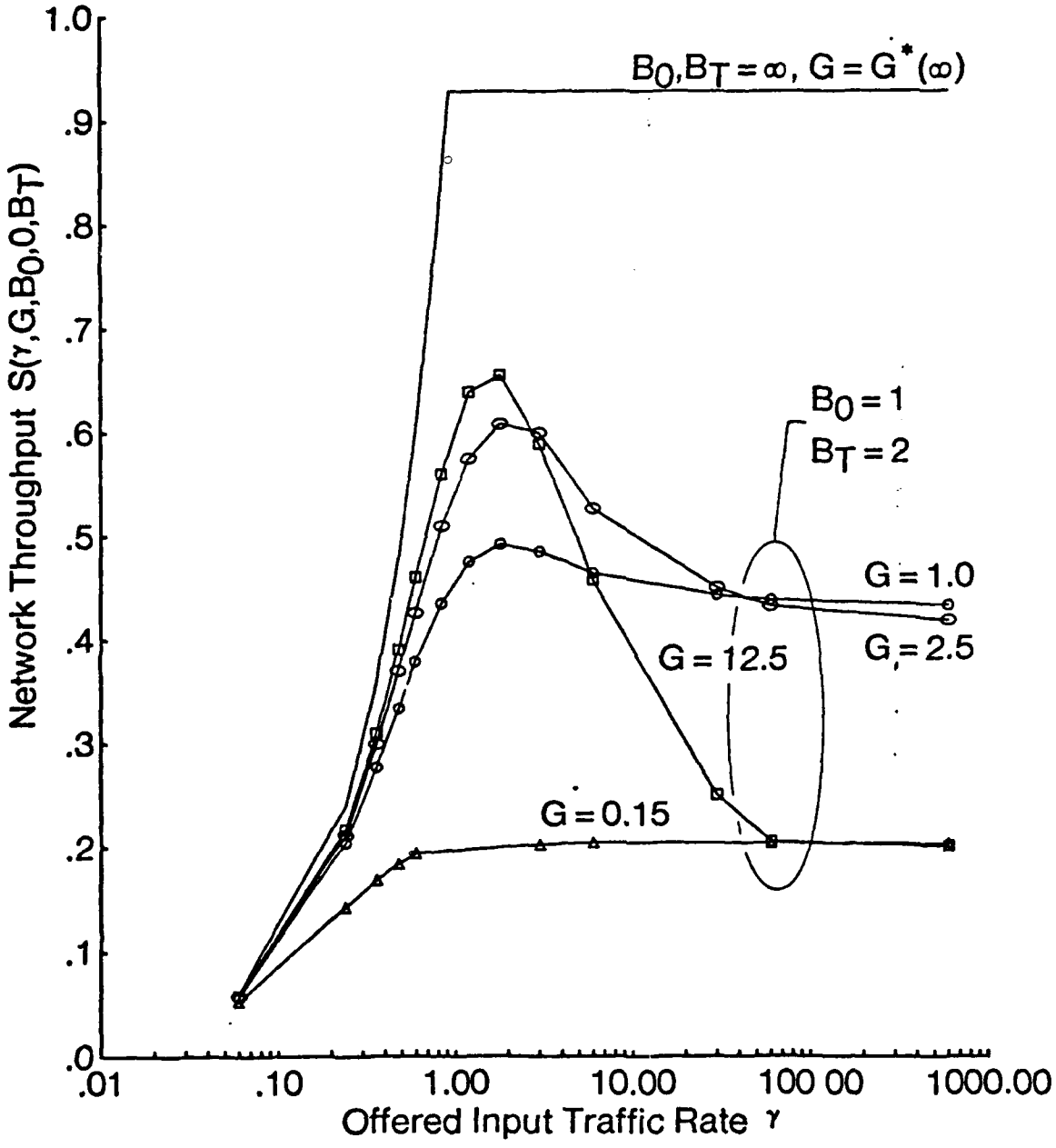

Fig. 4.13 Network throughput versus offered input traffic rate in a six PRU ring network, with the C-BTMA protocol, the HSF buffer scheme, a single queue per PRU, $B_T = 2, B_0 = 1$, and various values of G.

higher throughput is achieved in figure 4.13 for the $B_0 = 1$ case due to the sharing of the single B_0 buffer by both new and transit packets.

We now consider the case of the HTG scheme. In this case, a new packet may be of class 0 through $h_{max} - 1$. Indeed, new packets associated with source-destination pairs that are i hops apart are of class $h_{max} - i$; thus, given the fact that packets in $B - m$ are serviced according to their class as described in section 2, access for new packets to both the PRU buffers and the transmitter is a function of their ultimate destination. In particular (for $B_0 - m > 0$), packets that travel shorter distances receive higher priority service than packets that travel longer distances. (For $B_0 = m$, new packets are processed according to the FCFS discipline which ensures equal access to the PRU buffers and transmitter for all new packets irrespective of their final destination. Thus each source-destination pair achieves the same end-to-end throughput as every other.) In certain cases (as described below), this may result in discriminatory behaviour. A fair allocation of resources may be accomplished by means of a simple modification, namely, distinguishing between new and transit packets, and treating all new packets as if they were class 0. Consider the latter fair scheme and $B_0 - m = \infty$. Let γ_i and S_i denote the offered traffic and the network throughput respectively for packets that travel i hops. Note that $\sum_{i=1}^{h_{max}} \gamma_i = \gamma$ and $\sum_{i=1}^{h_{max}} S_i = S$. Let $\alpha_i = \gamma_i/\gamma,\ i = 1, \cdots, h_{max}$. In this case, for $\gamma < C(G, B_T)$, $S_i = \gamma_i$ and for $\gamma > C(G, B_T)$, $S_i = \alpha_i C(G, B_T)$. Note that $S_i/S = \alpha_i$ for all values of γ. Without the above modification to ensure fairness, as stated above, discriminatory behaviour may result. Consider the unmodified scheme with $B_0 - m = \infty$. The overall behaviour corresponding to this case is typical of priority queueing networks. As before, for $\gamma < C(G, B_T)$, $S_i = \gamma_i$. As γ increases beyond $C(G, B_T)$, the network capacity for successive classes of traffic beginning with traffic that travels h_{max} hops and ending with traffic that travels 1 hop is exceeded. Furthermore, sooner

or later S_i goes to zero, for $i = 2, \cdots, h_{max}$, as γ increases further. The fraction of the server capacity that was previously allocated to packets of class i is now divided equally among traffic of the remaining classes which in turn increases the throughput achievable by these traffic classes. Only the throughput associated with the traffic that travels 1 hop does not ultimately go to zero; in fact, $S_1 = \gamma_1$ until a value of throughput equal to the 1-hop capacity of the network is attained (which corresponds to the throughput achievable when traffic is destined to nearest neighbors only). Thereafter, it remains constant at that value. Both the above discriminatory and fair behaviour are seen in figure 4.14 for the example network and $B_T = \infty$. (For $B_T = \infty$ and the same value of G, the (S, γ) relationship for the fair HTG scheme is identical with that of the HSF scheme). Note that for the unmodified scheme, the overall behaviour for the case of $B_0 - m = \infty$ will differ from the case of $B_0 - m < \infty$. In the latter case, new packets contend equally for the finite buffers of $B_0 - m$, and the relationship between throughput and traffic rate is given by $S_i = \gamma_i(1 - P_l)$, so that $S_i/S = \alpha_i$ for all values of γ. The (S, γ) curves in this case would differ from those of the fair HTG scheme due to the non-zero value of P_l.

4.4.2 Variants of the SBP schemes

In this section we examine the effect of the variants of the SBP scheme considered in this study, namely:

(i) the 'push-up' (PU) and 'push-down' (PD) policies for the placement of packets within the structured buffer set,

(ii) the HSF and HTG packet classification schemes,

(iii) the threshold service (TSBP) scheme,

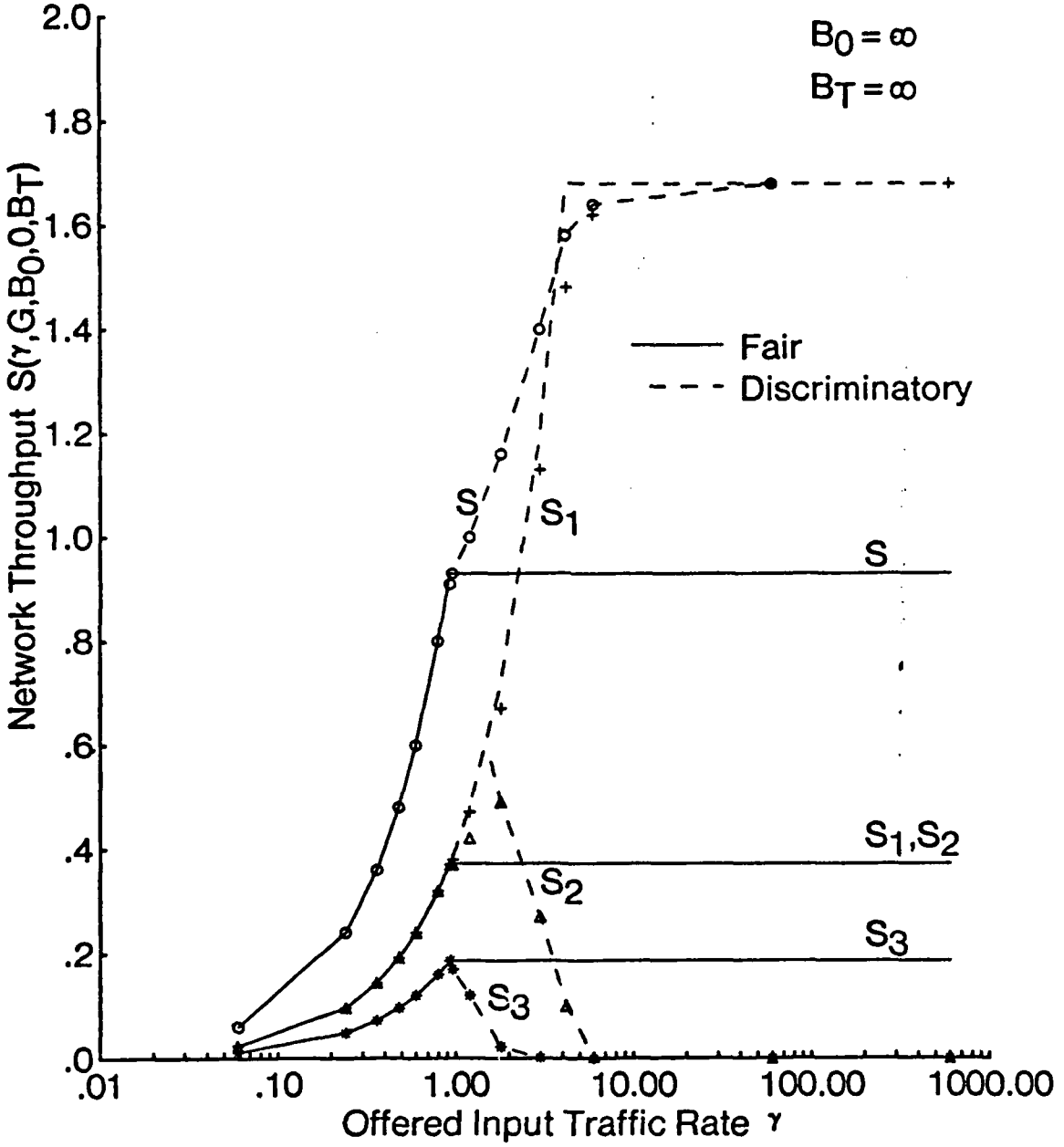

Fig. 4.14 Network throughput versus offered input traffic rate in a six PRU ring network, with the C-BTMA protocol, the HTG buffer scheme, a single queue per PRU, $B_0 = \infty$, $B_T = \infty$, and $G = G^*(\infty)$.

(iv) the separate queues per link and single queue per PRU outbound queueing structures.

Throughout this section we assume that $\gamma = \infty$. At this value of γ, as has already been stated, the network throughput S is exactly $C(G, B_T)$. For the case of $B_0 = m = \infty$ and given values of G and B_T, knowledge of $C(G, B_T)$ determines exactly the complete (S, γ) relationship. For a given value of B_T, the maximum throughput that the network can support is $C(G^*, B_T)$. We therefore limit this section to a study of the SBP variants on the basis of graphs which depict their $C(G^*, B_T)$ versus B_T performance. Note that, for the case of $B_0 > m$ and given values of G and B_T, in the HSF scheme and the modified HTG scheme of subsection 4.4.1.2 knowledge of $C(G, \infty)$ and $C(G, B_T)$ determines both an upper bound on S, and its limiting value as $\gamma \rightarrow \infty$, respectively.

We now compare the PU and PD placement policies for the HSF scheme with a single shared queue per PRU. We consider both the C-BTMA and CSMA access schemes. The results are depicted in figures 4.15 and 4.16 where $C(G^*, B_T)$ is plotted as a function of B_T for the six PRU ring and dodecahedron topologies. The PD scheme is consistently seen to be somewhat less efficient due to its more conservative placement policy. The difference in performance is, however, rather slight.

In figure 4.17, the HSF and HTG schemes are compared in the six PRU ring topology under C-BTMA for both the queue per neighbor and the single queue per PRU cases. The results indicate that the HTG scheme achieves a greater throughput than the HSF scheme. This is because of the particular form of prioritization in the HTG scheme, namely that packets which are within 1-hop of their final destination are serviced first. For such packets, P_b is always 0. In the HSF scheme, since order of service is according to distance travelled so far, the fact that a given packet may

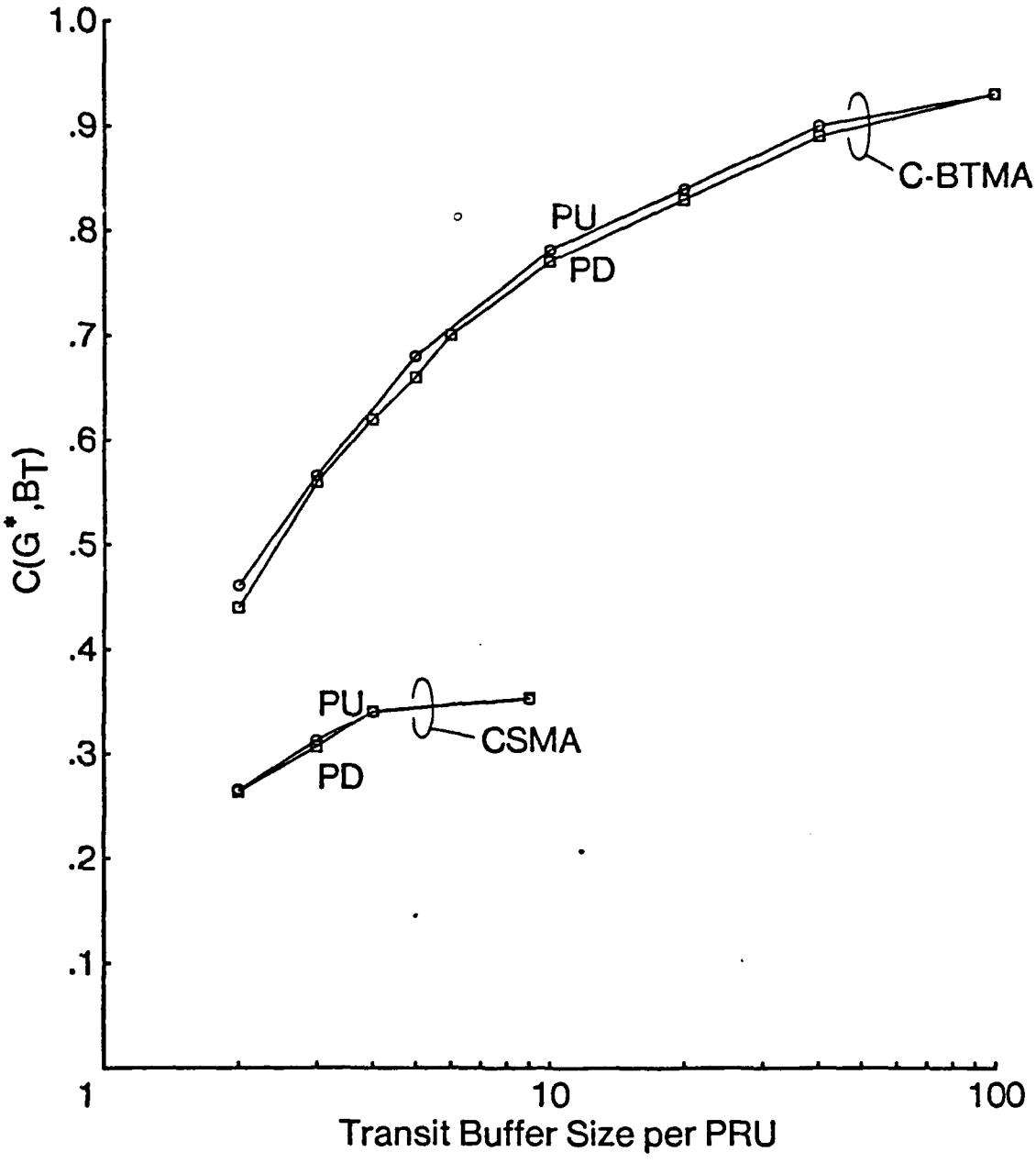

Fig. 4.15 $C(G^*, B_T)$ versus transit buffer size B_T in a six PRU ring network, under the C-BTMA and CSMA channel access protocols, with the HSF scheme, a single queue, for the PU and PD packet placement policies.

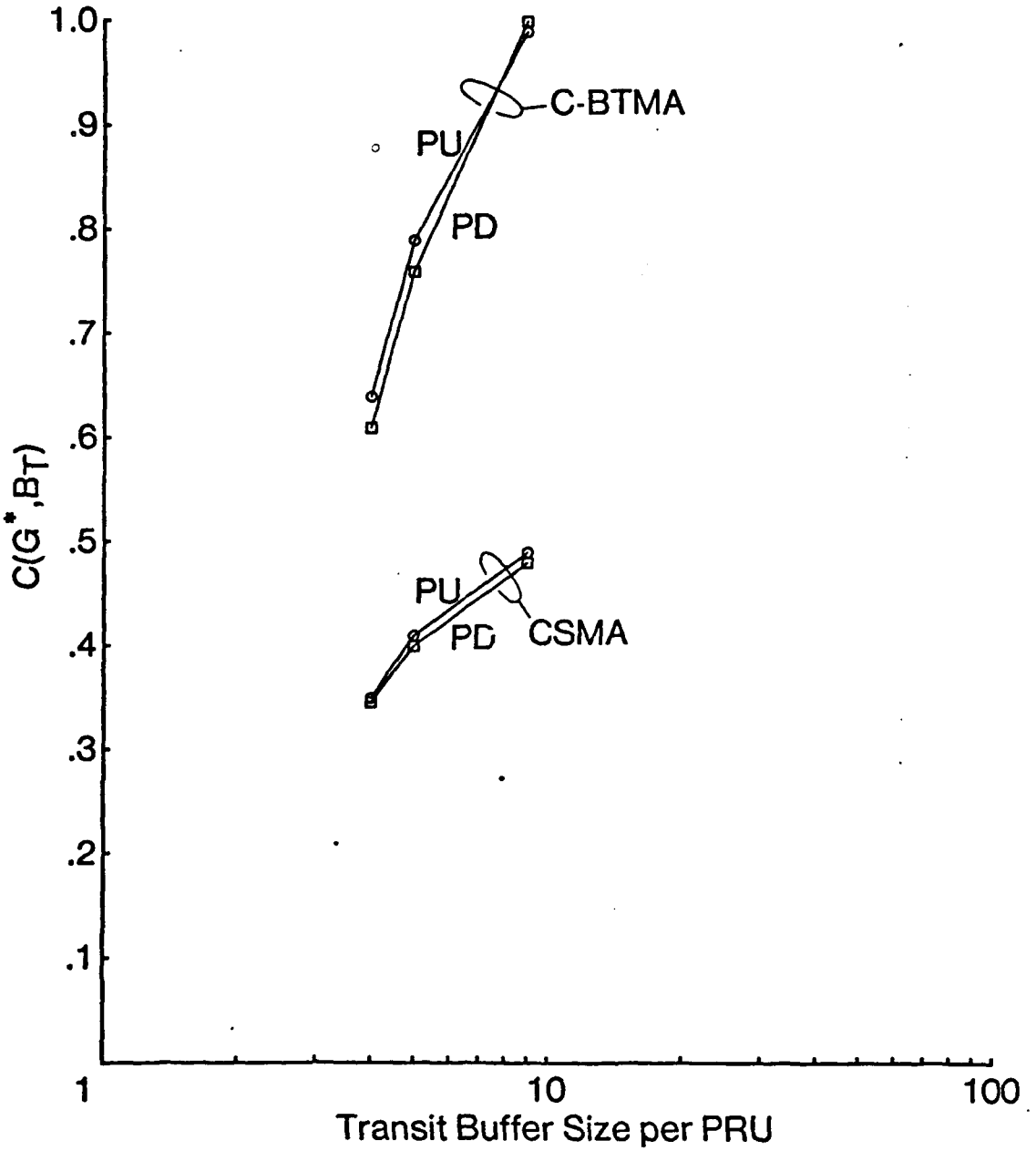

Fig. 4.16 $C(G^*, B_T)$ versus transit buffer size B_T in a dodecahedron network, under the C-BTMA and CSMA channel access protocols, with the HSF scheme, a single queue, for the PU and PD packet placement policies.

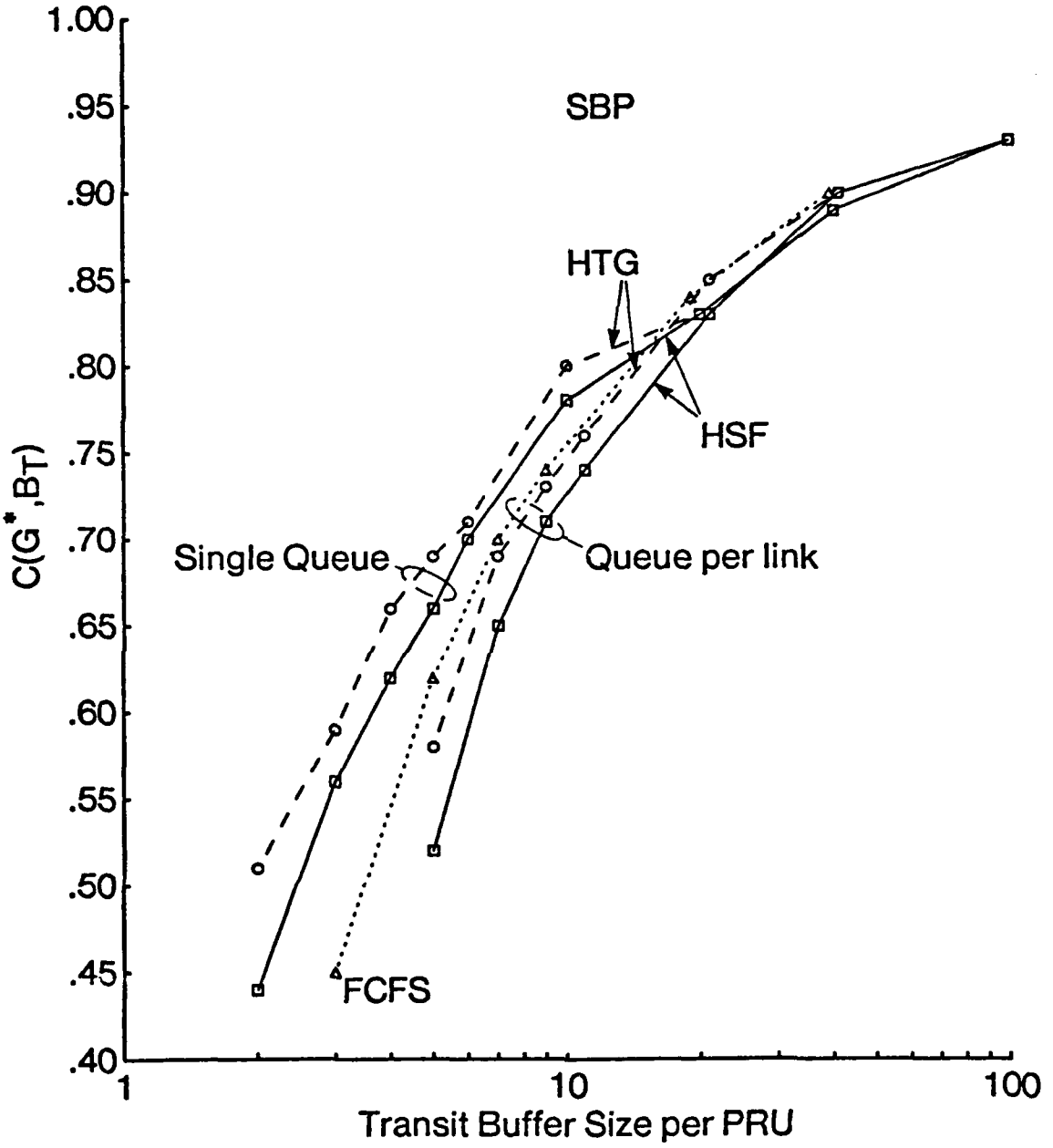

Fig. 4.17 $C(G^*, B_T)$ versus buffer size B_T in a six PRU ring network, under the C-BTMA protocol, for the HSF and HTG schemes.

be within 1-hop of its final destination is not taken into account. In general, the relative performance of these two schemes will depend both on the network topology and on the traffic pattern. Regarding the TSBP variant, we plot $C(G^*, B_T)$ versus B_T for both the HSF and HTG classifications and the single queue and queue per link structures in figure 4.18. These results are virtually identical to those of the SBP scheme in figure 4.17. It will be seen that the main difference between the TSBP and SBP schemes lies in their respective delay performances (refer to section 4.4.4). Note that in figures 4.17 and 4.18, for $B_T = \infty$ $P_b = 0$ and hence, given a queueing structure, in the SBP and TSBP schemes both the HSF and HTG variants achieve the same throughput. In many cases, for a given buffer management scheme the single queue and the queue per link structures achieve the same throughput at $B_T = \infty$, as exemplified in figures 4.17 and 4.18 for the C-BTMA access scheme. In certain other cases, as described below, each structure may achieve a different throughput. This is because of the difference in the scheduling process for packet transmissions that exists between the single queue and queue per link cases. Consider for the moment that the single queue scheme is employed. If a packet at the head-of-queue of a given PRU is not successfully received, then the same packet is reconsidered for retransmission until such time as it is successfully received. It is conceivable that during this time period another neighboring PRU might be idle, and if this information was known to the source PRU, a transmission to such a neighbor may be successful if it was allowed to take place. Clearly, in the queue per link scheme the above information may be exploited since each queue contends for access to the PRU's transmitter at every scheduling point. It turns out that only in the CASMA channel access protocol is information about the identity and state of neighboring nodes available to a PRU. For all other access protocols considered here this information is not available to a PRU; for these other schemes and $B_T = \infty$, each queueing structure achieves the same throughput in the regular

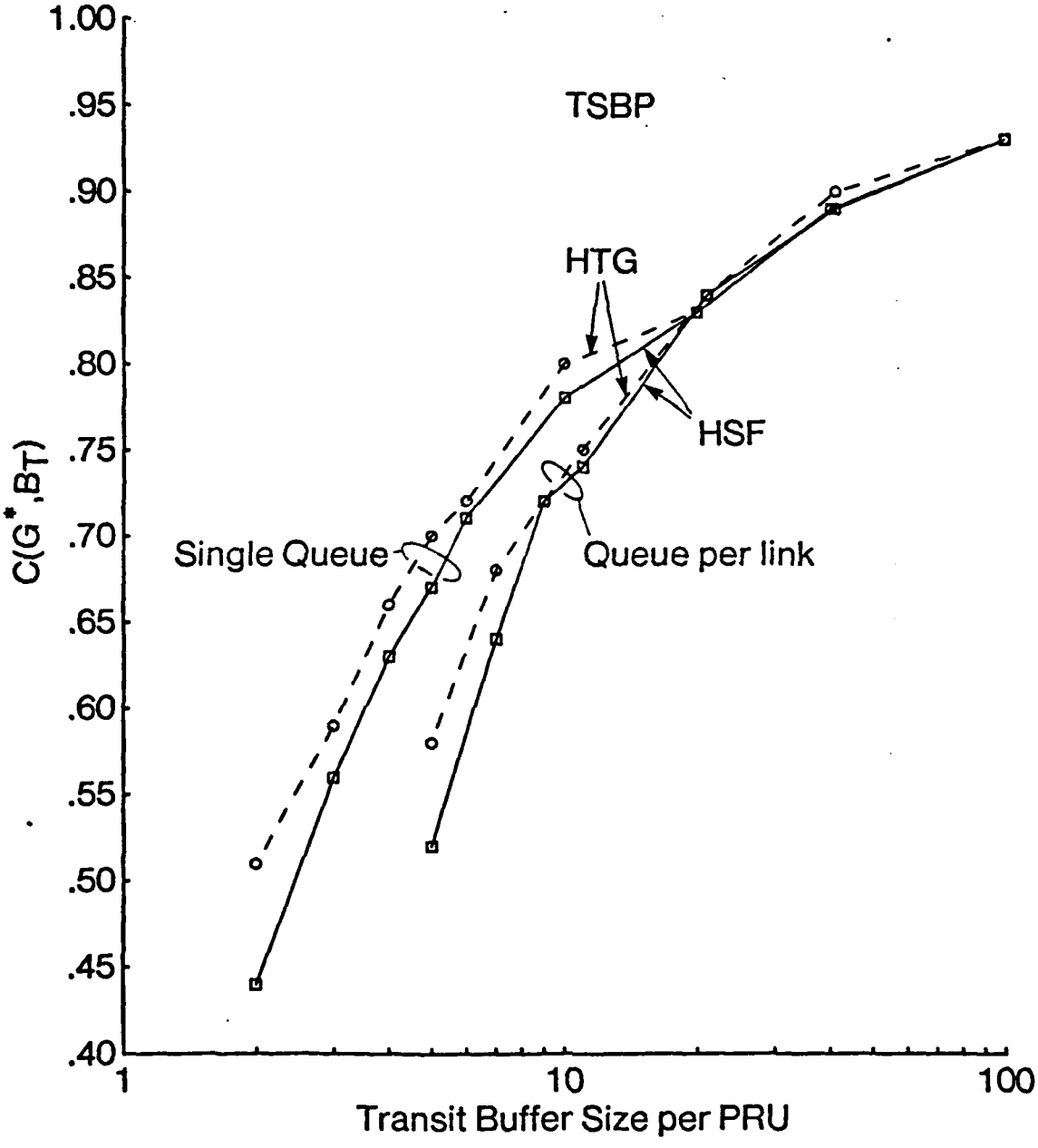

Fig. 4.18 $C(G^*, B_T)$ versus buffer size B_T in a six PRU ring network, under the C-BTMA protocol, for the TSBP schemes.

networks under study. When the CASMA access protocol is employed, the queue per link scheme may achieve a higher throughput than the single queue per PRU scheme, depending on the network topology and traffic pattern. In figure 4.19, we compare the alternative queue structuring schemes for the case of the TSBP buffer management scheme with HTG classification and the CASMA channel access protocol in the six PRU ring and dodecahedron topologies. Clearly the effect is present in the case of the dodecahedron, but not in the case of the ring. In general, it is believed that the above behaviour will occur only in topologies where at capacity, the number of *unused* nodes is zero (i.e., when all nodes are either transmitting or receiving). It is evident from figures 4.17, 4.18 and 4.19 that when the same capacity is achieved by both outbound queueing structures, then the single queue per PRU structure achieves a higher throughput than the queue per link scheme for the same number of transit buffers per PRU. This is because, as is well known (refer to [58]), the sharing of buffer resources (in the single queue case) is more efficient than the partitioning of these resources (employed here in the queue per link case). If, in the queue per link scheme, the sharing of buffers among all intra-node queues was employed (instead of partitioning), then, for networks where $C(G^*, \infty)$ is the same for both queueing structures, we would expect a performance similar to that of the single queue structure for all values of transit buffer size. Refering to figure 4.17, note results for the case of a separate unstructured queue per link, but with network access flow control and utilized with a global FCFS service discipline. (Recall from section 4.2 that this configuration with FCFS service and network access flow control is deadlock-free). This scheme is seen to be the most efficient of the queue per link schemes, again due to a more complete sharing of the buffer resources among packets of all classes. Furthermore, the latter results indicate that the structuring of the buffers introduced to ensure deadlock-free operation does indeed result in a small performance penalty.

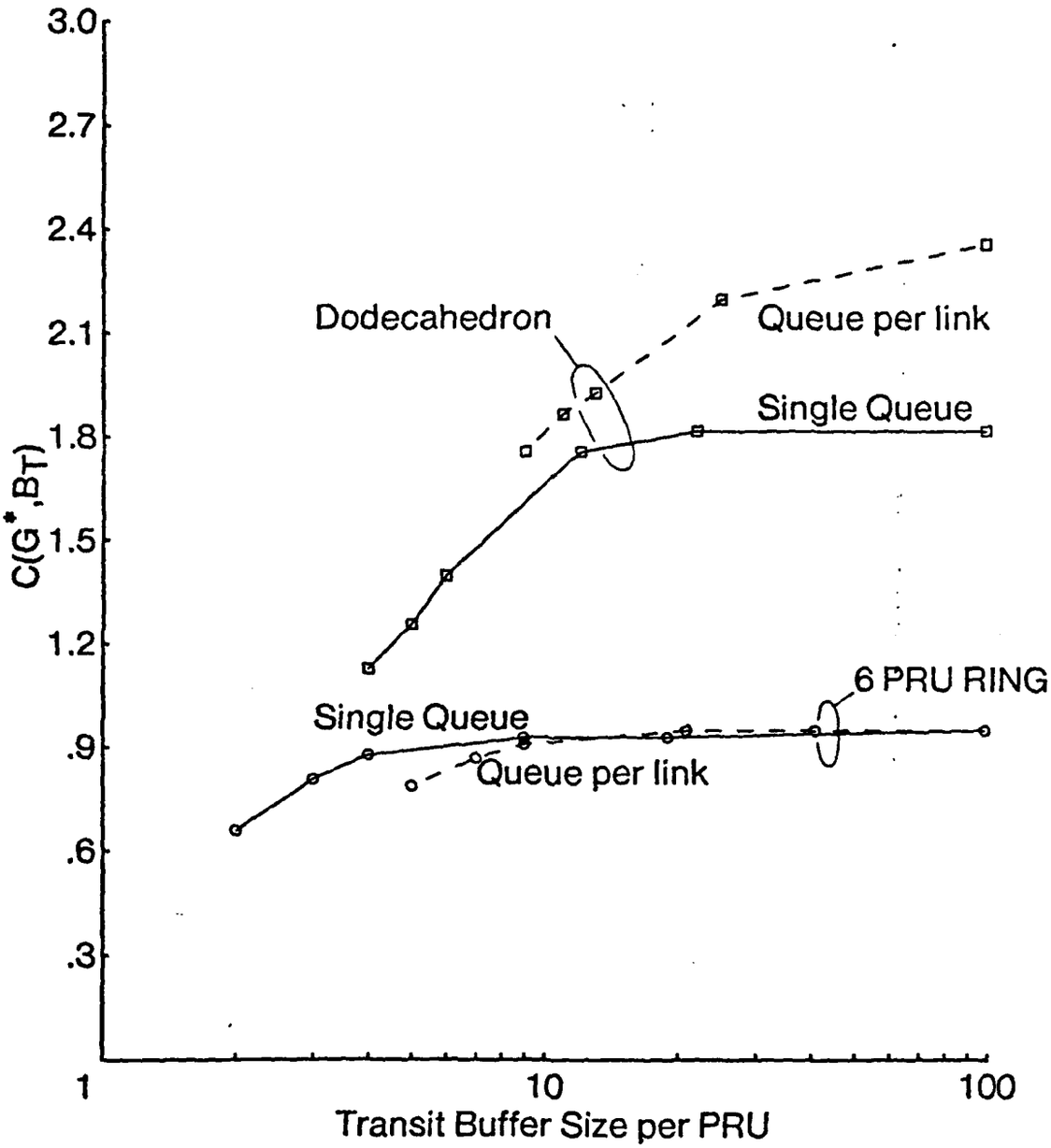

Fig. 4.19 $C(G^*, B_T)$ versus buffer size B_T in the six PRU ring and dodecahedron networks, under the CASMA protocol, the TSBP scheme with HTG classification, for the single queue per PRU and queue per link structures.

4.4.3 Comparison of channel access schemes

We now consider the effect of finite buffer size on the network throughput for the various channel access schemes. Out of the many combinations of buffer management schemes and queueing structures, we have selected one efficient pair for study, namely, the TSBP scheme with HTG classification and the single queue per PRU structure. Two examples of regular topologies, i.e., the 6 PRU ring and the dodecahedron are considered. In figures 4.20 and 4.21, we plot $C(G^*, B_T)$ vs. B_T for the various access schemes in the six PRU ring and the dodecahedron topologies respectively. We note that at $B_T = \infty$, the CASMA, C-BTMA and CDMA access schemes achieve the highest throughputs while ALOHA and CSMA achieve the lowest throughputs (as in the previous chapter).

The effect of the finite transit buffer size on the achievable network throughput is seen by considering the percentage degradation in throughput when B_T is decreased from ∞ to the minimum value set by the constraints of the SBP scheme (denoted ${B_T}^{min}$). The latter percentage degradation is equal to $100(C(G^*, \infty) - C(G^*, {B_T}^{min}))/C(G^*, \infty)$ and is denoted by Δ. Table 4.1 exhibits $C(G^*, {B_T}^{min})$, $C(G^*, \infty)$ and Δ for the various access schemes in the 6 PRU ring and dodecahedron topologies. It is evident that the C-BTMA and CASMA access schemes have the highest values of Δ and hence they are mostly storage bound. For the remaining access schemes, Δ is between 10 and 20%, indicating that the latter schemes are mainly channel bound. The results given here on the channel bound CSMA and ALOHA schemes are consistent with those in [16] and [17], where the slotted ALOHA and CSMA access schemes were studied in certain two-hop centralized networks.

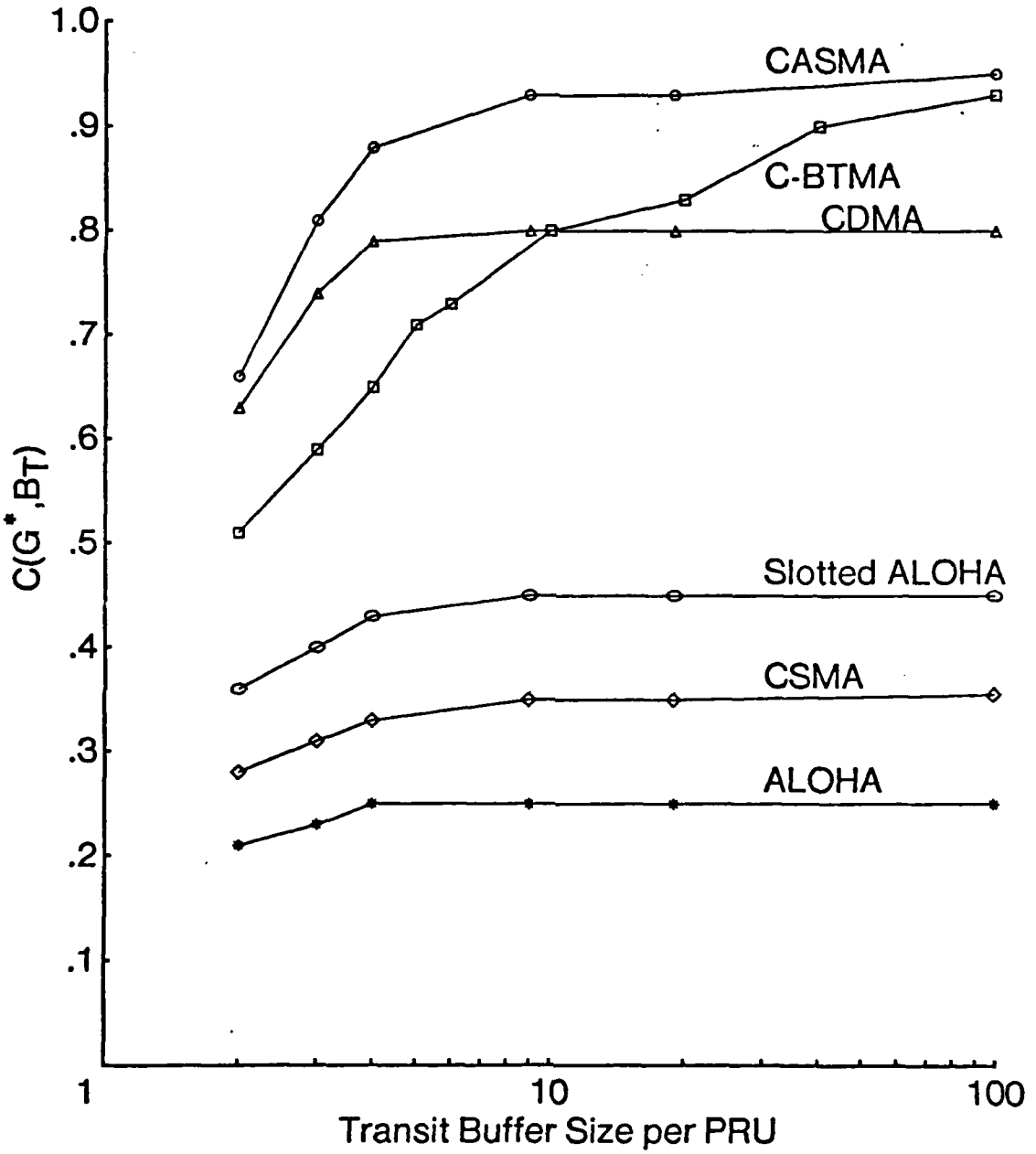

Fig. 4.20 $C(G^*, B_T)$ versus buffer size B_T in a six PRU ring network, with the TSBP scheme with HTG classification, a single queue per PRU, for various channel access schemes.

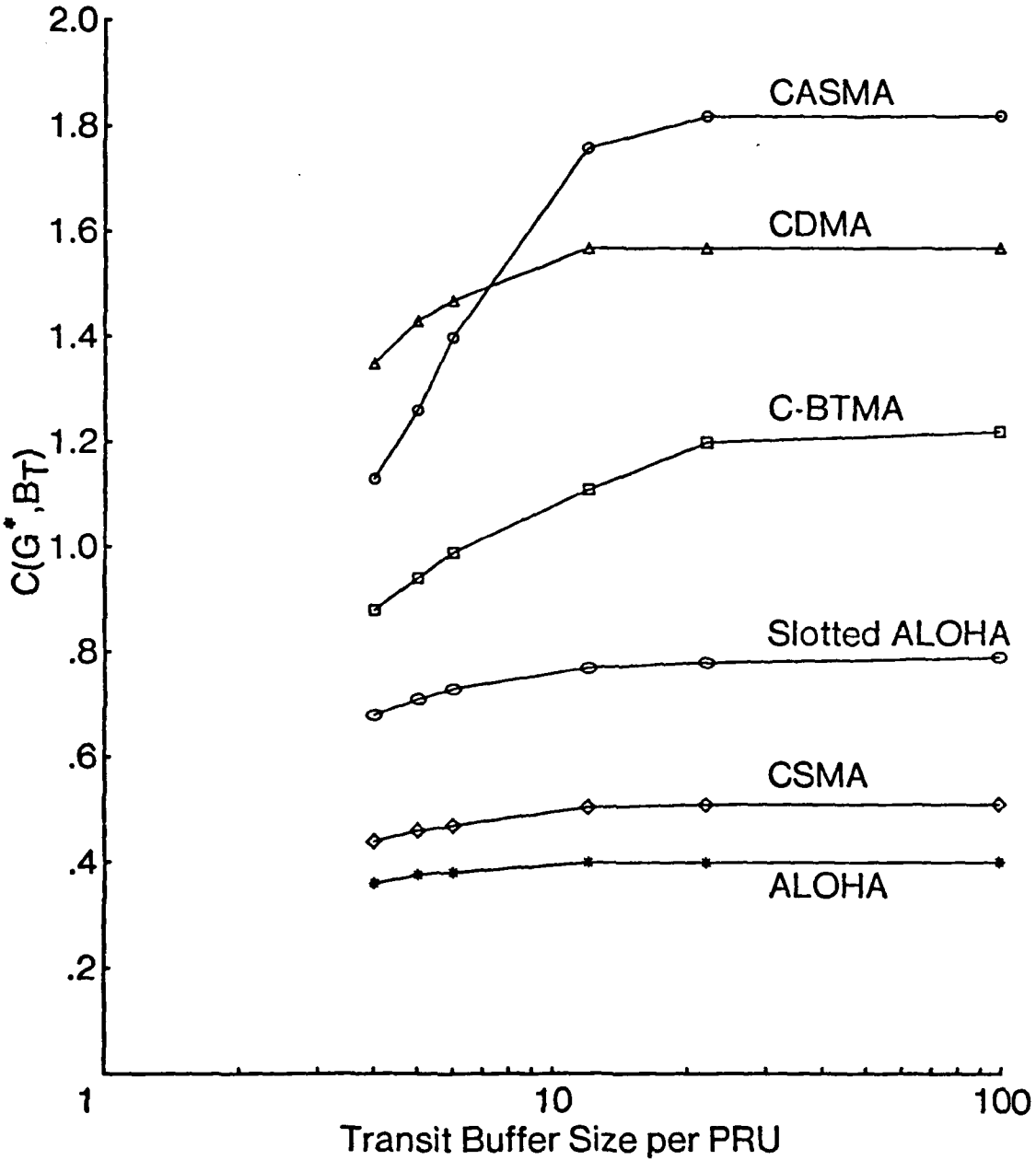

Fig. 4.21 $C(G^*, B_T)$ versus buffer size B_T in a dodecahedron network, the TSBP scheme with HTG classification, a single queue per PRU, for various channel access schemes.

	6 PRU Ring			Dodecahedron		
Access Scheme	$C(G^*, 2)$	$C(G^*, \infty)$	$\Delta(\%)$	$C(G^*, 4)$	$C(G^*, \infty)$	$\Delta(\%)$
pure ALOHA	0.21	0.25	16	0.36	0.40	10
CSMA	0.28	0.36	21	0.44	0.51	14
slotted ALOHA	0.36	0.45	20	0.68	0.79	14
CDMA	0.63	0.80	21	1.35	1.57	14
C-BTMA	0.51	0.93	45	0.88	1.22	28
CASMA	0.66	0.95	30	1.13	1.82	38

Table 4.1. The effect of transit buffer limitation on achievable throughput for the various channel access schemes in the 6 PRU ring and dodecahedron topologies.

4.4.4 Throughput-delay performance

In evaluating the throughput-delay tradeoff, we first assume that $B_0 = m = \infty$ (i.e., the user has an unlimited buffering capability) so that no new packets are ever lost. We again consider the example network of section 4.4.1, namely, the six PRU ring operating under the C-BTMA channel access protocol with a single queue per PRU. For the case of $B_0 = m$ (all packets in B_0 reserved for new packets), we fi. d (as

in the previous chapter) that for $\gamma < C(G^*, B_T)$, the network delay is minimized by a particular value of G denoted $G_{opt}(\gamma)$ and that as $\gamma \rightarrow C(G^*, B_T)$, the network delay becomes unbounded. The optimum throughput-delay performance for the HSF scheme is depicted in figure 4.22. For $B_0 = m$, curves depicting the cases of $B_T = 2, 10$, and ∞ are shown. A fourth curve shows the case of $B_0 - m = 8$ and $B_T = 2$. In the latter case, the network delay goes to infinity at a value of throughput that lies in between $C(G^*, 2)$ and $C(G^*, 10)$. Such behaviour is to be expected due to the sharing of $B_0 - m$ buffers by new and transit packets (refer to figure 4.12). The optimum throughput-delay performance for the HTG scheme is depicted in figure 4.23. Comparing the performance of the HSF and HTG schemes in figures 4.22 and 4.23, we find that for $B_T = \infty$ and $B_T = 10$, the throughput delay performance is much the same, while it differs for $B_T = 2$ due to the differing values of $C(G^*, B_T)$. The case of $B_T = 2$ is detailed in figure 4.24, where the 1-, 2- and 3-hop delays are plotted for both schemes and the case of $B_T = \infty$ is detailed in figure 4.25 where, for clarity, only the 1- and 3-hop delays are plotted. The differences in the 1-, 2-, and 3-hop delays between the two schemes are due to:

(i) for a given B_T, the larger value of $C(G^*, B_T)$ in the HTG scheme than in the HSF scheme,

(ii) the lower priority of service given to packets that travel short distances in the HSF scheme,

(iii) the higher priority of service given to packets that are close to their final destination (including, in this case, packets that travel only 1-hop) in the HTG scheme.

Note that, for $B_T = 2$ the 1-, 2-, and 3-hop delays are all higher for the HSF scheme than for the HTG scheme since effect (i) predominates. For the case of $B_T = \infty$, since $C(G^*, \infty)$ is identical in either case, only effects (ii) and (iii) are present. We

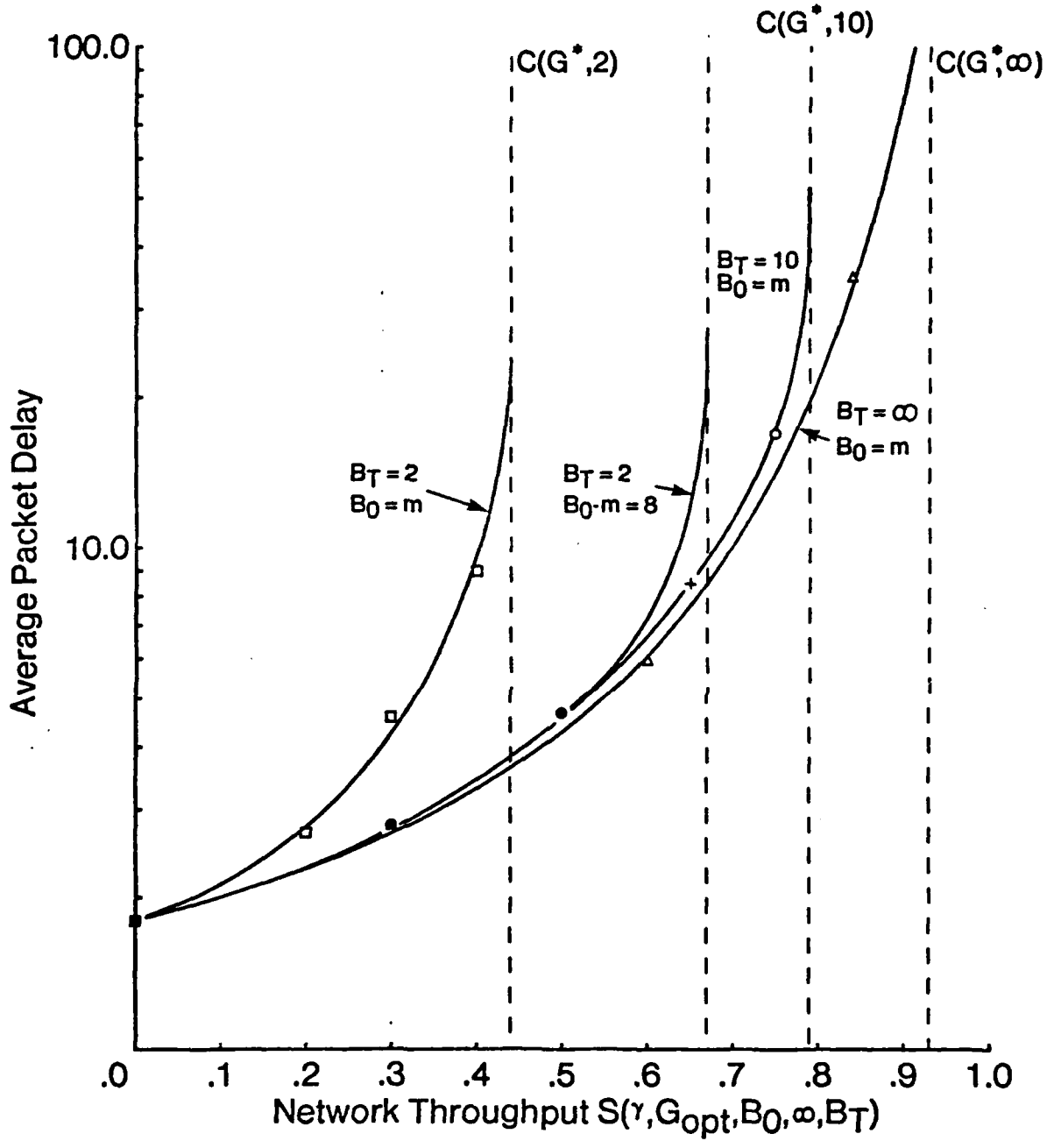

Fig. 4.22 Average packet delay versus network throughput in the six PRU ring network, under the C-BTMA protocol, the HSF buffer structuring scheme with a single queue per PRU, $m = \infty$ and various values of B_T.

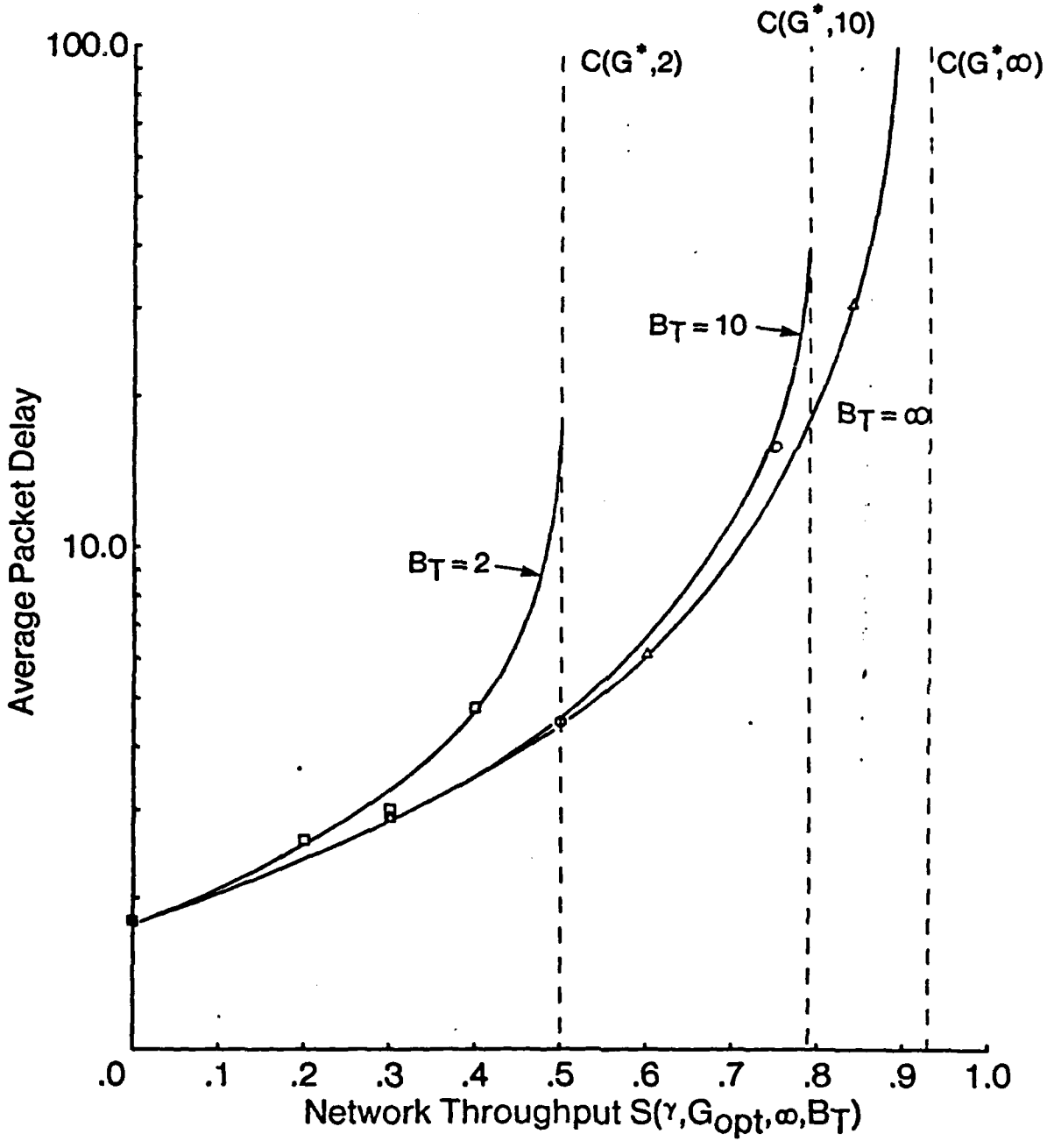

Fig. 4.23 Average packet delay versus network throughput in the six PRU ring network, under the C-BTMA protocol, the HTG buffer structuring scheme with a single queue per PRU, $n_i = \infty$ and various values of B_T.

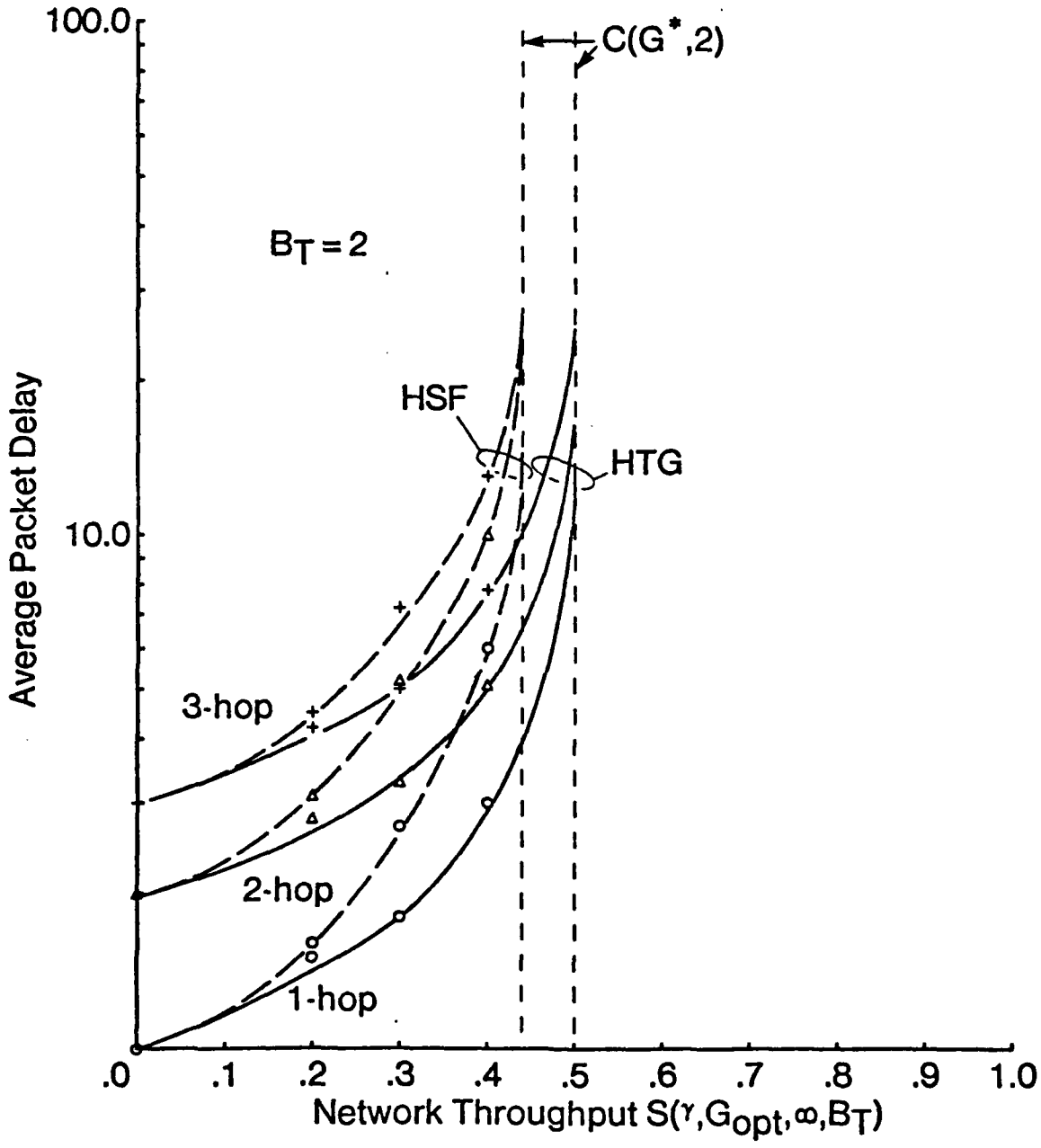

Fig. 4.24 1-, 2- and 3-hop delays versus network throughput in the six PRU ring network, under the C-BTMA protocol, for the HSF and HTG buffer structuring schemes with a single queue per PRU, $m = \infty$ and $B_T = 2$.

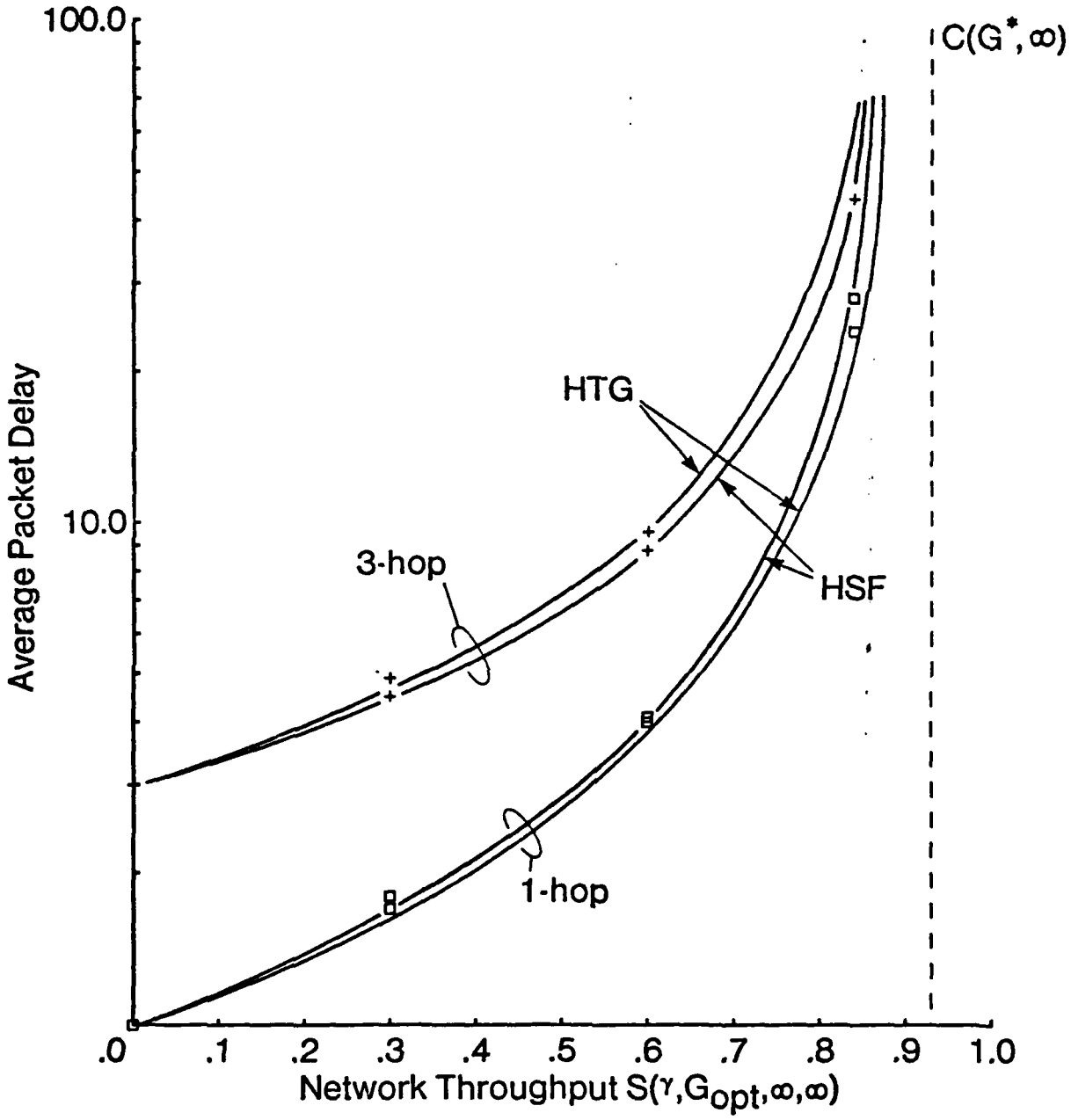

Fig. 4.25 1- and 3-hop delays versus network throughput in the six PRU ring network, under the C-BTMA protocol, for the HSF and HTG buffer structuring schemes with a single queue per PRU, $m = \infty$ and $B_T = \infty$.

observe that, as expected, for the HSF scheme the 1-hop delay is increased and the 3-hop delay is decreased over the corresponding 1- and 3-hop delays for the HTG scheme. The difference is however very small.

We now consider the case $B_0 - m = \infty$. Recall that for this case, the unmodified HTG scheme is characterized by the discriminatory behaviour that is typical of priority queueing networks*. We now consider the effect of this discrimination on packet delay. We will compare the delay performance of the HSF and unmodified HTG schemes using the performance of the TSBP scheme as a benchmark. Recall that in the SBP scheme, the order of service is highest class first only over the packets stored in the $B - m$ (PRU) buffers. Thus, in the $B_0 = m = \infty$ case, the prioritization of service extends only to transit packets, while in the $B_0 - m = \infty$ case, it extends to both new and transit packets. Since, in the HSF scheme all new packets are of class 0, the global prioritization over all packets in the $B_0 - m = \infty$ case does not result in any difference in the order of service as compared with the $B_0 = m = \infty$ case, and hence the respective delay performances will be the same. In the HTG scheme, new packets may be of class 0 through $h_{max} - 1$, and thus, as previously indicated, the prioritization over all packets in the $B_0 - m = \infty$ case will tend to increase discrimination in favour of packets that travel shorter distances. The effect on delay is clearly seen in figure 4.26, where the case $B_0 - m = \infty$ for the HSF, HTG and TSBP schemes is depicted. We note that in the HTG scheme, at $\gamma = C(G^*, \infty)$ the delay for the 3-hop traffic is unbounded, while that of the 2- and 1-hop traffic remains bounded (due to the priority structure of this scheme). As noted in subsection 4.1.2, the delay for the i-hop traffic ($i = 1, 2$) goes to infinity at values of γ greater than $C(G^*, \infty)$. As expected, we see a much greater difference in performance between the HSF and HTG schemes in figure 4.26 as compared

*The modified HTG scheme in which all new packets are treated the same way irrespective of class will have an identical performance to the case of $B_0 = m = \infty$ and $B_T = \infty$ depicted in figure 4.23.

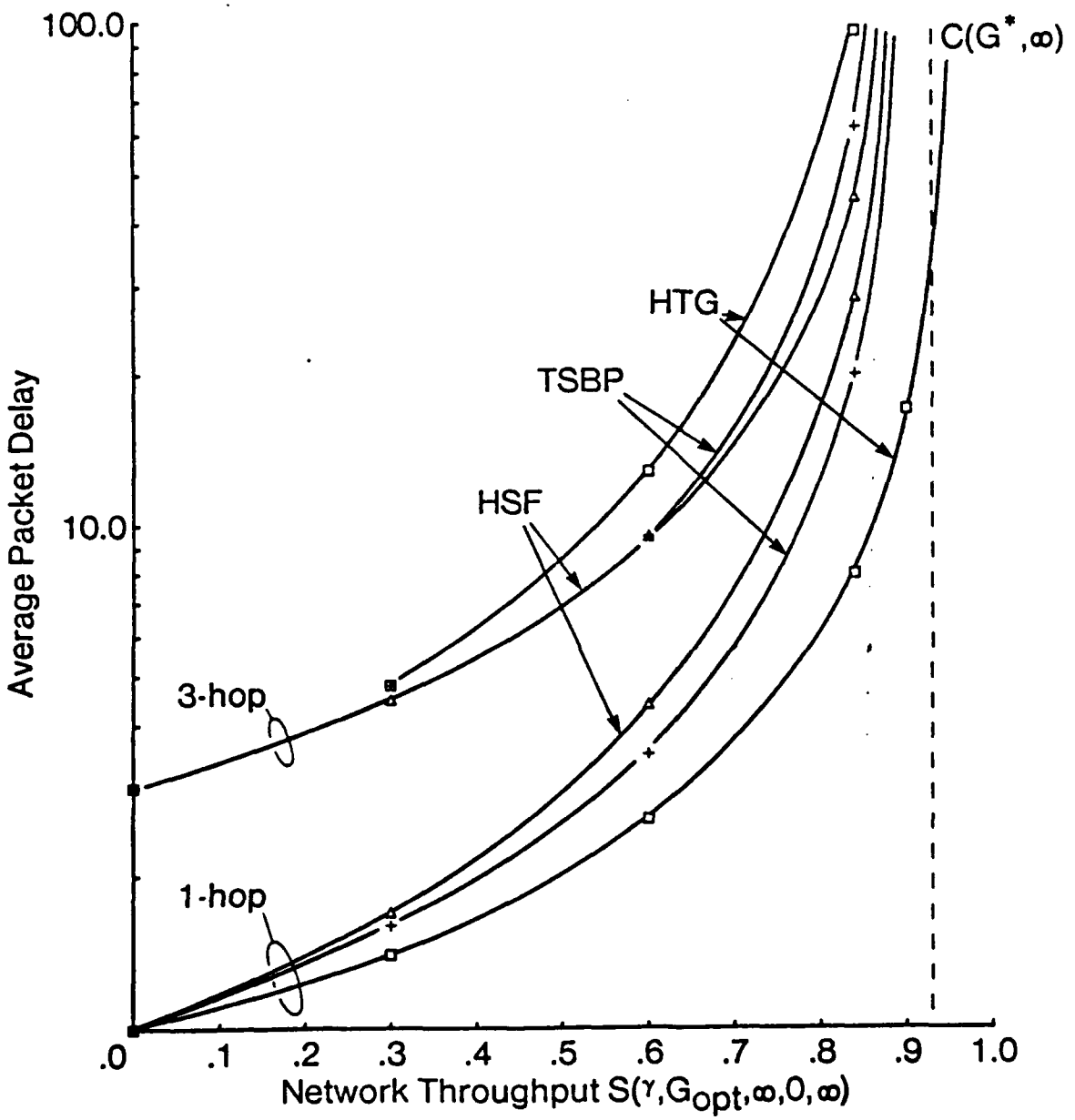

Fig. 4.26 1- and 3-hop delays versus network throughput in the six PRU ring network, under the C-BTMA protocol, for the HSF, HTG and TSBP schemes with a single queue per PRU, $m = 0$, $B_0 = \infty$ and $B_T = \infty$.

with figure 4.25, where the $B_0 = m = \infty$ case is depicted. Regarding the TSBP scheme, we note that for $B_0 - m = \infty$, this scheme achieves the same performance as the global FCFS service discipline. The 1-hop and 3-hop delays for the TSBP scheme are seen to lie in between the corresponding curves for the HSF and HTG schemes. This is to be expected since no discrimination, neither in favour of packets that travel long distances (as in HSF), nor in favour of packets that travel short distances (as in HTG) is present.

4.5 Summary

In this chapter, we have studied the performance of multihop packet radio networks with finite buffers. A deadlock-free buffer management scheme called the SBP scheme was employed. We considered a user model in which users are able to buffer new packets separately whenever space is not available among the PRU buffers. We observed that the optimal allocation of buffers among new and transit buffer classes, and the selection of the scheduling and traffic rates that optimized capacity depended on the number of user buffers m. When m was large (as would be the case if the users corresponded to computer processes carrying out data transfer operations) then for a given number of PRU buffers (i.e., $B - m$) the achievable network throughput is maximized by maximizing the transit buffer size B_T and setting $G = G^*(B_T)$. No improvement was to be had by varying the input traffic rate γ beyond the network capacity $C(G, B_T)$. When m was small (which could correspond to the case of interactive terminal users), the loss probability P_l was non-negligible for $\gamma < C(G, B_T)$. For this case and a given value of B_T, we observed that the network throughput could be increased to a value somewhat greater than $C(G^*, B_T)$ by both tuning G to a value $> G^*(B_T)$ and adjusting γ to a value

$> C(G^*, B_T)$. Note that if γ was constrained to be less than some bound and when m is small, then given a finite buffer size $B = B_0 + B_T$, improved performance may be obtained by increasing the number of buffers in B_0 in order to reduce the loss probability P_l. The latter case could arise in practice if the offered input traffic is generated by PRUs of another packet radio network (operating possibly at a different frequency), and using for example the ALOHA access scheme. In this instance, γ would be limited by the ALOHA channel throughput.

We considered a number of variants of the SBP scheme. We noted only a minor performance difference between the PU and PD packet placement policies with PU achieving a slightly higher throughput than PD. The TSBP scheme (which at $B_T = \infty$ reaches the throughput-delay performance of the global FCFS service discipline), was seen to achieve essentially the same throughput as the SBP scheme. It was observed that while in the HSF scheme resource allocation was intrinsically fair, for certain cases in the HTG scheme the resource allocation was discriminatory with packets travelling shorter distances being favoured over packets travelling longer distances. This discrimination was removed by treating all new packets in the same way (i.e, as class 0). The HTG scheme was seen to achieve a higher throughput than the HSF scheme where the transit buffer size was limited. Regarding the different outbound queueing structures, a performance difference was observed among these only in the case of the CASMA access protocol; for this access protocol, the queue per link scheme achieved a higher throughput than the single queue per PRU scheme. For all the remaining access schemes no difference in performance was observed among the outbound queueing structures. As expected, we observed that the sharing of the buffer resources was more efficient than the partitioning of these resources. We also showed that, depending on the channel access scheme, the effect of finite buffer size on network performance could be significant. The greatest impact on performance was seen for the C-BTMA and CASMA access schemes (which

are predominantly storage bound). A lesser effect was seen for the remaining access schemes (namely, ALOHA, CSMA and CDMA) which are predominantly channel bound.

Chapter 5

More General Networks

5.1 Introduction

In chapters 3 and 4, we have studied several aspects of the performance of multihop packet radio networks. In chapter 3, the performance of various channel access schemes was studied in networks with an entirely regular structure, and under the idealized assumption of infinite buffers. In chapter 4, the restriction of infinite buffer resources was removed. In the present chapter, we consider networks with more general topologies. Such networks are more complicated to study since, contrary to the situation in the previous chapters, not all nodes and links achieve an identical performance. Therefore, while previously scalar measures of performance such as the network throughput and the average packet delay sufficed, here vector or matrix measures corresponding to nodal and link throughputs and delays may be required. In addition, network variables such as nodal transmission scheduling rate and nodal buffer size may no longer be scalar.

The differing behaviour among individual nodes and individual links in the more general networks leads to some nodes and links becoming saturated at capacity as described in section 5.2. In section 5.3, in order to illustrate the aforementioned effects we first consider some simple non-regular networks for which the size of the parameter space is not excessively large. Any effects observed in these simple networks would almost certainly occur in a more realistic, large-scale network. In the particular cases considered here, it is feasible to exhaustively search the entire space of parameters thereby determining the regions of feasible nodal and link capacities. In section 5.4 we turn to the question of more complex and realistic large-scale topologies. As such networks typically have hundreds or thousands of radio links, the space of scheduling parameters is extremely large and is thus impractical to search over by means of simulation. Therefore an alternative approach is taken whereby a number of simple sub-optimal transmission scheduling algorithms are considered. *Numerical results are given for an example consisting of a 51 node* network obtained from measurement over real terrain.

5.2 Saturated Links and PRUs and Bottlenecks

Suppose that we are given a non-regular network topology, a set of operational protocols (i.e., a channel access scheme, a set of link transmission scheduling rates, a buffer management scheme, a fixed routing scheme), and an end-to-end traffic pattern matrix (denoted $[\alpha]$). Assume that the buffer storage space available for new packets (B_0) is unlimited, and let S be a real scalar. We define the network capacity as the maximum value of S such that the offered traffic matrix $[S\alpha]$ may be achieved*. When the network is operating at capacity, the utilization factor of

*Note that for entirely regular networks with buffer management such that $B_0 = m = \infty$ or unlimited transit buffer size, this definition reduces to our previous definition of network capacity.

a subset of the queues of the network is equal to 1. We define the links associated with these queues to be saturated links, and the PRUs that transmit on saturated links to be saturated PRUs. For a given topology, and with all other operational protocols and parameters fixed, the set of scheduling rates determine the network capacity and the set of saturated links and PRUs. Clearly, the network capacity may be optimized over the set of scheduling rates. If the scheduling rates are sub-optimal, then certain links and nodes may be saturated according to the above definition when in fact they need not be. On the other hand, when the scheduling rates are optimal then at least one link must be saturated. Accordingly, we classify saturated links and PRUs into one of two classes. Given a set of scheduling rates, a resulting network capacity and a set of saturated links, a saturated link is said to be a scheduling saturated link if, without reducing the network capacity, it is possible to decrease the utilization factor of the associated queue to be < 1 by adjusting the scheduling rates. A saturated link is called a network saturated link if it is not a scheduling saturated link. Note that if the scheduling rates are set at sub-optimal values then all saturated links are scheduling saturated links.

In the previous chapters, the networks considered had an entirely regular structure, and when the network was operating at its optimal capacity, all PRUs and all links were network saturated. However, in more general networks at optimal capacity not all PRUs and links are necessarily network saturated, as is shown in two examples below.

Example 5.2.1: Consider a 3 node chain topology (as depicted in figure 5.1) under slotted ALOHA. PRU 1 generates traffic which is destined to PRU 3 and vice versa. Both PRUs transmit a packet in a slot with probability G_1. (This assumption is equivalent to assuming that the scheduling probability of each PRU is G_1, and that the utilization of each PRU is 1.) PRU 2 generates no traffic of its own, but

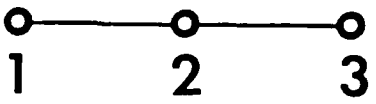

THREE NODE CHAIN

FOUR NODE CHAIN

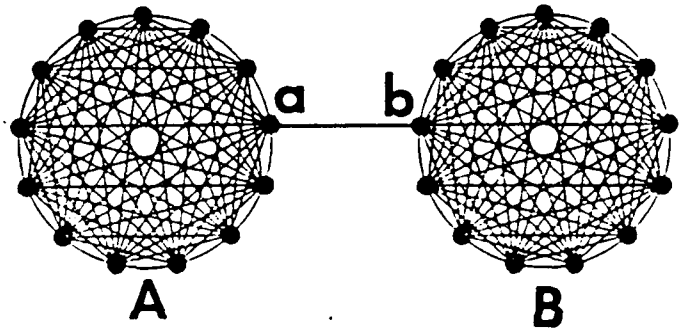

TWO CLUSTERS (M nodes each)

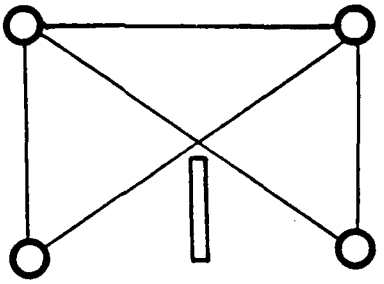

FOUR NODE WALL

Fig. 5.1 Simple multi-parameter networks.

buffers those packets that are successfully received from PRUs 1 and 3 in one of two queues corresponding to each outgoing link. Each queue is assumed to have an infinite buffering capability. If at a given slot PRU 2 has at least one packet in its buffers, then it transmits a packet with probability G_2, selecting the head of one of the non-empty queues with equal probability. We denote the network capacity by $C(G_1, G_2)$ and the utilization of PRU 2 (defined as the probability that at least one packet resides in one of the queues of 2) by $\rho_2(G_1, G_2)$. It is straightforward to show that the network capacity is expressed as

$$C(G_1, G_2) = \begin{cases} \dfrac{2G_1(1-G_1)}{1+2G_1}, & \dfrac{2G_1}{1+2G_1} < G_2 \leq 1; \\ G_2(1-G_1), & 0 \leq G_2 \leq \dfrac{2G_1}{1+2G_1}. \end{cases}$$

The utilization factor is expressed as

$$\rho_2(G_1, G_2) = \begin{cases} \dfrac{2G_1}{G_2(1+2G_1)}, & \dfrac{2G_1}{1+2G_1} < G_2 \leq 1; \\ 1, & 0 \leq G_2 \leq \dfrac{2G_1}{1+2G_1}. \end{cases}$$

In figure 5.2, we plot $C(G_1, G_2)$ as a function of G_1 for various values of G_2 and in figure 5.3 we plot $C(G_1, G_2)$ as a function of G_2 for various values of G_1. The optimal network capacity C^*, is equal to 0.268 and is attained for $G_1 = 0.366$ and $G_2 \geq 0.423$. Note that for a given value of G_1 and $G_2 \leq 2G_1/(1+2G_1)$ all PRUs are scheduling saturated PRUs. However, for $G_2 > 2G_1/(1+2G_1)$, $\rho_2 < 1$, $C(G_1, G_2)$ is independent of G_2, and PRU 2 is neither a network nor a scheduling saturated PRU.

Example 5.2.2: Consider a 4 PRU chain topology (as depicted in figure 5.1) under slotted ALOHA. Traffic is generated at PRUs 1 and 3 according to Bernoulli processes with rates λ_1 and λ_3 respectively. Each PRU is assumed to have infinite

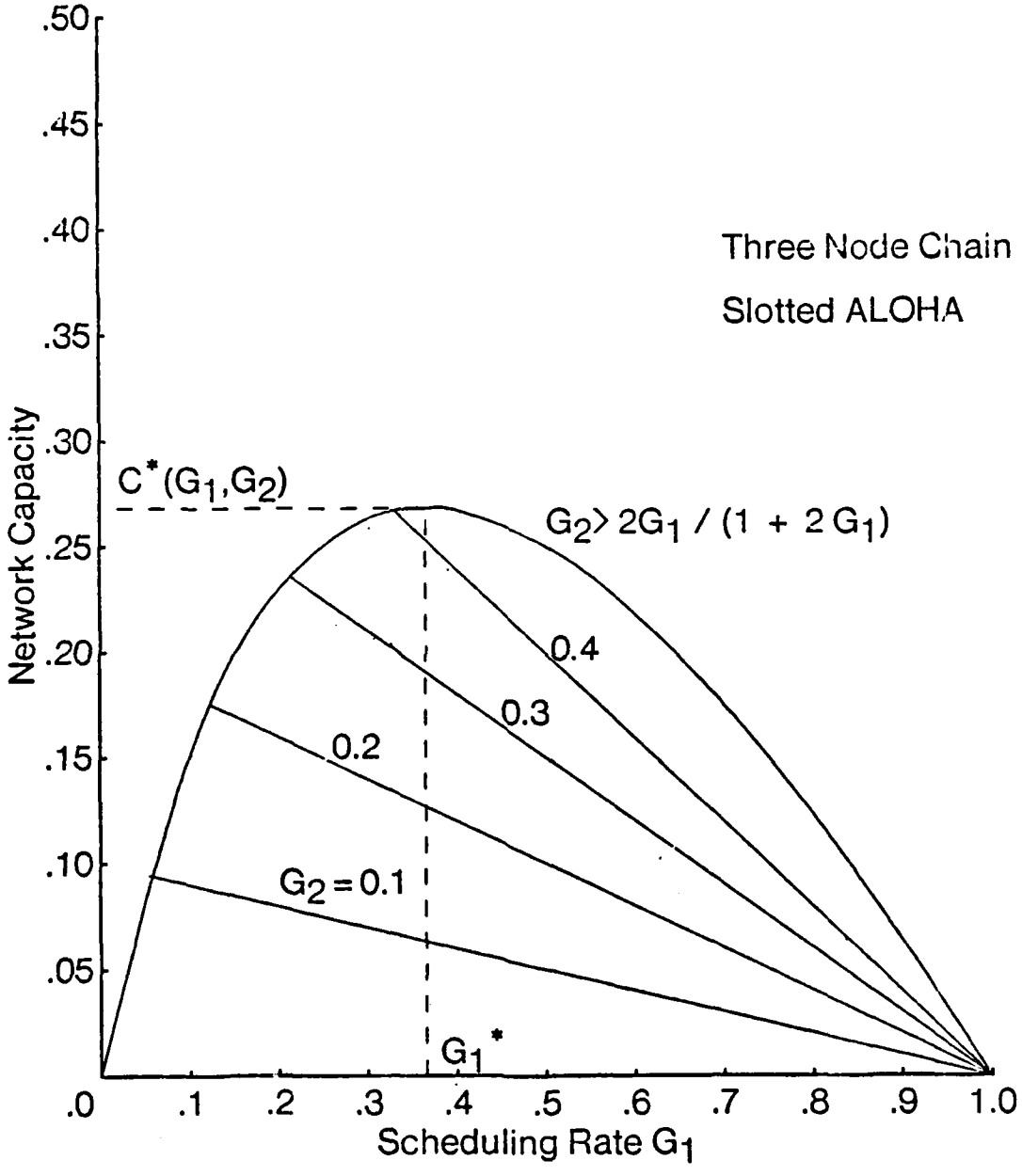

Fig. 5.2 Network capacity versus G_1 for various values of G_2 in a three node chain network under slotted ALOHA.

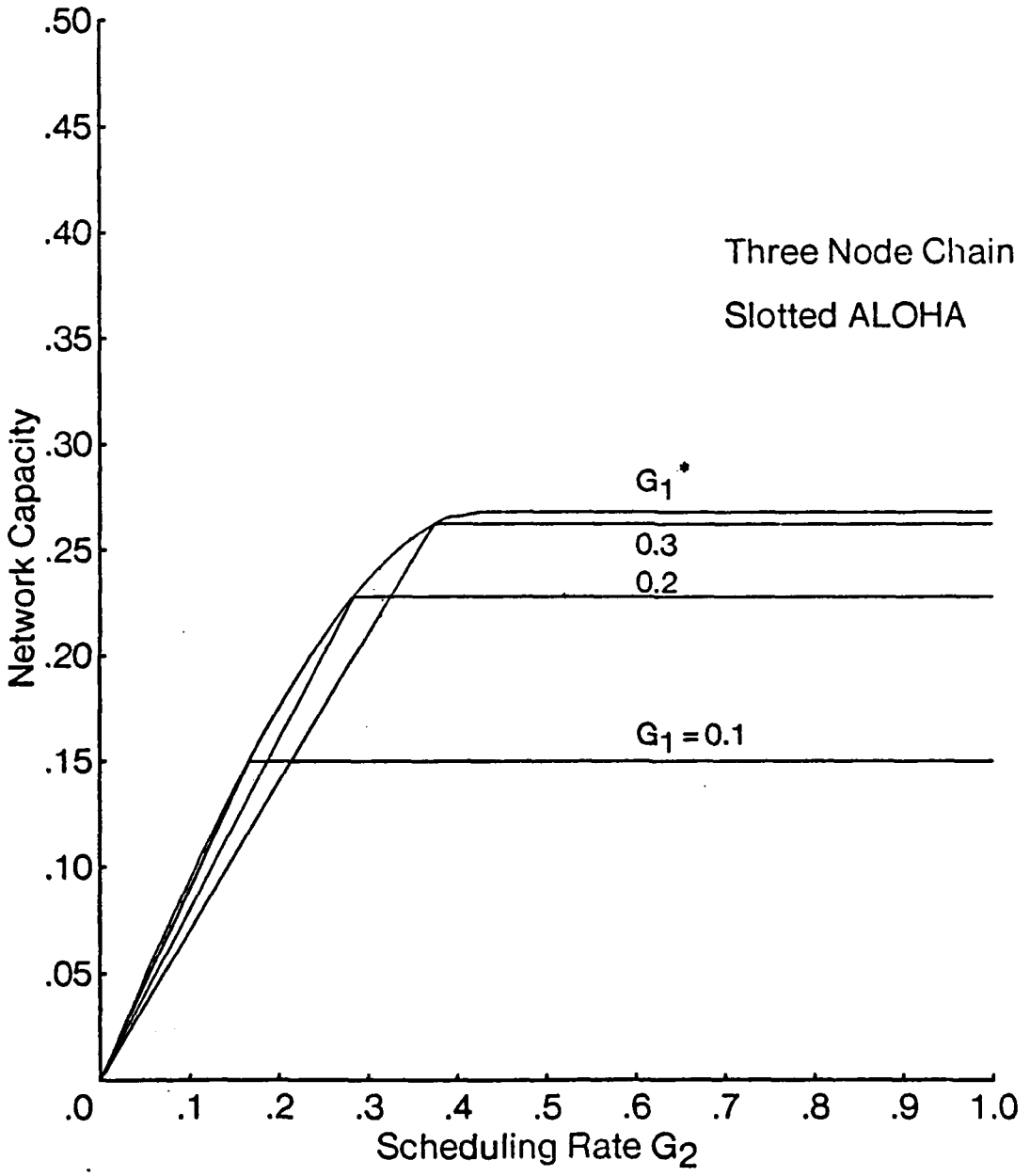

Fig. 5.3 Network capacity versus G_2 for various values of G_1 in a three node chain network under slotted ALOHA.

buffering capability. The traffic of PRU 1 is destined to PRU 2 while that of PRU 3 is destined to PRU 4. The scheduling probabilities of nodes 1 and 3 are denoted G_1 and G_3 respectively. Consider the traffic pattern $\lambda_1 = \lambda_3$. It is straightforward to show that the network capacity is expressed as

$$C(G_1, G_3) = \begin{cases} \dfrac{G_1}{1+G_1}, & \dfrac{G_1}{1+G_1} < G_3 \leq 1; \\ G_3, & 0 \leq G_3 \leq \dfrac{G_1}{1+G_1}. \end{cases}$$

In figure 5.4, we plot the network capacity $C(G_1, G_3)$ versus G_1 for various values of G_3 and in figure 5.5 the network capacity is plotted versus G_3 for various values of G_1. We observe that when the capacity is optimized (for $G_1 = 1.0$ and $G_3 \geq 0.5$), PRU 1 is a network saturated PRU while PRU 3, on the other hand, is not. For $G_3 > 0.5$, PRU 3 is neither a scheduling nor a network saturated PRU while for $G_3 = 0.5$ PRU 3 is a scheduling saturated PRU.

In general, at capacity the links of the network can be partitioned into two subsets, namely, ω_1 containing links that are saturated, and ω_2 containing links that are not saturated. If ω_2 is not empty, then the links in ω_1 are referred to as bottleneck links, and the PRUs that transmit on bottleneck links are referred to as bottleneck PRUs. Bottlenecks will be further discussed in section 5.4.

5.3 Small-Scale Networks

In this subsection, we consider a number of small-scale networks in which we illustrate (i) how the network capacity depends on the scheduling rate of topologically different nodes and links, and (ii) the differing achievable throughputs among differing links and nodes. The topologies considered are depicted in figure 5.1.

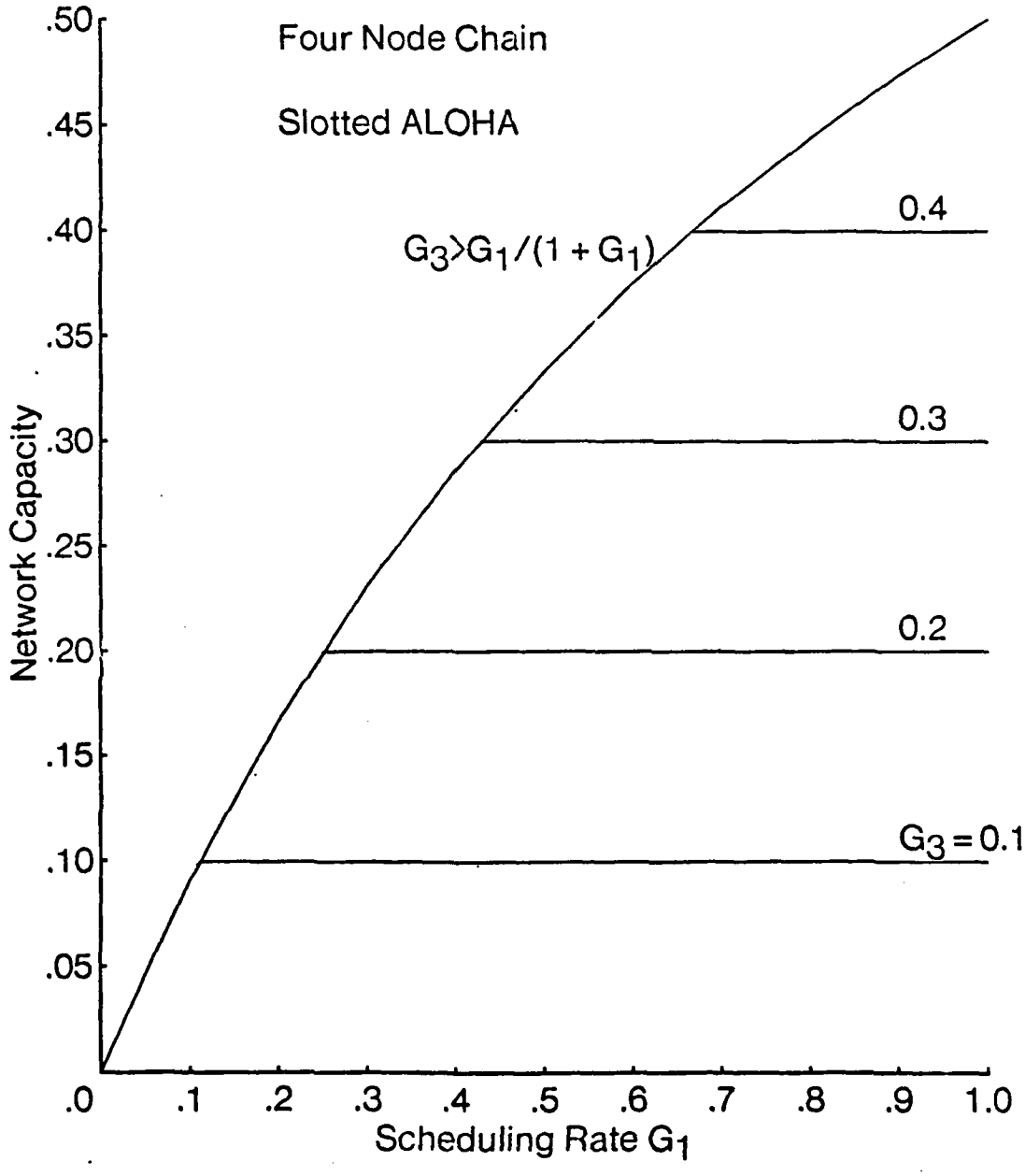

Fig. 5.4 Network capacity versus G_1 for various values of G_3 in a four node chain network under slotted ALOHA.

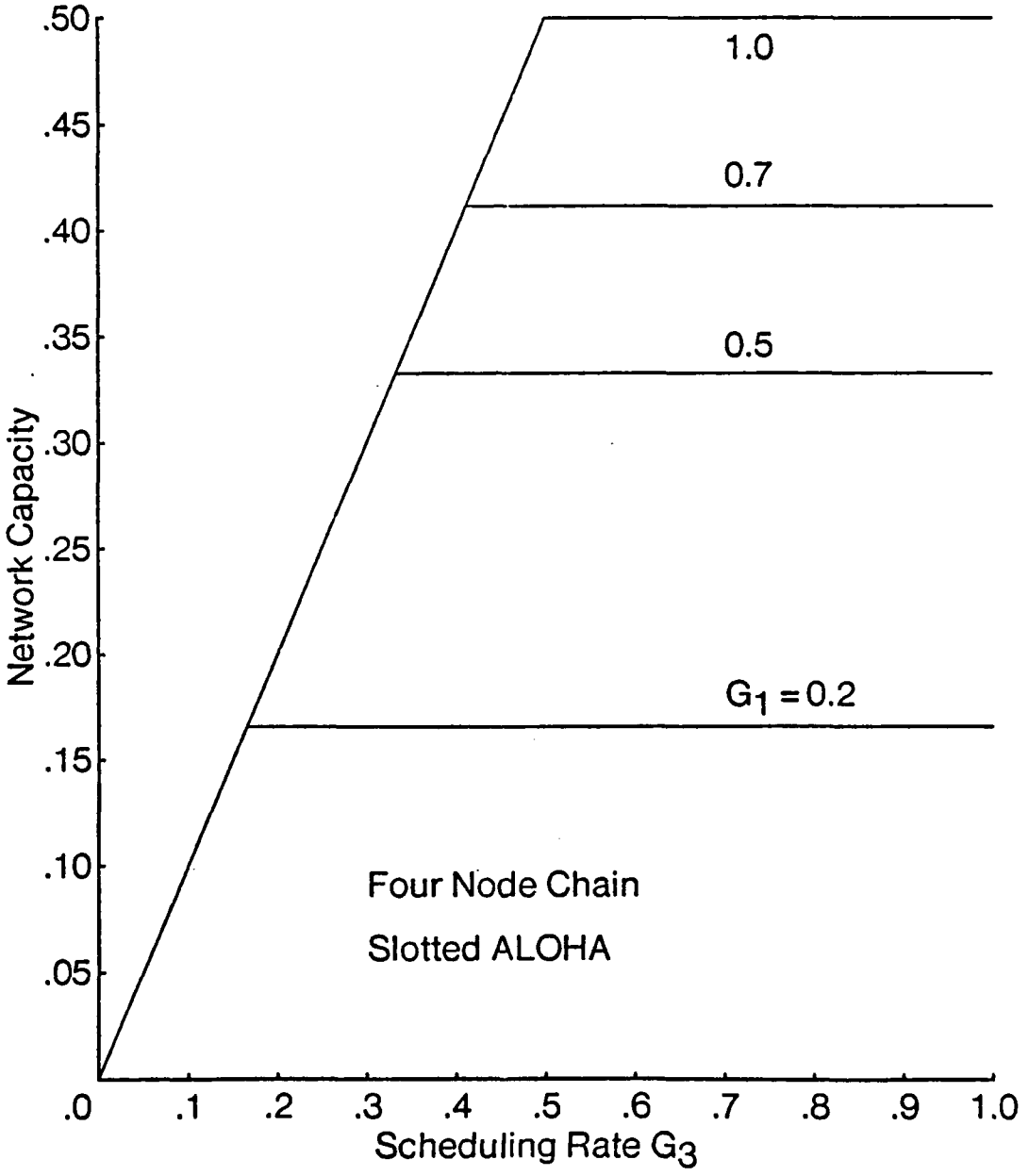

Fig. 5.5 Network capacity versus G_3 for various values of G_1 in a four node chain network under slotted ALOHA.

5.3.1 Two Clusters with a Single Intercluster Link

The simplest example of such a network is the four node chain with each end node serving as the ultimate destination for the other. We initially consider the four node chain network, assumed to be operating under the slotted ALOHA access scheme. Let the probability of transmission for both PRUs 1 and 4 be denoted G_1. Suppose that PRUs 2 and 3 generate no traffic of their own, but store and then forward packets that are successfully received from their neighbors. The buffer structure of each of PRUs 2 and 3 consists of a separate queue with infinite storage for each outgoing link. Each of PRUs 2 and 3 schedule packet transmissions as follows: if at a given slot, there are one or more packets in the PRU buffers, then the PRU transmits in that slot with probability G_2. If both queues are non-empty, then the queue on the intercluster link is selected with probability β and the other with probability 1-β. The network capacity, (i.e, the achievable network throughput) is denoted by $C(G_1, G_2, \beta)$. In figure 5.6, we plot the network capacity (obtained via simulation) as a function of G_2 for various values of G_1 and $\beta = 0.5$. We note the existence of unique values G_1^* and G_2^* which maximize the network capacity. For $G_1 < G_1^*$, the capacity is approximately constant over a range of G_2 that is wide for $G_1 << G_1^*$ but which narrows to a point as $G_1 \rightarrow G_1^*$. In contrast to situation of example 5.2.1, we see here that at optimal capacity the store-and-forward PRUs are always network saturated PRUs. This is because, in example 5.2.1 increasing the transmission probability of the central node did not decrease the network capacity, while in this case, as transmissions from PRUs 2 and 3 may interfere with one another, increasing their transmission probability above a certain value would cause a decrease in network capacity. While these results are given for $\beta = 0.5$, we observed that the optimal capacity remained approximately constant for $0.3 \leq \beta \leq 0.7$ and decreased for β outside this range. Also shown in the figure is the optimal capacity obtained via analysis under the assumption of heavy traffic (i.e.,

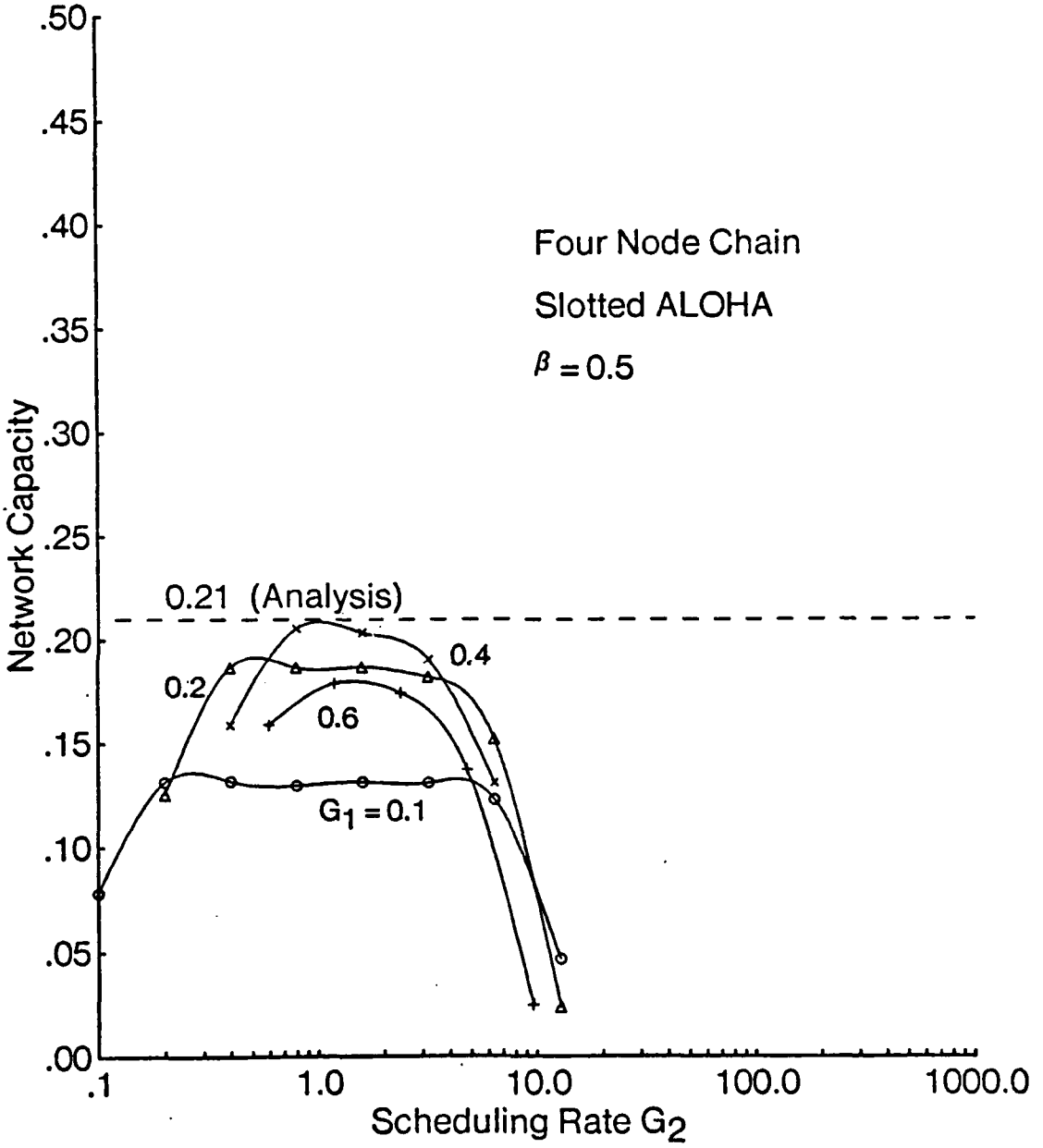

Fig. 5.6 Network capacity versus G_2 for various values of G_1 in a four node chain network under slotted ALOHA.

all PRUs have a packet available for transmission at every scheduling point). As this condition is met in the simulation model at optimal capacity, it is not unexpected that the same optimal capacity is reached. For this network we have also simulated various other access schemes, such as C-BTMA, RD-BTMA, CDMA, CASMA, pure ALOHA and CSMA, in addition to slotted ALOHA. The same general behaviour is seen except for the fact that the resulting network capacities differ. The ordering of the access schemes according to their capacities remains the same as was seen in chapter 3.

We now turn to the case where each fully connected cluster contains an arbitrary number of nodes M (refer to figure 5.1). Assume heavy traffic conditions at each PRU. Each PRU except a and b is a traffic source and transmits a packet in a slot with probability G_1. We assume that all traffic generated in cluster A is forwarded by nodes a and b to ultimate destination PRUs in cluster B, chosen at random according to a uniform distribution, and vice versa. As in the previous example, PRUs a and b each transmit a packet in a slot with probability G_2; the transmission is directed along the link between and a and b with probability β and along a link directed into the adjacent cluster with probability $1 - \beta$. In figure 5.7, we plot the optimal network capacity (obtained via analysis) as a function of the cluster size M. We note that for $M \leq 4$ the capacity decreases (due to a slightly reduced interference within each cluster), while for $M > 4$, the capacity remains essentially constant. The scheduling rate G_2 exhibits only a slight decrease as M increases due to the slight increase in the probability of collision within the clusters, while G_1 decreases rather sharply with M.

5.3.2 The Multiconnected Ring

The multiconnected ring with varying number of nodes and varying nodal degree was studied in chapter 3. In that chapter it was assumed that the queue

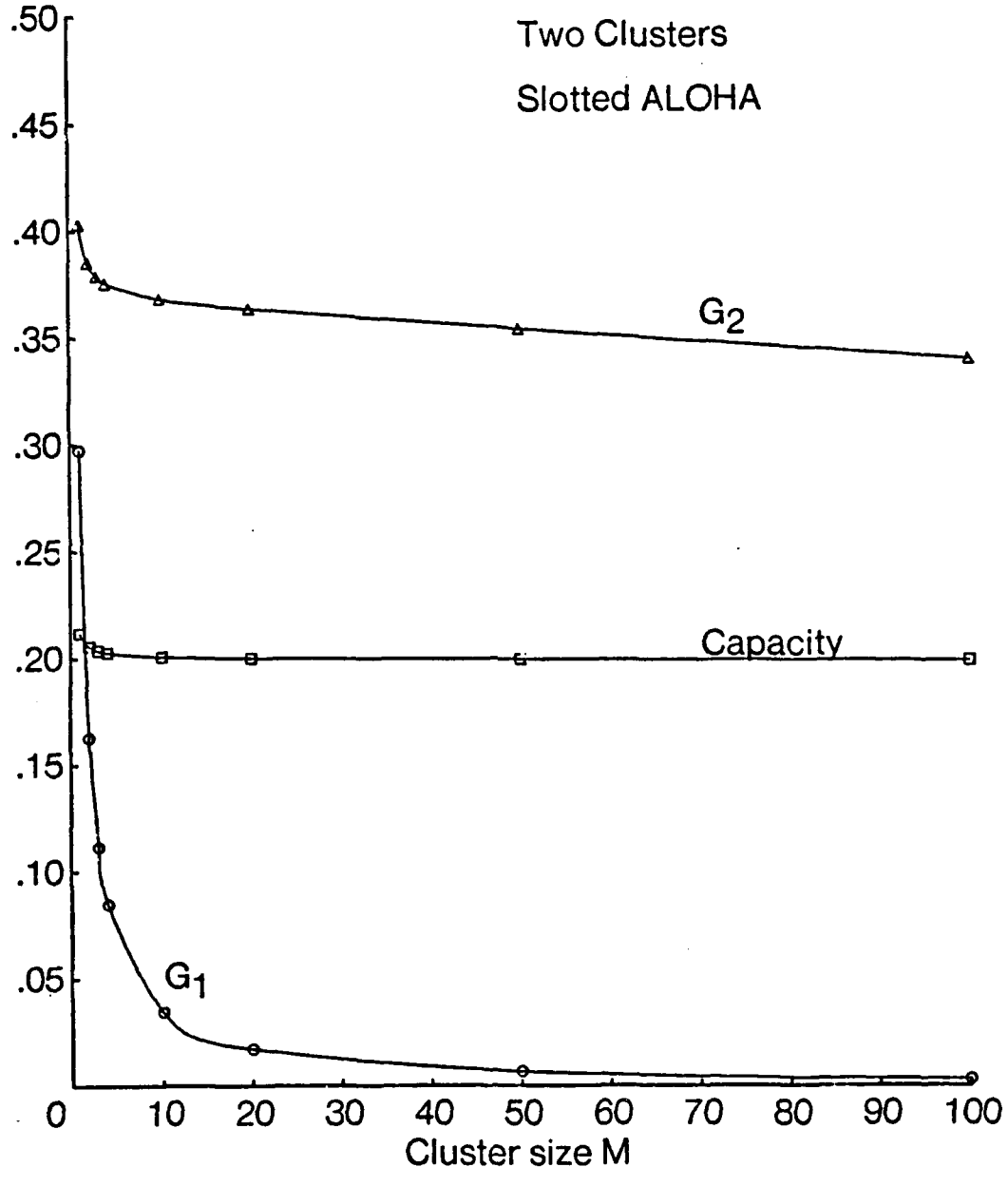

Fig. 5.7 Network capacity versus cluster size in a two cluster network under slotted ALOHA.

scheduling distribution was uniform and it was noted that under CSMA, BTMA and CASMA the link traffic processes were not all statistically identical; the latter phenomenon occurs because the number of hidden nodes relative to a transmission depends on the link that the transmission was undertaken on. This is illustrated in the example cited in chapter 3 and reviewed here: consider a multiconnected ring with N nodes of degree 4, operating under CSMA with $a = 0$. Let the nodes be numbered sequentially from 1 through N and consider transmissions from node 1 to its neighbors (i.e, nodes 2, 3, $N-1$, and N). The transmission $< 1, 2 >$ is vulnerable to transmissions from node 4 only, (the other neighbors of 2 being blocked by carrier sensing), while $< 1, 3 >$ is vulnerable to transmissions from both nodes 4 and 5. This suggests that the capacity along each link will be different. Therefore we consider the case where the transmission scheduling rates along each type of link may be independently set. (Recall that in chapter 3 these were equal). This is accomplished by varying both the nodal *transmission* scheduling rate and the nodal queue scheduling distribution. Let the rates of the scheduling processes along links between PRUs whose labels differ by 1 be denoted G_{12}. Let rates of the scheduling processes along the remaining links be denoted G_{13}. Consider a neighbors-only traffic matrix. Let C_{12} and C_{13} denote the link capacities corresponding to G_{12} and G_{13}. As G_{12} and G_{13} each vary over the set $[0, \infty)$, the resulting capacities C_{12} and C_{13} both lie within a bounded region in the (C_{12}, C_{13}) space which defines the set of feasible link capacities. The boundaries of such capacity regions are shown in figure 5.8 where the (C_{12}, C_{13}) feasibility region is plotted for the 12 node multiconnected ring with nodal degree 4, and $a = 0.01$ under various channel access schemes. We note that for ALOHA (pure and slotted) and CDMA, the feasibility region is symmetric about a 45° line thus indicating that the achievable throughput along each link is the same. This is because in both ALOHA and CDMA, the probability of successful reception depend only on the number of neighbors of

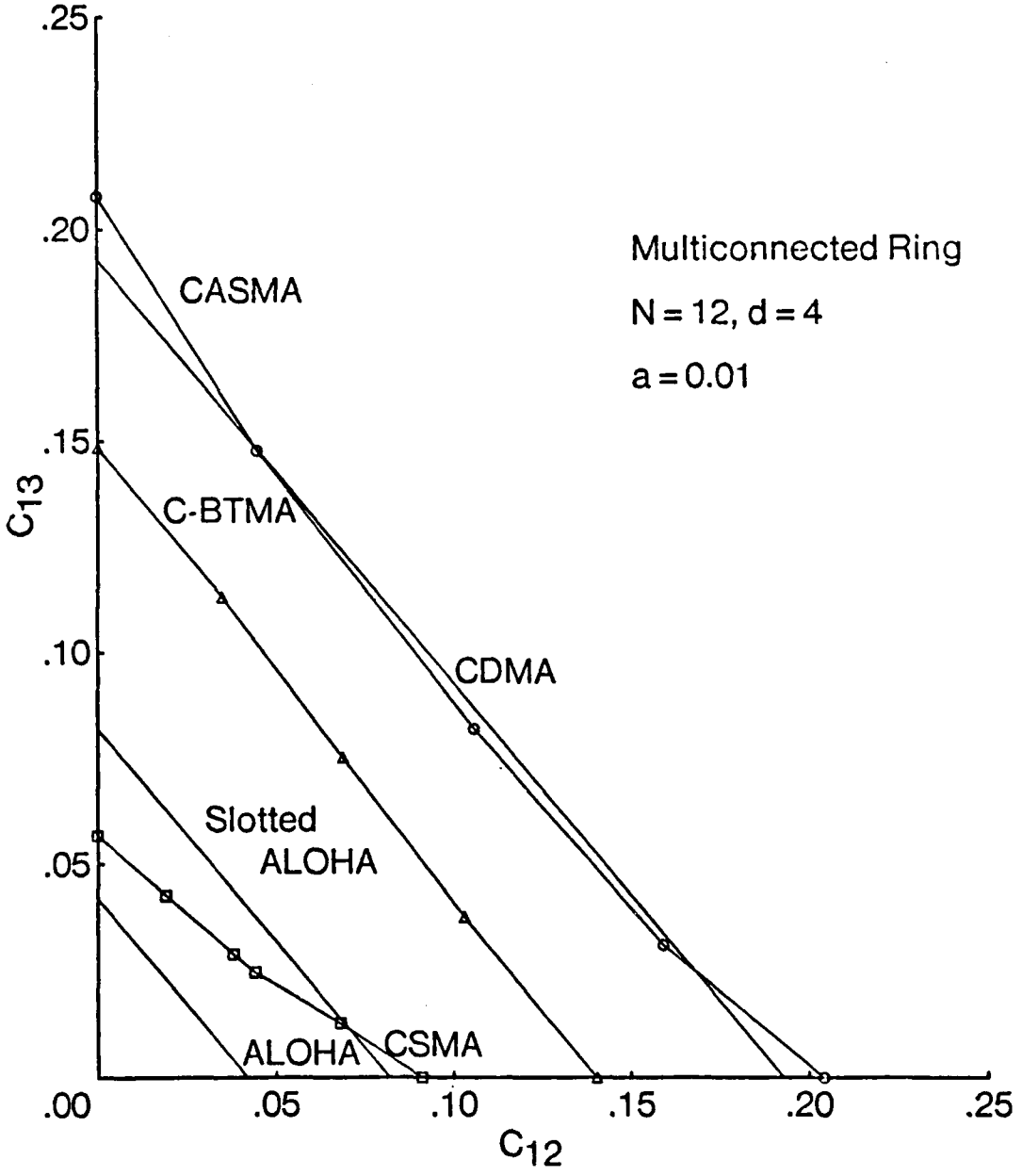

Fig. 5.8 Feasible region for link capacities in a 12 node multiconnected ring network with nodal degree 4, neighbors-only traffic pattern, $a = 0.01$, under various channel access schemes.

the intended destination which is the same on both links. For CSMA the region is skewed in the direction of C_{12} indicating that the throughput achievable along this link is greater than along C_{13}. This is due to the greater number of hidden nodes relative to transmission $< 1,3 >$ than relative to $< 1,2 >$. Note that for $C_{12} >> C_{13}$ (a highly unbalanced traffic pattern), contrary to what was observed in chapters 3 and 4, the performance of CSMA exceeds that of slotted ALOHA with the same pattern due to the reduced number of hidden nodes per transmission in CSMA. For both C-BTMA and CASMA, the feasibility region is only slightly skewed as the effect of hidden nodes is rendered minor due to the utilization of the busy and carrier sense tones. Note that the direction of the skew cannot be easily predicted as the probability that a given transmission is successful is a function of the network state immediately prior to and during that transmission; furthermore, the probability distribution of the network state is not available *a priori*. In the example considered here we see that the achievable throughput on link $< 1,3 >$ is slightly higher than that on link $< 1,2 >$. In an example with 7 nodes and degree 4, and under the C-BTMA access scheme the reverse was seen to be true.

In the following subsection, our aim is to emphasize the different performance that is achieved by PRUs according to the subset of the PRUs of the network that they hear.

5.3.3 The Wall Configuration

The wall configuration represents a situation where there exists a set of PRUs all of whom communicate with a central station only, but where a subset of the PRU's are able to hear all other PRUs in the network. Due to the existence of a 'wall', the remaining PRUs are able to hear only a subset of the PRUs of the network. Note that this configuration was considered in [6]. In that work the network performance under CSMA and BTMA was obtained by means of approximate

analysis and simulation. Additional approximate analysis taking into account time capture and (mini) slotting under the CSMA access scheme was performed in [19]. In both these studies, the purpose was to show the effect of hidden nodes on the overall network capacity, and the feasible capacity regions were not shown. In the present work, the feasibility region for C-BTMA is obtained by means of the analysis of C-BTMA in two-hop networks described in appendix 7.1.3. The results for ALOHA was obtained using analysis as described in appendix 7.1.1, and for CDMA by an approach similar to that in appendix 7.1.1. For the CSMA access scheme, the results were obtained by simulation.

We first consider the 4 node wall under the C-BTMA access scheme. Let C_1 denote the capacity of a PRU that hears all other PRUs and C_2 denote the capacity of a PRU that does not. In figure 5.9, the (C_1, C_2) feasibility region is plotted for various values of a. We note that for $a = 0$, $C_1 + C_2 = 0.5$. For $a > 0$, the feasible nodal capacities lie below this line, and we also observe that the fully connected PRUs are able to achieve a slightly higher capacity than PRUs that are not fully connected. For a given traffic pattern, as a increases the nodal capacities decrease and furthermore, the difference between the achievable capacities for the PRUs that are fully connected versus those that are not increases. This is because, the vulnerable period for PRUs that are fully connected is equal to a while that of PRUs that are not is equal to $2a$. In figure 5.10. the feasible region for the various access schemes is depicted for $a = 0.01$. We note that for ALOHA and CDMA, the feasibility region is symmetric indicating that the achievable throughput for all nodes is the same. The reason for this is the same as in the multiconnected ring case, namely, that the probability that a transmission is successful is independent of whether nodes are hidden or not. As indicated above, for C-BTMA nodes that are fully connected are able to achieve a slightly higher throughput than those that are not. For CSMA, the performance of nodes that are not fully connected is degraded

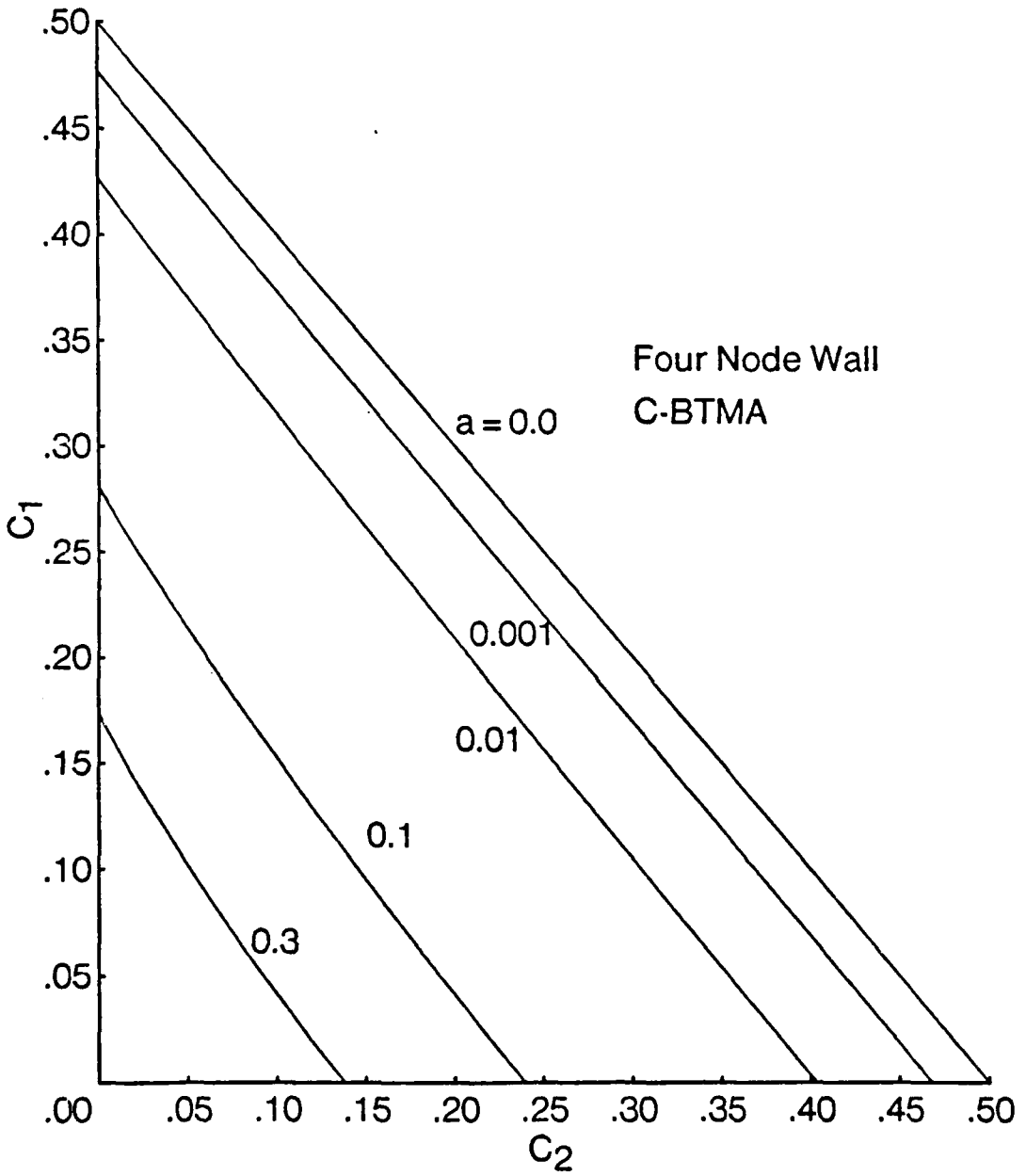

Fig. 5.9 Feasible region for nodal capacities in a 4 node wall network, under the C-BTMA access scheme for various values of a.

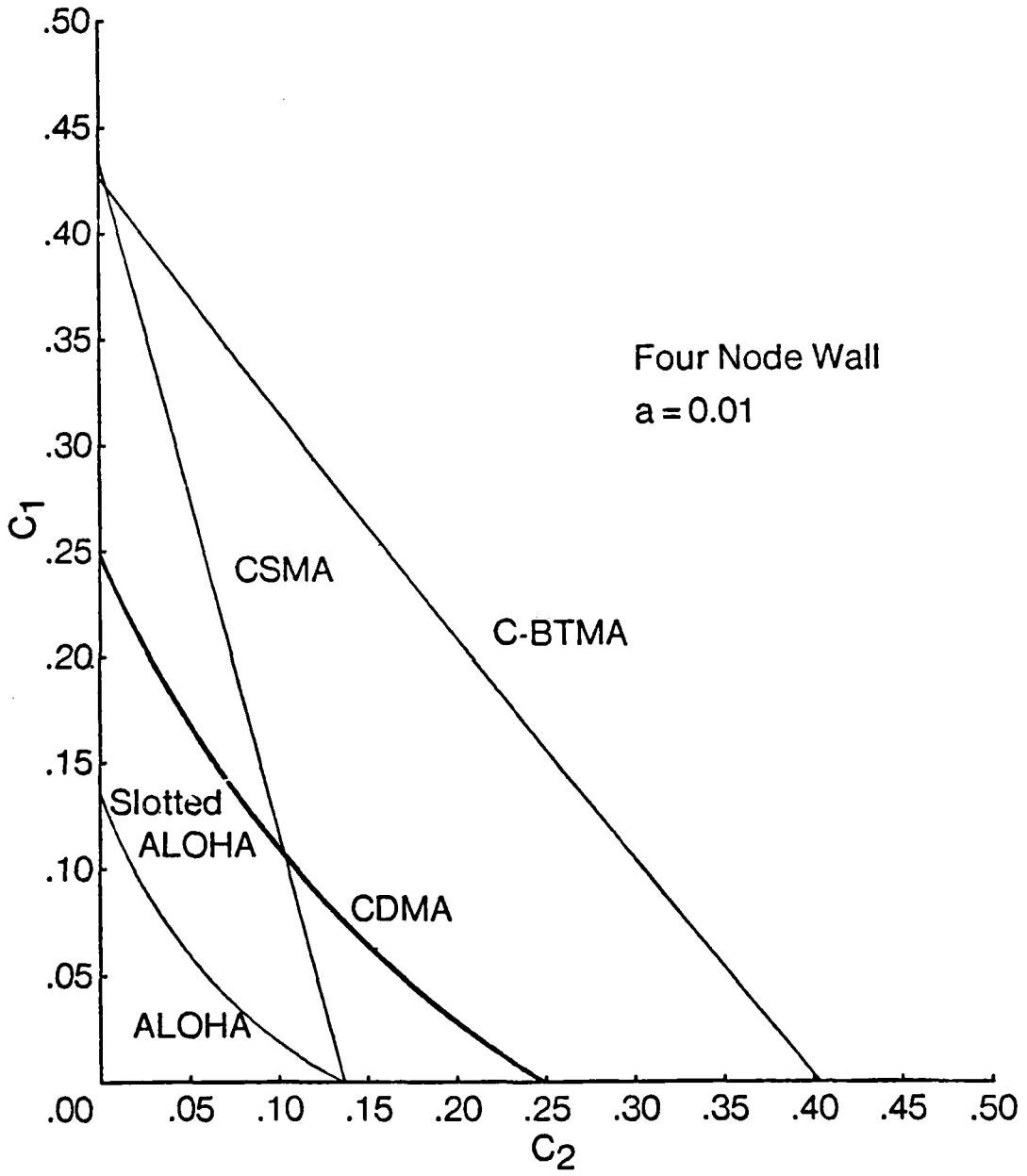

Fig. 5.10 Feasible region for nodal capacities in a 4 node wall network, with $a = 0.01$, under various channel access schemes.

versus those nodes that are fully connected. Indeed, for $C_1 = 0$, the performance of CSMA is identical to that of ALOHA since, in this case, the network is like a 2 node star. For $C_2 = 0$, the performance of CSMA is slightly better than that of C-BTMA. As noted in chapter 3, this improvement is due to the additional period of time (a) for which nodes are blocked from transmitting in C-BTMA because of the busy-tone as compared with CSMA.

5.4 Large-Scale Networks

Large-scale realistic networks typically have a non-regular structure and hundreds or thousands of radio links. The space of scheduling parameters is thus extremely large and is impractical to search over by means of simulation. We therefore do not utilize the approach of parameter space search and instead consider a number of simple sub-optimal transmission scheduling algorithms. The simplest such algorithm consists of specifying that all radio units use the same scheduling rate G. Note that having employed this approach and specified a particular value of G for all the PRUs of the network, at capacity particular links are saturated while others are not saturated. The capacity on saturated bottleneck links can be increased by perturbing the scheduling rates of the links and PRUs of the network. While such perturbations can be carried out globally over all the scheduling parameters of the network, here we consider only local perturbations in the vicinity of bottleneck PRUs. In particular, we consider the improvement in capacity to be gained by increasing both the scheduling rate and the probability that a transmission is undertaken and successfully received, on a given bottleneck link. Clearly this approach has limitations since it is unlikely that a local algorithm would reach the network capacity optimized over all scheduling parameters. Nevertheless, it is of

interest to investigate the capacity achievable by these simple sub-optimal schemes, referred to hereafter as local perturbation schemes.

The example topology considered for such investigations was obtained by measurement over real terrain near Yuma, Arizona and is depicted in figure 5.11*. The topology consists of 51 nodes, 432 directed links, and has nodal degree varying from 1 to 28 (with average nodal degree = 8.47). Note that there are no isolated subnetworks. The traffic pattern is considered to be uniform end-to-end and shortest path routing is employed. Assuming that each PRU generates unit traffic, the distribution of nodal traffic (both new and in transit) is shown in figure 5.12. Note that the average path length is 2.685 hops. We also consider the same propagation delay on all links corresponding to a value of $a = 0.01$.

5.4.1 Transmission Scheduling Algorithms

As stated above, the simplest transmission scheduling algorithm is to specify that all radio units use the same scheduling rate G. (Such a simple algorithm is also desirable from a network management point of view). We first consider this algorithm utilized with the separate queue per link scheme, with $B_0 = m = 40$ and $B_T = \infty$. Note that the former value is chosen to be large enough so that the probability of loss for new packets is negligible for loads below capacity. In figure 5.13, the network capacity is plotted as a function of the nodal scheduling rate for the various channel access schemes. We see that for each access scheme there exists a value of G denoted G_{max} which maximizes the capacity. It is interesting to observe that the range of optimal scheduling rates G obtained from the study of regular topologies (of degree 2 through 10) roughly corresponds to the range of highest capacity here. This suggest that for a given access scheme, the results

*Courtesy Paul Sass, U. S. Army Cencoms, Ft. Monmouth, NJ 07703.

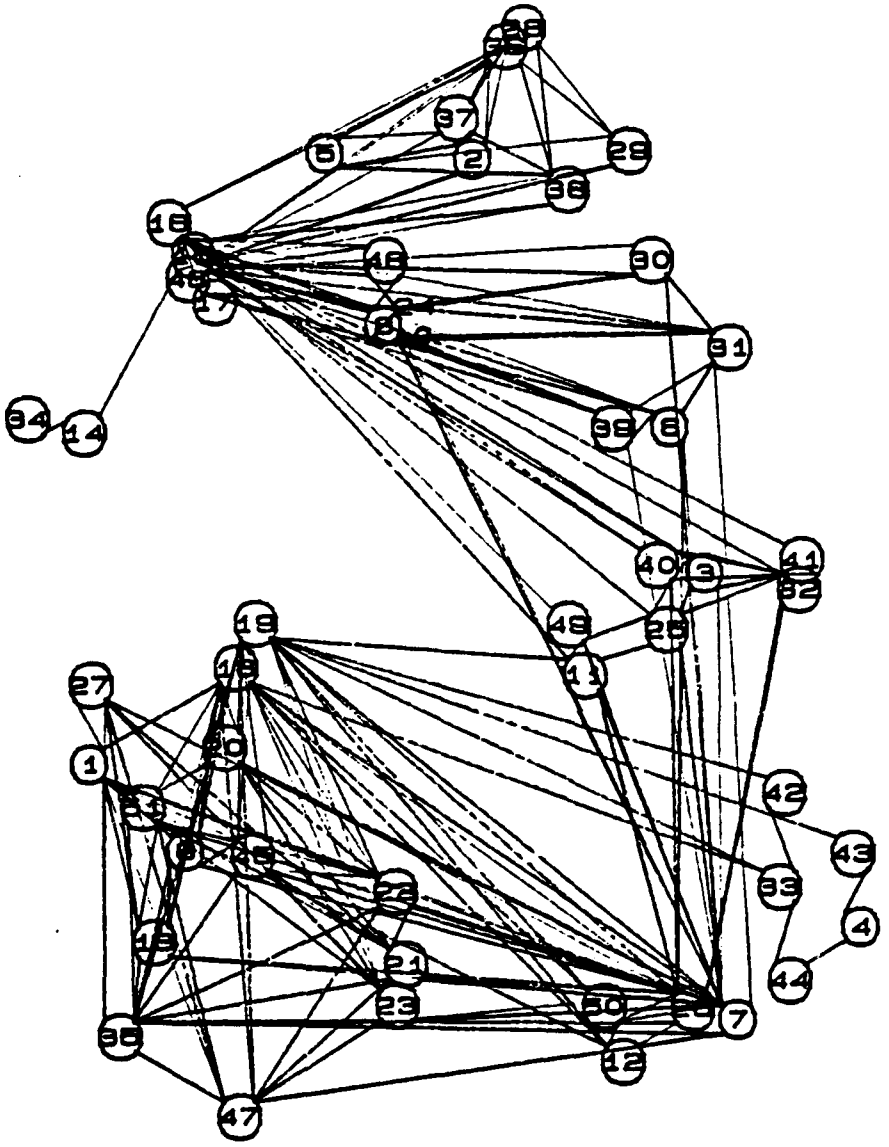

Fig. 5.11 A large-scale packet radio topology (Yuma).

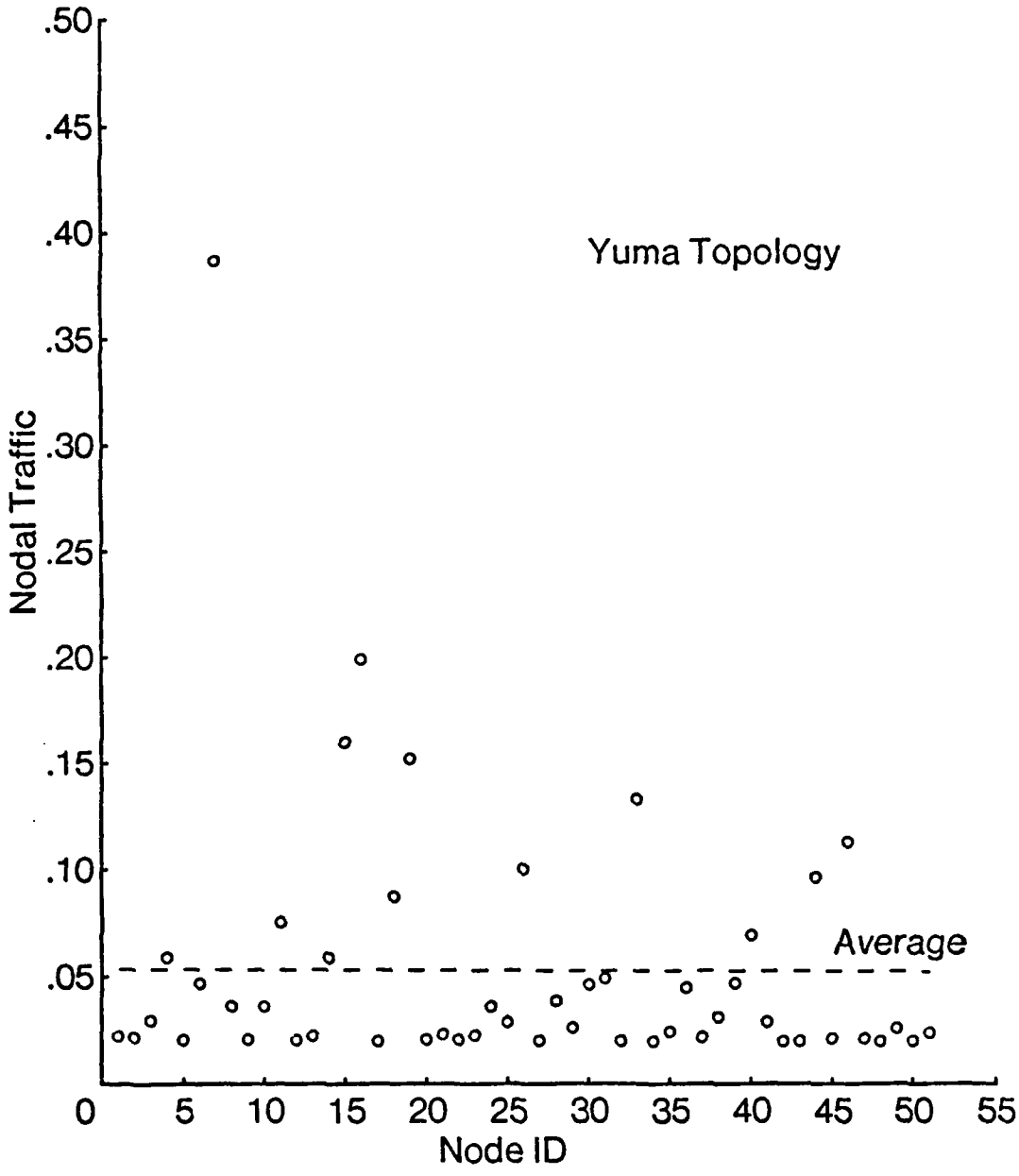

Fig. 5.12 Distribution of nodal traffic in Yuma network for a uniform traffic requirement and shortest path routing.

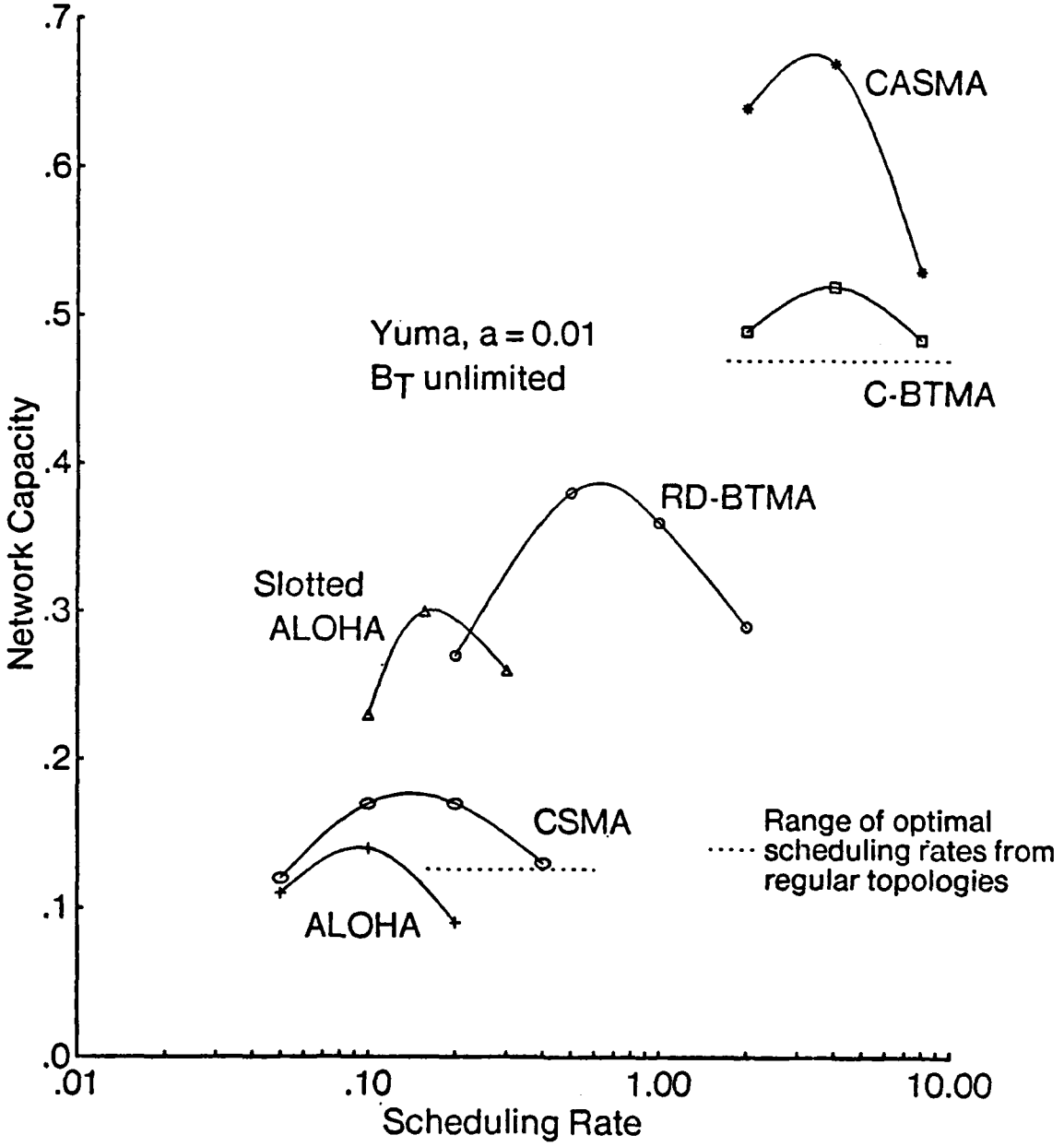

Fig. 5.13 Network capacity versus nodal scheduling rate in the Yuma topology for various channel access schemes.

from the study of regular topologies may serve as a crude guide in the selection of scheduling rates. We observe that the ordering of the access schemes in terms of their maximum capacities is the same as was seen in the regular topologies. Furthermore, also similar to what was seen in the regular topologies, the network capacity is somewhat insensitive to the scheduling rate G, for values of G within about a factor of 2 or 3 of G_{max}.

The scheduling rate on a given bottleneck link may be increased by increasing the associated PRUs scheduling rate, keeping the queue scheduling distribution uniform and with the scheduling rates of all other PRUs fixed at G_{max}*. In all cases in figure 5.13, a single PRU (denoted K) was detected as the bottleneck In figure 5.14, we plot network capacity versus the scheduling rate of PRU K for the C-BTMA, CSMA and ALOHA access schemes. In all cases $K = 7$. This is not unexpected as PRU 7 carries the highest traffic of all nodes (refer to figure 5.12) and thus we may expect PRU 7 to be a bottleneck PRU *a priori*. We observe that the capacity under each scheme initially increases with G_7, reaches a maximum and then decreases. Note that the decrease in capacity coincides with a PRU other than PRU 7 becoming the new bottleneck PRU. The total improvement in capacity achieved relative to the case where all PRUs utilize scheduling rate G_{max} depends on the access scheme and amounted to 5% in the case of C-BTMA to 30% in the case of CSMA. In the sequel, we consider two experiments in which it is attempted to increase the probability of successful reception over a bottleneck link by decreasing the scheduling rates of the neighbors of the source and the neighbors of the destination independently of one another. The set of scheduling rates that resulted in the maximum capacity in figure 5.14 are used as the operating values about which perturbations are made.

*Note that in general, not only the saturated PRUs scheduling rate but also its queue scheduling distribution could be varied.

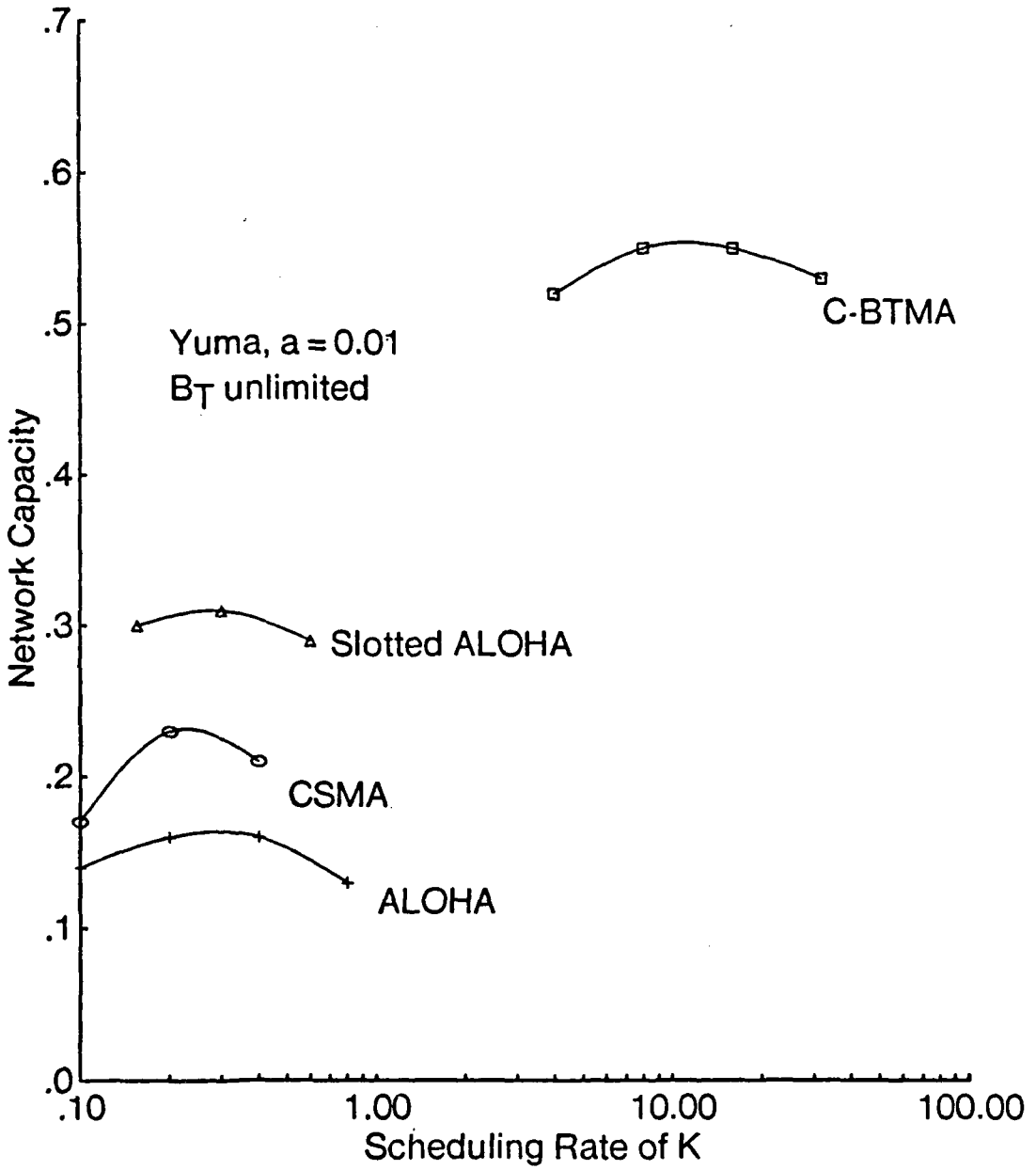

Fig. 5.14 Network capacity versus bottleneck PRUs scheduling rate in the Yuma topology for various channel access schemes.

We first consider reducing the scheduling rate of neighbors of the source node on the bottleneck link. This measure trades off the improvement in the capacity of the bottleneck link for degradation in the capacity of neighboring nodes of the source, as explained below. Let i represent the source PRU and j the destination PRU of a given bottleneck link denoted (i, j). Decreasing the scheduling rate of PRUs in $\mathcal{N}(i)$ may increase the likelihood of PRU i gaining access to the channel at a scheduling point for access schemes which employ carrier sensing. Furthermore, if $\mathcal{N}^*(i) \cap \mathcal{N}^*(j) \neq \phi$ then the probability of collision on link (i, j) may be reduced. The above two effects tend to improve the capacity of the bottleneck link at the cost of possibly reducing the capacity of PRUs in $\mathcal{N}(i)$, one of which may then become the new bottleneck PRU. In order to study this tradeoff we let G_7 be fixed at its maximizing value as depicted in figure 5.14, with the rates of all other PRUs besides those in $\mathcal{N}(7)$ be fixed at G_{max}. In figure 5.15 we plot the network capacity versus the scheduling rate of PRUs in $\mathcal{N}(7)$ for the C-BTMA and CSMA access schemes. We observe for C-BTMA some benefit in that a small increase in capacity (about 5%) is achieved. On the other hand, for CSMA no increase in capacity was observed, indicating that the decrease in the capacity of PRUs in $\mathcal{N}(7)$ is limiting the network capacity.

We now consider the decreasing of the scheduling rates of PRUs in $\mathcal{N}(j)$. This measure trades off the improvement in the capacity of the bottleneck link for degradation in the capacity of the neighboring nodes of the destination. Note that on link (i, j), the probability of collision is decreased, and the probability that a transmission is undertaken may be affected by this strategy depending on the access scheme. On the other hand, the capacity of PRUs that are neighbors of destinations on bottleneck links may be reduced. Let D_b denote the set of destinations on bottleneck links and, if A is a set of nodes whose scheduling rates are the held the same, let G_A denote the scheduling rate of the nodes in set A. Let G_7 be fixed at its maximizing

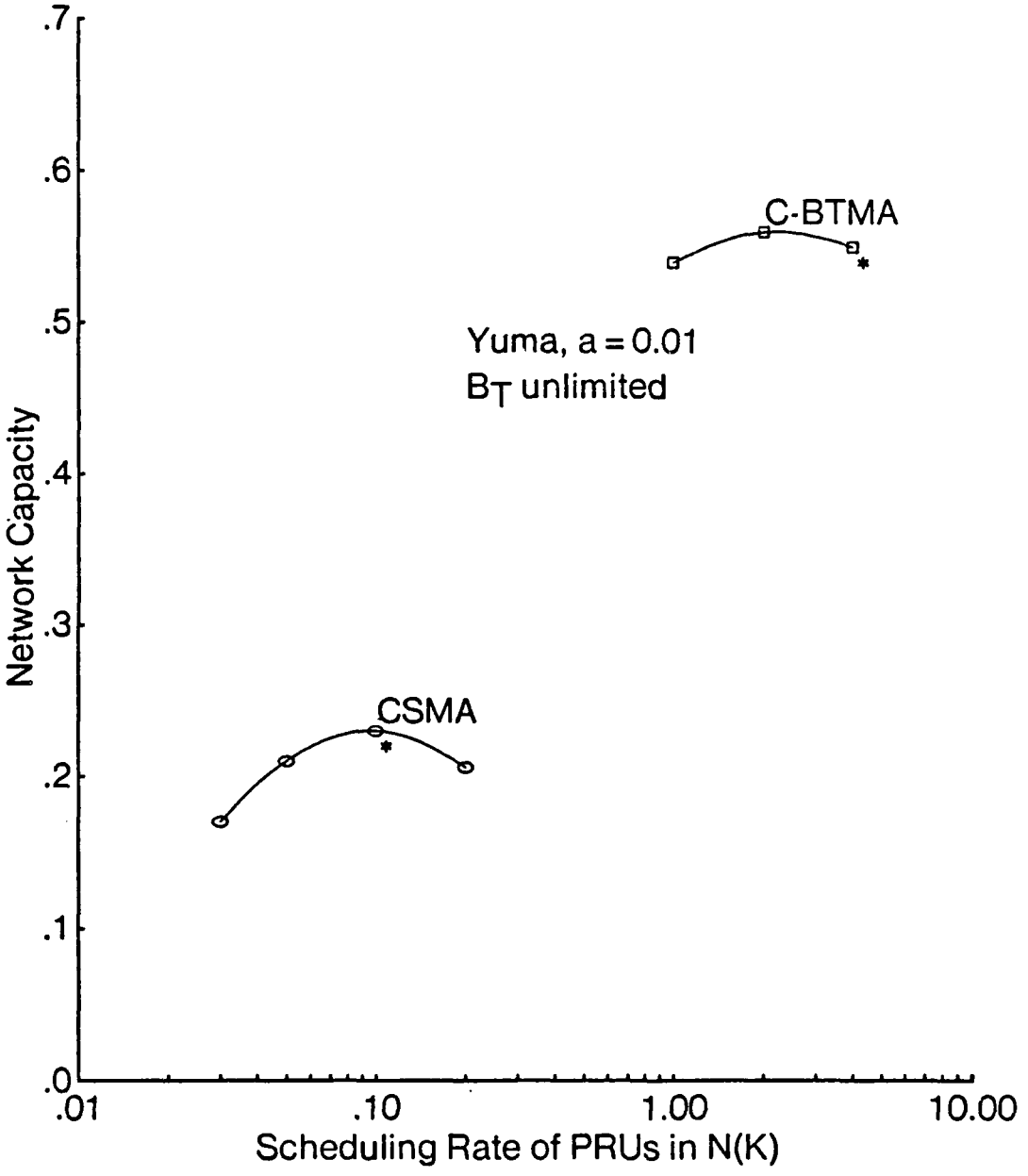

Fig. 5.15 Network capacity versus scheduling rate of neighbors of the bottleneck PRU in the Yuma topology for various channel access schemes.

value as depicted in figure 5.14, and the rates of all other PRUs besides those in D_b be fixed at G_{max}. In figure 5.16 we plot the network capacity versus the scheduling rate of nodes in $\mathcal{N}(D_b)$, $G_{\mathcal{N}(D_b)}$ for the C-BTMA and CSMA access schemes. In the case of C-BTMA, $D_b = (8, 19, 39)$ and a slight benefit is seen in that an increase in capacity of about 5% is observed. For CSMA $D_b = (6, 19, 31)$ and the network capacity was seen to only decrease as $G_{\mathcal{N}(D_b)}$ decreases. This indicates that the decrease in the capacity of links terminating on PRUs in D_b is limiting the network capacity.

There are many additional local perturbations that can be performed, such as decreasing the scheduling rates of PRUs that are neighbors of the source and destination of a bottleneck link simultaneously, or repeating many of the above experiments but with the scheduling rates of PRUs other than those in the vicinity of the bottleneck PRU held fixed at a value different from G_{max}. Rather than continuing to exhaustively check all variations, we limit the remainder of this section to a partial assessment of the absolute performance of the schemes we have examined so far. In order to accomplish this, it is necessary to compare the results obtained here with a global maximization over the entire set of scheduling parameters. Unfortunately, such a global maximization is infeasible by means of simulation. Under the assumptions made in this study, analytic solutions to the network capacity problem are known for the pure and slotted ALOHA schemes only (see Appendix 7.1). We therefore are able to assess the absolute performance of the algorithms proposed here only for the ALOHA schemes. In table 5.1, the capacity of the local perturbation algorithm where only the scheduling rate of the bottleneck PRU is varied (all other scheduling rates being held fixed at G_{max}), is compared with the optimum capacity obtained from analysis. We observe that a capacity of approximately 80% of the optimum value is achievable. For comparative purposes, we also show results obtained using a local traffic flow algorithm proposed in [41] for slotted ALOHA

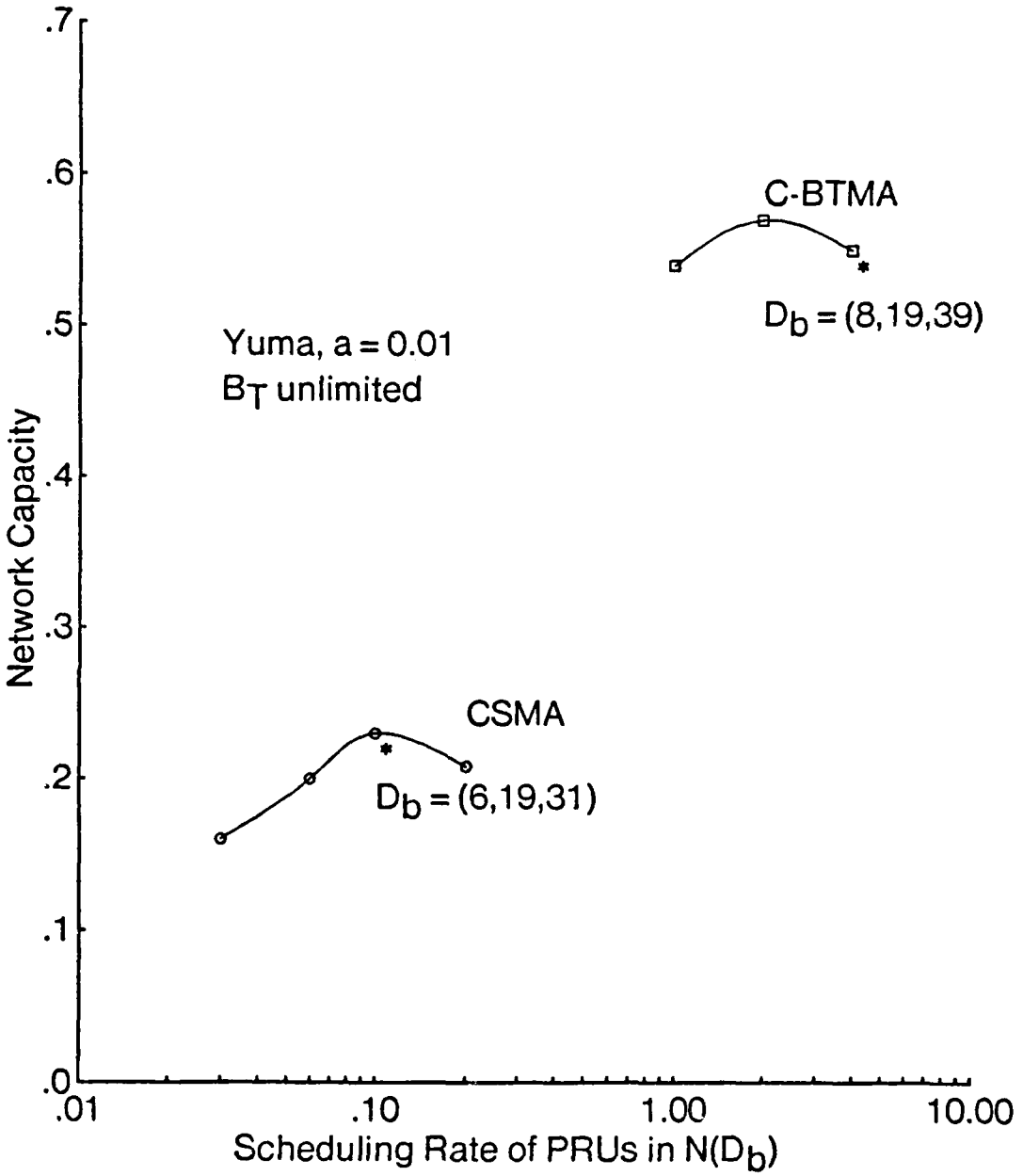

Fig. 5.16 Network capacity versus scheduling rate of neighbors of destinations of bottleneck links in the Yuma topology for various channel access schemes.

and a similar algorithm given here for pure ALOHA.

	Pure ALOHA	Slotted ALOHA
Optimum	0.20	0.39
Local Perturbation	0.16	0.31
Traffic Flow	0.18	0.36

Table 5.1. The capacity of transmission scheduling algorithms for pure and slotted ALOHA.

These local traffic flow algorithms are based on two elements:

(i) For a given PRU i, an assumed proportional relationship between the scheduling rate and the sum of all outgoing link traffic, and

(ii) A heuristic functional relationship among the scheduling rates of PRU's in $\mathcal{N}(i)$; the relationship is heuristic as it is based upon an optimality criterion which holds either exactly or approximately in fully connected, single-hop networks but which does not necessarily hold in multihop networks.

For slotted ALOHA, the two relationships are $G_i = K_s\lambda_i$, where λ_i is the sum of the link traffic over all outgoing links of PRU i, and $\sum_{j\in\mathcal{N}(i)} G_j = 1$, which yields the local flow scheduling algorithm

$$G_i = \frac{\lambda_i}{\sum_{j\in\mathcal{N}(i)} \lambda_j}.$$

For pure ALOHA letting $d_i \triangleq |\mathcal{N}(i)| - 1$, the two relationships are $G_i = K_p\lambda_i$ and $\prod_{j\in\mathcal{N}(i)} G_j = G^*(d_i)^{1+d_i}$. Note that $G^*(d)$ is the scheduling rate that maximizes the capacity of regular networks of degree d (appendix 7.1.1) and is expressed as

$$G^*(d) = \sqrt{\frac{d+1}{d}} - 1.$$

This yields the local flow scheduling algorithm

$$G_i = \frac{\lambda_i(\sqrt{\frac{d_i+1}{d_i}} - 1)}{(\prod_{j \in \mathcal{N}(i)} \lambda_j)^{\frac{1}{1+d_i}}}.$$

We observe that the "local-flow" heuristics for pure and slotted ALOHA perform well and achieved a capacity of approximately 90% of the theoretical maximum. Unfortunately, the operation of the remaining channel access schemes is characterized by a strong coupling among all the PRUs of the network, and the relationship among the scheduling rates is thus more complex. For these schemes it is unlikely that a local heuristic relationship among the scheduling rates of PRUs of the type described above would lead to a good performance. Furthermore, the variation of $G(d)$ with d over the range of interest (i.e, 1 through 28) is not completely known and would be costly to obtain by means of simulation. Therefore we do not consider local traffic flow algorithms for the remaining access schemes. The remainder of this chapter is limited to studying the effect of finite transit buffer size in the Yuma network.

5.4.2 Finite Transit Buffer Size

Having considered the case of infinite transit buffer size we now consider the case of finite transit buffer size. We assume that all PRUs have the same buffer storage size. For simplicity, the single queue per PRU scheme is utilized here with $B_0 = m = 40$ and various values of B_T. Consider now the case where all PRUs utilize the same scheduling rate G. In figure 5.17, for the C-BTMA access scheme the network capacity is plotted as a function of G for various values of B_T. The general behaviour is seen to be similar to that observed in chapter 4 for regular topologies; in particular, we see that for low values of B_T C-BTMA is storage bound. The

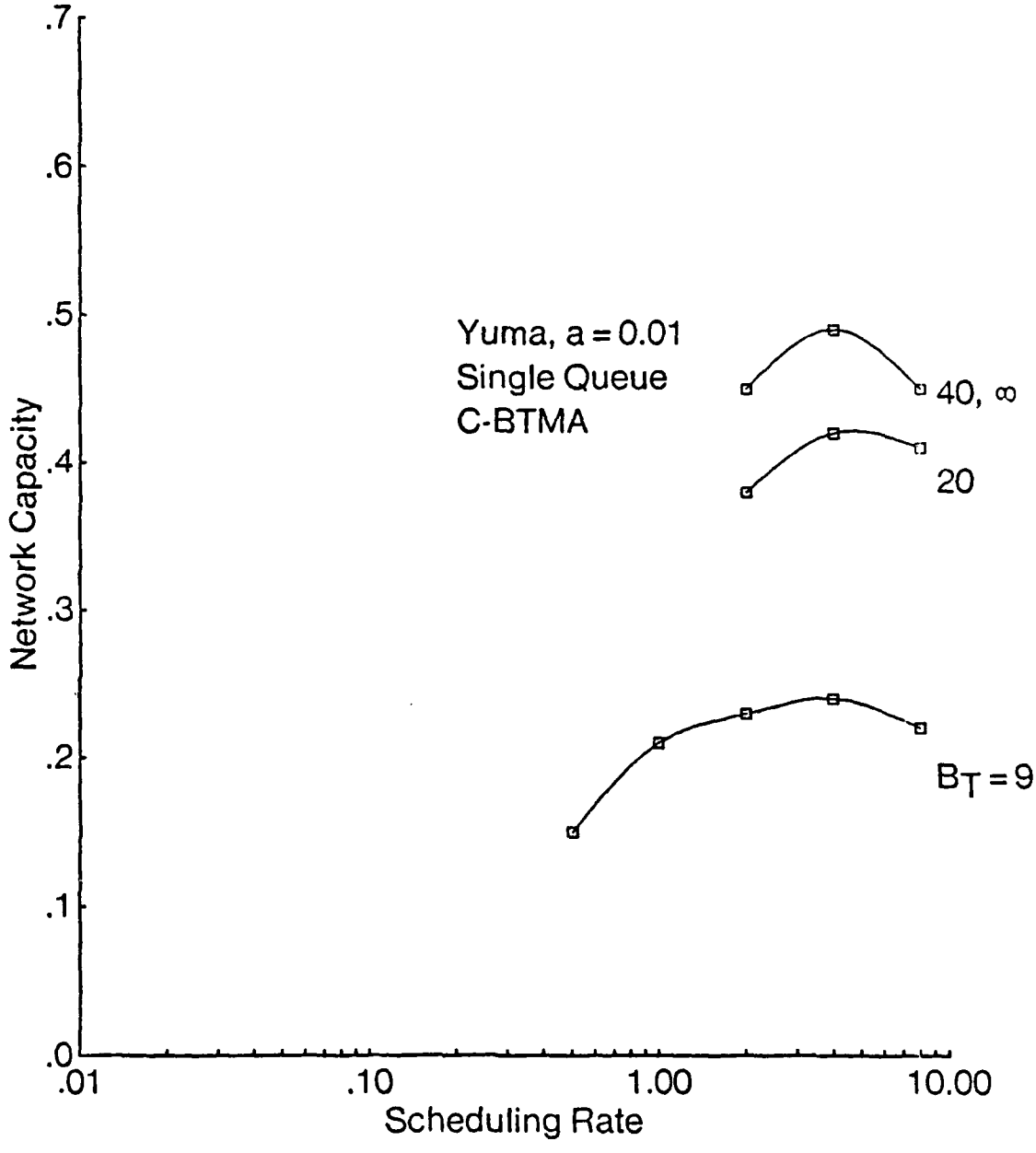

Fig. 5.17 Network capacity versus nodal scheduling rate in the Yuma topology, for the single queue per PRU scheme with $B_0 = m = 40$ and various values of B_T under the C-BTMA channel access scheme.

improvement in performance achievable by tuning the bottleneck PRUs scheduling rate is shown in figure 5.18 and amounts to 25% relative to the case where all PRUs use the same scheduling rate. Also considered is the case where the three PRUs with the highest average buffer occupancies at capacity, namely, PRUs 7, 11, and 19 are treated as bottleneck PRUs. (In the figure, these are denoted K_s). For this case a certain amount of improvement in capacity is also seen although it is less than for $K = 7$. This is because PRUs 7, 11 and 19 are neighbors of one another and hence the improvement in capacity is limited by the increase in interference among these nodes as their scheduling rates increase.

5.5 Summary

We have investigated a number of characteristics of multihop packet radio networks not found in entirely regular networks by considering several simple two and three parameter networks. Most notably we have shown that for CSMA the difference in achievable performance among different PRUs and links is significant compared with the remaining access schemes. With respect to large-scale networks, in a particular example we have studied a number of simple transmission scheduling strategies. These strategies consisted of the selection of a single scheduling rate for all PRUs followed by local perturbation of scheduling rates in the vicinity of a bottleneck PRU. For the case of ALOHA, we have shown that a capacity within 20% of the theoretical maximum is achievable. The preliminary results obtained so far suggest that this is a promising approach to packet scheduling in large multihop networks, deserving of additional research.

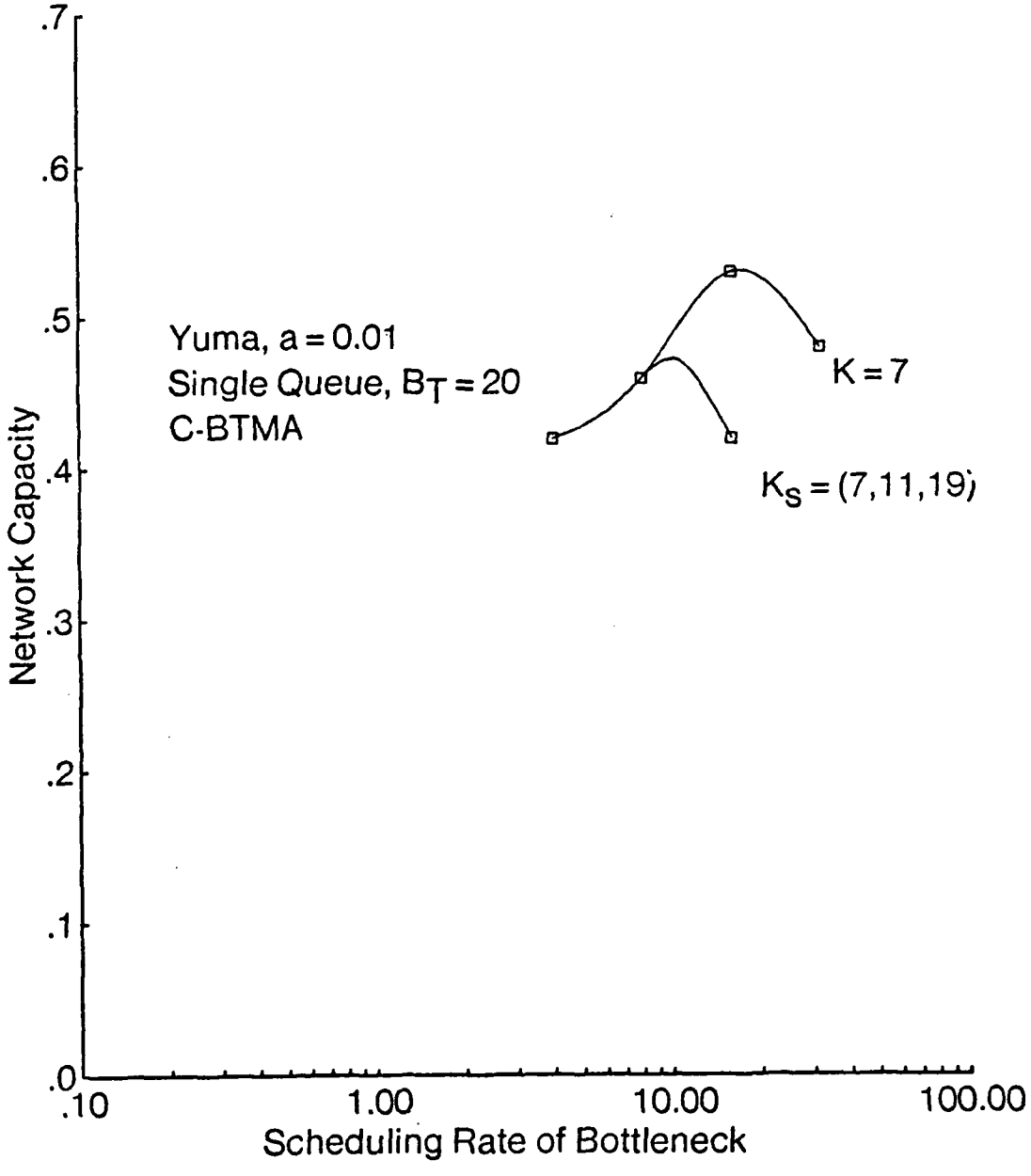

Fig. 5.18 Network capacity versus bottleneck PRUs scheduling rate in the Yuma topology, for the single queue per PRU scheme with $B_0 = m = 40$ and $B_T = 20$ under the C-BTMA channel access scheme.

Chapter 6

Concluding Remarks and Future Research

6.1 Concluding Remarks

In this dissertation, a number of aspects of multihop packet radio networks have been addressed. In networks with a regular structure and balanced traffic flow, the effect of transmission scheduling rate, the ratio of propagation delay to packet transmission time, store-and-forward buffer size, and to some extent network access flow control on throughput and delay performance was examined. The performance of various existing channel access schemes, namely, ALOHA, CSMA, CDMA, and BTMA and a new scheme referred to as Coded Activity Signalling Multiple Access (CASMA) was investigated. We observed that for all access schemes and in large enough networks, the nodal degree was the topological parameter primarily determining the optimum scheduling rate. We showed that contrary to the case of single-hop, fully connected networks [5], CSMA is little affected by propagation delay (its performance being primarily degraded due to hidden nodes). Propagation

delay was also shown to have little effect on ALOHA and CDMA, but it had a major limiting effect on the performance of BTMA and CASMA. The results obtained also implied that analytic models that use the zero propagation delay assumption are more applicable for ALOHA, CSMA and CDMA than for BTMA and CASMA. Regarding the relative performance of the BTMA schemes, it was observed that C-BTMA outperformed ID-BTMA in all examples considered, suggesting that the collisions allowed by the ID-BTMA protocol were more harmful to performance than the superfluous blocking of transmissions by C-BTMA. If more efficient random access schemes than C-BTMA are desired, then by comparing the performance of CASMA and C-BTMA for values of a in the practical range ($0.01 \leq a \leq 0.1$), we conclude that there exists a margin for improvement over C-BTMA of about 20% to 40%. Regarding the effect of finite buffer size, the results obtained indicated that ALOHA and CSMA are channel bound, implying that relatively few buffers per repeater may be utilized without incurring a performance penalty. We also showed that this was not the case for BTMA and CASMA as these schemes exhibited a capacity degradation of up to 50% in certain examples where the buffer storage size per repeater was too small. In all the examples studied, the largest value of buffer storage size required in order to correct this degradation was approximately 40. Note that the amount of buffering required is expected to increase if acknowledgments are not for free.

The performance of a number of variants of the SBP buffer management scheme was also obtained. For storage bound access schemes and where the buffer size was limited, the HTG variant achieved a slightly higher capacity than the HSF, while the differences in capacity among the remaining variants was minor. The variants differed more noticibly in terms of packet delay. In the HTG scheme with a HCF service discipline, packet delay was reduced for packets that travel shorter distances, and increased for packets that travel longer distances, as compared with

a benchmark consisting of FCFS service with infinite buffers. The opposite was true for the HSF scheme, namely, delay was increased for packets that travelled shorter distances, and decreased for packets that travelled longer distances.

In networks with a more general structure, we showed that the CSMA scheme exhibited a high degree of variance in the achievable capacity among different PRUs and links, as compared with the remaining access schemes. Due to the large size of the parameter space in general multihop networks, a number of simple sub-optimal transmission scheduling algorithms were introduced. We showed that in the case of ALOHA, the strategy of selecting a single scheduling rate for all PRUs, followed by a local perturbation of scheduling rates in the vicinity of saturated PRUs led to a capacity of within 20% of the theoretical maximum in a realistic example. As the remaining channel access schemes also appeared to perform well using the same scheduling algorithm, we therefore conclude that this approach to packet scheduling in large multihop networks appears promising.

6.2 Suggestions for Future Research

Our suggestions for future research fall into two categories. The first category consists of system issues relating to packet radio networks that have not been studied in this dissertation or (to any satisfactory extent) in the literature. The second category consists of topics that build on or are suggested by the research reported on here.

In the first category is the study of hop-by-hop acknowledgment schemes. While some work has on acknowledgments been has been carried out in the single-hop environment [59,60], little work has been done in the multihop environment. A hop-by-hop acknowledgment can be obtained by a source PRU by detecting the

transmission of the packet in question being forwarded over the next hop; such a scheme is referred to as an echo-ACK. Alternatively, an explicit acknowledgment possibly contained in a dedicated packet may be sent, referred to as an active-ACK. In both the echo-ACK and the active-ACK schemes the channel access protocol can be modified to improve acknowledgment efficiency as has been suggested in [7] for BTMA. The performance of both the echo-ACK scheme and the active-ACK scheme needs to be established, most likely by means of simulation. Note also that in the active-ACK scheme, acknowledgments are often given priority over data packets, and hence such a scheme may be integrated rather naturally within the priority structure of the SBP scheme.

Routing is another important system issue that has so far been little addressed. Unlike the situation in point-to-point wire-based networks, the routing problem in packet radio is complicated by the fact that the capacity of network links is a function of the link traffic and the channel access policy. Given the progress in the understanding of the channel access policy achieved in this dissertation and other recent works (refer to section 1.5), the time may be ripe for an attack on the routing problem.

This research has also suggested a number of interesting problems. The issue of real-time control of the scheduling rates is basic, and the surface of this subject has barely been scratched in chapter 5 of this dissertation. The results obtained there are encouraging in that they suggest that adequate performance can be achieved with rather crude schemes. The design of more sophisticated schemes will surely prove a fruitful area of research. Regarding the issue of buffer management, it would be interesting to study 'lossy' schemes, whereby packets are dropped from the network after a set number of unsuccessful retries, and compare results with those already obtained for lossless deadlock-free schemes. This would quantify the tradeoff

between the overhead incurred in the lossless schemes due to the prioritization versus the presumable degradation in performance for the lossy schemes; such results would prove valuable to packet radio system designers.

Chapter 7

Appendices

7.1 Capacity Analysis

7.1.1 Pure and Slotted ALOHA in Arbitrary Topologies

Let G_{ij} be the rate of the scheduling process at node i for packets destined to node j. It is assumed that G_{ij} is non-zero only if $j \in N^*(i)$, $(i = 1, \cdots, N)$. Let $G_i = \sum_{j \in N^*(i)} G_{ij}$. Let c_{ij} denote the average number of packets transmitted successfully from node i to node j per packet transmission time, and let $c_i = \sum_{j \in N^*(i)} c_{ij}$.

For each node i, c_{ij} is zero for $j \notin N^*(i)$, while for $j \in N^*(i)$

$$\frac{c_{ij}}{G_{ij}} = \Pr\{\text{scheduling point at node } i \text{ results in a transmission}$$

$$\text{and the transmission is successful}\}$$

$$= \Pr\{\text{node } i \text{ is not transmitting}\} \Pr\{\text{transmission } < i, j > \text{ is successful}\},$$

$$= P_i^I P_{ij}^s$$

Pure ALOHA: From renewal theory arguments, $P_i^I = 1/(1+G_i)$. Furthermore,

$P_{ij}^s = \Pr\{\text{transmission } < i,j > \text{ is successful}\}$

$= \Pr\{j$ and it's neighbors excluding i are idle at start of reception and no node in $N(j)$ transmits during the transmission $< i,j >\}$.

Let $N'(j) = N(j) - i$. Then

$$P_{ij}^s = \prod_{l \in N'(j)} \left(\frac{1}{1+G_l}\right) \prod_{k \in N'(j)} e^{-G_k},$$

$$c_{ij} = G_{ij} \prod_{l \in N(j)} \left(\frac{1}{1+G_l}\right) \prod_{k \in N'(j)} e^{-G_k},$$

$$c_i = \sum_{j \in N^*(i)} G_{ij} \prod_{l \in N(j)} \left(\frac{1}{1+G_l}\right) \prod_{k \in N'(j)} e^{-G_k},$$

$$= \sum_{j \in N^*(i)} G_{ij} \prod_{l \in N(j)} \left(\frac{1}{1+G_l}\right) \exp(-\sum_{k \in N'(j)} G_k),$$

For the case of the regular topologies (with degree d), $G_i = G$ and $c_i = c(G)\ \forall i$. Hence the nodal capacity is expressed as

$$c(G) = \frac{G}{\left(1+G\right)^{d+1}} e^{-dG},$$

is maximized by

$$G = \sqrt{\frac{d+1}{d}} - 1$$

and hence the optimum nodal capacity is expressed as

$$c(G^*) = \left(\sqrt{\frac{d}{d+1}}\right)^{d+1} \frac{\sqrt{d+1} - \sqrt{d}}{\sqrt{d}} e^{-(\sqrt{d^2+d}-d)}, \qquad (7.1)$$

Slotted ALOHA: Note that $P_i^I = 1, \ \forall i$.

$$P_{ij}^s = \prod_{k \in N'(j)} (1 - G_k)$$

$$S_{ij} = \frac{1}{1+a} G_{ij} \prod_{k \in N'(j)} (1 - G_k).$$

For the case of regular topologies (with degree d), the nodal capacity is expressed as

$$c(G) = \frac{1}{1+a} G(1-G)^d.$$

This is maximized by $G = 1/(1+d)$, and hence

$$\begin{aligned} c(G^*) &= \frac{1}{1+a} \frac{1}{d+1} (1 - \frac{1}{d+1})^d \\ &= \frac{1}{(1+a)(d+1)} \Big(\frac{d}{d+1}\Big)^d. \end{aligned}$$

7.1.2 CSMA, C-BTMA and CASMA in Fully Connected Topologies

Using renewal theory arguments as in [5], the nodal capacity is expressed as

$$c(G) = \frac{1}{N} \frac{E(U)}{E(B) + E(I)}$$

where $E(\cdot)$ denotes the expected value, U denotes the channel utilization, B denotes the busy period, and I denotes the idle period.

CSMA: From [61], the above quantities are expressed as

$$E(U) = e^{-a(N-1)G},$$

$$E(I) = \frac{1}{NG},$$

$$E(B) = 1 + 2a - \int_0^a (1 - e^{-yG} + e^{-aG})^{N-1} dy.$$

The latter expression is rather cumbersome to evaluate even for moderate values of N. However, note that for N large with NG fixed, $E(B)$ can be approximately expressed as

$$E(B) = 1 + 2a - \frac{1}{(N-1)G}(1 - e^{-a(N-1)G}).$$

For the case of the tetrahedron topology ($N = 4$), this approximation has been used in calculating $c(G^*)$ and compared with the results obtained using the exact expression for $E(B)$. The difference was found to be $< 2\%$ for $0.0001 \leq a \leq 0.3$, and hence the approximate expression for $E(B)$ is utilized. This yields

$$\begin{aligned} c_{CSMA}(G) &= \frac{1}{N} \frac{e^{-a(N-1)G}}{\frac{1}{NG} + 1 + 2a - \frac{1}{(N-1)G}(1 - e^{-a(N-1)G})} \\ &= \frac{1}{N} \frac{(N-1)Ge^{-a(N-1)G}}{\frac{N-1}{N} + (1+2a)(N-1)G - (1 - e^{-a(N-1)G})}. \end{aligned}$$

Note that for N large, the network capacity is expressed as

$$C_{CSMA}(g) = \frac{ge^{-ag}}{(1+2a)g + e^{-ag}},$$

where we have set $g = (N-1)G$. This is the same expression as in [5], where it was assumed that the generation process of the entire population of nodes constituted a Poisson process of rate g.

For the C-BTMA and CASMA schemes, the same 'large N' approximation as was used for the case of CSMA is utilized.

C-BTMA: The analysis for this case is very similar to that for the case of CSMA. For $N > 2$, the only difference is the fact that the period of time for which nodes are blocked is longer by an additional amount a, due to the busy-tone. Hence

$$c_{C-BTMA}(G) = \frac{1}{N} \frac{(N-1)Ge^{-a(N-1)G}}{\frac{N-1}{N} + (1+3a)(N-1)G - (1 - e^{-a(N-1)G})}.$$

CASMA: In this case, both the vulnerable period and the period of time for which nodes are blocked are longer by an additional amount a as compared to C-BTMA. In this instance for $N > 2$

$$E(U) = e^{-aG(2N-3)},$$

$$E(I) = \frac{1}{NG},$$

$$E(B) = 1 + 4a - \frac{e^{-aG(N-2)}}{(N-1)G}(1 - e^{-aG(N-1)}) - \frac{1}{(N-2)G}(1 - e^{-aG(N-2)})$$

Hence

$$c_{CASMA}(G) = \frac{(N-1)(N-2)Ge^{-aG(2N-3)}}{(N-1)[N(N-2)(1+4a)G - 2] + Ne^{-aG(N-2)} + N(N-2)e^{-aG(2N-3)}}.$$

7.1.3 C-BTMA in Arbitrary Two-hop Topologies

Note that the capacity analysis of C-BTMA in fully connected topologies contained in appendix 7.1.2 is a special case of the analysis given here. A two-hop topology is defined to be a topology in which the maximum shortest pathlength over all pairs of PRUs is two. Let G_{ij} be the rate of the scheduling process at node i for packets destined to node j. It is assumed that G_{ij} is non-zero only if $j \in N^*(i)$, $i = 1, \cdots, N$. Let

$$G_i = \sum_{j \in N^*(i)} G_{ij},$$

$$G = \sum_{i=1}^{N} G_i,$$

$$G_1(i,j) = \sum_{k \in N(j)-i} G_k,$$

$$G_2(i,j) = \sum_{k \in N(j)-N(i)} G_k.$$

Using renewal theory arguments as in [5] and [19], the capacity of node i c_i and the network capacity C are expressed as

$$c_i = \frac{\gamma_i}{E(B) + E(I)},$$

$$C(G) = \frac{\gamma}{E(B) + E(I)}$$

Note that $E(\cdot)$ denotes the expected value, B denotes the busy period, I denotes the idle period, $\gamma_i \triangleq \Pr\{$ transmission of PRU i is successful given that PRU i started the busy period $\}$, and $\gamma \triangleq \Pr\{$ transmission of any PRU is successful given that that PRU initiated the busy period $\}$. We also let $Y_i \triangleq$ the starting time of the last overlapping packet of the busy period given that PRU i starts the busy period.

The above quantities are expressed as

$$\gamma_i = \sum_{j \in N^*(i)} \frac{G_{ij}}{G_i} e^{-a(G_1(i,j)+G_2(i,j)}$$

$$\gamma = \sum_{i=1}^{N} \frac{G_i}{G} \gamma_i$$

$$= \frac{1}{G} \sum_{i=1}^{N} \sum_{j \in N^*(i)} G_{ij} e^{-a(G_1(i,j)+G_2(i,j)}$$

$$E(I) = \frac{1}{G},$$

$$E(B) = 1 + 2a + \frac{1}{G} \sum_{i=1}^{N} G_i E(Y_i).$$

The probability distribution for Y_i is given by

$$F_{Y_i}(y) = \begin{cases} F^b_{Y_i}(y), & y \in (0, a]; \\ F^c_{Y_i}(y) & y \in (a, 2a]. \end{cases}$$

Note that

$$F^b_{Y_i}(y) = \sum_{\substack{m \subset x_i^1 \\ m \neq \phi}} \left\{ \prod_{k \in m} (1 - e^{-yG_k}) \cdot \prod_{l \in x_i^2} e^{-aG_l} \cdot \prod_{j \in x_j^2} e^{-aG_j} \right\},$$

$$F^c_{Y_i}(y) = \sum_{m \subset x_i^1)} \left\{ \prod_{k \in m} (1 - e^{-aG_k}) \cdot \prod_{l \in x_i^2} e^{-aG_l} \cdot \sum_{\substack{q \subset x_i^3 \\ q \neq \phi}} \left\{ \prod_{j \in x_i^4} e^{-aG_j} \cdot \prod_{n \in q} (1 - e^{-(y-a)G_n}) \right\} \right\},$$

where $x_i^1 = N^2(i) - i$, $x_i^2 = x_i^1 - m$, $x_i^3 = N^2(i) - N(i) - m$, and $x_i^4 = x_i^3 - q$.

$E(Y_i)$ is expressed as

$$E(Y_i) = aF^b_{Y_i}(a) - \int_0^a F^b_{Y_i}(y)dy + 2aF^c_{Y_i}(2a) - \int_a^{2a} F^c_{Y_i}(y)dy.$$

As the above expression for $E(Y_i)$ is rather cumbersome, we consider the following approximation for calculating this quantity. We assume that the set of nodes B that may transmit at any point in time constitutes a Poisson process with rate equal to $\sum_{i \in B} G_i$.

Let $G_3(i) = \sum_{k \in N^2(i) - i} G_k$ and $G_4(i) = \sum_{k \in N^2(i) - N(i)} G_k$. In this case,

$$F_{Y_i}(y) = \begin{cases} e^{-(a-y)G_3(i)}(1 - e^{-yG_3(i)}), & y \in (0, a]; \\ e^{-(2a-y)G_4(i)}(1 - e^{-(y-a)G_4(i)}), & y \in (a, 2a], \end{cases}$$

and

$$E(Y_i) = 2a - \frac{1}{G_3(i)} e^{-aG_4(i)}(1 - e^{-aG_3(i)}) - \frac{1}{G_4(i)}(1 - e^{-aG_3(i)}).$$

The above approximation is considerably more simple than the exact expression. Results using the approximation have been compared with those derived from the exact expression for fully connected and star topologies with $0 < a < 1$. (Note that

these two topologies represent two extremes among the set of two-hop topologies in that the average path lengths are 1 and 2 respectively). An extremely close match was noted in all cases. In topologies other than the fully-connected and star cases the capacities were derived using the approximate expression.

7.2 The Simulation Program

In this appendix we briefly describe the aspects of the simulation program structure, the validation of the simulation, and the estimation of the measures of performance that pertain to the packet radio network simulation program. The subject of the simulation of computer systems and queueing networks are discussed more generally in a number of texts [62,63].

7.2.1 Simulation Program Structure

In this section, our intent is to give a top-level description of the program structure without going into the complete details, and to highlight any points that pertain especially to the packet radio aspects of the simulator. The simulation program is a model in software of the packet radio network and channel access protocols as described in chapter 2. The program was written in the Pascal language and consists of approximately 3000 lines of code. The program is portable and has been run under the TOPS20 operating system on several DEC2060 machines and under UNIX on VAX 11/780, 11/750 and microvax II machines.

The program utilizes the event driven technique rather than the synchronous timing technique for advancing the simulation clock, the reasons being greater efficiency and ease of programming [62]. In the event driven technique, the program is

thought of as a finite state machine whose state is updated upon the occurrence of certain events. (The particular events of interest here are described in subsection 7.2.1.1). In the packet radio network simulation program, the state of the machine is a vector whose components are the states of individual PRUs as described in subsection 7.2.1.2, and the states of the packets in the network as described in subsection 7.2.1.3. The sequencing of the simulation events is controlled by means of an event scheduler, which manages the event heap from which the system events are obtained and to which events are added. At any point in time, the next event to occur is the minimum time-ordered event on the heap. Whenever an event occurs, an event handling procedure corresponding to that event is invoked. The event handling procedure may cause the state of the finite state machine to be updated, new traffic to be generated or future events to be scheduled. The input to the simulation program is a set of parameters contained in several input files. The input parameters are: *network parameters such as the non-zero elements of* the hearing matrix, the propagation delay and the access scheme; PRU parameters such as the buffer size and the nodal scheduling rate; traffic parameters such as the traffic generation rate and the packet length; and simulation parameters such as the length of the transient period and confidence interval length (refer to section 7.2.3). The output of the program consists of a number of performance measures, the main ones being throughput average packet delay, loss probability and collision probability matrices, as well as corresponding scalar values, obtained by averaging over all source-destination pairs. The simulation program structure is depicted in figure 7.1. Regarding the event heap, we note that its implementation has a major impact on the amount of CPU time of the program runs since the simulator executes the event scheduling code a large percentage of the time. In the past, the eventheap has often been implemented as a linear list structure [62], which is characterized by $O(n)$ insertion and deletion characteristics (n being the number of events in

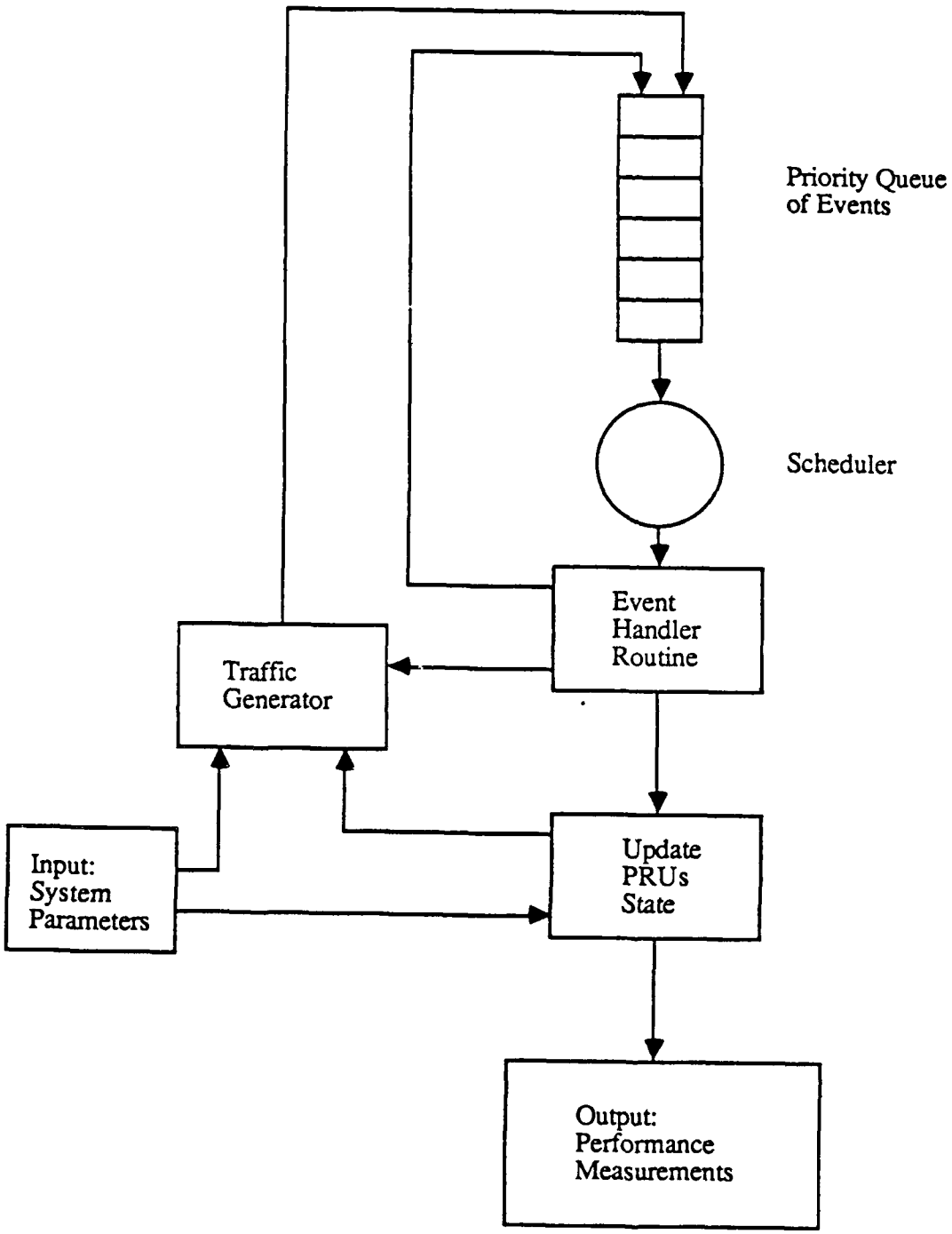

Fig. 7.1 The simulation program structure.

the list). In this program, we have implemented the eventheap as a priority queue having a partially ordered tree structure [64]. For this case, insertion and deletion is $O(\log n)$, which implies a significant savings in execution time particularly for large scale networks.

7.2.1.1 Simulation Events

The simulation events are implemented as record types having fields for the type of the event, the time of the event, and the source PRU associated with this event (among others). The event types consist of: a new arrival of a packet, an attempt to begin to transmit, an end of transmission, a beginning of a reception, an end of a reception, an end of processing of the header, a beginning of reception of busy-tone, an end of reception of busy-tone, a beginning of reception of carrier-sense tone, and an end of reception of carrier-sense tone.

7.2.1.2 PRU Structure

Contrary to the case of fully connected networks, in multihop networks (which are implicitly not fully connected) there is no single shared channel from which users may derive network state information (such as the number of transmitting users). Hence in this simulation, there does not exist a "channel module"; instead, the network state information is derived from the state of the individual PRUs. Each PRU is implemented as a record type. Within each record are fields comprising a set of queues in which packets are stored, and a set of variables indicating the state of that PRU. The queues are managed by a set of buffer management routines. The state variables indicate whether or not the PRU is transmitting or receiving, whether or not a collision has occurred, the number of overlapping transmissions sensed, the number of busy tones sensed, the number of each type of carrier sense

tone sensed, the identity of the transmitting PRU that has captured the receiver, etc. The status of the variables is used to determine both whether or not to transmit, and at the end of a packet reception whether or not a collision has occurred. The PRU structure is depicted in figure 7.2.

7.2.1.3 Packet Structure

Each packet is implemented as a record type having fields for the identities of the source, the ultimate destination and the immediate destination PRUs, as well as the packetlength, and the hopcount.

7.2.1.4 Extensibility

The simulation program was developed with the intent of being modular in structure and extendible. As changes to accomodate new protocols were made to the program, it was observed that many procedures in the program remained unchanged. These included the event heap manipulation routines, traffic generation routines, shortest path routing routine and many buffer manipulation routines. The I/O routines changed only slightly as new variables corresponding to protocols were added. As new buffer management schemes were studied, these were accomodated very simply by adding new procedures. The addition of new access protocols was accomplished by augmenting the list of access protocol types, adding switches corresponding to these types in those eventhandler routines that were common to all access schemes, and adding new event types and eventhandling procedures as required.

7.2.2 Validation of the Simulation

As mentioned in the previous subsection, the packet radio network simulation software consists of approximately 3000 lines of Pascal code. This software must

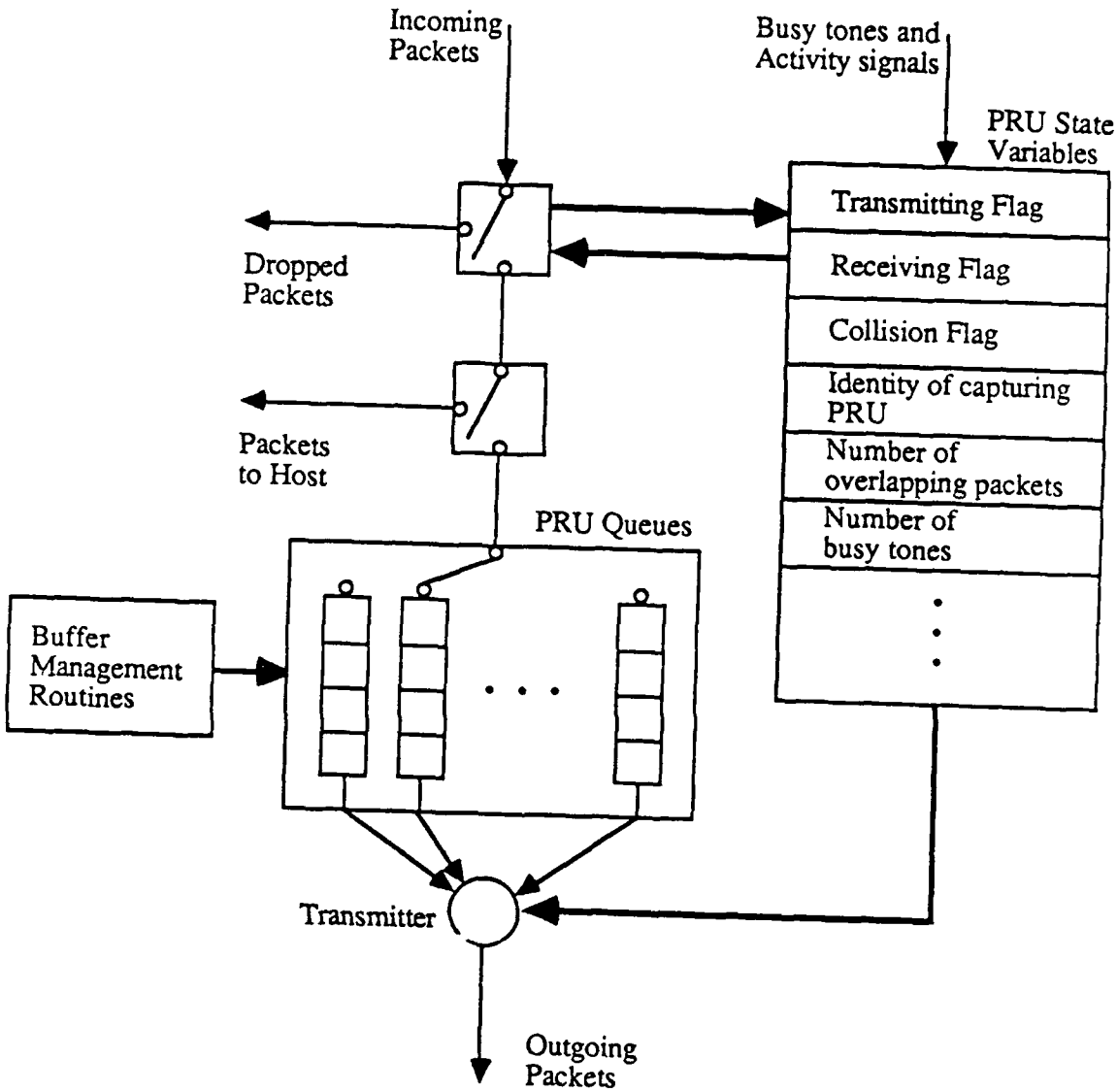

Fig. 7.2 The structure of a PRU.

be validated to be a correct representation of the packet radio network model. It is desirable to validate the simulation by comparison with measurements obtained from real packet radio networks. Unfortunately, such measurements are not available as many of the schemes and features considered in this study have not been implemented. Indeed, a major motivation for the simulation study was to serve as a guide for future network design. In the absence of real system data, the approach we have taken to validation is based on a comparison of the simulation output with the results of mathematical analyses. Such analyses are of course only available for a restricted subset of the simulation parameter settings; however, within this subset a number of access schemes, topologies and performance measures are included and hence different aspects of the simulation may be checked. We have performed such checks for the following situations:

(i) Nodal capacity of pure and slotted ALOHA in regular topologies,

(ii) Nodal capacity of CSMA, C-BTMA and CASMA in the fully connected tetrahedron,

(iii) Nodal capacity of C-BTMA in the (two-hop) octahedron,

(iv) Throughput-delay performance of CSMA in a fully connected network with 50 PRUs, each with a single packet buffer.

In all cases an extremely close match between simulation and analysis was seen, which enhanced our confidence in the correctness of the simulation program.

7.2.3 Estimation of the Performance Measures

Each simulation run can be considered to be composed of an initial transient period followed by a 'steady-state'. The objective is to obtain accurate estimates of the system performance measures when the system is in steady state. As the data

gathered during the transient period are clearly not representative of the steady state, such data may need to be discarded. The approach taken here is to measure the length of the transient period in several typical scenarios, record the 'worst case' value (i.e, where the transient period is longest), and to use this value plus an substantial factor of safety in subsequent runs. The 'worst case' value is periodically checked and updated if necessary as additional experiments on the network are performed. Note that in cases where the transient period is very long, a judicious selection of the initial state can significantly improve simulation efficiency by shortening the transient period, as is illustrated in the following example. Consider a packet radio network consisting of the 6 PRU ring topology under the C-BTMA access scheme, the HSF buffer management scheme with a single queue per PRU, $B_0 = m = \infty$, $B_T = 2$, $G = 5.0$ and $a = 0.01$. As has been pointed out in an earlier chapter, when the load exceeds the network capacity all PRUs are in a heavy traffic situation, and the throughput is equal to the capacity. Let us refer to that subset of the system state space consisting of those states where every PRU has at least one packet in its buffers as the HT (for heavy traffic) set. Let τ denote the mean time to hit the HT set starting from the initial state in which all queues are entirely empty. Since for $\gamma \geq C(G)$ the states of the HT set are recurrent, while all other states are transient, for this case τ is a good indicator of the length of the transient period*.

In figure 7.3 we plot τ versus γ for $\gamma \geq C(G)$. We observe that as γ increases beyond $C(G)$ τ decreases, and for γ large enough τ is negligible as compared with the length of a typical simulation run. Note that for values of γ slightly greater than $C(G)$ τ is extremely large. In this case τ and hence the transient period would be considerably diminished were the initial state a member of the HT set.

In order to measure the degree of precision in the measures of system performance, confidence intervals at some high confidence level (typically 95%) are

*Note that for $\gamma < C(G)$ all states are recurrent.

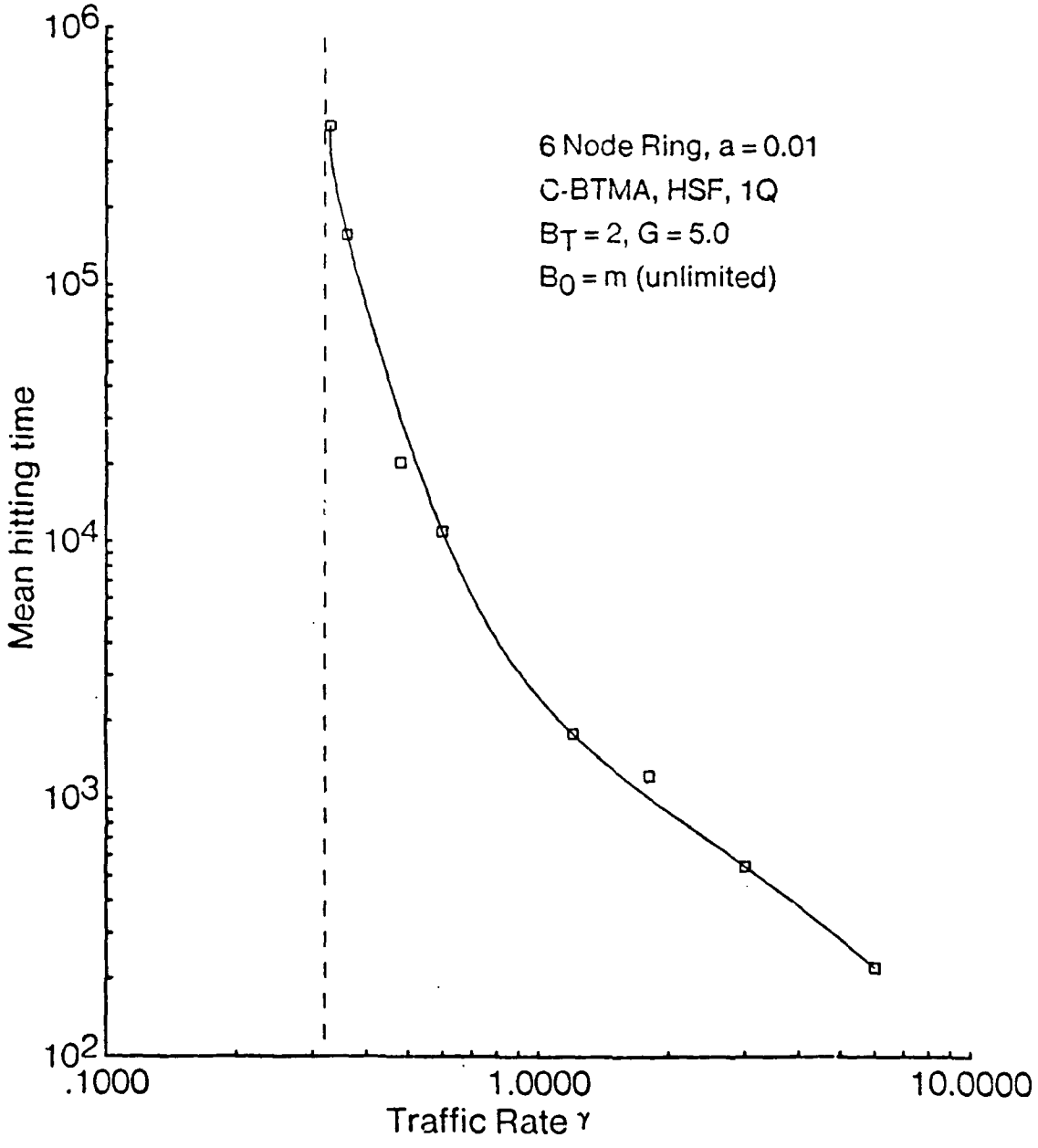

Fig. 7.3 The effect of offered traffic load on the length of the transient period.

required. There are a number of methods proposed in the literature for confidence interval estimation. Among these are:

(i) Method of independent replications,

(ii) Method of sub-runs,

(iii) Regenerative method,

(iv) Autoregressive method,

We have investigated each of the above methods in order to determine which was most appropriate for our purposes. In method (iv) it is assumed that the measured samples of the performance measures are generated by an underlying linear model of known form but of unknown order. Various methods exist for estimating that order. In applying this method in a typical simulation, it was found that the order of the assumed underlying model turned out to be extremely high (of the order of thousands of coefficients). For this reason, the autoregressive approach was deemed unsuitable here. We next considered the regenerative method. The regenerative method is applicable when the system state returns successively to a 'regeneration state' over and over again; samples gathered over such 'cycles' are mutually independent and identically distributed. The regenerative method possesses several desirable features. Not only are independent samples of the system output obtained, but it is unnecessary to discard the transient period. (Note that the selection of a suitable regeneration state is left to the simulation analyst). While the packet radio networks that we simulate are indeed regenerative, unfortunately we found that in several cases of interest the cycle (recurrence) times were intolerably long. This is illustrated in the following example. Consider the same network as described in the previous example. Suppose that we are interested in the average delay performance whereupon a natural choice of a regeneration state is the idle state (i.e, the state in which all queues are entirely empty). In figure 7.4, we plot the mean recurrence time

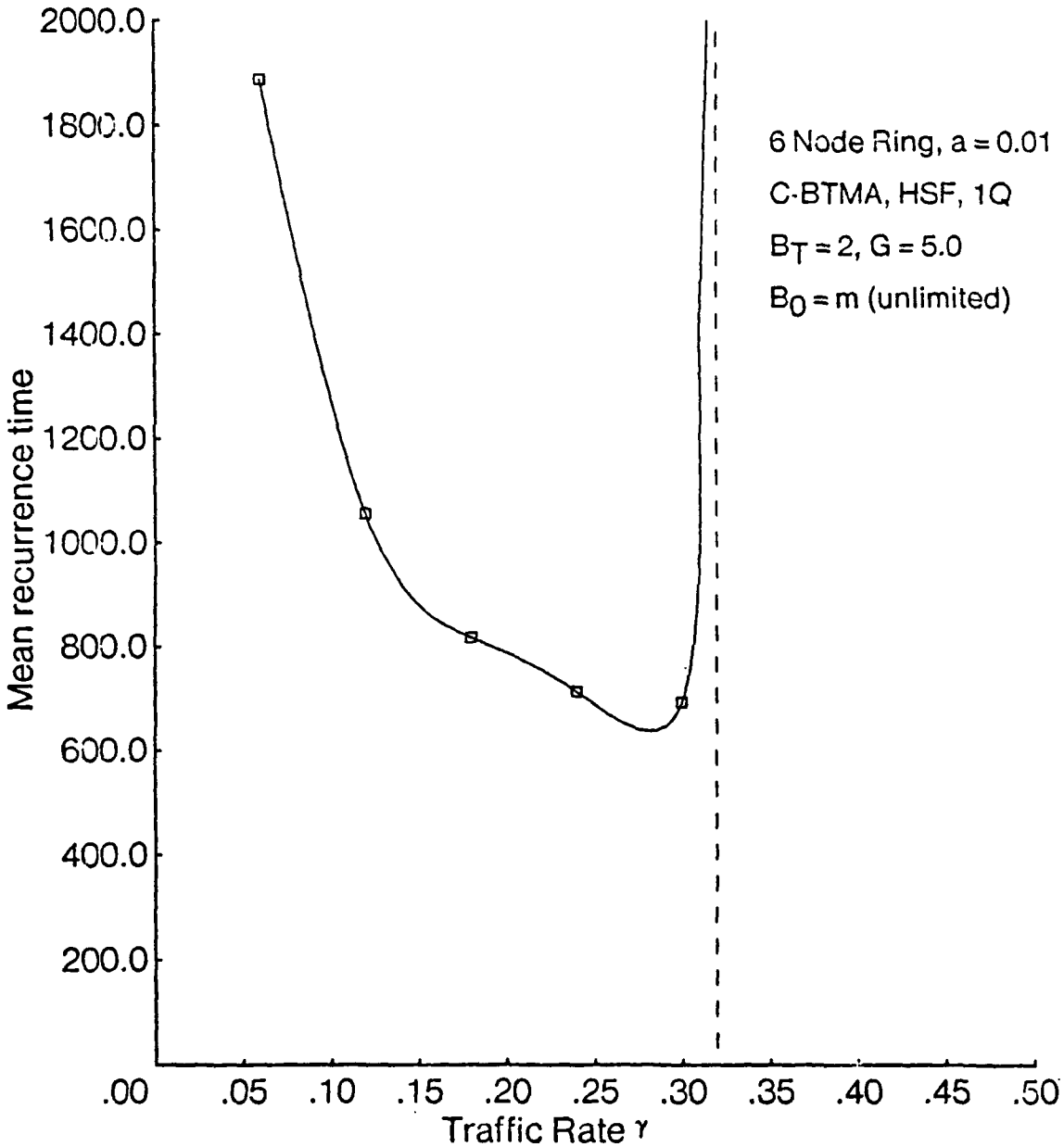

Fig. 7.4 Mean recurrence time to the idle state versus the offered load.

as a function of the offered traffic. It is not surprising to observe that as $\gamma \rightarrow C(G)$ (a region of load that we are clearly interested in), the recurrence time approaches ∞. Thus the regenerative method is impractical here and we are left to consider methods (i) and (ii). Both the latter methods are similar in that no assumptions about the underlying structure of the simulation process are made. In the method of independent replications the samples produced are independent. However, as the transient period associated with each replication needs to be discarded, this method is costly. In the method of sub-runs (or batch means), the transient period is discarded only once. The sub-run method is thus more cost-effective, and for this reason we have used the sub-run method extensively. In the method of sub-runs, it is necessary for the simulation analyst to specify the length of the sub-runs. As the samples generated over each sub-run are not strictly speaking independent, the length of the sub-runs must be chosen large enough so that for all practical purposes the samples are uncorrelated. The length of the sub-run required to achieve the latter condition depends not only on the network structure, the protocols and the load, but also on the measure of performance under consideration. This is illustrated in figure 7.5 in a typical network where the effect of the sub-run length is shown for both the network capacity and the delay performance measures. The example considered consists of an icosahedron topology under the CSMA access scheme, with a uniform traffic matrix, and $a = 0.001$, $B_T = \infty$, $B_0 = 1(m = 0)$, $G = 0.05$, and $\gamma = \infty$. The length of the run in this case was 6×10^5 in time units normalized to the packet transmission time (hereafter denoted ntus) with a discarded initial 'warm-up' period of 1.6×10^3 ntus. The network capacity and the average packet delay were measured as 0.238 and 4.56×10^2 respectively. We note that the confidence intervals for network capacity are essentially constant with sub-run length indicating that the smallest value considered, namely, 2×10^3 ntus is sufficiently large. On the other hand, for the delay we see that the confidence

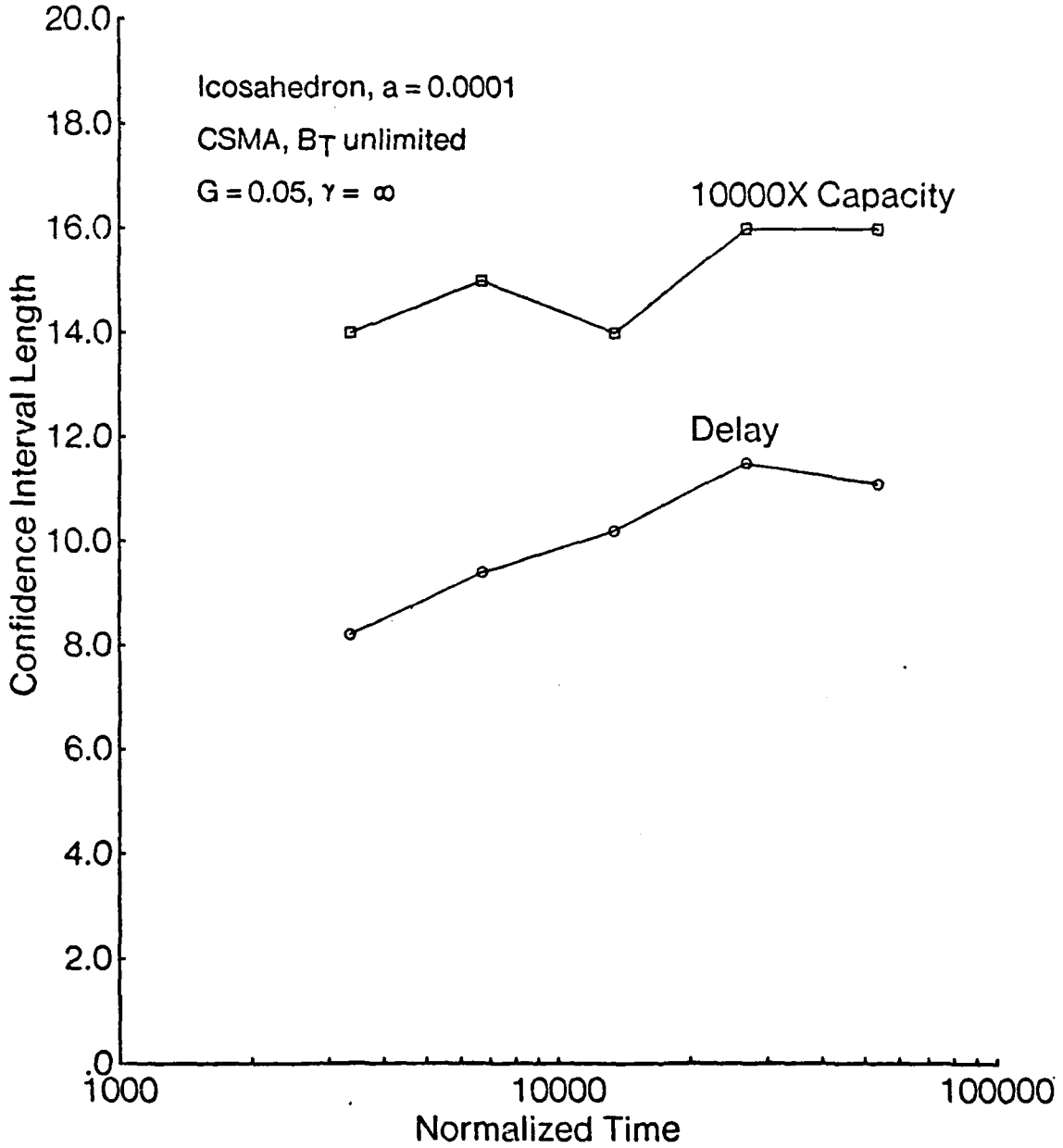

Fig. 7.5 Effect of sub-run length on confidence interval length for network capacity and average packet delay.

interval length increases with sub-run length until the sub-run length is 1.6×10^4 ntus, indicating that for delay the sub-run length should be at least that value. Once the sub-run lengths are specified, the number of such sub-runs determines the confidence interval at the given confidence level. Typically, a confidence interval whose length is within 5% of the performance estimate in question is sought. The simulation is run in an iterative mode until such a confidence interval length is attained or some maximum run time is exceeded.

References

[1] L. Kleinrock, *Queueing Systems, Volume 2: Computer Applications*, John Wiley and Sons, New York, 1976.

[2] N. Abramson, "The ALOHA system - Another Alternative for Computer Communication," *1970 Fall Joint Comput. Conf. AFIPS Conf. Proc.*,Vol. 37, pp281-285.

[3] R. Kahn, S. Gronemeyer, J. Burchfiel and R. Kunzelman, "Advances in Packet Radio Technology," *Proc. IEEE,* Vol. 66, Nov. 1978, pp1468-1496.

[4] F. Tobagi, "Multiaccess Protocols in Packet Communication Systems," *IEEE Trans. Commun.,* Vol. COM-28, No. 4, April 1980, pp468-488.

[5] L. Kleinrock and F. Tobagi, "Packet Switching in Radio Channels: Part 1 - Carrier Sense Multiple-Access Modes and their Throughput-Delay Characteristics," *IEEE Trans. Commun.*, Vol. COM-23, No. 12, December 1975, pp1400-1416.

[6] F. Tobagi and L. Kleinrock , "Packet Switching in Radio Channels: Part 2 - The Hidden Terminal Problem in Carrier Sense Multiple-Access and the Busy-Tone Solution," *IEEE Trans. Commun.*, Vol. COM-23, No. 12, December 1975, pp1417-1433.

[7] P. Spilling and F. Tobagi, "Activity Signalling and Improved Hop Acknowledgements in Packet Radio Systems," *Packet Radio Temporary Note No. 283,* January 1980.

[8] S. S. Lam and L. Kleinrock, "Packet Switching in a Multiaccess Broadcast Channel: Dynamic Control Procedures," *IEEE Trans. Commun.*, vol. COM-23, no. 9, Sept. 1975, pp891–904.

[9] F. A. Tobagi and L. Kleinrock, "Packet Switching in Radio Broadcast Channels: Part IV – Stability Considerations and Dynamic Control in Carrier Sense Multiple Access," *IEEE Trans. Commun.*, vol. COM-24, no. 10, Oct. 1977, pp1103–1119.

[10] R. M. Metcalfe and D. R. Boggs, "Ethernet: Distributed Packet Switching for Local Computer Networks," *Comm. ACM,* Vol. 19, No. 7, July 1976, pp395-404.

[11] T. A. Gonsalves and F. A. Tobagi, "On the Performance Effects of Station Locations and Access Protocol Parameters in Ethernet Networks," *SEL Technical Report No. 86-292*, Stanford University, Stanford, California, January 1986.

[12] F. Tobagi, "On the Analysis and Simulation of Buffered Packet Radio Systems," *Proc. 9th Hawaii Int. Conf. Syst. Sci.*, Honolulu, HI, Jan. 1976, pp42-45.

[13] M. Sidi and A. Segall, "Two Interfering Queues in Packet-Radio Networks," *IEEE Trans. Commun.*, vol. COM-31, no. 1, Jan. 1983.

[14] F. Tobagi, "Modeling and Performance Analysis of Multihop Packet Radio Networks," *Proc. IEEE*, Vol. 75, No. 1, January 1987.

[15] I. Gitman, "On the Capacity of Slotted ALOHA Networks and Some Design Problems," *IEEE Trans. Commun.*, vol. COM-23, no. 3, Mar. 1975, pp305-317.

[16] F. Tobagi, "Analysis of a Two-Hop Centralized Packet Radio Network—Part I: Slotted ALOHA," *IEEE Trans. Commun.*, Vol. COM-28, No. 2, February 1980, pp196-207.

[17] F. Tobagi, "Analysis of a Two-Hop Centralized Packet Radio Network—Part II: Carrier Sense Multiple Access," *IEEE Trans. Commun.*, Vol. COM-28, No. 2, February 1980, pp208-216.

[18] Y. Yemini, "On Channel Sharing in Discrete-Time, Multi-Access Broadcast Communication," Computer Science Department, School of Engineering and Applied Science, University of California, Los Angeles, *UCLA Tech. Report* UCLA-ENG-8061, Sept. 1980.

[19] H. Takagi and L. Kleinrock, "Throughput-Delay Characteristics of Some Slotted-ALOHA Multihop Packet Radio Networks," *IEEE Trans. Commun.*, vol. COM-33, no. 11, Nov. 1985, pp1200-1207.

[20] J. Silvester and L. Kleinrock, "On the Capacity of Multihop Slotted ALOHA Networks with Regular Structure," *IEEE Trans. Commun.* Vol. COM-31, No. 8, August 1983, pp974-982.

[21] J. Silvester and L. Kleinrock, "On the Capacity of Single-Hop Slotted ALOHA Networks with Various Traffic Matrices and Transmission Strategies," *IEEE Trans. Commun.* Vol. COM-31, No. 8, August 1983, pp983-991.

[22] R. Nelson and L. Kleinrock, "The Spatial Capacity of a Slotted ALOHA Multihop Packet Radio Network with Capture," *IEEE Trans. Commun.*, vol. COM-32, no. 6, Jan. 1984, pp684–694.

[23] H. Takagi and L. Kleinrock, "Optimal Transmission Ranges for Randomly Distributed Packet Radio Terminals," *IEEE Trans. Commun.*, vol. COM-32, no. 3, Mar. 1984, pp246–257.

[24] T.-C. Hou and V. O. K. Li, "Transmission Range Control in Multihop Packet Radio Networks," *IEEE Trans. Commun.*, vol. COM-34, no. 1, Jan. 1986, pp38-44.

[25] E. Sousa and J. A. Silvester, "Determination of Optimum Transmission Ranges in a Multi-Hop Spread Spectrum Network," *Proceedings MILCOM'85,* Boston, Oct. 1985, pp25.3.1–25.3.5.

[26] R. Nelson and I . Kleinrock, "Rude CSMA: A Multihop Channel Access Protocol," *IEEE Trans. Commun.*, vol. COM-33, no. 8, Aug. 1985, pp785-791.

[27] R. Nelson and L. Kleinrock, "Spatial-TDMA: A Collision-Free Multihop Channel Access Protocol," *IEEE Trans. Commun.*, vol. COM-33, no. 9, Sept. 1985, pp934-944.

[28] B. Leiner, "A Simple Model for Computation of Packet Radio Network Communication Performance," *IEEE Trans. Commun.*, Vol. COM-28, no. 12, December 1980, pp2020-2023.

[29] I. Lee and J. A. Silvester, "An Iterative Scheme for Performance Modeling of Slotted ALOHA Packet Radio Networks," *Proc. ICC'82,* June 1982, pp 6G.1.1–6G.1.5.

[30] J. A. Silvester and I. Lee, "Performance Modeling of Buffered CSMA – An Iterative Approach," *Conf. Record GLOBECOM'82,* Miami, Nov. 1982, ppF1.6.1–F1.6.5.

[31] R. Boorstyn and A. Kershenbaum,"Throughput Analysis of Multihop Packet Radio," *Proceedings of ICC,* Seattle, June 1980, pp 13.6.1- 13.6.6.

[32] R. Boorstyn , A. Kershenbaum and V. Sahin,"A new Acknowledgement Protocol for Analysis of Multihop Packet Radio Networks," *Proceedings of COMPCON,* Washington, 1982.

[33] F. Tobagi and J. Brazio, "Throughput Analysis of Multihop Packet Radio Networks Under Various Channel Access Schemes," *Proc. INFOCOM,* San Diego, May 1983.

[34] B. Maglaris, R. Boorstyn and A. Kershenbaum,"Extensions to the Analysis of Multihop Packet Radio Networks," *Proc. INFOCOM,* San Diego, California, May 1983.

[35] A. Kershenbaum and R. R. Boorstyn, "Evaluation of Throughput in Multihop Packet Radio Networks with Complex Topologies," *Proc. INFOCOM'84,* San Francisco, California, Apr. 1984.

[36] J. Brazio and F. Tobagi, "Theoretical Results in Throughput Analysis of Multihop Packet Radio Networks," *Proc. ICC,* Amsterdam, May 1984.

[37] J. Brazio and F. Tobagi, "Throughput Analysis of Spread Spectrum Multihop Packet Radio Networks," *Proc. INFOCOM,* Washington, DC., March 1985.

[38] O. deSouza, M. Chen and R. Boorstyn, "A Comparison of the Performance of Protocols in Packet Radio Networks," *Proc. MILCOM,* Boston, Massachusetts, October 1985.

[39] M. Chen and R. Boorstyn, "Throughput Analysis of Code Division Multiple Access (CDMA) Multihop Packet Radio Networks in the Presence of Noise," *Proc. Infocom,* Washington D. C., April 1985

[40] H. Frank, I. Gitman and R. Van Slyke, " Packet Radio System - Network Considerations," *AFIPS Conf. Proc.,* Vol. 44, Montvale, NJ, 1975, pp217-231.

[41] J. Silvester, "On the Spatial Capacity of Packet Radio Networks," *UCLA-ENG-8021,* Computer Science Department, School of Engineering and Applied Science, UCLA, May 1980.

[42] M. Elsanadidi and W. Chu, "Simulation Studies of the Behaviour of Multi-hop Broadcast Networks," *ACM SIGCOMM Symposium on Communications Architectures and Protocols,* Austin, Texas, March 1983, pp170-177.

[43] F. Tobagi, R. Binder and B. Leiner, "Packet Radio and Satellite Networks," *IEEE Communications Magazine,* Vol. 22, No. 11, November 1984, pp24-40.

[44] D. Baker and A. Ephremides, "The Architectural Organization of a Mobile Radio Network via a Distributed Algorithm," *IEEE Trans. Commun.,* Vol. COM-29, No. 11, November 1981, pp1694-1701.

[45] M. Flynn, C. Spangler, and A. Zimmerman, "The Stanford Packet Radio Network," *Proc. COMPCON,* San Francisco, California, Spring 1986.

[46] M. Hazell and B. Davies, "A Fully Distributed Approach to the Design of a 16Kbit/sec VHF Packet Radio Network," *Proc. IEEE MILCOM,* Washington, DC, January 1983, pp645-649.

[47] E. Raso (Editor), *Gateway: The ARRL Packet Radio Newsletter,* ARRL, Newington, Connecticut.

[48] F. Tobagi and J. Storey, "Improvements in Throughput of a CDMA Packet Radio Network due to a Channel Load Sense Access Protocol," *22nd Allerton Conf.,* Urbana, ILL, October, 1984.

[49] M. Gerla and L. Kleinrock, "Flow Control: A Comparative Survey," *IEEE Trans. Commun.,* Vol. COM-28, No. 4, April 1980, pp553-574.

[50] L. Kleinrock and S. Lam, "Packet switching in a multiaccess broadcast channel: Performance evaluation," *IEEE Trans. Commun.*, Vol. COM-23, Apr. 1975, pp410-423.

[51] L. Kleinrock, "Principles and Lessons in Packet Communication", *Proc. IEEE*, Vol. 66, No. 11, November 1978, pp1320-1329

[52] R. Holt, "Some Deadlock Properties of Computer Systems", *ACM Comput. Surveys.*, vol. 4, No. 3, Sept. 1972, pp179-196.

[53] K. Gunther, "Prevention of Deadlocks in Packet-Switched Data Transport Systems", *IEEE Trans. Commun.* COM-29, No. 4, April 1981.

[54] P. Merlin and P. Schweitzer, "Deadlock Avoidance in Store-and-Forward Networks - I: Store-and-Forward Deadlock", *IEEE Trans. Commun.*, Vol. COM-28, No. 3, March 1980, pp345-354.

[55] A. Giessler et al., "Free Buffer Allocation - An Investigation by Simulation," *Computer Networks (2)*, 1978, pp191-208.

[56] S. Toueg and J. Ullman,"Deadlock-free Packet-Switching Networks," *Proc. 11th Annu. ACM Symp. Theory Comput.*, Atlanta, GA., May 1979, pp89-98.

[57] I. Gopal, "Prevention of Store-and-Forward Deadlock in Computer Networks," *IEEE Trans. Commun.*, Vol. COM-33, No. 12, December 1985, pp1258-1264.

[58] F. Kamoun, "Design Considerations for Large Computer Communication Networks", *UCLA-ENG-7642*, Computer Science Department, School of Engineering and Applied Science, UCLA, April 1976.

[59] F. Tobagi and L. Kleinrock, "The Effect of Acknowledgement Traffic on the Capacity of Packet-Switched Radio Channels," *IEEE Trans. Commun.*, Vol. COM-36, No. 6, June 1978, pp815-826.

[60] M. Elsanadidi and W. Chu, "Study of Ackowledgements in a Star Multi-Access Network,"*IEEE Trans. Commun.*, Vol. COM-30, No. 7, July 1982, pp1657-1667.

[61] H. Takagi and L. Kleinrock, "Output Processes in Contention Packet Broadcasting Networks," *IEEE Trans. Commun.*, Vol. COM-33, No. 11, November 1985, pp1191-1199.

[62] H. Kobayashi, *Modeling and Analysis: An Introduction to System Performance Evaluation Methodology*,, Addison-Wesley, Massachusetts, 1978.

[63] G. Fishman, *Principles of Discrete Event Simulation*, John Wiley and Sons, New York, 1978.

[64] A. Aho, J. Hopcroft, J. Ullman, *Data Structures and Algorithms*, Addison Wesley, Massachusetts, 1983.